The University Of Sheffield.

Mutational and Biochemical Analysis of the Yeast Ribonuclease Rex1

By:

Taib Ahmed Hama Soor

A thesis submitted in partial fulfilment of the requirements for the degree of Doctor of Philosophy

The University of Sheffield

Department of Molecular Biology and Biotechnology

August 2017

Abstract

Cellular RNAs are transcribed as precursor molecules and need to be processed to become fully functional RNAs. RNAs are processed either solely by exoribonucleolytic trimming reactions or in combination with one or more endonucleolytic cleavages. This study focuses on the mutational and biochemical analysis of the 3'→5' exoribonuclease Rex1 from *Saccharomyces cerevisiae*. Rex1 is a nuclear protein that is required for the correct 3' end maturation of specific cellular RNAs, including 5S rRNA. Although yeast expresses a family of four distinct Rex Proteins that show strong sequence homology within the catalytic domain, Rex1 is uniquely able to substitute for the function of the yeast exoribonuclease Rrp6 *in vivo*. The catalytic domain of Rex1 is flanked by N-terminal and C-terminal regions that are not shared by the other Rex proteins, suggesting these additional structural features may contribute to its ability to substitute for Rrp6 function. Deletion of either the N-terminal or C-terminal region of Rex1 caused a loss of function, and northern blot analyses demonstrated that these mutants were defective in 5S rRNA processing *in vivo*. Using an RNA processing assay developed in our laboratory that accurately recapitulates Rex1-dependent 5S rRNA maturation, I showed that deletion of either the N- or C-terminal region of Rex1 blocked 5S rRNA processing *in vitro*. Interestingly, full-length *rex1* mutants that express the catalytic domain of either Rex2 or Rex3 are also nonfunctional. GFP fluorescence studies showed that the N-terminal region of Rex1 contains a nuclear localization signal(NLS). Glycerol gradient ultracentrifugation studies and size exclusion chromatography of Rex1 indicated that the protein is expressed as part of a complex of approximately 125 kDa. Together, these results suggest that features within the N- and C-terminal region of Rex1 (in addition to the catalytic domain) are required for Rex1 function, while the N-terminal region of Rex1 is also critical for its nuclear localization. CRAC (cross linking and analysis of cDNAs) analysis of Rex1 showed that the protein binds directly to a diverse range of RNAs *in vivo* but is predominantly associated with tRNA, and showed a preference for certain isoacceptor species and intron-containing transcripts. Rex1 broadly bound to the same RNAs in the absence of Rrp6 but did show accentuated recruitment to characterized Rrp6 substrates, such as snoRNAs and 5.8S rRNA. These data catalogue the transcripts

that are processed or degraded by either Rex1 or Rrp6, and reveal that Rex1 is selectively recruited to Rrp6 substrates in the absence of Rrp6.

Acknowledgements

First of all I am deeply grateful to my supervisor Dr Phil Mitchell, who gave me great support and encouragement to achieve this research during my PhD studies. Special thanks to my parents for their guidance and looking after me. I would also like to thank the support staff at the molecular biology department.

I would like to acknowledge my lovely lab colleagues of Mitchell Lab. Their companionship kept my spirits up when things were not going so well in the lab.

I'd also like to thank my advisors Ewald Hettema and Stuart Wilson for their critical advice and support during this time.

I' would like to thank to colleagues in Edinburg University, Elizabeth Petfalski, David Tollervey and Sander Granneman for their collaboration with the CRAC analysis of Rex1. And Rosie Staniforth and her lab colleagues for their help with the Size exclusion chromatography assay.

Finally, I would also like to mention my sponsorship Iraqi-HCED (Higher Committee for Education Development) and the University of Sulaimani for essential financial support over the course of my studies.

Index of Contents

List of abbreviations used in this study

Endo	endonuclease
CUT	cryptic unstable transcript
DEPC	diethylpyrocarbonate
DMSO	dimethyl sulfoxide
dNTP	deoxyribonucleotide triphosphate
ds	double stranded
DTT	dithiothreitol
5-FOA	5'fluoroorotic acid
ATP	adenosine triphosphate
CIP	calf-intestinal alkaline phosphatase
CTD	C-terminal domain
ETS	external transcribed spacer
His	histidine
IPTG	isopropyl -D-1-thigalactopyranoside
mRNA	messenger RNA
MW	molecular weight
ncRNA	non-coding RNA
NTD	N-terminal domain
OD	optical density
Exo	exonuclease
gDNA	genomic DNA
GST	glutathione-S-transferase
GTC	guanidine thiocynate
HCl	hydrochloric acid
Ori	origin of replication
PCR	polymerase chain reaction
PEG	polyethyleneglycol
PMSF	phenylmethylsulphonylfluoride
PNK	polynucleotide kinase
poly(A)	polyadenylated
poly(U)	polyuridylated
ORF	open reading frame
RBD	RNA binding domain
RNA	pol DNA dependent RNA polymerase
RNase	ribonuclease
RNP	ribonucleoprotein
rDNA	ribosomal DNA
snRNA	small nuclear RNA
ss	single stranded
TAP	tandem affinity purification
TCA	trichloroacetic acid
rRNA	ribosomal RNA
SD	synthetic dextrose medium
SDM	site directed mutagenesis
SDS	sodium dodecyl sulphate

SGal	synthetic galactose medium
snoRNA	small nucleolar RNA
TEMED	*N*,*N*,*N*′,*N*′-Tetramethylethylenediamine
Tm	melting temperature
tRNA	ransfer RNA
WT	wildtype
ZnK	zinc-knuckle
zz	protein A tag
Rs	stoke's radius
TS	temperature sensitive
UTR	untranslated region
UV	ultraviolet
v/v	percentage volume per volume
w/v	percentage weight per volume
5S RNP	5S rRNA ribosomal protein

Units used in this study

cpm	counts per minute
Da	daltons
bp	base pair
CFU	colony forming units
g	gram
g-force	g-force(relativeentrifugal force)
kb	kilobase
kDa	kiladalton
rpm	revolutions per minute
S	Svedberg
U	units (of enzyme)
µg	microgram
µM	micromolar
µ	microlitre
l	litre
mg	milligram
ml	millilitre
mM	millimolar
ng	nanogram
nM	nanomolar
pmol	picomolar

Chapter one

1.1 Introduction

RNA processing reactions are of fundamental importance to the process of gene expression (Houseley and Tollervey, 2009; Parker, 2012; Jackowiak et al., 2011). All characterized cellular RNAs are synthesized as primary RNA transcripts that are subsequently converted to shorter, mature RNAs by a set of molecular processes that are collectively known as RNA processing events. Cellular RNA processing reactions are diverse, comprising the splicing, 5' end capping and coupled 3' end cleavage and polyadenylation typical of pre-mRNA transcripts, the post-transcriptional ribose 2'-O-methylation and base modification of ribosomal RNA and other stable RNAs (Yamada-Okabe ET AL, 1999; Lodish, 2007), as well as endonucleolytic cleavage events and/or exonucleolytic trimming of RNA from either the 3' or 5' end (Bernstein and Toth, 2012; Arraio et al, 2010). Of these distinct types of RNA processing events, 3'-5' exoribonucleolytic trimming is probably the most fundamental and widespread (Bernstein and Toth, 2012). Indeed, all characterized nascently transcribed RNAs have at least one additional nucleotide present at their 3' end and these extra nucleotides have to be removed to produce a functional, mature RNA (Butler, 2002). In contrast, not all RNAs require endonucleolytic cleavage, 5' end RNA trimming or other RNA processing events.

Exoribonucleases show directionality that is they remove terminal nucleotides from either the 3' or 5' end of RNA. Nucleotides can be removed from the 3' end of RNA by either a hydrolytic or phosphorolytic mechanism (Deutscher and Reuven, 1991). Enzymes with phosphorolytic activity such as polynucleotide phosphorylase (PNPase) from *Escherichia coli* use an inorganic phosphate ion to attack the 5' phosphodiester linkage of the terminal nucleotide, leaving a 3' hydroxyl group and releasing a nucleoside5' diphosphate. In contrast, hydrolytic exoribonucleases use a water molecule to attack the phosphodiester bond and release nucleoside 5' monophosphates (figure 1). Ribonucleases are also classified as being either "processive" or "distributive", based on their kinetic properties (Ptsahne, 1986; Mazur and Record, 1989; Lohman 1986; von Hippe, 1989). Processive enzymes remain bound

to the substrate molecule after release of the nucleotide product and degrade or process individual substrate molecules to completion. Intermediates are not observed and processing/degradation is generally rapid. In contrast, distributive enzymes bind less tightly to their substrates and dissociate readily after release of one or more nucleotides. In this case, the whole population of substrate molecules is progressively shortened and intermediates of various lengths are observed.

The major source of 3' to 5' exoribonuclease activity in eukaryotic cells is the exosome ribonuclease complex (Allmang et al, 1999b; Mitchell et al, 1997). The exosome complex was initially characterised in the bakers' yeast *Saccharomyces cerevisiae* but is conserved throughout eukarya and archaea (Chlebowski et al, 2013; Lykke-Andersen et al, 2009; Liu et al, 2006) (figure 2). The exosome is a multi subunit complex of ca. 400 kDa and, furthermore, must interact functionally and physically with additional cofactor proteins and complexes in order to process or degrade its substrates. The structural "core" of the exosome complex comprises six different proteins that are structurally related to the bacterial phosphorolytic exoribonuclease RNase PH, together with three structurally related "cap" proteins that contain S1 and/or KH RNA-binding domains. The 6 RNase PH homologous proteins (known as Rrp41, Rrp42, Rrp43, Rrp45, Rrp46 and Mtr3) are organized in a hexameric ring arrangement consisting of three paired subunits (Rrp41/Rrp45, Rrp46/Rrp43 and Mtr3/Rrp42) (Liu et al., 2006; Makino et al., 2013a). This ring structure is stabilized by interactions with the cap proteins Rrp4, Rrp40 and Csl4, where by each cap protein stabilizes interactions between two adjacent RNase PH heterodimers (Lorentzen et al, 2007; 2008). The cap proteins also interact with one another, forming a second tier. Together, these 9 subunits form a stable, two-tiered barrel-shaped complex with a central channel that is broad enough to accommodate single-stranded RNA. The archaeal complex is somewhat simpler, with the hexameric ring comprising three Rrp41/Rrp42 heterodimers and a cap structure comprised of a combination of Rrp4 and Csl4 proteins. The hexameric ring of the archaeal exosome contains three catalytic sites for a phosphorolytic activity that are composed of both subunits of each Rrp41/Rrp42 heterodimer (Houseley *et al*, 2006; Büttner K *et al*, 2005 and Lorentzen, and Conti, 2005).In contrast, the core of the eukaryotic exosome complex lacks

catalytic activity (Lorentzen et al, 2008; Dziembowski et al, 2007). Ribonuclease activity is associated with two additional subunits, Rrp6 (Allmang et al., 1999b; Briggs et al., 1998; Butler, 2008) and Rrp44/Dis3 (Lorentzen et al, 2008; Mitchell et al, 1997), that are bound to the top and bottom of the core complex, respectively. Both Rrp6 and Rrp44 are hydrolytic enzymes. Rrp44/Dis3 is ubiquitously associated with exosome complexes. In contrast, yeast Rrp6 is associated specifically with the exosome complexes in the nucleus. Rrp6 functions in the degradation or processing of a number of distinct substrates, including 5.8S rRNA (Briggs et al., 1998; Mitchell et al., 1997; Mitchell et al., 2003; Briggs et al., 1998) and box C/D snoRNAs (Stead et al, 2007).

SnoRNAs can be transcribed from independent gene or from polycistronic transcripts by

Pol II in *S. cerevisiae*, which guide pseudouridylation and methylation. There are two major types of snoRNAs: snoRNA containing H/ACA box and snoRNA containing C/D box. Box C/D snoRNA contains two motifs; box C (UGAUGA) and box D (CUGA) at the 5' and 3'ends. To form distinctive structural motifs, the c and D motifs should be brought together in the pre-snoRNA. The function of these motifs is to stabilize, localize and process snoRNAs in the nucleolus (Bally et al. 1988; Hughes and Ares 1991; Li et al. 1990; Ooi SL et al, 1998; Morrissey and Tollervey 1993, 1997; Lemay et al. 2011).

Rrp6 interacts directly with the nuclear RNA-binding protein Rrp47 (Costello et al, 2011; Feigenbutz et al, 2013; Mitchell et al., 2003; Stead et al, 2007). Rrp6 and Rrp47 proteins provide mutual stability (Feigenbutz et al, 2013) and consequently *rrp6Δ* and *rrp47Δ* mutants have largely overlapping RNA degradation and processing phenotypes (Arigo et al, 2006; Costello et al, 2011; Milligan et al, 2008; Mitchell et al, 2003). Accumulation of some pre-rRNA processing intermediates includes 21S and 23S pre-rRNAs are observed in cells lacking Rrp6 (Canavan and Bond, 2007).

In eukaryotes, RNA polymerase I initiates rRNA synthesis in nucleolus. RNA polymerase I transcribes the 35S pre-rRNA, this includes 18S, 5.8S and 25S ribosomal subunits seperated internal transcribed spacers (ITSs) and flanked by external transcribed spacers (ETSs) (Henras et al 2008; Fang; et al, 2005). Through several

events of cleavage and processing, mature rRNAs are generated from a long polycistronic precursor 35S rRNA. Through these events several intermediates are released includes 21S and 23S (de la Cruz et al, 1998; Fang; et al, 2005).

The structural organization of the eukaryotic exosome core is closely related to bacterial phosphorolytic enzyme, PNPase. PNPase is a homotrimeric protein and each subunit has two topologically identical core domains that have diverged in sequence, only one of which containing residues that are critical for catalysis. In addition to the duplicated core domain, each PNPase monomer contains a KH and an S1 domain in the C-terminal region (Aloy et al, 2002). In an analogous arrangement to the structure of the exosome complex, the duplicated core domains of the three monomeric PNPase proteins are arranged as a trimeric ring, while the KH and S1 domains of each monomer are positioned on the surface of the ring. Similarly, RNase PH is a homohexameric enzyme with an analogous ring structure wherein a catalytic site is located at the interface between each pair of sub units. The structural similarity between these different exonuclease complexes suggest that they are evolutionarily related, with a single domain phosphorolytic enzyme having evolved into PNPase, RNase PH and the two archaeal Rrp41 and Rrp42 proteins. The six eukaryotic RNase PH homologues can be divided into Rrp41-related (Rrp41, Rrp46, Mtr3) and Rrp42-related (Rrp42, Rrp43, Rrp45) groups, suggesting that they have evolved from the archaeal proteins through subsequent gene duplications.

In addition to the PNPase/RNase PH family, cells express other 3'-5' exoribonucleases that are grouped by their relationship to either bacterial RNase II (RNase B) (which includes Rrp44/Dis3)or to RNase D (which includes Rrp6) (Mian, 1997). Members of all three enzyme families perform critical functions in RNA processing, turnover and degradation. A further enzyme, called RNase BN, is found in a number of eubacteria but appears to be absent in archaea and eukaryotes (Zuo and Deutscher, 2001). In contrast to the exosome and PNPase complexes, many cellular exoribonucleases that have been structurally characterized have a much simpler organization and are expressed either as monomeric proteins (e.g. RNase II from *E. coli*) (Zilha˜o et al., 1993, 1995a,1996b) or homodimers (e.g. RNase T from *E. coli*) (Li et al., 1996; Zuo et al., 2007).

1.2 The DEDD superfamily of exoribonucleases

One major group of cellular 3’ to 5’ exoribonucleases is the DEDD family (figure 3), which includes the bacterial enzyme RNase D, the related bacterial enzymes RNase T and oligoribonuclease, and the yeast enzymes Rrp6, Rex1, Rex2, Rex3, Rex4, Pan2 and Caf1. The DEDD family of RNases is related in sequence to the 3’ to 5’ exodeoxyribonuclease proof-reading domain of DNA polymerases. The 3' to 5' exonuclease domain has three motifs known as ExoI, Exo II, and Exo III (Bernard et al, 1989; Delarue et al, 1990; Ito and Braithwaite, 1991; Braithwaite and Ito, 1993), which are gathered around the active site of the exoribonuclease domain (Beese and Steitz, 1991). The term “DEDD family” is derived from the presence of four invariant aspartate and glutamate residues within these three structural motifs at the active site of the enzymes. These negatively charged amino acid residues function to coordinate the binding of two divalent metal cations such as Mg^{2+}. The mechanism of action of the proofreading activity of DNA polymerases has been well established and shown to be dependent upon the divalent metal cations (Steitz and Steitz, 1993). Nucleophilic attack on the phosphorus atom of the last nucleotide is carried out by a hydroxide ion that is activated by one of the divalent cations, whilst the second divalent metal ion stabilizes the leaving oxy anion and pentacoordinate transition state (Beese, and Steitz, 1991). The proof-reading activity of the exodeoxyribonuclease domain is inhibited by mutation of any of the four conserved acidic residues (Joyce and Steitz, 1994). All members of this family (including DNases and RNases) are proposed to have the same mechanism of action to catalyse different substrates, which is characterized by the requirement of two divalent metal cations (Steitz and Steitz, 1993). Consistent with this, mutagenesis studies have found that the four conserved acidic residues are essential for the catalytic activity of bacterial RNase T (Zuo and Deutscher, 2002) and yeast Rrp6 (Phillips and Butler, 2003).

In addition to the presence of the four invariant acidic amino acids in the DEDD super-family of proteins, a fifth highly conserved acidic residue is found between motifs II and III (Barnes *et al*, 1995) and this has made the identification of motif III problematic (Koonin, 1997; Nguyen et al, 2000). This conserved residue does not interact with the substrate directly and does not constitute part of the active site of the protein in the

DNA polymerase proof-reading domain (Brautigam et al, 1999). However, it may have a role in catalysis through interactions with residues within motif II since mutation of the corresponding amino acid blocks the catalytic activity of DNA polymerase III in *B. subtilis* (Barnes et al, 1995) and RNase T in *E. coli* (Huang and Deutscher, 1992).

Members of the DEDD family can be divided into two groups, according to the nature of the amino acid sequence of motif III. A tyrosine residue in motif III helps to orientate an activated water molecule for nucleophilic attack at the terminal phosphodiester bond (Beese and Steitz, 1991). Furthermore, mutation of the corresponding position within yeast Rrp6 (Y361A, Y361F) was shown to inhibit exonuclease activity (Phillips and Butler, 2003). However, other DEDD enzymes such as DNA polymerase III, RNase T, oligoribonuclease, the Rex Proteins and Pan2 lack this tyrosine residue and contain a conserved histidine residue at an adjacent position. These distinct subfamilies are referred to as DEDDy and DEDDh enzymes.

The mechanistic consequence of having a tyrosine or histidine residue within motif III is not yet clear. The presence of either a histidine or tyrosine residue does not correlate simply with DNase or RNase activity, both types of catalytic activity being exhibited by members of the DEDDy and the DEDDh groups.

1.3 The yeast DEDD family of exoribonucleases

There are six different enzymes in *S. cerevisiae* that have 3' to 5' exonuclease activity and which belong to the DEDD super family: Rrp6, Pan2, Caf1, Rex1, Rex2, Rex3 and Rex4 (Moser et al, 1997). Each of the genes encoding these proteins is nonessential for mitotic cellular growth (Briggs et al, 1998; van Hoof et al, 2000) although the lack of Rrp6 causes a temperature-sensitive phenotype (Allmang et al., 1999).Indeed, a *rex1Δ, rex2Δ, rex3Δ, rex4Δ, pan2Δ* pentuple mutant shows no obvious growth defect (van Hoof et al, 2000). Each of these enzymes functions in the processing or degradation of specific transcripts, while some exonucleases are redundant with other exonucleases for specific pathways (van Hoof et al, 2000).

Rrp6 (ribosomal RNA-processing 6) is a nuclear protein that is associated with the core exosome complex and functions in the processing of 3’ extended forms of some types

of ribosomal RNAs (Briggs et al, 1998; Allmang et al, 2000). The accumulation of an extended form of 5.8S rRNA was found in mutant forms of Rrp6 (Mitchell et al, 2003, 1997; Briggs et al, 1998). Rrp6 is important for the maturation of some types of RNA such as 5.8 rRNA, snRNA and snoRNAs (Stead et al, 2007; Carneiro et al, 2007; Allmang et al, 1999a; van Hoof et al, 2000a; Briggs et al., 1998). In addition, it has a role the degradation of a wide range of processing fragments and unstable transcripts. Lack of Rrp6 in the cell causes an accumulation of some processing intermediates such as 21S and 23S pre-rRNAs (Canavan and Bond, 2007). Rrp6 also degrades aberrant mRNP particles as a part of quality control pathways (Butler and Mitchell, 2011). Recombinant Rrp6 protein exhibits a distributive 3'-5' exonuclease activity *in vitro* on poly(A) substrates but shows much weaker activity against structured RNA (Burkhard and Butler, 2000; Liu et al, 2006).In addition to its DEDD exonuclease domain, Rrp6 contains an N-terminal PMC2NT (polymyositis autoantigen 2, N-terminus) domain (Staub et al, 2004) with which it interacts with its cofactor Rrp47 (Stead et al., 2007), an HRDC (helicase and RNase D C-terminal) domain that contributes to substrate binding (Makino et al., 2015) and an extended C-terminal region that allows association with the exosome complex (Callahan and Butler, 2008; Makino et al., 2013). The interaction between Rrp6 with Rrp47 is important for the mutual stability of these two proteins (Feigenbutz et al., 2013) and the heterodimeric interface provides a platform for the interaction between the Rrp6/Rrp47 heterodimer and the RNA helicase, Mtr4 (Schuch et al, 2014).

The yeast *PAN2*gene encodes a 135 kDa protein that functions in shortening the poly (A) tail of mRNA (Boeck et al, 1996; Brown and Sachs, 1998). Pan2 is associated with another protein, Pan3, and the Pan2/Pan3 complex has an adenylate-specific exonuclease (deadenylase) activity. The PAN deadenylase shortens newly synthesised mRNA poly (A) tails from approximately 200 nucleotides to around 60-80 nucleotides and is important in establishing specific poly(A) tail lengths for each mRNA transcript, a process that is conserved from yeast to humans (Brown and Sachs, 1998; Yamashita et al, 2005). A detailed atomic resolution crystal structure of the yeast PAN deadenylase enzyme has been reported (Schäfer et al., 2014). Pan2 contains an N-terminal WD40 domain that is shared with other RNA processing factors such as Prp19

and Pwp2, a linker region and a central domain that has similarity with deubiquitinases (but which lacks the catalytic triad of residues necessary for proteolysis), in addition to the C-terminal DEDD domain (see figure 4). Pan3 contains an N-terminal zinc finger, a region of low complexity that contains a poly(A)-binding protein (Pab1) interaction motif and a structurally compact C-terminal region comprising a pseudokinase domain, a coiled coil region and a knob domain (Brown et al, 1996; Mangus et al, 2004; Christie, 2013). The Pan2/Pan3 complex consists of an asymmetric Pan3 dimer in association with a single molecule of Pan2 (figure 4).

Formation of a catalytically active Pan2/Pan3 complex is dependent upon the linker region, the deubiquitinase-like domain and the DEDD domain of Pan2, as well as the C-terminal region of Pan3. The C-terminal regions of the two Pan3 proteins are packed together, and the deubiquitinase domain of Pan2 is stacked on top of the DEDD domain. Pan2 interacts with the Pan3 homodimer mainly through its linker region, which wraps around the knob domains of the Pan3 homodimer. Furthermore, an extended loop within the DEDD domain of Pan2 makes contacts with a beta sheet within the N-terminal lobe of the psuedokinase domain of the Pan3 protein. Deletion of the corresponding residues within the pseudokinase domain of the Drosophila Pan3 homologue blocked PAN activity (Christie et al, 2013), emphasising the importance of this interaction for PAN function .Mutation of residues within the nucleotide binding site of the pseudokinase domain of Pan3 partially block Pan2 deadenylase activity in vitro (Schäfer et al., 2014) and impacted on mRNA deadenylation in vivo (Christie et al., 2013). The ATP binding site of Pan3 is separated from the catalytic site of Pan2 by approximately 50 angstrom, suggesting that it may stimulate Pan2 deadenylase activity by contributing to poly(A) binding.

The structure and properties of the Pan3 dimer is similar to RNase L, a homodimer with a dual endoribonuclease-pseudokinase domain structure which is an interferon-inducible antiviral protein (Zhou et al, 1993, 1997). RNase L is present under normal conditions as a none active monomer and it becomes activated by 2',5' oligoadenylate ligands to make a dimeric complex (Floyd-Smith et al, 1981; Wreschner et al, 1981). The RNase L dimer protein, similar to Pan3, is composed of a single rigid complex consisting of the two dual RNase and pseudokinase region modules in a parallel back-

to-back arrangement (Huang et al 2014). The pseudokinase domain of RNase L has nucleotide binding activity (Dong and Silverman, 1999; Huang et al, 2014). Moreover, the pseudokinase domain of Pan3 helps to thread RNA into the active site of the enzyme to increase the efficiency of distributive degradation the RNA (Schäfer et al, 2014).

Caf1/Pop2 was initially characterised as a conserved component of the Ccr4 transcription factor complex (Draper et al., 1995). Yeast *pop2* mutants were subsequently shown to be defective in mRNA deadenylation *in vivo* (Daugeron et al., 2001). Furthermore, a recombinant polypeptide fragment of Pop2 encompassing the DEDD domain showed ribonuclease activity *in vitro*. Interestingly, yeast Pop2 contains noncanonical residues at three of the four acidic residues that constitute the catalytic active site (the canonical "DEDD" residues are substituted for the residues "SETQ" in yeast Pop2). However, the acidic residues are conserved in the putative orthologues from other species and the yeast protein does contain the fifth, highly conserved acidic residue between motifs II and III (see figure 3).
In addition to the *RRP6*, *PAN2* and *POP2* genes, the genome of *S. cerevisiae* encodes 4 additional genes that have sequence homology with members of the DEDD superfamily (Moser et al., 1997). On the basis of their homology with known exoribonucleases, these proteins were named Rex1 (RNA exonuclease 1), Rex2, Rex3 and Rex4 (van Hoof et al., 2000).

The YNT20/REX2 gene was cloned through genetic interactions with *yme* mutants, which cause a high rate of mitochondrial DNA loss. A loss of function *ynt20* mutant exhibited a cold-sensitive respiratory growth defect and an epitope-tagged form of the protein was shown to cosediment with mitochondria (Hanekamp and Thorsness, 1999). Notably, overexpression of *REX2* causes a block in cell growth and a clustered mitochondria phenotype (Sopko et al, 2006). An analysis of the role of the *REX* genes on stable RNA synthesis has revealed that approximately half of the U4 snRNA molecules in a *rex2Δ* mutant are extended at the 3' end, while a *rex2Δ rrp6Δ* double mutant had little U4 snRNA of the correct, mature size (van Hoof et al., 2000). This

suggests that Rex2 and Rrp6 (or the exosome complex) have redundant functions in the final 3' end maturation of U4 snRNA (Figure 5).

Strains that are deleted for the *REX3* gene show a specific defect in the 3' end maturation of the RNase MRP RNA, accumulating transcripts that are approximately 7 nucleotides longer than those seen in the wild-type strain. Rex3 has overlapping functions with other Rex proteins in the 3' maturation of U5 snRNA and RNase P RNA transcripts (Figure 5) (van Hoof et al, 2000) and in the autoregulated degradation of the *RTR1* mRNA transcript (Hodko et al, 2016). Rex3 is related in sequence to the putative exoribonuclease pqe-1 of *Caenorhabditis elegans*, which has a protective effect on neuronal cells and decreases the toxic effects of glutamine/proline triplet expansion diseases (Faber et al, 2002).

The function of yeast Rex4 has been less well studied, although one report suggests a role for the protein in pre-rRNA processing and ribosome assembly (Eppens et al, 2002). Consistent with this, the protein is localized to the nucleus and nucleolus in yeast cells (Hu et al, 2003). Rex4 is highly conserved and the orthologous proteins in humans and *Xenopuslaevis* have been studied. The human Rex4 homologous protein, ISG20/HEM45, is also localized to the nucleus. Little is known about the functional role(s) of the human protein but its expression was shown to be strongly induced upon treatment of cells with interferon or estrogen (Gongora et al, 1997; Pentecost, 1998). The gene encoding the Rex4 homologous protein in *X. laevis*, XPMC2, was cloned through its ability to rescue mitotic catastrophe in the fission yeast *Schizosaccharomyces pombe*, which occurs due to hyperactivity of the Cdc2 protein kinase and the ensuing premature entry into mitosis (Su and Maller, 1995).The mechanism by which XPMC2 inhibits Cdc2 kinase activity is unclear.

1.4 Rex1

The *rex1Δ* mutant shows a specific defect in the 3' end maturation of 5S rRNA, accumulating molecules that are approximately 3 nucleotides longer than the 5S rRNA observed in wild-type cells (van Hoof et al, 2000). Strains lacking Rex1 are also defective in the 3' processing of tRNA-Arg(UCU), which is encoded not only by seven

monocistronic genes but also by four copies of a dicistronic tRNA-Arg-tRNA-Asp gene. The dicistronic transcript is processed initially into tRNA-Arg and tRNA-Asp species by endonucleolytic cleavage. tRNA-Arg(UCU) RNAs accumulate in the *rex1Δ* mutant that are incompletely processed at their 3' end (van Hoof et al., 2000), consistent with a defect in 3' maturation following endonucleolytic processing.

The RNA processing defects observed in the *rex1Δ* mutant phenotypically matches those previously reported for the *rna82-1* allele (Piper et al, 1983). The *rex1Δ* and *rna82-1*mutations were subsequently shown to be allelic and sequence analysis revealed a single nucleotide substitution within the *rna82-1* allele that converts the TGG codon encoding residue W433 into a TGA premature termination codon. The truncated Rex1 protein encoded by the *rna82-1* allele comprises the complete DEDD catalytic domain but lacks 100 residues at the C–terminus of the protein.

Pulse-chase labeling studies in wild-type yeast cells revealed that the 121 nucleotide long 5S rRNA is processed from longer (128 and 131 nucleotide long) primary transcripts without any detectable intermediates (Piper et al, 1983). This is consistent with earlier in vitro processing studies using solubilized yeast chromatin (Tekamp et al, 1980). In addition to the longer transcripts, the in vitro transcription and processing system revealed a processing intermediate that is extended by 3 nucleotides (Tekamp et al, 1980). Notably, processing of the 5S rRNA transcript is incomplete in the *rna82-1* mutant, the predominant species being 124 nucleotides in length (Piper et al, 1983). The observed 3' extended forms of 5S rRNA in wild-type yeast extracts, the accumulation of the 3 nucleotide extended 5S rRNA species in the*rna82-1* mutant and the sequence homology between Rex1 and other DEDD family members strongly suggests that the final maturation of 5S rRNA involves a Rex1-dependent exonucleolytic trimming mechanism.

There is convincing data to support the hypothesis that the yeast Rex1 protein does indeed have 3'-5' exoribonuclease activity. Rex1 was purified as an overexpressed fusion protein from cell extracts of *S. cerevisiae* and shown to accurately trim a pre-tRNA-Met substrate to the mature tRNA form in vitro (Ozanick et al, 2009). As predicted by its sequence similarity with other members of the DEDD family, Rex1

required the presence of Mg^{2+} ions for its catalytic activity in vitro (Ozanick et al, 2009). Furthermore, mutation of two of the conserved acidic residues (D229A/E231A) within Rex1, which had previously been shown to inactivate the homologous *E. coli* enzyme RNase T (Zuo and Deutscher, 2002), caused complete loss of catalytic activity (Ozanick *et al,* 2009).

tRNA maturation involves removal of the 5' leader and 3' trailer sequences and, in some instances, the removal of intronic sequences within their anticodon loops by a dedicated cleavage and ligation machinery. The order of tRNA processing events is not obligatory in yeast but typically 5' processing through endonucleolytic cleavage by RNase P precedes 3' end processing, and splicing normally occurs after removal of the 5' leader and 3' trailer sequences (Xiao et al, 2001; O'Connor and Peebles 1991; Kufel et al, 2003; Evans et al. 2006; Späth et al. 2007; Hartmann et al. 2009). The fact that tRNA splicing in yeast typically occurs after 5' and 3' end processing reflects the fact that the tRNA splicing machinery in yeast is located on the surface of the mitochondria (Copela et al*,* 2008; Lee et al. 1991; Hopper 2006; Yoshihisa et al, 2003; Huh et al, 2003) and so tRNA molecules must be exported from the nucleus to the cytoplasm for splicing to occur. tRNA can undergo retrograde transport from the cytoplasm to the nucleus, at least under stress conditions (Shaheen and Hopper, 2005; Shaheen et al., 2007; Takano et al., 2005; Murthi et al., 2010; Park et al, 2005; Whitney et al., 2007). Furthermore, tRNAs are extensively modified post-transcriptionally by a diverse group of protein enzymes. These modification events not only impact on tRNA function during translation in the cytoplasm but can also influence whether the pre-tRNA is correctly processed or subjected to degradation in the nucleus (Copela et al, 2008; Ozanick et al, 2009; Kadaba et al, 2004, 2006; Vanacova et al, 2005) Probably as a result of the complexity of tRNA production, approximately half of the tRNA made by RNA polymerase III is degraded shortly after synthesis through quality control pathways that occur in both the nucleus and the cytoplasm (Gudipati et al, 2012; Schneider et al, 2012; Dewe et al, 2012).

Our understanding of the molecular function of many tRNA processing factors has been hampered by the complexities of the synthesis pathway for even this small RNAs, namely existence of redundant processing pathways, a nonobligatory order of

processing events, distinct subcellular distributions of processing activities, and the fact that the same ribonuclease enzymes are involved in both the productive processing of pre-tRNA to mature tRNA molecules and the complete destruction of their substrates. The complexity of this biological process is reflected by the results of a recent study that identified 174 genes required for tRNA production in yeast (Wu et al, 2015).

As noted above, *rex1* mutants are defective in the 3' end maturation of tRNA-Arg(UCU) that is encoded by the dicistronic tRNA-Arg-tRNA-Asp transcript (Skowronek et al, 2014; van Hoof et al, 2000; Ozanick et al, 2009). Deletion of the *REX1* gene also leads to the accumulation of 3' extended forms of different types of monocistronic tRNAs, suggesting that Rex1 has a more general role in the 3' end processing of pre-tRNAs. These tRNAs include, but are not limited to, unspliced, intron-containing tRNAs such as tRNA-Tyr(GUA) and tRNA-Lys(UUU) (Copela et al*,* 2008). Some of the pre-tRNA transcripts that accumulate in the *rex1* mutant also contain the 5' leader sequence. These observations suggest that recruitment of Rex1 to its (intron-containing) pre-tRNA substrates occurs independently of the pre-tRNA splicing machinery or the 5' end processing endonuclease, RNase P. The accumulation of a diverse set of 3' extended tRNA species in the rex1Δ mutant that either do or do not contain the 5' leader sequence or the intronic sequence is consistent with the model that the steps in tRNA processing occur in a nonobligatory order. Under certain circumstances, the activity of Rex1 may be important in providing a sufficient period of time for other processing steps to be completed. In support of this hypothesis, absence of the TRAMP subunit Trf4 (that typically polyadenylates RNAs and targets them to subsequent exonucleolytic degradation) leads to the accumulation of unspliced pre-tRNAs that are 3' end processed in a Rex1-dependent manner (Copela et al*,* 2008). In contrast, the study by (Ozanick et al, 2009) provides strong evidence for a role of Rex1 in tRNA quality control. Expression of initiator tRNA-Met_i is dependent upon the methyltransferase Trm6, which methylates A58 in the TYC loop. The expression levels of mature tRNA-Met_i are similarly low in the *trm6* and*rex1Δ trm6* mutants, compared to the wild-type strain, but there is a large increase in the 3' extended precursor in the absence of Rex1 and these RNAs are oligoadenylated.

Whether 3’ processing of pre-tRNAs involves an endo- or exonucleolytic process is largely influenced by the RNA-binding protein La (known as Lhp1 in yeast). La protects the 3’ end of the pre-tRNA transcripts from exonucleolytic attack and promotes endonucleolytic processing by RNase Z (Yoo and Wolin, 1997; Skowronek et al., 2013). In the absence of La, 3’ end processing involves Rex1 or Rrp6 (van Hoof et al., 2000; Copela et al., 2008).It follows that alteractions in the balance between the expression levels of Rex1 and La in the cell can result in changes in Rex1 activity (Yoo and Wolin, 1997; Skowronek et al, 2013). Elevated temperature and/or addition of glycerol to the growth medium lead to a decrease in the production of tRNA. A cellular stress response results in an increase in the expression of La, which binds to the 3’ end of tRNA-Tyr and tRNA-lle(UAU) and inhibits exoribonuclease processing by Rex1 (figure 6) (Foretek et al, 2016).

Yeast *rex1Δ rrp6Δ* double mutants are synthetic lethal.

Although there are many Rex Proteins in yeast, only Rex1 can substitute for the function of Rrp6 in one or more pathways that are required for cell growth (Peng et al, 2003; van Hoof et al, 2000b). This specificity may be related to the structure of Rex1, which has N- and C-terminal domains in addition to the central catalytic domain that are not shared with other Rex proteins. The critical cellular function that is dependent upon either Rrp6 or Rex1 has not been equivocally demonstrated but the available data suggests a role in snoRNA processing. A viable *rrp47 rex1* double mutant exhibited an enhanced defect in the 3’ end maturation of box C/D snoRNAs, while disruption of the interaction between Rrp47 and Rrp6 in the *rex1Δ* mutant blocked cell growth and led to the accumulation of 3’ extended snoRNAs and the depletion of the corresponding mature species (Garland *et al,* 2013). However, the reason why snoRNA depletion would cause a rapid cessation of growth (before depletion of the available pool of cellular ribosomes) is not clear.

The *E. coli* Rex1 homologue, RNase T, is also nonessential for cell growth and has been shown to function in a redundant manner in the 3’ end processing of tRNA (Kelly and Deutscher, 1992). Any one of five exoribonucleases (RNase T, RNase PH, RNase D, RNase II, and RNase BN) is required for the correct 3’ end maturation of tRNA and

mutation of the genes encoding these five proteins accumulatively leads to synthetic lethality.

The structural organization of Rex1

Residues 225-373 of yeast Rex1 comprise a central domain that shares sequence homology with other members of the Rex family of DEDD exoribonucleases (figure 3). Moreover,Rex1 purified from yeast cell extracts has been shown to exhibit exoribonuclease activity *in vitro* (Ozanick et al, 2009).The unique ability of Rex1 to substitute functionally for Rrp6 is most likely reflected in specific structural features of this protein that are not present in the other Rex proteins. Notably, the central DEDD catalytic domain of Rex1 is flanked by C-terminal and N-terminal regions that do not share any notable sequence homology with other members of the Rex Protein family. A central hypothesis of this project was that one or more regions within the N- or C-terminal portions of Rex1 would be critical for its function *in vivo.* Upon initiating this project, the only structural features or motifs that could be identified within yeast Rex1 (in addition to the catalytic DEDD domain) were a short predicted coiled coil region within the N-terminal region from residues 167-194, and two predicted coiled coil regions within the C-terminal region encompassing residues 428-458 and 509-533 (figure 3). Subsequently, it became apparent that the polypeptide sequence encompassing residues 428-505 (which directly flanks the catalytic DEDD domain) can be threaded to the resolved three-dimensional structure of alkaline phosphatase and phosphoglycerate mutase (Kelley and Sternberg, 2009), although the stretch of homology is not sufficient to constitute a complete structural fold within these proteins (see figure 20, below). Nevertheless, it is of note that alkaline phosphatase and phosphoglycerate mutase are enzymes that are involved in the binding of ligands containing phosphate groups (see figure 20, below). This region of Rex1 may therefore potentially contribute to the binding of the RNA substrate or the released nucleoside monophosphate. Finally, a number of residues within yeast Rex1 have been demonstrated to be sites of phosphorylation *in vivo*, including S24, T26, S27, T34 (in the N-terminal region) and T287 (in the DEDD catalytic domain) (Li et al, 2007; Holt et al, 2009; Albuquerque et al, 2008). The post-translational modification of these

residues may potentially have an impact on the function of Rex1 through alteration of its catalytic properties or through altering another aspect of the protein's function, such as substrate recruitment.

Rex1 homologues are found in *E. coli* and Man

The homologue of Rex1 in *E. coli* is RNase T. RNase T is an exoribonuclease with 3' to 5' exoribonuclease activity and it is able to hydrolyse both RNA and DNA (Viswanathan et al, 1998; Moser et al, 1997; Zuo & Deutscher, 2001). It belongs to the super-family of DEDDh exo(deoxy)ribonucleases and is dependent upon divalent metal ions such as Mg^{2+} for its catalytic activity (Zuo & Deutscher, 2002; Deutscher & Marlor, 1985; Moser et al, 1997; Zuo & Deutscher, 2001). RNase T is required to generate the mature 3' end of 23S and 5S rRNA (Li & Deutscher, 1995; Li et al, 1999a) and has a role in the turnover of tRNAs (Deutscher et al, 1985). Structural and biochemical analyses of RNase T from *E. coli* revealed a homodimeric architecture similar to that of oligoribonuclease that is critical for catalytic activity (Li et al, 1996; Zuo et al, 2007). The subunits are aligned in an antiparallel fashion, such that the nucleic acid binding site of one monomer is facing the catalytic active site of the second monomer. This structural arrangement allows RNA substrates to be channeled from the substrate binding site of one monomer to the catalytic active site of the other subunit (Zuo et al, 2007).

The human proteinTREX1 shows sequence and structural homology to RNase T of *E. coli* (Mazur and Perrin, 1999; Zuo and Deutscher, 2001) and has 3' to 5' end exoribonuclease activity *in vitro* that is dependent upon its homodimeric structure (Mazur and Perrino, 1999; Orebaugh et al, 2011; Li et al, 1996; Zuo and Deutscher, 2002). In addition, both proteins have exodeoxyribonuclease and exoribonuclease activity (Fenghua et al*,* 2015; Zuo and Deutscher, 1999) and they have a higher Km for single stranded RNA rather than single stranded DNA (Fenghua et al*,* 2015; Zuo, and Deutscher, 1999; Mazur, and Perrino, 2001).

TREX1 functions as a 3' to 5' deoxyexoribonuclease in mammalian cells (Mazur and Perrino, 1999; Mazur, and Perrino, 2001; Hoss et al*,* 1999), in addition to its function

in tRNA processing (Fenghua *et al,* 2015). Failure of TREX1 to degrade DNA in cytosol is believed to be the cause of TREX1-mediated autoimmune disease (Bailey et al, 2012*;* Fye et al, 2011; Barber, 2011). Several autoimmune disorders are associated with mutations in TREX1, such as Aicardi-Goutieres syndrome (AGS) type 1, chilblain lupus, systemic lupus erythematosus, and retinal vasculopathy with cerebral leukodystrophy (Richards et al, 2007; Lee-Kirsch et al, 2007a; Lee-Kirsch et al, 2007b; Crow et al, 2006; Kavanagh, 2008). Defects in TREX1 in mammalian cells has also been linked to an increased resistance of RNA viruses such as human immunodeficiency virus (HIV), influenza virus, vesicular stomatitis virus, West Nile virus, and Sendai virus (Yan et al, 2010; Hassan et al, 2013).

5S rRNA and its assembly into ribosomes

The small 5S ribosomal RNA is the most well characterised Rex1 substrate (Piper et al, 1983 and Van Hoof et al, 2000). 5S rRNA is a component of the large ribosomal subunit and is the smallest ribosomal RNA molecule, with a length of 120-121nt and a molecular weight of 40 kDa. It has a highly conserved secondary and tertiary structure, consisting of five short helices, four loops (two hairpins and two internal), and one hinge which folds the molecule into a Y-shaped structure (Lee et al*,* 2006). 5S rRNA is the only ribosomal RNA molecule that is transcribed by RNA polymerase III, rather than by RNA polymerase I. Prior to assembly into ribosomal complexes, 5S rRNA interacts with the large ribosomal subunit proteins L5 and L11 to form a 5S rRNP complex (Deshmukh et al*,* 1995; Zhang et al*,* 2007). The 5S rRNP particle is then assembled into 90S pre-ribosomal complexes within the nucleolus (Deshmukh et al*,* 1995), together with further accessory factors in yeast such as Rpf2 and Rrs1 (Zhang et al*,* 2007). The 90S pre-ribosomal complexes undergo a complex series of nucleolytic processing reactions and structural rearrangements in order to generate the mature 40S small ribosomal subunits and large 60S ribosomal subunits (Venema and Tollervey, 1999; Schafer et al, 2003). The 5S rRNA constitutes part of a structural feature of the mature, large ribosomal subunit known as the central protuberance (CP) and is positioned at the interface between the 40S and the 60S subunits of the translating ribosome. The precise function of 5S rRNA in translation is still not well

known but it is believed to be involved in some RNA-RNA and protein-RNA interactions within the ribosome (Spahn et al*,* 2001).

1.5 Protein import into the nucleus

Nuclear processes are dependent upon the import of specific proteins from the cytoplasm to the cell nucleus. Transport of proteins into the eukaryotic cell nucleus is dependent upon the presence of specific targeting signals known as nuclear localization signals (NLSs), specific transporter proteins that mediate protein import and nuclear pore complexes that provide access sites through the double-layered nuclear membrane.

Some nuclear proteins do not contain an NLS and are imported into nucleus through interaction with other nuclear proteins that do contain an NLS (Leslie et al 2004; Jonas et al, 1997; Shiota et al, 1999; Xia et al, 1992). The mutant form of the hepatitis D virus antigen depends on these types of nuclear import mechanism (Xia et al, 1992). Rex1 is a nuclear protein (Frank et al, 1999) but whether or not it contains a functional NLS has not been established.

The eukaryotic cell nucleus is differentiated from the cytosol by a double-layered membrane called the nuclear envelope. Transport across the nuclear envelope occurs via large nuclear pore complexes and an underline lamina of nucleus (Fahrenkrog and Aebi, 2003; Stoffler et al*,* 1999; Allen et al*,* 2000; Fahrenkrog and Aebi 2002). Small proteins (around 40 kDa or less), metabolites and ions can pass through nuclear pore complexes by passive diffusion, while the transport of larger macromolecules is restricted, such that only those proteins containing an appropriate targeting signal can pass through the pores (Paine et al*,* 1975; Bonner, 1975). Specific carrier proteins known as karyopherins facilitate the transport of macromolecules between the nucleus and cytoplasm compartments (Radu et al*,* 1995). Those karyopherins that function in export and import are named exportins (Stade et al*,* 1997) and importins (Gorlich et al*,* 1994), respectively. Karyopherins typically bind directly to their cargo proteins. However, in the initially characterised “classic” nuclear import pathway (Go¨rlich, *et al,* 1995), this interaction is mediated via an adaptor protein called importin α and in this case transport involves an α/β heterodimer. Importins mediate

transport of proteins through the nuclear pore complexes through their ability to interact with the F/G repeat nucleoporin subunits that line the pore.

The “classical” NLS (cNLS) is the most well characterized nuclear transport signal and is widely employed as a module to artificially target heterologous proteins to the eukaryotic cell nucleus. It is composed of either one stretch of predominantly basic amino acids (a monopartite signal) or two such sequences (a so-called bipartite signal), separated by a short spacer sequence. The first NLS characterized was that of the SV40 virus large T antigen, a monopartite classical NLS with the sequence PKKKRRV. In contrast, nucleoplasmin has a bipartite NLS with the sequence KRPAATKKAGQAKKKK, where the sequence PAATKKAGQ separates the two basic motifs (Kalderon et al, 1994; Robbins et al*,* 1991; Dingwall and Laskey, 1991). Monopartite NLSs have the loose consensus sequence K(K/R)*X*(K/R), wherein a lysine residue in the p1 position and a basic residue (either a lysine or arginine residue) at position p2 and p4 is required (Hodel et al*,* 2001).

The steady state nuclear accumulation and import rate of a cNLS cargo *in vivo* correlates with the affinity of binding of the cargo cNLS with importin, which can be measured *in vitro* (Hodel et al*,* 2001, Hodel et al*,* 2006). Non-functional cNLS sequences may bind to importin very weakly and not be imported effectively, or they may bind to importin very tightly and not be separated from the receptor efficiently in the nucleus (Gilchrist et al*,* 2002; Matsuura et al, 2003; Matsuura and Stewart, 2005; Matsuura and Stewart, 2004; Gilchrist and Rexach, 2003).The rate of cargo import is also affected by the effective concentration of importin (Riddick and Macara, 2005). Therefore, the concentration of the receptor (importin) and the affinity of binding between importin and cargo affects the nuclear accumulation and import rate of cNLS cargoes (Riddick and Macara, 2005, Hodel et al*,* 2006).

1.6 Aims of the study

Our laboratory has a long-standing interest in understanding the molecular functions of eukaryotic ribonucleases in the processing and degradation pathways that target cellular RNA transcripts. To date, much work has focused on the role of the exosome RNase complex and the activities of its catalytic subunits Rrp6 and Rrp44 (Allmang et al, 1999b; Mitchell et al, 1997; Lorentzen et al, 2008; Allmang et al, 1999b; Briggs et al,

1998). The function of Rrp6 is somewhat overshadowed by that of Rrp44, largely because expression of Rrp6 is not strictly required for cell viability (Mitchell et al, 1997; Briggs et al,1998; Allmang et al, 1999b). However, *rrp6Δ* mutants do have a conditional, temperature-sensitive growth phenotype and growth of this mutant is affected by a diverse set of cellular stress conditions. Moreover, loss of both Rrp6 and Rex1 exonucleases does causes a block in cell growth under normal laboratory growth conditions (Costello et al, 2011; Peng et al, 2003; van Hoof et al, 2000b), indicating that either Rrp6 or Rex1 is required for one or more RNA processing or turnover pathways that are critical for cell growth. The exact nature of this Rrp6/Rex1-dependent pathway is currently unclear. One study suggests that one of these two proteins is required for the 3' end maturation of box C/D snoRNAs (Garland et al, 2013; Stead et al, 2007), although it is probable that these enzymes are also required for the processing or degradation of other transcripts. It is also unclear how Rex1 is uniquely able to compensate for the lack of Rrp6 activity, whereas the other DEDD family exoribonucleases that are closely related to Rex1 in sequence and enzymatic activity are not able to do so. One trivial explanation would be that Rex1 is physically associated with the exosome RNase complex. However, Rex1 has not been identified in any reported purification of the exosome complex or associated complex such as the TRAMP or Nrd1/Nab3/Sen1 complexes (Chlebowski et al, 2013; Steinmetz et al, 2000, Houseley and Tollervey, 2006; LaCava et al, 2005; Vanácová et al, 2005; Wyers et al, 2005; Mitchell et al, 1997). This suggests that Rex1 and Rrp6 can be targeted independently to their shared substrate(s). The underlying hypothesis of this project was that specific structural features of Rex1 (that are not present in other yeast DEDD exoribonucleases) enable the protein to act on RNA transcripts and to share these substrates with Rrp6. Therefore, a central aim of this project was to define the physical features of Rex1 (in addition to its catalytic domain) that are important for its ability to function in the cell, using appropriate genetic and biochemical assays. To this end, a set of *rex1* deletion mutants were generated by site-directed mutagenesis and the phentoypes of the resultant mutations were analysed.

Rex1 is known to function in the 3' end maturation of two well characterized substrates: 5S rRNA and tRNA-Arg, which is processed from the dicistronict RNA-

Arg/tRNA-Asp transcript. Notably, processing of neither of these RNAs is significantly affected in *rrp6Δ* mutants (Van Hoof, 2000; and Piper et al, 1983). This suggests these previously characterized Rex1 substrates are not the RNAs whose processing is critically dependent upon either Rex1 or Rrp6. A further aim of this study was to catalogue the diversity of cellular substrates that are processed or degraded by Rex1 and to address whether its substrate profile is altered in cells that lack Rrp6. To address this, yeast strains expressing HTP fusions of Rex1 were generated that either did or did not express Rrp6. These strains were then used to perform CRAC analyses (Granneman et al, 2009) to identify the cellular RNA substrates of Rex1 on a genome-wide scale.

The Rex1 homologous proteins RNase T and TREX are both homodimeric proteins and this structural arrangement is fundamental to the catalytic activity of the enzyme (Orebaugh et al, 2011; Zuo et al., 2007; Zuo and Deutscher, 2002; Mazur and Perrino, 1999; Li et al, 1996). It would therefore be anticipated that yeast Rex1 is also expressed as a dimer. The only biochemical purification of Rex1 reported to date suggests that the protein is monomeric (Frank et al, 1999). However, the protein was purified using buffers containing 2M NaCl, which could disrupt potential protein interactions. A final aim of this study was to address the physical properties of Rex1 isolated from yeast cells. The experimental approach taken was to generate strains expressing epitope-tagged Rex1 fusion proteins, confirm that the fusion protein is functional and to purify the protein from yeast cell lysates using a combination of affinity chromatography and ion exchange chromatography. The native molecular weight of the Rex1 fusion protein was estimated by a combination of size exclusion chromatography and velocity sedimentation centrifugation on both purifed protein preparations and on nonfractionated cell extracts. Furthermore, coimmunoprecipitation experiments were carried out on lysates from cells expressing two different Rex1 fusion proteins to address specifically whether Rex1 is expressed as a dimeric protein.

Chapter Two

Materials and Methods

1.1 Media

Concentrations of constituents are given as weight per volume (w/v) percentages. To prepare solid medium, Bactoagar was added to 2% final concentration before autoclaving. Appropriate nitrogenous bases and amino acids were added to yeast minimal medium preparations from 100 x stocks (see Table 2.3) prior to autoclaving. 5-FOA was dissolved in DMSO and filter-sterilised into warm autoclaved medium prior to pouring plates. Bases, amino acids and kanamycin were obtained from Sigma-Aldrich. Otherwise, unless stated, chemicals were obtained from`` Melford Laboratories.

Table 1 List of Media

LB (Lysogeny Broth)	0.5% yeast extract, 1% tryptone, 1% NaCl(Fisher).
YPD	1% Yeast Extract, 2% Peptone, 2% Glucose
Yeast Minimal Media	0.5% ammonium sulphate, 0.17% yeast nitrogen base, 2% glucose and appropriate nitrogenous bases and amino acids (see Table 2.3).
5'FOA Minimal Media	0.5% ammonium sulphate , 0.17% yeast nitrogen base, 2% glucose, 20mg/L adenine hemisulphate, 20mg/L arginine monohydrochloride, 20mg/Lhistidine monohydrochloride, 60mg/L leucine, 30mg/L lysine monohydrochloride, 20mg/L methionine, 50mg/L phenylalanine, 200mg/L threonine, 20mg/L tryptophan, 30mg/L tyrosine, 50mg/L uracil, 1g/L 5-fluoroortic acid.

Table 2 List of yeast and *E. coli* trains used in this study

Strain	Genotype	Source
DH5α *(E. coli)*	fhuA2Δ(argF-lacZ)U169 phoA glnV44 Φ80 Δ(lacZ)M15 gyrA96 recA1 relA1 endA1 thi-1 hsdR17	Stratagene
P596	*ade2 ade3 his3 leu2 trp1-1 ura3 can1-100? rrp47-Δ::kanMX4 rex1-Δ::kanMX4 + p265* (=pRS416[*RRP47*, ADE3])	Costello et al, 2011
P364	Mata *his3Δ1 leu2Δ0 met15Δ0 ura3Δ0*	BY4741. Euroscarf, The University of Frankfurt, Germany
P550	Mat *his3Δ1 leu2Δ1 lys2Δ0 ura3Δ0 rex1-Δ::kanMX4*	Y07293Euroscarf, The University of Frankfurt, Germany
P1022	*rex1-TAP::URA3*	Rebecca Jones, Mitchell lab
P1601	Mata*his3Δ1 leu2Δ0 met15Δ0 ura3Δ0 rrp6Δ::kanMX4 rex1-TAP::URA3*	this study
P1604	Mat *his3Δ1 leu2Δ1 lys2Δ0 ura3Δ0 rex1-Δ::kanMX4* *rrp47Δ::hphMX4* strain	this study
P1810	Mata*his3Δ1 leu2Δ0 met15Δ0 ura3Δ0 rex1-TAP::URA3*	this study
P2100	Mata *his3Δ1 leu2Δ0 met15Δ0 ura3Δ0 rex1-HTP::URA3*	this study
P2101	Mata *his3Δ1 leu2Δ0 met15Δ0 ura3Δ0 rex1-HTP::URA3 rrp6Δ::kanMX4*	this study

Table 3 List of Antibiotic/drug with their concentrations used in this study

Solutions of ampicillin sodium salt and kanamycin monosulphate were prepared as 1000 x stocks, stored at -20°C and added to autoclaved medium prior to pouring for solid plate medium or for selective growth in liquid medium**.**

Antibiotic	Abbreviation	Source	Stock	Preparation	Final Concentration
Ampicillin Sodium Salt	Amp	Melford Laboratories	1000 X in 50% ethanol	4 g in 50 ml 50% ethanol	80 µg/ml
Kanamycin A Monosulphate (from*S. kanamyceticus)*	Kan	Sigma-Aldrich	1000 X, aqueous solution	2.5 g in 50 ml sterile water	50 µg/ml

Table 4 Weights of bases and L-aminoacids used in this study to generate 100 X stocks.

Individual 100 X stock solutions were prepared using Millipore filtered water and stored at 20 °C. NaOH was added to a final concentration of 30 mM NaOH and 20 mM to dissolve tyrosine and adenine, respectively.

Amino Acid/Base	Abbreviation	Mass per litre (g) for 100 x stock	Final concentration (mg/litre)
Adenosine hemisulphate*	Ade	2	20
Arginine monohydrochloride	Arg	2	20
Histidine monohydrochhloride	His	2	20
Leucine	Leu	6	60
Lysine monohydrochloride	Lys	3	30
Methionine	Met	2	20
Phenyalanine	Phe	5	50
Threonine	Thr	20	200
Tryptophan	Trp	2	20
Tyrosine*	Tyr	3	30
Uracil	Ura	2	20

1.2 Buffers and solutions

In this study, water filtered through a Milli-Q 4 Bowl reagent grade water system (MP H2O)) was used to prepare all buffers and solutions. All buffers and solutions were autoclaved at 126 °C, 121 psi for 11 minutes. Buffer and solutions were filter-sterilized by passing through 0.2 µm Minisart filters (Sartorius Stedim).

Table 5 Buffers and solutions used in this study.

1 X TE Buffer	10mM Tris-HCl pH 8, 1mM EDTA pH 8,
1 X TBE	90mM Tris, 90mM Boric acid, 2 mMEDTA
1 X TGS	25mM Tris, 192mM Glycine, 0.1% SDS (w/v)
1 X TBS	10mM Tris-HCl pH 7.4, 150mM NaCl
1 X SSPE	9mM NaH_2PO_4, 150mM NaCl, 1mMEDTA, pH 7
6 X DNA Loading Dye	0.25% (w/v) bromophenol Blue, 0.25% (w/v) xylene cyanol30% (v/v) glycerol.
2 X Protein Loading Dye	160 mM Tris-HCl pH 6.8, 10% (v/v)β-mercaptoethanol, 2% (w/v) SDS, 10% (v/v) glycerol, 0.05% (w/v) bromophenol blue
2 X RNA Loading Dye	95% (v/v) formamide,20mM EDTA, 0.05% (w/v) bromophenol blue, 0.05% (w/v)xylene cyanol
Western Blot Transfer Buffer	12.5mM Tris, 96mM Glycine, 0.1%(w/v) SDS, 20% (v/v) methanol
TMN150 Lysis Buffer	10mM Tris-HCl pH 7.6, 150mM NaCl, 5mM $MgCl_2$
HEPES Extraction Buffer	50 mM HEPES-NaOH pH 7.4, 50 mM KCl, 5 mM $MgCl_2$, 10% (v/v) glycerol. Filter sterilised and stored at 4°C. PMSF was added to 2 mM final concentration prior to use.

GTC Mix	75mM Tris-HCl pH 8, 6.1M guanidinium thiocyanate,15mM EDTA pH 8.0,3% (v/v) sarkosyl, 1.5% (v/v) β-mercaptoethanol
NaAc Mix	100mM sodium acetate pH 5, 10mM Tris-HCl pH 8.0, 1mM EDTA pH 8.0
ECL Solution 1	100mM Tris- HCl pH 8.7, 400µM p-coumaric acid, 2.5mM Luminol.Stored at 4 °C
ECL Solution 2	100mM Tris HCl pH 8.7, 5.4mM H_2O_2. Stored at 4°C
Alkaline Lysis Solution I	25mM Tris-HCl pH 8.0, 50mM glucose, 10mM EDTA pH 8.0
Alkaline Lysis Solution II	0.2M NaOH, 1% (v/v) SDS
Alkaline Lysis Solution III	3M potassium acetate, 11.5% (v/v) acetic acid. Solution was pre-chilled onice prior to use.
DEPC-H_2O	Diethylpyrocarbonate (DEPC) was added to Millipore-filtered water to a concentration of 0.1% (v/v), mixed and left to stand overnight at room temperature. Excess DEPC was then degraded by autoclaving.
Northern Blot Stripping Buffer	0.1 X SSPE, 0.1% (v/v) SDS
50 X Denhardt's Solution	2% (w/v) polyvinylpyrrolidone, 2% (w/v) ficoll, 2% (w/v) BSA in DEPC-H_20. Stored at -80C for long term storage and -20C for short term storage
Oligo-Hybridisation Buffer	5 X Denhardt's Solution, 6 X SSPE, 0.2% (v/v) SDS in DEPC-H_2O.

LiT Buffer	10mM Tris-HCl pH 7.6,1mM EDTA pH 8.0, 100mM Lithium acetate pH7.5
LiT/PEG solution	A 1:1 (w/v) mixture of PEG 4000 and LiT buffer, microwaved to dissolve and filter-sterilised. Prepared fresh.
Western Blot Blocking Buffer	TBS containing 10% (w/v) skimmed milk powder.
Neutralisation Buffer	0.5M Tris-HCl pH 7.4, 1.5M NaCl.
Breaking Buffer	10mM Tris-HCl pH 8, 100mM NaCl, 1mM EDTA pH 8, 1% (v/v) SDS, 2% (v/v) Triton X-100
Alkaline Lysis Extraction Buffer	0.2M NaOH, 0.2% (v/v) β-mercaptoethanol. Prepared fresh.
TfbI Solution	100mM $RbCl_2$, 10mM $CaCl_2$, 50mM $MnCl_2$, 10mM KAc, 15% (v/v) glycerol. The pH was set to5.8 using acetic acid
TfbII Solution	10mM MOPS, 75mM $CaCl_2$, 10mM $RbCl_2$, 15% (v/v) glycerol. The pH was set to 6.5 using KOH

1.3 Oligonucleotides

Oligonucleotides were synthesized by Operon (Eurofins MWG Operon, Ebersberg, Germany) at a 10nmol scale and purchased in a desalted condition. Lyophilized oligonucleotides were resuspended in Millipore-filtered water to generate stock solutions at a concentration of 100µM. Working dilutions of 5µM were then made using Milipore-filtered water. Sequences are written in the 5' – 3' direction.

Table 6 Oligonucleotides used in this study.

Oligos	Sequence	Purpose	Location
o191	AAACTCGAGGAACTGACTACTGA	(+) PCR primer with *XhoI* site to amplify *RRP47* gene	upstream of the *RRP47* gene
o192	AAAGAGCTCAAACTTTCGCTGG	(-) PCR primer with *SacI* site to amplify *RRP47* gene	downstream of the *RRP47* gene
o261	AGAACTAGTTCCCTTAAG	(+) PCR primer with *SpeI* site to amplify *REX1* gene	upstream of the *REX1* gene
o264	GGTGAGCTCCAATGTG	(-) PCR primer with *SacI* site to amplify *REX1* gene	downstream of the *REX1* gene
o263	ATTGGTACCAACCATCTA	(-) PCR primer with *KpnI* site to amplify *REX1* gene	downstream of the *REX1* gene
o468	CTGGGATCCATGATACACGATGCAGG	(+) PCR primer with *BamHI* site to amplify *REX1* gene	upstream of the *REX1* gene
o560	AAACTCGAGGTATGATTGGTACC	(-) PCR primer with *KpnI* site to amplify *REX1* gene	downstream of the *REX1* gene
o559	AAAGGATCCGATGAGCTCTTGCAAA	(+) PCR primer with *BamHI* site to amplify *REX1* gene	upstream of the *REX1* gene

o869	CGCGAATTCAATGCAAGTAGAAGGGCC	(+) PCR primer with *EcoRI* site to amplify *REX1* gene	upstream of the *REX1* gene
o870	GAATTTGTTGTCTACTTTCG	(+) Primer to sequence *rex1-zz or rex1-TAP* gene	middle of the tag gene
o774	CGAAAGTAGACAACAAATTC	(-) Primer to sequence *rex1-zz or rex1-TAP* gene	middle of the tag gene
o884	CTGGATTCTGGAGACAC	(+) Primer to sequence *REX1* gene	middle of the *REX1* gene
o457	CAGTCTAGACTTCGAGATGAGCTTG	(+) PCR primer with *XbaI* site to amplify *RRP6* gene	upstream of the *RRP6* gene
o458	GCTGGGCCCACCTCAGTATTACAGC	(-) PCR primer with *EcoRI* site to amplify *RRP6* gene	downstream of the *RRP6* gene
o875	CACGATTCTGTCGAAGATGCAAGGGCTTGTCTTG	(+) SDM PCR primer to correct a single mutation in the catalytic domain of *REX1* gene	Catalytic domain of the *REX1* gene
o876	CAAGACAAGCCCTTGCATCTTCGACAGAATCGTG	(-) SDM PCR primer to correct a single mutation in the catalytic domain of *REX1* gene	Catalytic domain of the *REX1* gene
o959	CGGGGTGGTGTAGCATCCTTTACTGTAAAACGGATCCCCGGGTTAATTAA	(+) PCR primer used to amplify *13MYC* tag gene to generate rex1-13Myc by homologues recombination	upstream of the *13MYC* tag gene of p750
o960	AGGAAAAGTATTATGCATATATATATATATGAATTCGAGCTCGTTTAAAC	(-) PCR primer used to amplify *13MYC* tag gene to generate rex1-13Myc by homologues recombination	downstream of the *13MYC* tag gene of p750
o961	GGGAACCTGAAATAGTAGAAGCCAT	(+) PCR primer used to extend o959 primer to improve the	upstream of the o959 primer

	AAAGTTAGCCCGGGGTGGTGT	homologous recombination	sequence
o1069	ATTCCGAAGAAGAAGCGTAAAGTGGAC	(+) PCR primer with *XmaI* site to amplify *SV40NLS* gene	upstream of the *SV40NLS* gene
o1070	GTCCACTTTACGCTTCTTCTTCGGAAT	(-) PCR primer with *XmaI* site to amplify *SV40NLS* gene	downstream of the *SV40NLS* gene
o1037	AATTCATTGGGATCAAAGAAA	(REX1_NLS_1) A complementary primer to generate *REX1NLS* gene	N-terminal of the *REX1* gene
o1038	AGAAGGTTATCCAAGACTTCTGTACAAGAGGATGATCATACAAATGTGGT	(REX1_NLS_2) A complementary primer to generate *REX1NLS* gene	N-terminal of the *REX1* gene
o1039	ATCGGAAGTGAATAAGAATAAGAAGAAAAAAAAGGCATAAC	(REX1_NLS_3) A complementary primer to generate *REX1NLS* gene	N-terminal of the *REX1* gene
o1040	CCGGGTTATGCCTTTTTTTTCT	(REX1_NLS_4) A complementary primer to generate *REX1NLS* gene	N-terminal of the *REX1* gene
o1041	TCTTATTCTTATTCACTTCCGATACCACATTTGTATGATCATCCTCTTGT(	REX1_NLS_5) A complementary primer to generate *REX1NLS* gene	N-terminal of the *REX1* gene
o1042	ACAGAAGTCTTGGATAACCTTCTTTTCTTTGATCCCAATG	(REX1_NLS_6) A complementary primer to generate *REX1NLS* gene	N-terminal of the *REX1* gene

o1017	GAAGAAAAAAAAGGCAAGGCCTATG ACATGCACATTGCTAAAGTCTG	(+) SDM PCR primer with *StuI* site to generate *rex1-NLSΔ* gene	N-terminal of the *REX1* gene
o1018	CAGACTTTAGCAATGTGCATGTCATA GGCCTTGCCTTTTTTTTCTTC	(-) SDM PCR primer with *StuI* site to generate *rex1-NLSΔ* gene	N-terminal of the *REX1* gene
o1020	GAAGGGCCTGACACTAACTTCGTGAG TGATAGGCCTTTGGGATCAAAG	(+) SDM PCR primer with *StuI* site to generate *rex1-NLSΔ* gene	N-terminal of the *REX1* gene
o1021	CTTTGATCCCAAAGGCCTATCACTCAC GAAGTTAGTGTCAGGCCCTTC	(-) SDM PCR primer with *StuI* site to generate *rex1-NLSΔ* gene	N-terminal of the *REX1* gene
o993	TGTTGACTTTACCCATGGTGGCTCCCA CATCTTTGTCTGGATCGACTGCG	(+) PCR primer to amplify a catalytic domain of *REX2* gene	upstream of the catalytic domain of *REX2* gene
o994	ATGCTAACCCATTTAAGATTTTTAATT TCGTTTGAGCTATGCTCTCTTTG	(-) PCR primer to amplify a catalytic domain of *REX2* gene	downstream of the catalytic domain of *REX2* gene
o995	GACACCAATTTTGATACAGACTGGGT ACAAACTGTTGACTTTACCCATGG	(+) PCR primer to amplify a catalytic domain of *REX2* gene	Upstream of the catalytic domain of *REX2* gene
o996	TTGACTTTACCCATGGTGGCTCCCACA TCTTTTCTCTTGACTGTGAAATG	(+) PCR primer to amplify a catalytic domain of *REX3* gene	Upstream of the catalytic domain of *REX3* gene
o997	ATGCTAACCCATTTAAGATTTTTAATT	(-) PCR primer to amplify a catalytic domain of *REX3* gene	downstream of the catalytic

	TCGTAACGTCCATCGTTGCTA		domain of *REX3* gene
o989	GCGTAAACAGCCATGGCAGATATCGC GCAACACGATGAAGCCG REX1_NT_RV+	(+) SDM PCR primer with *EcoRV* site to insert *EcoRV* site into *zz* tag gene of p44 vector	N-terminal of the *REX1* gene
o990	CGGCTTCATCGTGTTGCGCGATATCT GCCATGGCTGTTTACGC	(-) SDM PCR primer with *EcoRV* site to insert *EcoRV* site into *zz* tag gene of p44 vector	upstream of the *REX1* gene
o897	CCAAGACTTCTGTACAAGAGGATGAT CATGCAAATGTGGTATCGG	(+) SDM PCR primer to generate a point base mutation (T34A) in *REX1* gene	N-terminal of the *REX1* gene
o898	CCGATACCACATTTGCATGATCATCCT CTTGTACAGAAGTCTTGG	(-) SDM PCR primer to generate a point base mutation (T34A) in *REX1* gene	N-terminal of the *REX1* gene
o899	CTGTTGGTGCCAAGAAAGCATTGCGA GAAGTAC	(+) SDM PCR primer to generate a point base mutation (T287A) in *REX1* gene	middle of the *REX1* gene
o900	GTACTTCTCGCAATGCTTTCTTGGCAC CAACAG	(-) SDM PCR primer to generate a point base mutation (T287A) in *REX1* gene	middle of the *REX1* gene
o901	TCCCACATCTTTGCACTAGCCTGTGAA ATGTGTCTTTCCGA	(+) SDM PCR primer to generate a point base mutation (D229A) in *REX1* gene	middle of the *REX1* gene
o902	TCGGAAAGACACATTTCACAGGCTAG	(-) SDM PCR primer to generate a point base mutation	middle of the *REX1* gene

	TGCAAAGATGTGGGA	(D229A) in *REX1* gene	
o903	GGGTACAGGCGACACAAGACCATAG AACAATCTTTCAACTG rex1 509X+	(+) SDM PCR primer to generate a point base mutation (W509X) in *REX1* gene	C-terminal of the *REX1* gene
o904	CAGTTGAAAGATTGTTCTATGGTCTTG TGTCGCCTGTACCC	(+) SDM PCR primer to generate a point base mutation (W509X) in *REX1* gene	C-terminal of the *REX1* gene
o905	CTCAATACTTGTTGCAGGCTGAAAAG AATTCTCCCAAATGGATTG rex1 246RI+	(+) SDM PCR primer to insert *EcoRI* site into *REX1* gene	N-terminal of the *REX1* gene
o906	CAATCCATTTGGGAGAATTCTTTTCAG CCTGCAACAAGTATTGAG	(-) SDM PCR primer to insert *EcoRI* site into *REX1* gene	N-terminal of the *REX1* gene
o907	GCAAACGATTACCCACTGAATTCTGG AGACACC	(+) SDM PCR primer to insert *EcoRI* site into *REX1* gene	N-terminal of the *REX1* gene
o908	GGTGTCTCCAGAATTCAGTGGGTAAT CGTTTGC	(-) SDM PCR primer to insert *EcoRI* site into *REX1* gene	N-terminal of the *REX1* gene
o909	GCCAGTTAATCCGTTGCGTCGACGAT GATTAGACATGGACCCATA	(+) SDM PCR primer to insert *SalI* site into *REX1* gene	C-terminal of the *REX1* gene
o910	TATGGGTCCATGTCTAATCATCGTCGA	(-) SDM PCR primer to insert *SalI* site into *REX1* gene	C-terminal of the *REX1* gene

	CGCAACGGATTAACTGGC		
O911	AAGGAAACTCCTTCGGTCGACGCGTC CATGGTTCTTC	(+) SDM PCR primer to insert *SalI* site into *REX1* gene	C-terminal of the *REX1* gene
O912	GAAGAACCATGGACGCGTCGACCGA AGGAGTTTCCTT	(-) SDM PCR primer to insert *SalI* site into *REX1* gene	C-terminal of the *REX1* gene
O236	GCGTTGTTCATCGATGC	Northern probe to detect 5.8S rRNA	complementary to B1S in 5.8S rRNA
O237	TGAGAAGGAAATGACGCT	Northern probe to detect 5.8S + 30nt rRNA	complementary to the 5.8S/ITS2 junction
O238	TCACTCAGACATCCTAGG	Northern probe to detect U14 snoRNA	complementary to the 5' end 108-126nt
O242	AAGGACCCAGAACTACCTTG	Northern probe to detect SCR1 RNA	complementary to the 5’ end 295-315nt

1.4 Plasmids

Table 7 List of plasmids used in this study

Plasmid	Description	Reference/Source
p44	pRS416 derivative bearing *URA3* marker containing the *RRP4* promoter upstream of a zz tag cassette. It uses to express of zz-N-terminal fusion proteins in yeast.	(Mitchell et al, 1996)
pRS314	Yeast/*E.coli* expression vector bearing *TRP1* marker uses to express a non-tagged yeast protein	(Sikorski and Hieter, 1989)
pRS313	Yeast/*E.coli* expression vector bearing *HIS3* marker uses to express a tagged or non-tagged yeast protein	(Sikorski and Hieter, 1989)
pRS415	Yeast/*E.coli* expression vector bearing *LEU2* marker uses to express a tagged or non-tagged yeast protein	(Sikorski and Hieter, 1989)
pRS425	Yeast/*E.coli* multi-copy expression vector bearing *LEU2* marker uses to express a tagged or non-tagged yeast protein	(Sikorski and Hieter, 1989)
p750	Yeast/*E.coli* expression vector. The *13Myc* tag of this vector was PCR amplified and used to generate *rex1-13Myc*.	Hetteme LAb
p727	Yeast/*E.coli* expression vector. The *GFP* tag of this vector was PCR amplified and used to generate *GFP-rex1.*	Hetteme LAb

p772	The genomic sequence of the *REX1* gene cloned into pRS314 as a *BamH*I/*Kpn*I fragment using primers o559 and o560.	This study
p752	The *13Myc* tag of p750 was PCR amplified using o959/0960 and cloned into p772 to generate *rex1-13Myc* by homologous recombination	This study
P659	The genomic sequence of the *REX1* gene cloned into p44 as an *EcoR*I/*Kpn*I fragment using primers o869 and o560 to generate *zz-rex1.*	This study
P674	*zz-rex1* gene was subcloned from p659 into pRS313 by homologous recombination using *Pvu*II.	This study
p675	*zz-rex1* gene was subcloned from p659 into pRS415 by homologous recombination using *Pvu*II.	This study
p679	Catalytic inactive mutant of *REX1* (*zz-rex1D229A*) generated by SDM on p675 using o901/o902	This study
p680	*zz-rex1W509X* generated by SDM on p675 using o903/o904	This study
p701	*zz-rex1Δ1-202* generated by SDM on p675 using o907/o908	This study
p706	*zz-rex1Δ1-82* generated by SDM on p675 using o905/o906	This study
p713	*zz-rex1Δ82-202* generated by sub cloning of *REX1-1-82* of p706 into p701 using *EcoR*I	This study
p716	*zz-rex1Δ428-456* generated by SDM on p675 as a *Sal*I fragment using o909/o910 and o911/o912	This study
p775	*GFP-rex1* generated through replacing *zz* tag gene of p674 into a *GFP* tag from p772 using *EcoR*V/*EcoR*I	This study
p804	*GFP-rex1Δ17-52* generated by SDM on p775 as a *Stu*I fragment using o1017/o1018 and o1020/1021	This study
p817	*GFP-rex117-52* generated through cloning of *rex117-52* which was generated by annealing 6 primers (o1037-o1042) containing *EcoR*I/*Sma*I into p775	This study
p823	Yeast expression vector (*mRFP-Nic96*) /URA3	This study

p819	Yeast expression vector (*mRFP-Nic96*) /TRP1	This study
P779	*GFP-rex1Δ1-202* generated through replacing *REX1* gene of p775 by a *rex1Δ1-202* of p701 using *EcoR*I/*Age*I	This study
P780	*GFP-rex1Δ1-82* generated through replacing *REX1* gene of p775 by a *rex1Δ1-82* of p706 using *EcoR*I/*Age*I	This study
P781	*GFP-rex1Δ428-456* generated through replacing *REX1* gene of p775 by a *rex1Δ1-82* of p716 using *EcoR*I/*Age*I	This study
P778	*GFP-rex1W509X* generated through replacing *REX1* gene of p775 by a *rex1W509X* of p680 using *EcoR*I/*Age*I	This study
P782	*GFP-rex1Δ82-202* generated through replacing *REX1* gene of p775 by a *rex1Δ82-202* of p713 using *EcoR*I/*Age*I	This study

1.5 Methods

1.5.1 Growth and Handling of *E. coli* and Yeast

Preparation of transformation-competent E. coli

A freshly saturated, starter culture of *E. coli (DH5α strain)* was prepared by inoculating a colony from an LB medium plate into 5ml of liquid LB medium and incubating the culture overnight at 37°C. The following day, the starter culture was inoculated into fresh LB medium to an OD_{595nm} of 0.1 and the cells were grown at 37°C until the spectrophotometric absorbance of the culture achieved an OD_{595nm} of 0.48. The cells were harvested by centrifugation at 3100*g* for 5 minutes in a chilled centrifuge. After removing the medium, the pellet was resuspended in 40ml ice cold TfbI buffer (see Table 7) and left on ice for 10 minutes. The cells were recovered by centrifugation and resuspended in 5ml ice cold TfbII buffer and was left on ice for 10 minutes. Aliquots (50-100µl) were transferred into chilled microfuge tubes, frozen in liquid nitrogen and stored at -80°C. To determine the level of competency for a batch of cells prepared as described above, a transformation reaction was carried out (see below) using an aliquot of a standard plasmid preparation of known concentration (1µl of a 0.1ng/µl solution of pUC18 DNA). The transformation efficiency was then determined by calculating the number of colonies obtained per ng plasmid DNA. Transformation efficiencies of more than 100 CFU/ng pUC18 DNA was taken as being indicative of a sufficient degree of competency to use for transformation for routine cloning applications.

Plasmid transformation of competent cells

Aliquots of competent bacterial cells were taken from deep freezer (-80◦C) and thawed on ice. 50 to 500ng plasmid DNA were added to the thawed cells and the mixture was left on ice for half an hour before subjecting to heat shock at42 ◦C for 1.5 minutes. The cells were then returned immediately on ice and incubated for a further minute. 800-1000µlof LB medium (without antibiotic) was added to the bacteria and the cells were incubated at 37 ◦C for 60 minutes with mild agitation.

The cells were then pelleted using a microfuge, resuspended in 100µl LB, bacteria and spread out on selective growth medium using autoclaved ColiRoller glass beads (Novagen). The plates were incubated at 37◦C overnight.

E.coli inoculation and propagation

A single colony of *E.coli* from a selective growth medium plate was inoculated into 5ml LB broth containing the appropriate antibiotic in glass culture tubes and incubated overnight at 37 ◦C with agitation. These starter cultures provided sufficient material for plasmid minipreps; for larger plasmid preps of for recombinant protein expression experiments, a small volume of the starter culture was inoculated into an appropriate larger volume of selective growth medium.

Yeast growth assays

A single yeast colony was inoculated into 5ml of selective liquid growth medium and incubated overnight at 30°C. 50ml of pre-warmed culture medium was then inoculated with the overnight culture to obtain an optical density at 600nm of 0.05 AU. The cells were grown up through incubation at 30°C and the increase in OD_{600nm} was determined spectrophotometrically at regular time intervals and followed until a optical density of 1 AU was achieved.

Replica plating of yeast

Replica plating of yeast strains was used in this study to test their ability to grow on different solids elective growth medium, for example medium lacking a specific amino acid or containing 5-FOA. A master plate was initially generated on permissive YPD medium by patching the yeast strains under investigation in an ordered array and allowing them to grow at 30°C for 1-2 days. A non-symmetrical grid patterns to allow easy subsequent identification of strains showing the appropriate growth characteristics. Cells on the master plate were then impressed into sterile, approximately $10cm^2$ squares of velveteen that were stretched tightly over an aluminium block to provide a level surface. Growth plates were then

reiteratively pressed onto the velveteen squares to print the cells onto a range of selective growth media. These plates were subsequently incubated at 30°C for 2-3 days to determine the growth phenotypes of the yeast strains.

Spot growth assays

The growth characteristics of yeast strains were also compared using spot growth assays. This assay allows the comparison of the relative growth of different yeast strains on solid medium under different conditions.

5ml of freshly saturated cultures were prepared under selective growth conditions. The optical density of each culture was measured at 600nm and normalized with each other by dilution of the cultures with fresh medium. 10 fold serial dilutions of each strain were then generated using selective growth medium and 4ul aliquots of each dilution were spotted onto plates containing either selective or permissive medium in an ordered array. The plates were incubated for 2-4 days to allow visualization of differential growth properties, typically at 30°C.

Mating yeast

Freshly growing colonies of haploid *S. cerevisiae* strains of opposite type were patched together on an YPD plate and incubated at 30°C overnight. Resultant diploid cells were isolated by streaking the mixed cell population on appropriate selective growth medium, followed by incubation for 2-3 days at 30°C.

1.5.2 Recombinant DNA Techniques

Ethanol precipitation of DNA

Ethanol precipitation of DNA was routinely performed to concentrate samples, desalt enzymatic restriction digestion mixtures and to purify DNA from other material such as primers and nucleotides following PCR or organic solvents following phenol/chloroform extractions. Typically, 3M NaAc pH 5 was added to a final concentration of 300mM and the DNA was precipitated by the addition of two volumes of 100% ethanol, followed by incubation at -20°C for at least one hour. The DNA was recovered by centrifugation at 16,300*g* for 20 minutes and the pellet

was washed with ice cold 70% (v/v) ethanol to remove traces of salt or organic solvents. After washing, the pellet was briefly centrifuged for 5 minutes at 16,300g, the liquid supernatant was removed and the pellet was air-dried at room temperature by leaving the microfuge tube to stand with the lid open for 10 minutes on the bench. The pellet was then dissolved in Millipore-filtered water or TE buffer for further processing.

Agarose gel electrophoresis

Agarose gel electrophoresis was routinely performed using 1% (w/v) agarose (Geneflow) in0.5 x TBE buffer. The agarose suspension was melted using a microwave and, when completely dissolved, ethidium bromide was added to a final concentration of 100ng/ml. The gel mix was poured into an electrophoresis gel casting mould with a positioned comb of the appropriate number and size of wells. 10cm long gels (BioRad mini sub gel) were routinely run with combs containing 6mm wide teeth, which allow a maximum of approximately 40µl of sample to be loaded in each lane. DNA samples and a standard range of molecular weight markers of known quantity (GeneRuler 1kb ladder, Thermo Scientific, 0.5µg) samples were added into different wells after mixing with 6x DNA loading buffer. Electrophoresis was performed using 0.5 X TBE running buffer at 100 volts until the bromophenol blue dye had migrated approximately three quaters of the length of the gel. DNA was visualised by fluorescence and images were captured using a CCD camera, using a G-box imaging system (Syngene, Synoptics, Cambridge, UK).

Purification of DNA fragments from agarose gels

Visualised bands of DNA were cut out of agarose gels using a clean scalpel blade and transferred into a microfuge tube. The tube containing the agarose gel slice was weighed and the mass of the gel slice determined, assuming the microfuge tube weighed 1g.The density of the gel slice was taken to be 1g/ml. DNA was recovered from the gel slice using E.Z.N.A® gel extraction kits (Omega-biotek), according to the manufacturer's instructions. Depending on the downsteam application, DNA was eluted from the spin column with 30-50µl elution buffer. For

maximal recovery, a second elution step was performed. The quantity of the recovered DNA was assessed by analysinga 1µl aliquotby agarose gel electrophoresis.

Alkaline lysis plasmid extraction from *E.coli*

The DNA was extracted by this method according the principles originally described by Barenboim and Doly (Sambrook and Russell, 2006).1.5ml of an overnight, saturated *E. coli* culture was added into amicrofuge tube and centrifuged at 13,000 x_g for 1 minute. The supernatant was removed and the pellet was re-suspended in 100 µl alkaline lysis solution I (see table 7 for the composition of buffers used). 200ul of solution II was added, mixed by inversion and left on ice for 5 minutes. 150ul of pre-chilled solution III was added and the contents were mixed again by inversion. The tubes were incubated on ice for 5 minutes and then centrifuged for 10 minutes at 13,000 x_g. The supernatant containing the plasmid DNA was transferred into a fresh microfuge tube and an equal volume of phenol/chloroform was added. The contents of the tube were vortexed briefly and the aqueous and organic phases were then separated by centrifugation for 5 minutes at 13,000 x_g. The upper, aqueous phase was transferred to a fresh microfuge tube and nucleic acids were precipitated by the addition of two volumes of pre-chilled 100% ethanol. The mixtures were incubated at room temperature for 10 minutes to ensure efficient precipitation before centrifugation for 20 minutes. The pelleted material was washed by addition of pre-chilled 70% ethanol, centrifugation for 5 minutes and the removal of the supernatant. The pellet was left to air-dry for 5 minutes and then resuspended in 20µl H_2O containing 50 ng/µl RNase A.

Plasmid extraction from *E.coli* using spin columns

Plasmid was isolated from bacterial cells using commercial spin column kits (E.Z.N.A. Plasmid minikit I, Omega bio-tek) according to the manufacturer's instructions (Maniatis, 1982). Briefly, the cells were lysed and the protein and SDS

precipitated as above but the solution I contained RNase A. Instead of performing a phenol/chloroform extraction, the neutralized cell lysate was passed through a spin column by centrifugation at 13,000 g for 1 minute. Material retained on the column was washed with 500 µl HB buffer followed by 700 µl of DNA wash buffer before a final extended centrifugation to remove any residual wash buffer. The column was left open to stand on the bench for five minutes to allow residual ethanol to evaporate. Retained DNA was incubated for 5 minutes in 30-50µl elution buffer and recovered by centrifugation at 13,000 x g for 1 minute. The elution step was repeated to maximize the plasmid yield. The recovery of DNA was assessed by analysing1µl of the eluted DNA by agarose gel electrophoresis.

Polymerase chain reaction (PCR)

Recombinant or genomic DNA sequences were amplified by PCR, using *Taq* DNA polymerase (GoTaq®, Promega). PCR was performed using a Cleaver TC32/80 (Cleaver Scientific LTD., Warwickshire, UK) or a Techne TC312 (Techne., Cambridge, UK) thermocycler. Optimal annealing temperatures for a given set of DNA primers were established empirically. It was observed that the best yield of amplicon was often achieved by performing the annealing step at two temperatures, involving an initial phase at 45°C followed by a second phase at 50°C.

A typical 25µl PCR mixture contained 1 x GoTaq buffer, 2.5µM $MgCl_2$, 200µMof each dNTP, 0.1µM of each DNA oligonucleotide primer, 50-100ng of DNA template and 2.5 units of GoTaq DNA polymerase. Reactions were routinely performed by denaturation of the template at 95 °C for 1 minute, followed by 30 cycles comprising a denaturation step at 95°C for 1 minute, an annealing step at 45°C for 1 minute (followed in some circumstances by a further incubation at 50°C for 1 minute) and an extension period at 72°C of 1 min/kb. After 30 cycles, the mixture was further incubated at 72°C for 5 minutes to ensure optimal completion of the extension reactions. 1-5µl of the PCR product was resolved through an agarose gel to assess the yield and homogeneity of the product.

Site-Directed Mutagenesis (SDM)

Site-directed mutagenesis (SDM) was carried out using a commercial kit (Quikchange^{TM} Site Directed Mutagenesis I Kit, Stratagene) and performed with minor modifications to the manufacturer's instructions. Reactions were carried out in 25µl volumes to increase the number of reactions possible per kit, and 10µl aliquots of the *Dpn*I digests were transformed into aliquots of competent cells prepared in the laboratory. PCR mixtures comprised 1 x reaction buffer, 50-100ng plasmid DNA template, 0.2µMof each primer, 0.5µl of the proprietary dNTP solution and 1.25 units of *PfuTurbo* DNA polymerase. The SDM PCR Thermocycler programme consisted of a denaturation step at 95°C for 30 seconds, followed by 18 cycles involving a denaturation step at 95°C for 30 seconds, an annealing step at 55°C for 1 minute and an extension period at 68°C for 12 minutes. The mixture was subsequently treated to incubation at 68°C for 10 minutes.

Following thermocycling reactions, mixtures were incubated with 1µl Dpn1 enzyme (20 U) at 37 °C for one hour and an aliquot of the digested PCR mixtures were transformed into DH5α *E. coli* cells.

Restriction digests of DNA

Restriction enzymes (New England Biolabs) were used to cut recombinant plasmid DNA to obtain suitable ends with compatible ends that can be used in ligation and cloning reactions. The appropriate NEB reaction buffer/buffers was/were selected that provides maximal enzyme activity. A typical 50µl restriction enzyme mixture comprised of 1 x appropriate NEB buffer, 100 µg/ml N-acetylated BSA, 0.1-5µg of recombinant DNA (plasmid or PCR amplicon), and 5-10 units of restriction enzyme. Mixtures were incubated either at 37◦C for 2 hours or at room temperature overnight. Aliquots of the digested mixtures were analysed by agarose gel electrophoresis and specific DNA fragments were purified from the mixtures using preparative agarose gels, if required.

Alkaline phosphatase digestion of DNA

To minimise the self-ligation of restriction digested vector DNA fragments during cloning reactions, 5' phosphate groups were removed by treatment with either Calf-Intestinal Phosphatase (Roche) or the heat labile shrimp alkaline phosphatase (New England BioLAbs).

After restriction digestion,1 tenth of the volume of 10 x CIP buffer and1 U CIP (1U/µl) was added to the vector DNA and the mixture was incubated for one hour at 37°C, or 30 minutes in the case of the Artic shrimp alkaline phosphatase. CIP-treated samples were diluted fourfold using Millipore treated water and 3M NaAc pH 5.0 was added to a final concentration of 300mM. The mixture was extracted with an equal volume of phenol/chloroform by vortexing briefly and then centrifuged at 16,300*g* for 5 minutes. The aqueous phase was transferred in to a new microfuge tube and the DNA was ethanol precipitated. The washed DNA pellet was dissolved in 50 µl 1X TE buffer. Samples treated with artic shrimp alkaline phosphatase were incubated for 10 minutes at 65°C to inactivate the enzyme. Dephosphorylated DNA samples were then purified by agarose gel electrophoresis.

Klenow fragment treatment of DNA

For blunt end ligation of DNA restriction fragments, 5' single stranded overhangs were filled in by treatment with the Klenow fragment of *E. coli* DNA polymerase I. After adding dNTPs to the restriction enzyme digest mixture to a final concentration of 200µM, 10U of Klenow fragment (Fermentas) were added and the mixture was incubated for 10 minutes at 37°C. The Klenow fragment was denatured by incubation of the mixture at 65°C for 5 minutes. The DNA fragment was then purified by agarose gel electrophoresis.

Ligation of DNA fragments

To generate new recombinant DNA constructs, DNA restriction fragments and digested plasmids were incubated together with DNA ligase in the presence of ATP.100-500ng of compatible DNA fragments were incubated together in 20µl

reaction volumes containing5 units of DNA ligase at 15°C overnight, using a thermocycler. The yield of purified insert and vector DNA fragments was assessed by agarose gel electrophoresis and the fragments were combined at a ratio of approximately 2:1. A further 5units of T4 ligase was added the following morning and the mixtures were incubated for a further 6 hours. A 5-10µl aliquot of the ligation mixtures were then transformed into bacterial cells.

1.5.3 Genetic manipulation of Yeast

Yeast transformation for homologous recombination

Yeast transformations were carried out by the lithium acetate method (Gietz et al., 1992). A freshly grown, saturated culture of the appropriate yeast strain in YPD medium was diluted 1:25 into 50ml YPD medium and the culture was incubated at 30°C until the absorbance reached an OD_{600nm} of 0.5.The cells were harvested by centrifugation at 4000g for 5 minutes and once with TE buffer and then with LiT buffer. The cell pellet was resuspended in 500µl LiT buffer and 100µl aliquots were added to microfuge tubes containing1-2µg DNA and 5µl herring sperm carrier DNA (10mg/ml, Roche). 300 µl of LiT buffer containing 40% (w/v) PEG4000 was added and the mixtures were incubated at room temperature for 30 minutes. 50µl DMSO (Sigma Aldrich) was then added and the mixture was incubated at 42°C in a water bath for 15 minutes and then placed on to ice for 1 minute. After the heat shock treatment, the cells were pelleted at 4000g for 5 minutes, washed in 1 X TE buffer and plated onto selective solid growth medium using ColiRoller beads (Novagen). Transformants were isolated by growth at 30°C for 3-4 days.

Transformation of plasmids into yeast

Recombinant plasmids were introduced into yeast using a colony transformation protocol (Gietz et al., 1992). Cells were streaked out on solid YPD medium and incubated for 2-3 days until small colonies (that predominantly contain dividing cells) were clearly visible. Several colonies were taken using an inoculating loop,

resuspended in 1ml Millipore filtered water and centrifuged at 13,000g for 1 minute .The cells were washed two times , firstly with 1ml 1 X TE buffer and secondly with 1ml 1 X LiT buffer. The cells were resuspended in 1 X LiT buffer and 50µl aliquots were used per transformation. The resuspendend cells were added to mirofuge tubes containing 1µl plasmid miniprep DNA and 5µl herring sperm carrier DNA (10 mg/ml, Roche). Two volumes of LiT buffer containing 40% (w/v) PEG 4000 were added and the mixtures were incubated at room temperature for 30 minutes. After adding 50µl DMSO, the cells were heat shocked at 42 °C for 15 minutes, washed with TE buffer and plated on to selective yeast solid growth medium. The plats were incubated at 30°C for 3-4 days before colonies of yeast transformants were visible.

Plasmid recovery from yeast

The high efficiency of homologous recombination in yeast was exploited for cloning purposes where insert and vector fragments could be designed to have a significant sequence overlap. The resultant recombinant DNA episomal plasmids were recovered from yeast transformants using a commercial kit (E.Z.N.A® Yeast Plasmid kit, Omega bio-tek), according to the manufacturer's instructions. For this purpose, yeast cells containing a target plasmid were inoculated in to 5ml selective growth medium and incubated overnight at 30°C. Cells were harvested from 3ml of saturated culture harvested by centrifugation at 3,200*g* for 5 minutes. The harvested cells were digested with lyticase to remove the cell wall and then disrupted by vortexing in the presence of glass beads. Plasmid DNA was extracted by alkaline lysis and purified using proprietary HiBind spin columns. The retained DNA was eluted from the column matrix using 30µl elution buffer (10mM Tris pH 8.5). An aliquot of the recovered plasmid was then transformed into DH5α *E. coli* cells and individual colonies were isolated on appropriate selective solid growth medium.

Preparation of yeast genomic DNA

Genomic DNA preparations were made to validate the genotype of yeast strains that were generated by homologous recombination and to provide templates for the amplification of yeast DNA sequences. Genmic DNA was prepared from approximately 10ml of saturated yeast cultures grown up in YPD medium. Yeast cells were harvested by centrifugation at 13,000g for 5 minutes and washed in 5ml TE buffer to remove any remaining culture medium. The cell pellet was ressupended in 200µl cell breaking buffer and the mixture was vortexed for 5 minutes after addition of 300µl glass beads (425-600µm, Sigma) and one volume of phenol/chloroform. One volume of TE buffer was then added and the mixture was briefly vortexed and centrifuged for 5 minutes at 4,000g. The upper aqueous layer was carefully transferred into a clean microfuge tube and two volumes of cold 100% ethanol were added. The mixture was incubated on ice for 20 minutes and the precipitated DNA was recovered by centrifugation at 4,000g for 10 minutes. The pellet was washed with cold 70% ethanol to remove salts and traces of organic solvents, and the microfuge tube was left at room temperature with the lid open for 10 minutes to air-dry the pellet. Finally, the genomic DNA was re-suspended in 95µl dH_2O or TE buffer and 5µl RNAse A (1mg/ml) was added. A 1µl aliquot of the recovered DNA was analysed by agarose gel electrophoresis to estimate the concentration of the sample. Alternatively, the spectrophotometric absorbance was measured at 260nm using a Nanodrop spectrophotometer (Nanodrop Lite, Thermo Scientific).

Colony PCR on yeast

Colony PCR was performed on yeast to validate the genotype of strains generated through homologous recombination as a rapid alternative to preparing yeast genomic DNA. In this case, PCR reactions were carried out directly on freshly growing yeast colonies that were collected from solid growth media. Single colonies were resuspendedin the PCR reaction mixture and heated at 95°C for 10 minutes to lyse the cells, prior to a normal PCR run. .PCR was carried out using the two stage annealing cycle mentioned above. Cellular debris was pelleted by

centrifugation at 16,300g for 2 minutes and the amplified DNA fragments were purified from excess primers, nucleotides and cellular contaminants using a commercial PCR cleanup kit (E.Z.N.A. Cycle Pure kit, Omega-biotek), according to the manufacturer's instructions.

1.5.4 Protein Analyses

SDS-PAGE analyses

SDS-PAGE was carried out according to the standard laboratory method (Shapiro *et al*, 1967). A 10% resolving gel solution was prepared by mixing 3.333ml 30% Acrylamide (37.5:1 acrylamide/bis-acrylamide, Protogel Geneflow), 4.334ml H_20, 2.8ml 1M Tris pH 8.7,100µl 10% ammonium persulphate solution (APS) and 100µl 10% SDS. Polymerisation was initiated by the addition of 10µl TEMED. After pouring into the SDS-PAGE gel mould, the gel solution was overlaid with 100µl of isopropanol to ensure a flat surface and allowed to set. After polymerisation, the surface of the gel was rinsed with H_20 and the stacking gel was added. The stacking gel was prepared by mixing 467µl 30% acrylamide solution, 350µl 1M Tris pH 6.8, 2.118ml H_20, 30µl APS and 30 µl 10% SDS. 5µl TEMED was added to polymerised the gel solution and the stacking gel was poured after setting an appropriate comb within the gel mould. Protein samples were loaded on to the gel after mixing with 2x SDS_PAGE loading buffer and heat denaturation by incubation at 95 °C for 5 minutes.1X TGS buffer was used as an electrophoresis buffer. Electrophoresis was routinely carried out using the Mini-Protean cell electrophoresis system (BioRad).The gel was run at 75V until the bromophenol dye had entered the resolving gel, after which the voltage was increased to 100V. Electrophoresis was continued until the dye had nearly reached the bottom of the resolving gel.

Staining of SDS-PAGE gels

Proteins resolved by electrophoresis through SDS-PAGE gels were visualized by staining with a proprietary form of a colloidal Coomassie Blue stain (InstantBlue, Expedion), which provides a sensitive detection method for proteins (Neuhoff et al.

1988). After staining, gels were briefly rinsed in Millipore-filtered water and documented usinga G:Box gel documentation system fits with GeneSnap software (SynGene).

Western Blotting

In order to analyse the expression of proteins using specific antibodies, the proteins resolved by SDS-PAGE were transferred onto nitrocellulose membranes (Amersham Protran, GE Healthcare). A sandwich cast was made by putting the gel on to the membrane, in between two or three sheets of Whatman 3M paper that were cut to an appropriate size (generally, 10cm x10cm squares). Transfer was performed overnight at 15 volts in 1X Transfer buffer, using a HSI, TE Series Tran-sphor Electrophoresis Unit (HSI, Hoefer Scientific Instruments, San Francisco, USA). To verify efficient transfer of protein from the SDS-APGE gel to the membrane, the membrane was washed in TBS buffer and the transferred protein wasvisualised by reversible staining with Ponceau S solution (Sigma Aldrich). After visualisation of the protein, the ponceau S stain was removed from the blot by repeated washing with 1 x TBS buffer. The blot was then blocked to prevent nonspecific protein binding by incubation in TBS buffer containing 5% milk. The blocking solution was then removed by washing in 1 x TBSand the membrane was incubated in 1 x TBS buffer containing the primary antibody at an appropriate dilution. Antibody incubations were performed with gentle mixing on a slowly rotating platform shaker at room temperature for 1-2 hours. Subsequently, the primary antibody was removed by washing the membrane three times for 5 minutes and the membrane was incubated with TBS buffer containing an appropriate dilution of the horseradish peroxidase (HRP) coupled secondary antibody. After a further incubation for 1 hour, the membrane was washed three times with TBS, as described above. The antibody/protein complexes were visualised by enhanced chemiluminescence (ECL), using reagents prepared in the laboratory. The chemiluminescence signal was detected using a G box Gel documentation system

equipped with a CCD camera and GeneSnap software (SynGene, Synoptics, Cambridge, UK).

Preparation of yeast cell extracts under denaturing conditions using SDS-PAGE loading buffer

Yeast strains were inoculated into 20ml YPD medium and incubated until the cell density achieved an optical density of 0.5-1.0 OD_{600nm}/ml. 10 OD_{600} cells were harvested by centrifugation at 4000 rpm for 5 minutes, resuspended in 1ml YPD medium and transferred to a microfuge tube, and then recentrifuged at 4000 rpm for 1 minute. The cells were resuspended in 100 ul of breaking buffer (160mM Tris-HCl pH 6.8, 2% SDS), and lysed by repeatedly (5 times) vortexing in the presence of approximately 100µl glass beads for 1 minute, followed by heating at 95 °C for 1 minute. Non-lysed cells and debris were pelleted by centrifugation at 13,000 x g for 5 minutes; the lysate was transferred to a new microfuge tube and stored at -20 °C.

Preparation of yeast cell extracts under denaturing conditions using alkaline lysis

The method is carried out according to the protocol of Motley et al. (Motley et al., 2012) and it's originally described in (Von der Haar, 2007). Yeast cultures were grown in log phase until they approached 1 OD_{600}/ml. 10 OD_{600} of yeast cells were collected by centrifugation. The cell pellet was resuspended in 500µl freshly prepared, ice-cold alkaline lysis solution (Table 7) and the mixture was incubated for 10 minutes on ice. 100µl of 30% TCA was added and the mixture was incubated on ice for a further 10 minutes. Precipitated protein was recovered by centrifugationat 13,000 x g in a chilled centrifuge and the pellet was re-suspended in 10µl of Tris buffer pH 9.4. Finally, the sample was made up to 100µl in 1 x SDS-PAGE gel loading buffer and heated at 90 for 5 minutes. $1OD_{600}$ equivalent (the amount of protein derived from $1OD_{600}$ of cells) (10µl) was resolved by SDS-PAGE.

Preparation of yeast cell Lysates under native conditions

Yeast cell pellets were resuspended in TMN150 or HEPES extraction buffer, using 2ml of buffer per litre of cell culture. PMSF was added to a final concentration of 0.5mM and the cells were lysed by vortexing in the presence of an equal volume of glass beads (425-600nm, Sigma Aldrich). The cells were vortexed for 10 cycles of 30 seconds, with a 1 minute period on ice between each cycle. Cell debris was removed by centrifugation at 3200g for 5 minutes. The cell lysate was then transferred to a fresh microfuge tube and clarified by centrifugation for 30 minutes at 15,000g in a cooled centrifuge.

Purification of tagged proteins from yeast

The versatile TAP tag (Nilsson et al, 1987) and zz tag (Mitchell et al, 1996; 1997) provide very useful tools that can be used for the physical characterization of specific individual proteins within complex mixtures of proteins such as whole cell lysates, for example through glycerol gradient centrifugation or size exclusion chromatography, or by affinity chromatography and "pull-down" analyses. For pulldowns on cell lysates expressing TAP-tagged or zz-tagged Rex1, 50µl of lgG Sepharose beads (GE Healthcare) were equilibriated with TMN150 buffer in a Poly-prep chromatography column (Bio-Rad). Clarified yeast lysate containing TAP-tagged or zz-tagged Rex1 was passed through the washed beads 10 to 15 times. The beads were then washed thoroughly with TMN150 buffer. Protein that had remained bound to the beads was eluted by adding 2 x SDS-PAGE loading buffer and heating to 95°C. The purified protein was then analysed by SDS-PAGE and western blotting was used to analyze purified protein.

Glycerol gradient ultracentrifugation

Clarified yeast cell lysates prepared in TMN150 buffer were subjected to ultracentrifugation analyses through 5-20% glycerol gradients, which were determined empirically to give the optimal resolution of the molecular weight marker proteins. . Strains expressing wild-type and Rex1 mutant proteins were grown up in 400ml minimal selective medium to an OD_{600} of 1-1.5. The cells were

harvested by centrifugation at 3,200*g* for 5 minutes, washed in 5ml of 1X TE buffer then stored at -80°C. Yeast cell lysates were prepared as described above.

Glycerol gradients were prepared using a Beckman Model 385 former (Beckman-Coulter, Beckman Coulter UK LTD, High Wycombe, UK). The front chamber was washed one time with water and one time with TMN150 buffer containing 5% glycerol. Then, 6ml TMN150 buffer containing 5% glycerol was loaded into the front chamber and 6ml of TN150 buffer containing 20% glycerol was loaded into the rear chamber. The connecting channel was opened to allow mixing of the solutions, the outlet tube was opened and the gradients were poured into 12ml Beckman SW41 ultracentrifuge tubes by underlaying. Each poured gradient was weighed using a top pan balance and their weights were normalized by adding additional TMN150 buffer containing 5% glycerol, as necessary. A 400µl aliquot of clarified lysate from a wild-type or mutant strain was on to the surface of the gradient using the inside surface of the gradient tube to apply the solution steadily.

Centrifuge runs were performed using an SW41 rotor in a Beckman-Optimer LE-80X ultracentrifuge for 24 hours at 36000 rpm and 4°C. After ultracentrifugation, 18 fractions of 680µl were collected manually from the top to the bottom of each glycerol gradient. Gradient fractions were analysed by SDS-PAGE and the distribution of proteins through the gradients was visualized by colloidal coomassie staining of the gels (Neuhoff et al, 1985), using Instant Blue (Expedion) or by western blot analyses. Typically for western analyses the signal obtained was weak and the protein within the fractions was therefore concentrated by precipitation with 5% TCA on ice for 30 minutes. The precipitated protein was pelleted by centrifugation at 16,300*g* for 20 minutes, washed with 1ml acetone, air-dried and resuspended in Tris-HCl pH 9.4 before being diluted to 100µl with SDS-PAGE loading dye.

In order to directly map the sedimentation profile of TAP-tagged Rex1 onto that of the molecular weight markers, the Rex1-TAP protein was initially purified by ion exchange chromatography using SP-Sepharose beads and then mixed with the set of sedimentation coefficient protein standards before resolution of the mixture by ultracentrifugation. Coomassie staining and western analyses were performed on

the same fractions to directly compare the profile of Rex1 with those of the protein standards. The sedimentation volume at which the maximum peak height was obtained for each protein was plotted against the values of the Stokes radius to empirically determine the S value of Rex1.

Size exclusion chromatography

Size exclusion chromatography was carried out using a high resolution Superdex 200 12ml column (GE Healthcare). The column was first equilibrated with HEPES cell extraction buffer overnight. Whole cell extract from a strain expressing the Rex1-TAP fusion protein was partially purified on SP sepharose beads and the eluate fraction containing Rex1-TAP was concentrated two-fold using a centrifugation filtration unit with a low molecular weight cut off. Samples were centrifuged for 30 minutes at 13,000g. A 200µl aliquot of the partialy purified protein was loaded on to the Superdex column. Chromatography was performed with a flow rate of 500µl/minute and fractions were collected every minute for one hour. A 100µl aliquot of each sample was denatured by heating at 95°C for 5 minutes in 1 X SDS-PAGE loading buffer. 50µlof each aliquot was resolved by SDS-PAGE and analysed by western blotting, using the PAP antibody complex. Characterised proteinstandards (BSA, ADH, BSA, Oval Albumin, and Lysosyme) were analysed under the same conditions and their elution profiles were analysed by SDS-PAGE and colloidal coomassie blue staining of the resolved proteins. The elution volume of each protein was determined by determining the maximal signal concentration for each protein on either western blots or SDS-PAGE gels, using ImageJ64 software. The Stoke's radius of the Rex1-TAP protein was determined by comparing its elution volume to those of the standard proteins of known Stokes radii.

Determination of the native molecular weight of Rex1-TAP

The native molecular weight of Rex1-TAPwas calculated using the equation:

$M = 4{,}205\ SRs$ (Siegel & Monte, 1966; Erikson, 2009)

Where *M* is the mass in daltons, *S* is the sedimentation coefficient in Svedberg units and *Rs* is the Stoke's radius in nanometers. This equation assumes a partial specific volume of 0.73 ml/g, which is typical for protein.

Co-immunoprecipitation (Co-IP) assays on Rex1 proteins.

To determine whether Rex1 is expressed in yeast as a homodimer, co-immunoprecipitation (co-ip) or "pull-down" assays were performed on lysates from strains expressing two differentially tagged Rex1 proteins. Cells expressing both zz-Rex1 and Rex1-13Myc fusion proteins were grown in appropriate selective medium until the optical density of the culture at 600nm reached 1-2 AU. The cells were harvested by centrifugation at 3600g for 5 minutes and lysed using HEPES cell extraction buffer. Clarified cell lysates were incubated on IgG sepharose fast flow beads (GE Healthcare) for one hour at room temperature on a rotating wheel. After removing the supernatant fraction, the beads were washed 3 times with lysis buffer. Retained protein was recovered by heat denaturation of the beads in SDS-PAGE gel loading buffer. Input, bound and non-bound fractions were resolved by SDS-PAGE and analysed by western blotting using antibodies specific to both the zz and myc epitope tags.

Purification of Rex1 proteins

Epitope-tagged zz fusions of wild-type and mutant Rex1 proteins were purified from yeast cell lysates for in vitro RNA binding and RNA degradation assays, using a combination of ion exchange and affinity chromatography. Yeast strains were grown up in appropriate selective or rich medium to an OD_{600nm} of 1-2 and harvested by centrifugation at 3600g for 5 minutes. Cells were lysed in HEPES cell extraction buffer (50mM HEPES/NaOH pH 7.4, 50mM KCl, 5mM $MgCl_2$, 2mM PMSF, 10% glycerol) and aliquots of the clarified lysates were incubated for one hour with an appropriate volume of Q sepharose beads (GE Healthcare), assuming a binding

capacity of 10mg/ml, on a rotating wheel. The non-bound fraction (containing the Rex1 protein) was then incubated with SP sepharose beads (GE Healthcare) for one hour at room temperature. The SP sepharose beads were collected by centrifugation at 360g for 5 minutes and washed three times for 5 minutes with HEPES cell extraction buffer. Protein retained on the SP sepharose beads was eluted by incubation in HEPES cell extraction buffer containing 300mM NaCl. The SP sepharose bead eluates were added to IgG sepharose beads and incubated for a further hour at room temperature. The beads were then washed three times with HEPES cell extraction buffer. Bound and non-bound fractions were analysed by SDS-PAGE and western blotting, using the peroxidase/antiperoxidase (PAP) antibody conjugate (Sigma Aldrich).

On-bead RNA binding assays

The RNA binding acitivity of wild-type and mutant Rex1 proteins was assessed by RNase-assisted RNA chromatography (Michlewski and Cáceres 2010). Poly(U)-coated agarose beads were prepared by mixing 1mg poly(U) RNA (Sigma Aldrich) with 0.1M NaOAc (pH 5) and 5mM sodium meta-periodate (Sigma Aldrich) in a volume of 200µl, and incubating the mixture at room temperature in the dark for one hour. The Poly(U) RNA was then precipitated with ethanol and resuspended in 500µl 0.1M NaOAc, pH 5. 250µl of a 50% slurry of adipic acid dehydrazide agarose bead (Sigma Aldrich) was washed four times with 10ml 0.1M NaOAc, pH 5, mixed with the poly(U) RNA and incubated overnight at 4°C. The coupled beads were washed three times with 2M KCl and then equilibrated with HEPES cell extraction buffer. The beads were resuspended in 3ml HEPES cell extraction buffer and 250µl volumes were aliquoted into 10 microfuge tubes. Rex1 proteins that had been purified by Q sepharose and SP sepharose ion exchange chromatography was then added to the poly(U)-agarose beads and incubated for 1 hour at room temperature on a rotating wheel. The beads were washed3 times with HEPES cell extraction buffer and RNA binding proteins were specifically eluted by incubation with 100µl buffer containing 2 µg RNase A. The eluates were denatured by heating at 95°C for

5 minutesin SDS-PAGE loading buffer and the proteins were analysed by SDS-PAGE and western blotting, using the PAP antibody complex.

Purification of yeast rRNP particles for in vitro RNA degradation assays

The release and purification of RNP particles containing 5S rRNA from yeast ribosomes was based on early sucrose gradient ultracentrifugation studies (Comb & Sakar, 1967). 500ml cultures of the yeast *rex1Δ*mutant strain P550 were grown in YPD medium at 30°C up to an OD_{600} of 0.5-1. Cells were then harvested by centrifugation and the cell pellets were stored at -80°C. Frozen cell pellets were thawed on ice and lysed with glass beads in a buffer comprising 50mM HEPES pH 7.4, 50mM KCl, 5mM $MgCl_2$, 1mM EDTA. The lysate was then incubated on ice for 15 minutes after adding EDTA to a final concentration of 3mM. Cell lysates were then loaded onto10-50% sucrose gradients in a buffer comprising 10mM Tris-HCl pH 7.4, 50mMKCl, 1mM EDTA, prepared essentially as described for glycerol gradients above. Sucrose gradient ultracentrifugation was carried out in an SW41 rotor at 4°C using a Beckman-Optimer™, LE-80X Ultracentrifuge (Beckman-Coulter) at 36,000 rpm for 210 minutes. Sucrose gradients were aliquoted in to 12 fractions and $MgCl_2$ was added to each fraction to a final concentration of 10mM to facilitate the catalytic activity of Rex1 protein in subsequent RNA degradation assays. Gradient fractions were screened for 5S and 5.8S rRNAs by denaturing polyacrylamide acrylamide gel electrophoresis to identify fractions that contain 5S RNP particles and lack large ribosomal subunits.

The purification of 60S ribosomal subunits was carried out by sucrose density gradient ultracentrifugation using a similar protocol to that described above, except that the lysate and gradient buffers lacked EDTA.

On-bead RNA degradation assays

Epitope-tagged, zz fusions of wild-type and mutant Rex1 proteins were expressed from high copy number plasmids in yeast and purified from 500ml cultures by ion

exchange and affinity chromatography, as described above. A 250µl aliquot (20µg/ml) of purified 5S rRNP particles was then added to the beads and the mixture was incubated at 30°C on a shaking platform. 50µl aliquots of the supernatant were collected when the substrate was added and at time intervals of 10, 20 and 30 minutes. Reactions were stopped by snap-freezing the samples in liquid nitrogen. Frozen samples were thawed and the RNA was recovered by extraction with phenol/chloroform, followed by ethanol precipitation. The RNA pellets were dissolved in 40µl DEPC-treated water and 40µl formamide gel loading dye, denatured by heating at 65°C for 10 minutes and the reaction mixtures were resolved by electrophoresis through 6%polyacrylamide gels containing 50% urea.

Fluorescence microscopy

Florescence microscopy imaging of GFP- and RFP-tagged proteins was performed on living cells using an Axiovert 200M microscope (Zeiss) equipped with Exo X-cite 120 excitation light source, band pass filters (Zeiss and Chroma) and 100X/1.45 alpha alpha-Fluar, 63X/1.40 plan Pochromat or ph2 objective lance plan 40X/0.065 (Zeiss), and a Hamatsu Orca EU digital camera. 0.5 µm Z-stacks were collected. Several slices were taken during the z stack and were then merged together using OpenLab software. Velocity computer software was used for image acquisition. Photoshop software was then used to process green, red, and merged images.

1.5.5 Nucleic Acid Analyses

Southern blotting

Restriction digestion and Southern blotting (Southern et al, 1975) was routinely carried out to confirm new recombinant plasmid constructs. Through using capillary transfer, the DNA was transferred from agarose gels to Hybond-N+membrane membrane (GE Health care). Following resolution of DNA through agarose gels, the double-stranded DNA was denatured by soaking the gel in 0.4M NaOH for 15 minutes and then neutralized with neutralization buffer (0.5M Tris-HCl, pH 7.4, 1.5 M NaCl,). The gel was finally soaked in 10 X SSPE buffer for 15

minutes and the DNA was transferred onto Hybond-N^+ membranes (GE Healthcare) by downward capillary action using 10X SSPE buffer. Transferred DNA was crosslinked on to the membrane by irradiation with UV light at an exposure of 1200 joule/$cm^2$and a distance of 10 cm, using a UV crosslinking apparatus (CL1000, UVP Products).

RNA extraction from yeast

RNA was prepared from yeast using the hot phenol extraction method (Maniatis, 1982), as modified by David Tollervey (Tollervey and Mattaj, 1987). For these experiments, 50ml of culture medium was inoculated with an overnight starter culture and left it to grow at 30°C with shaking until it reached an optical density of OD_{600} 0.5 AU. The cells were harvested by centrifugation at 3,200*g* for 5 min. The cell pellet was mixed with approximately 1ml of DEPC-treated glass beads (425-600nm, Sigma Aldrich), 0.5ml of pre-chilled GTC mix and 0.5ml of phenol pH 4.0, and the cells were disrupted by vortexing for 5 min. A further 3.5ml of GTC mix and phenol were added after and the mixture was incubated at 65°C for 10 minutes. After briefly chilling on ice, 4ml chloroform and 2ml of the NaAc mix were added and the mixture was vortexed briefly and then centrifuged at 3,200*g* for 5 minutes to separate the aqueous and organic phases. The aqueous phase was transferred to a fresh falcon tube and re-extracted with 5ml phenol/chloroform/isoamyl alcohol. The aqueous phase from the second extraction was then transferred to a fresh falcon tube and the RNA was precipitated by the addition of 2 volumes of cold 100% ethanol. Precipitation was allowed to occur -80°C for 1-2 hrs or overnight at -20°C. The precipitated RNA was pelleted by centrifugation at 3,200*g* for 15 minutes. The RNA pellets were washed twice with ice cold 70% ethanol and then left to air dry for 20 minutes at room temperature. The isolated RNA was dissolved in 100µl DEPC-treated water and the concentration was determined spectrophotometrically, assuming the specific absorbance of RNA at 260nm to be 40 µg/OD.

Polyacrylamide gel electrophoresis of RNA

Total cellular RNA samples were analysed by electrophoresis through 15cm long 8% or 6%polyacrylamide (19:1) gels containing 50% (w/v) urea, using 0.5X TBE running buffer. 5µg aliquots of RNA in 8µl of formamide gel loading buffer were denatured by heating to 65°C for 10 minutes and loaded onto the gel shortly after rinsing the pockets with electrophoresis buffer to remove leached urea. Electrophoresis was performed at 70 volts overnight until the xylene cyanol blue dye in the gel loading buffer had migrated to the bottom of the gel. After electrophoresis, the gel was stained in buffer containing ethidium bromide (final concentration, 0.1µg/ml) and the RNA was visualised using a G:box gel documentation system (SynGene).

Northern Blotting

RNA was transferred from polyacrylamide gels to Hybond N^+ nylon membranes (GE Healthcare) by Northern blotting, according to the technique described by Alwine *et al* (Alwine et al, 1977) and Littlehales (Littlehales, 1989). Polyacrylamide gels were positioned onto pre-wetted, pre-cut Hybond N+ membranes under buffer and placed between sheets of Whatmann 3MM paper, ensuring that air was not trapped between the gel and membrane, and the sandwich was placed in an electroblotting transfer unit (Engineering &Design Plastics, Cambridge). Electrophoresis was performed in 0.5 X TBE buffer at 10 volts overnight. After transfer, RNA was cross-linked to the membrane blots by irradiation with short wavelength UV light (1200 joules/cm^2 at a distance of approximately 10cm), using a CL1000 crosslinker (UVP Products).

5' ^{32}P-Labelling of oligonucleotides

Commercially sourced oligodeoxyribonucleotides (Eurofins Genomics) synthesized supplied with a free 5' hydroxyl group were ^{32}P-labelled at their 5' ends for use as hybridisation probes for specific RNA transcripts on northern blots or for plasmid DNA on southern blots (Maniatis, 1982). Radiolabelling was carried out using polynucleotide kinase and γ-[^{32}P]-ATP (PerkinElmer, Mass, USA). 5 units of T4 polynucleotide kinase (New England BioLabs) were added to 20 ul of 1 x PNK buffer

containing 5pmol DNA oligonucleotide and 6 pmol[^{32}P]ATP (6000Ci/mmol) and the mixture was incubated at 37°C for 30 minutes. The mixture was then heated for 5 minutes at 65°C to inactivate the enzyme and then diluted in hybridization buffer before filtering directly into the hybridization solution through a 0.2 µm filter (Sartorius).

5' P-Labelling of oligonucleotides

Commercially sources complementary single stranded oligodeoxyribonucleotides (Eurofins Genomics) were 5'end labelled with an organic phosphate to facilitate cloning. 5 units of T4 polynucleotide kinase (New England BioLabs) were added to 20 ul of 1 x PNK buffer containing 5pmol DNA single stranded oligonucleotides and 5 pmol ATP and the mixture was incubated at 37°C for 30 minutes. The complementary single stranded oligonucleotides were then mixed together and incubated at room temperatures for 10 minute to generate double stranded 5' end labelled oligonucleotides with inorganic phosphate.

Hybridisation of ^{32}P-labelled probes to blots

Northern and Southern blots were hybridized with ^{32}P-labelled oligonucleotide probes in oligonucleotide hybridization buffer (see Table 7) at 37°C overnight. Blots were placed in flat-bottomed Tupperware boxes fitted with air-tight lids and pre-hybridised with 50ml Oligo-hybridisation buffer for one hour at 37°C to block nonspecific binding. Radiolabelled probes were filtered directly into the hybridization solution and the membrane was hybridized overnight. After hybridization, the radiolabelled probe solution was decanted into a falcon tube and stored at room temperature for further use for a period of one to two weeks. The membrane was rinsed briefly three times with 6 X SSPE buffer and then incubated with 6X SSPE buffer at 37°C for 30 minutes to remove any nonspecifically hybridized probe. The membrane was then removed from the hybridization box, dried on paper towels and wrapped in Sarawrap (Fisher). Blots were placed under phosphor storage screens (Kodak) in X-ray film cassettes and the screen was exposed overnight. PhosphorImager data were collected using a Personal Molecular Imager FX machine (BioRad).ImageJ64 software (NIH) was used to

visualise and quantifynon-saturated images. Northern blots were typically hybridized reiteratively with a number of probes. To remove the hybridized probes on the membrane, the membrane was soaked with boiling Northern stripping buffer (0.1 X SSPE, 0.1% SDS) and washed on a shaking bed platform for one hour.

1.6 Bioinformatics

Yeast genomic sequences were obtained from the *Saccharomyces* Genome Database (SGD) (http://www.yeastgenome.org). Blast searches (NCBI) were used to identify proteins with sequence homology (http://www.ncbi.nlm.nih.gov/BLAST/) and Clustal Omega (Sievers et al, 2011) was used to align different protein sequences. Phyre2 searches (Kelley and Sternberg, 2009) were also used to identify polypeptide sequences that are structurally related to yeast Rex1. Putative NLSs were identified using online NLS detecting databases (Kosugi et al, 2009; Nguyen et al, 2009). Lastly, Expasy (Artimo et al, 2012) was used to translate nucleotide sequences into protein sequences and to predict the size of the encoded protein products. CRAC analyses of the Rex1-HTP strains were carried out by Tollervey and Granneman labs (University of Edinburgh) and they analyzed the sequencing data using the PyCRAC data pipeline (Webb et al, 2014).

Chapter Three

Mutational and functional analysis of Rex1

3.1 Introduction

Rex1 is a 3'→5' exoribonuclease that functions in the 3' end maturation of different types of RNA, the best characterized substrates being 5S rRNA and $tRNA^{Arg}$ that is processed from the dicistronic $tRNA^{Arg}$ -$tRNA^{Asp}$ transcript (Piper et al, 1983 and van Hoof, 2000). Rex1 contains a central exonucleolytic catalytic domain (Ozanick et al., 2009) that is flanked by N- and C-terminal regions (figure 3). The catalytic domain of Rex1 is homologous in sequence to a family of exoribonucleases in yeast that include Rrp6, Rex2, Rex3, Rex4, and Pan2 and Caf1 (Moser et al, 1997; van Hoof et al, 2000; Zuo and Deutscher, 2001). These enzymes belong to the larger DEDD "superfamily"of exonucleases that act on DNA and/or RNA substrates, which contain four conserved acidic amino acids that are important for their catalytic activity These exoribonucleases process distinct but overlapping sets of RNA substrates in yeast and, despite the high degree of sequence homology between the polypeptide sequences of the catalytic domain of these proteins, only Rex1 was found to process 5S rRNA (van Hoof, 2000). This suggests that the N- and C-terminal regions of Rex1 that flank the central catalytic domain may contribute to its substrate specificity. These features have yet to be characterized, either functionally or structurally. However, the COILS software (Expasy Bioinformatics resource portal) (Lupas et al*,* 1991) predicts three coiled coil regions within the N- and C-terminal regions (figure 3). Rex1 is not an essential gene product but loss of function *rex1* alleles are synthetic lethal with loss of function mutations in the yeast 3'→5' exoribonuclease, Rrp6 or its associated cofactor, Rrp47 (Peng et al, 2003; van Hoof et al, 2000b). In contrast, loss of function mutations in Rex2, Rex3 or Rex4 are not synthetic lethal with loss of function *rrp6* mutants. Thus, Rex1 has a specific functional overlap with Rrp6 that is not shared with other members of the DEDD exonuclease family.

Rex1 has both sequence and functional homology with RNase T of *E. coli*, a 3'→5' exoribonuclease that is required for 3' end maturation of 5S rRNA (Li & Deutscher, 1995) and which functions redundantly in the processing of precursors to other stable RNAs, including tRNA (Kelly and Deutscher, 1992) . RNase T is a homodimeric protein that has a two-fold rotational symmetry, such that the nucleic acid binding region of one monomer is positioned adjacent to the catalytic domain of the other monomer, a feature that is critical for its function (Li et al, 1996; Zuo et al, 2007). It is a member of the DEDD family of exonucleases and the four highly conserved acidic amino acid residues are important for the catalytic activity of RNase T, mutation of any one of these amino acids completely abolishing the catalytic activity of the protein (Huang and Deutscher, 1992).

In this chapter, I report the results of a mutagenesis study to address the contribution of different regions of the Rex1 protein to its function in living yeast cells. Site-directed mutagenesis was used to generate specific N- or C-terminal truncations, internal deletions and point mutations within a plasmid-borne copy of the*REX1*gene, based on the limited known domain organisation of the encoded protein. The generated *rex1* mutants were assayed for protein expression levels, whether they function *in vivo* using a genetic complementation assay and for their ability to mediate the correct 3' end maturation of 5S rRNA.

Specific mutations can be assayed for their effect on the function of a yeast gene using a plasmid shuffle assay (Elledge & Davis, 1988). In this assay, the loss of growth phenotype caused through deletion of the gene under study is complemented by a plasmid that harbours a wild-type copy of the gene. Cells that lack this plasmid as a result of unequal plasmid segregation during mitotic cell division are unable to grow unless they harbour a second functional copy of the gene. This can be provided by transforming a second plasmid into the strain that carries the allele under scrutiny. Provided that a counter selectable marker is present on the first plasmid that harbours the wild-type allele, cells can be purged of this plasmid and will only grow if the allele encoded on the second plasmid is

functional. The most widely used counter selectable marker in yeast is the *URA3* gene. This gene encodes the enzyme orotidine-5'-phosphate (OMP) decarboxylase, which converts OMP into uridine 5'-monophosphate, and is required for a step in the pyrimidine biosynthetic pathway. Ura3 can also act on 5' flouro-orotic acid and converts this substrate into 5-fluorouracil, a toxic base analogue. Plasmids containing the *URA3* gene can therefore be selected for on medium lacking uracil and selected against on medium containing uracil and 5-FOA. Since the *REX1* gene is not required for cell growth but mutants lacking Rex1 and Rrp6 or Rrp47 are nonviable, *rex1* mutant alleles can be assayed using a plasmid shuffle strain that is deleted for both *REX1* and *RRP6* or *RRP47* genes and is complemented by a plasmid bearing a wild-type copy of either deleted gene (see Figure 7).

N-terminal epitope tagging of the Rex1 protein with the "zz" tag, comprising two copies of the z domain from protein A of *Staphylococcus aureus* (Nilsson et al., 1987), had no discernible detrimental effect on the function of the protein. Unexpectedly, however, deletion of either one of two non-overlapping portions of both the N-terminal and C-terminal regions of Rex1 that flank the central catalytic domain caused a loss of protein function, even when the mutant protein was expressed at levels equal or greater than that of a chromosomally encoded C-terminally tagged Rex1-TAP fusion protein. Furthermore, substitution of the catalytic domain of Rex1 for that encoded by either the *REX2* or *REX3* gene also led to loss of protein function. As predicted, mutation of a conserved acidic amino acid residue within the catalytic domain (analogous to the catalytically inactive D238A mutation of Rrp6) also caused loss of Rex1 function. Taken together, these data clearly demonstrate that the N-terminal region,the central catalytic domain and the C-terminal region of Rex1 are all critical for its function *in vivo*, and strongly support the conclusion that the catalytic domain of Rex1 has one or more functions in addition to catalysis.

3.2 Results

3.2.1 *Construction of a plasmid-borne zz-rex1 allele*

To generate specific mutants of the *REX1* gene and to assay them in a plasmid shuffle assay, a pair of plasmids were generated that expressed *REX1* and differed only in the selectable marker present; one harboured the *URA3* gene (to function as the complementing wild-type plasmid) and the other carried the *LEU2* gene (for the generation of mutated *rex1* alleles). In each case, the Rex1 protein was expressed from the constitutive *RRP4* promoter as an N-terminal fusion protein that contained the zz epitope tag. Mutation of a gene encoding an N-terminally tagged zz fusion of Rex1would allow a straightforward comparison of the relevant expression levels of mutant and wild-type proteins by western analyses that is independent of the mutation within the *REX1* ORF. Furthermore, the analysis of protein expression levels allows the potentially trivial explanation to be ruled out that a loss of function phenotype reflects poor steady state expression levels of the mutant protein. To provide an additional line of experimentation to exclude the possibility that phenotypes associated with the rex1 mutants may result from poor expression, the mutant alleles were also expressed from 2µhigh copy number plasmids (Christianson et al., 1992).

The DNA sequence encompassing both the complete *REX1* ORF and approximately 500 nucleotides downstream of the *REX1* termination codon was amplified by PCR, using genomic DNA from the BY4741 (P364) wild type yeast strain. The forward primer (o869) introduced a unique *EcoR*I restriction site into the PCR product immediately upstream of the *REX1* initiation codon, while the reverse primer (o560) introduced a *Kpn*I site at the other end of the amplicon. The amplified *REX1* gene was then cloned in-frame as an *EcoR*I-*Kpn*I fragment into the construct p44 (Mitchell et al., 1996), which is a derivative of the *URA3*-bearing pRS416 cloning vector (Sikorski & Hieter, 1989) that allows the expression of N-terminally tagged "zz" fusion proteins from the *RRP4* promoter (Figure 8). PCR amplification of the *REX1* gene from yeast genomic DNA using primers o869 and o560 gave a single

product with the expected size of 2.1 kb (see Figure 8 panel C, lane 2). The amplicon was cloned into p44 and plasmid DNA minipreps from candidate clones were initially screened by restriction digestion and subsequently validated by sequence analysis of the complete REX1 ORF, using a primer complementary to a sequence encoding part of the zz tag (o774) and to a sequence within the *REX1* ORF (o884). The selected clone (p659) gave rise to two restriction fragments of the predicted sizes upon digestion with *EcoR*I and *Kpn*I (Figure 8C, lane 3) and was correct at the sequence level throughout the length of the ORF (data not shown).

To determine whether the zz-Rex1 fusion protein is functional, the p659 construct and a control vector were transformed into a *rex1Δ* strain for RNA analysis. Cells lacking Rex1 protein are defective in the 3' end 5S rRNA processing (Piper et al., 1983; van Hoof et al., 2000). In order to know whether zz-Rex1 is functional, total RNA was extracted from cells after growing under a permissive growth condition in SD-Ura. Then the total RNA was loaded and fractionated on a 6% RNA acrylamide gel and stained with ethidium bromide. Then the RNA was transferred from the gel on to a northern membrane to carry out a northern analysis. To analyze the samples, northern blot was hybridized by using a specific probe against 5S rRNA to show the processing activity of zz-Rex1 and the phenotype was compared to the wild type, and *rex1Δ* strain. The RNA processing phenotype of zz-Rex1 is similar to wild type strain and it able to shorten 5S rRNA (figure 9 panel B). This indicates that zz-Rex1 is functional and it complements the RNA defective phenotype of *rex1Δ* strain.

To generate a second *REX1* plasmid in order to be able to perform plasmid shuffle assays, the insert from the zz-REX1 expression construct p659 was cloned into the centromeric yeast vector pRS415, which carries the *LEU2* marker gene, and pRS313, which carries the *HIS3* marker gene (Sikorski & Hieter, 1989).These cloning reactions were done by homologous recombination in a yeast strain that contains complete deletions of the *LEU2* and *HIS3* genes to suppress the isolation of false positives that could potentially arise through recombination between the

selectable marker on the plasmid and the auxotrophic chromosomal allele (Figure 10). A *Pvu*II fragment from p659, that contains the complete insert encoding the zz-Rex fusion protein plus 100-200 nucleotides on either side of the polylinker, was transformed into the yeast strain BY4741, together with pRS415 or pRS313 that had been linearized with their polylinker regions. Transformant colonies were isolated by growth on selective medium lacking either leucine or histidine, and the plasmids were recovered and screened by restriction digestion with *Pvu*II.

To determine whether the zz-Rex1 fusion protein is stably expressed in yeast, the p659 construct and a control vector were transformed into a *rex1Δ* strain and cell extracts from the resultant transformants were subjected to western blot analysis using the peroxidase/anti-peroxidase antibody complex. The cell lysates were made using the alkaline lysis method (Motley et al., 2012), which minimizes protein degradation during sample processing. The expression level of thezz-Rex1 protein was compared to that of a C-terminally TAP-tagged Rex1 fusion protein (Rex1-TAP) that is expressed from the homologous *REX1* chromosomal locus (a description of the generation of the REX1-TAP strain is given in the next Chapter). The level of expression of the Rex1-TAP fusion protein gives a good approximation for the normal expression levels of Rex1, as it is expressed from the homologous chromosomal locus and has the same epitope (i.e. two copies of the z domain of protein A) as the zz-Rex1 fusion, and was shown to be functional (see data below). As shown in Figure 9, both zz-Rex1 and Rex1-TAP proteins are clearly detected as single polypeptides of distinct sizes. This observation, and the fact that extracts from cells not expressing a fusion protein gave no signal upon western analysis (data not shown), demonstrates that the signal is specific for the fusion proteins. The Rex1-TAP protein has a clearly slower electrophoretic mobility than the zz-Rex1 protein. This can be explained, at least in part, by the difference in predicted molecular weights of the zz-Rex1 and Rex1-TAP fusion proteins (78kDa and 84kDa, respectively).The expression level of zz-Rex1 was clearly higher than that of the Rex1-TAP fusion protein (Figure 9). Quantitative analysis of three independent data

sets, normalizing the signals to that of the Pgk1 protein, revealed that the expression of zz-Rex1 is approximately five-fold higher than Rex1-TAP. This difference in expression level will partially reflect the fact that the zz-Rex1 protein is expressed from the *RRP4* promoter rather than the *REX1* promoter. Furthermore, genes are typically expressed at higher levels from plasmid DNA than from chromosomal loci because plasmid DNA is typically less densely packaged together with nucleosome complexes.

3.2.2 *Construction of a plasmid shuffle strain to test rex1 mutant alleles*

A plasmid shuffle strain to test *rex1* alleles was generated by deleting the *RRP47* gene in a *rex1Δ::kanMX4* strain, after initially transforming the strain with the p659 plasmid that encodes the Rex1 fusion protein zz-Rex1.The *RRP47* locus was disrupted in the *rex1Δ::kanMX4* strain, rather than the *RRP6* locus, because a strain bearing an *rrp47Δ::hphMX4* allele with the suitable hygromycin resistance selectable marker had been previously generated in the laboratory (Garland et al., 2013). The *rrp47Δ::hphMX4* allele was amplified from yeast genomic DNA by PCR using primers complementary to sequences approximately 500 nucleotides up- and downstream of the *RRP47* ORF (primers o191 and o192). After transformation with the *rrp47Δ::hphMX4* PCR amplicon, integrants were isolated by growth on YPD plates containing hygromycin. Genomic DNA was prepared from each isolate and the DNA samples were screened by PCR amplification using the same pair of primers originally used to amplify the *rrp47Δ::hphMX4* deletion allele. These primers generate products of clearly distinct lengths from *RRP47* and *rrp47Δ::hphMX4* alleles (Figure 11, panel A); genomic DNA from a wild-type *RRP47* strain and an *rrp47Δ::hphMX4*mutant were also analysed in parallel. PCR analysis of genomic DNA from the selected *rex1Δ rrp47Δ* candidate P1604 clearly shows that the product obtained migrated slower through agarose gels than the product from the *RRP47* wild-type control strain, and comigrated with the larger amplicon obtained from the *rrp47Δ::hphMX4* strain(Figure 11B, lanes1-3). The plasmid

shuffle strain has the 5.8S rRNA defect of an rrp47Δ mutant (Figure 37, palnel A, lane 4) which shows the fact that *RRP47* gene is successfullt deleted.

Since *rex1Δ rrp47Δ* double mutants are synthetic lethal (Peng et al., 2003), a *rex1Δ rrp47Δ* double mutant would be predicted to be dependent upon the plasmid p659 for growth. To confirm that the isolated strain showed the expected growth phenotype, it was transformed with either the cloning vector pRS415 (which carries a *LEU2* marker) or a derivative thereof that harbours the *zz-REX1* allele. The transformants were then tested for growth on medium containing 5-FOA and on medium lacking leucine. As shown in Figure 11 panel C, the *rex1Δ rrp47Δ* double mutant transformed with the cloning vector was unable to grow on medium containing 5-FOA whereas the strain transformed with the zz-Rex1 derivative of pRS415 was able to grow robustly. Furthermore, the parental *rex1Δ* strain transformed with the pRS415 vector also showed vigorous growth on medium containing 5-FOA. All three transformants grew well on minimal medium lacking leucine. Together with the genomic DNA analysis described above, these experiments show clearly that the *rex1Δ* derived strain P1604 harbours an *rrp47Δ* allele and, as predicted, its growth can be supported by a plasmid encoding the *REX1* gene. Since expression of the plasmid-borne REX1 ORF can complement the *rex1Δ rrp47Δ* double mutant, these experiments also clearly demonstrate that the zz-Rex1 fusion protein is clearly functional.

3.2.3 *Construction of a set of rex1 deletion mutants*

One principal aim of this study was to address the importance of the N- and C-terminal regions of Rex1 to its function. Upon initiating this study, it was not clear what, if any, function these regions of the protein may have. Notably, the catalytic domain of the RNase T homodimer is flanked by regions that are important for RNA binding and protein-protein interactions but they do not show clear homology with the equivalent regions of Rex1.

A set of N-terminal, C-terminal and internal deletions of the *REX1* ORF were generated by site-directed mutagenesis on the cloned *REX1* construct, which expresses the N-terminally epitope-tagged zz-Rex1 fusion protein (see Figure 12). The *rex1 W509X* C-terminal truncation, which lacks the last46 amino acid residues that includes a predicted coiled coil region, was made by inserting a premature termination codon within the *REX1* ORF. The *rex1Δ428-476* internal deletion mutant was generated by introducing a pair of in-frame *Sal*I restriction sites within the *REX1* ORF and deleting the intervening sequence by restriction digestion. The DNA sequence encoding the zz epitope tag contains an *EcoR*I site at its 3' end. This was exploited in the production of the *rex1Δ1-81* and *rex1Δ1-202*N-terminal deletion mutants by introducing in-frame *EcoR*I restriction sites within the *REX1* ORF and then deleting the internal *EcoR*I restriction fragments. Since the *LEU2*ORF within pRS415 contains an *EcoR*I site, N-terminal deletions could not be generated directly within the pRS415/zz-rex1 construct. To generate these mutants, inserts containing*rex1* alleles with the additional *EcoR*I site were cloned into pRS313 (which carries the *HIS3* gene and contains a single *EcoR*I site within the polylinker region)by homologous recombination, the internal *EcoR*I fragment was deleted, and then the shortened insert was transferred back into pRS415.The *rex1Δ82-202*internal deletion mutant was generated by subcloning the short *EcoR*I fragment that had been deleted upon production of the *rex1Δ1-82* mutant and introducing it into the *rex1Δ1-202* construct. As a control for a *rex1* loss-of-function mutant, the conserved aspartate residue D229 within the Rex1 catalytic domain was mutated to an alanine residue. The D229A mutant was strongly predicted to block the catalytic activity of the protein, based on the effect of the analogous mutation within Rrp6 (Phillips & Butler, 2003) and the effect of the *rex1*D229A, E231A double mutation reported in a previous study (Ozanick et al., 2008). Mutated plasmids were screened by sequence analysis of the corresponding region of the *REX1* ORF, with preliminary screening by restriction digestion analysis where feasible.

3.2.4 The N-terminal and C-terminal regions of Rex1 are critical for protein function

Plasmids encoding the *rex1* mutant proteins were transformed into the rex1Δ rrp47Δ plasmid shuffle strain and assayed for their ability to support growth on medium lacking leucine and on medium containing 5-FOA (Figure 13). The plasmid encoding the wild-type zz-Rex1 fusion and the pRS415 cloning vector were also transformed in parallel to serve as positive and negative controls, respectively, in the growth assays. All transformants grew comparably on the medium lacking leucine. As seen previously (Figure 11), transformants expressing the wild-type zz-Rex1 fusion protein from the *LEU2* containing vector were able to grow on medium containing 5-FOA whereas cells transformed with the pRS415 vector did not grow. Cells expressing the D229A *rex1* point mutant were not able to grow on medium containing 5-FOA, demonstrating that this mutant causes loss of Rex1 function. Strikingly, none of the N-terminal or C-terminal *rex1*deletion mutants supported growth on 5-FOA medium. The same effects were also observed using an independent *rex1Δ rrp47Δ*plasmid shuffle strain that is complemented with a plasmid bearing the *URA3* marker gene and a genomic clone of the *RRP47* gene (Costello et al., 2011) (data not shown). Thus, two independent deletions with the N-terminal region (Δ1-82 and Δ82-202) and within the C-terminal region (Δ428-476 , W509X)of Rex1 have a strong impact on protein function. These data clearly demonstrate that the N- and C-terminal regions of Rex1 are required for its function in mitotically dividing cells.

3.2.5 *The rex1 deletion mutants are expressed in yeast*

A trivial explanation for a mutation within a protein-coding gene causing a loss of function phenotype is that the mutant protein is not stably expressed. Plasmids encoding the *rex1* mutant proteins were transformed into a *rex1Δ* strain and whole cell extracts from these transformants were analysed by SDS-PAGE and western blotting (Figure 14). The apparent molecular weights of the Rex1 mutant proteins varied and the altered electrophoretic mobilities were consistent with the predicted changes in length of the mutant proteins. Relative protein expression

levels were determined in triplicate, normalizing the expression level to that of the constitutively expressed Pgk1 protein.

The D229A active site point mutation had no significant effect on the expression of Rex1. In contrast, the expression levels of all of the *rex1* deletion mutants were notably reduced compared to the full-length wild-type protein, with observed signal strengths ranging from 15-40%. This suggests that the expression level of the mutant Rex1 proteins may be below a critical threshold required for cell growth in the absence of Rrp47. However, it should be noted that expression of the plasmid-encoded zz-Rex1 wild-type protein was observed to be approximately five-fold higher than the C-terminal Rex1-TAP fusion protein (Figure 9), which itself is sufficient to support cell growth in the absence of Rrp6 (see Figure 24, below). Consistent with the previous experiments, the expression level of the Rex1-TAP fusion protein was also observed to be approximately 20% of the N-terminally tagged zz-Rex1 fusion protein (Figure 14, compare lanes 1 and 3). Therefore, the deletion mutants of the N-terminally tagged zz-Rex1 fusion protein were expressed at similar levels to that of the chromosomally encoded Rex1-TAP protein.

To address further whether the protein expression levels of the rex1 deletion mutants were limiting for Rex1 function, all the generated *rex1* deletion mutants were subcloned into a high copy number plasmid containing the 2µ origin of replication. These plasmids have a copy number of approximately10-30 per haploid genome (Christianson et al., 1992). SDS-PAGE and western analyses of extracts from *rex1Δ* cells harbouring these plasmids revealed that the expression levels of the *rex1Δ82-202*, *rex1Δ428-476* and *rex1* W509X mutant proteins were all clearly increased, compared to their expression from the pRS415 derivatives, and ranged from 40-80% of the zz-Rex1 full-length protein expressed from the centromeric plasmid (Figure 16). These mutant proteins were expressed from the 2µconstruct at levels equal or greater than the expression level of the chromosomally encoded Rex1-TAP protein. In contrast, similar expression levels were observed from the 2µ and centromeric plasmids for the*rex1Δ1-82* mutant. The reason for this observation is not clear. Nevertheless, the expression of the *rex1Δ1-82* mutant

protein is comparable to that of the Rex1-TAP fusion protein (Figure 14).Transformation of the 2µ variants into the *rex1Δ rrp47Δ* plasmid shuffle strain failed to support growth on medium containing 5-FOA (Figure 13). Taken together, these datasets demonstrate that the inability of the *rex1* deletion mutants to function is not due to limiting expression levels of the mutant proteins.

3.2.6 *All rex1 deletion mutants are defective in 5S rRNA maturation in yeast*

The most well characterized RNA processing defect that is observed in *rex1Δ* mutants is the block in 3' end maturation of 5S rRNA (Piper et al., 1983; van Hoof et al., 2000). The extended form of 5S rRNA observed in *rex1Δ* mutants and the normal form of 5S rRNA observed in wild-type cells can be easily resolved upon polyacrylamide gel electrophoresis under denaturing conditions. To screen the *rex1* mutants for a defect in 5S rRNA maturation, total cellular RNA was isolated from yeast cells, resolved in denaturing 6% polyacrylamide gels and the predominant short ribosomal RNAs (5.8S and 5S rRNAs) were visualized by staining with ethidium bromide. The 5S rRNA was also detected specifically by transferring the RNA to nylon membrane and carrying out northern hybridisation with an oligonucleotide probe complementary to a sequence within the mature 5S rRNA. Analyses was performed on RNA isolated from a wild-type strain, the isogenic *rex1Δ* mutant, an isogenic rex1-TAP strain and *rex1Δ* strains that express the plasmid-borne N-terminally tagged Rex1 proteins. As previously shown (van Hoof et al., 2000), the 5S rRNA species in the *rex1Δ* strain migrates slower than the fully matured 5S rRNA in wild-type cells (figure 15, compare lanes 1 and 3). The rex1-TAP strain expresses 5S rRNA of a normal length, demonstrating that the C-terminal Rex1 fusion protein is functional. Cells expressing the N-terminal Rex1 fusion protein also showed no defect in 5S rRNA maturation (Figure 15, lane 4). As predicted, the *rex1* D229A active site mutant was blocked in the final maturation of 5S rRNA. Notably, all the loss-of-function *rex1* deletion and truncation mutants were defective in the 3' end maturation of 5S rRNA (Figure 15, lanes 6-10). Expression of the *rex1* mutants from the high copy number 2µ plasmid did not allow suppression of the 5S rRNA maturation defect (Figure 16, panel C). These

experiments show that the N-terminal and C-terminal regions of Rex1, in addition to the catalytic domain, are required for the correct processing of 5S rRNA precursors in living cells.

3.2.7 *The catalytic domain of Rex1 has specific properties essential for its function*

Yeast expresses a number of proteins that share homology with the catalytic domain of Rex1 and which have been shown directly to have exoribonuclease activity through in vitro assays (Rrp6, Pan2) (Burkard & Butler, 2000; Schäfer et al., 2014) or to be required for the correct processing or degradation of cellular RNAs (van Hoof et al., 2000). A BLAST sequence alignment of the catalytic domain of these proteins is shown in (Figure 3). The catalytic domain is highly conserved across different members of the yeast DEDD family, with an identity of 38% and a similarity of 58% between residues corresponding to I225 to T373 in Rex1.

Differences in amino acid sequence within the DEDD catalytic domains of these proteins may reflect the specific function of particular exonucleases or may be functionally neutral changes in protein structure that have arisen through genetic drift. To address whether the catalytic domain of other members of the yeast DEDD family could substitute functionally for the catalytic domain of Rex1, “domain swap” experiments were performed. Yeast genomic DNA encoding the catalytic domain of Rex2 and Rex3 that is homologous to residues I225 to T373 of Rex1 was amplified by PCR and seamlessly inserted into the zz-Rex1 expression construct by homologous recombination. Candidate clones were pre-screened for loss of the *Xcm*I restriction site that is present in the sequence encoding the catalytic domain of Rex1 but not that of Rex2 or Rex3, and then subsequently confirmed by sequence analysis across the complete length of the catalytic domain. The resulting constructs expressed full-length zz-Rex1 fusion proteins where in the catalytic domain had been replaced by that of either Rex2 or Rex3. The catalytic domains of the Rex2 and Rex3 proteins were chosen because these proteins show the closest

homology to Rex1 (24 and 38% sequence identity across the length of the domain for Rex2 and Rex3, respectively). The mutants are denoted *rex1-cat-rex2* and *rex1-cat-rex3*, respectively.

The relative expression levels of the domain swap *rex1* mutants were determined by western analysis of denatured cell extracts. As can be seen in Figure 17, both mutants were expressed at lower levels than the zz-Rex1 protein containing the wild-type *REX1* ORF but at higher levels than the chromosomally encoded rex1-TAP fusion protein. Plasmid shuffle assays showed that neither of the *rex1-cat-rex2* or *rex1-cat-rex3* mutants was able to complement for the loss of the *REX1* gene in a *rex1Δ rrp47Δ* double mutant (Figure 17, panel D). These experiments demonstrate that the catalytic domain of Rex2 or Rex3 is not able to functionally substitute for that of Rex1.

The domain swap mutants were assayed for their ability to complement the 5S rRNA maturation defect of the *rex1Δ* mutant. Polyacrylamide gel electrophoresis and northern blot hybridization analyses of total cellular RNA revealed that the extended form of 5S rRNA seen in the *rex1Δ* mutant was also observed in the *rex1-cat-rex2* and *rex1-cat-rex3*mutants (Figure 17, panel C). In contrast, the shorter mature form of 5S rRNA was observed in cells expressing the full-length zz-Rex1 fusion protein. Thus, the *rex1-cat-rex2* and *rex1-cat-rex3* alleles are not able to complement the RNA processing defect of the *rex1Δ* mutant.

To rule out the possibility that the expression level of the domain swap mutant proteins was insufficient to complement for the lack of Rex1, the *rex1-cat-rex2* and *rex1-cat-rex3* alleles were sub-cloned into the high copy number 2µ plasmid pRS425 by homologous recombination. Expression from the pRS425 vector increased the levels of the domain swap mutant proteins to that of the wild-type Rex1 fusion protein (Figure 18, panel A). However, this increased expression was

not sufficient to complement for the loss of the wild-type Rex1 fusion in the *rex1Δ rrp47Δ* double mutant (Figure 18, panel D) or to support normal 5S rRNA maturation (Figure 18, panel C).

These experiments demonstrate that replacement of the catalytic domain of Rex1 with that of closely related proteins with demonstrated roles in RNA processing (van Hoof et al., 2000) does not generate a functional protein. This suggests that the catalytic domain of Rex1 has one or more specific functions, in addition to its role in RNA catalysis. The catalytic domain of Rex1 may make contacts with other regions of the protein and impact in some manner on its three-dimensional arrangement. Alternatively, the catalytic domain of Rex1 may contribute to an additional function such as substrate recognition or binding.

To test whether the domain swap mutants had a gross effect on the biophysical properties of Rex1, lysates from cells expressing either the wild-type zz-Rex1 fusion protein or the Rex1/Rex2 catalytic domain swap mutant were resolved by glycerol gradient centrifugation. The sedimentation profile of the rex1-cat-rex2 domain swap mutant was compared to that of the wild-type fusion protein and to a set of protein standards by a combination of SDS-PAGE and western blotting analyses. The wild-type zz-Rex1 fusion protein and rex1-cat-rex2 mutant protein sedimented through glycerol gradients with similar profiles (Figure 19). Although there was some trailing of the western signal down the gradients, the Rex1 proteins sedimented with a clear peak signal approximately the size of yeast alcohol dehydrogenase (ADH).This suggests that the Rex1/Rex2 domain swap mutation does not have a gross effect on the biophysical properties of the protein that causes it to aggregate or to be excluded from a protein complex. Hence, the loss-of-function phenotypes of the domain swap mutants do not appear to reflect a significant alteration of the physical state of the protein. Yeast ADH is a globular homotetramer with a molecular weight of approximately 150kDa. Since the

predicted molecular weight of the Rex1 fusion proteins is approximately 75kDa (Figure 18), this indicates that Rex1 may not be expressed simply as a monomeric protein.

3.3 Discussion

The yeast Rex1 protein contains acentral catalytic domain that is well conserved among members of the DEDD family of exonucleases, as well as N- and C-terminal regions that have not yet been functionally characterized. To address the functional importance of the distinct regions of the Rex1 protein, a set of deletion and point mutants were generated within a plasmid-borne copy of the gene and the constructs were assayed for their ability to support cell growth in a Rex1-dependent strain and to support normal 3'-end maturation of 5S rRNA, a well characterized Rex1-dependent RNA processing event (van Hoof et al., 2000). The data obtained from plasmid shuffle assays and northern blot analyses of cellular RNA showed that both the N-terminal region and the C-terminal region were required for Rex1 function. In addition, mutation of one of the conserved aspartate residues within the catalytic domain of Rex1 caused loss of function *in vivo*. Furthermore, substitution of the catalytic domain of Rex1 for the equivalent polypeptide sequence found in two other members of the DEDD family of exonucleases failed to generate a functional protein.

One trivial explanation for a mutation causing a loss-of-function phenotype is that the mutant protein is incorrectly folded. This can cause the mutant protein to be susceptible to protein degradationand/or be inefficiently incorporated into functional protein complexes. To address this, the expression levels of the generated mutants were compared with that of full-length Rex1protein that is encoded from the same plasmid construct, as well as with Rex1 that is expressed from a chromosomal allele. Assays included the chromosomally encoded protein because expression of a given gene is frequently higher from a plasmid than from a

chromosome. To facilitate comparative expression analyses, all full-length and deletion proteins were expressed as fusions that contained a common epitope. Western blot analyses revealed that all the mutant proteins were expressed at levels similar to or more than that of the chromosomally encoded Rex1 fusion protein. Furthermore, expression of the Rex1 mutant proteins from a high copy number plasmid increased the level of protein expression (with the possible exception of the *rex1Δ1-82* mutant) but failed to support Rex1-dependent growth or normal 5S rRNA maturation in vivo. The loss-of-function phenotypes associated with the *rex1* mutants are therefore clearly not as a result of poor expression of the mutant alleles. These data strongly support the conclusion that the N- and C-terminal regions of Rex1 contribute in some manner to the function of the protein. A truncation within an intricately folded protein domain may be expected to destabilize protein structure. It may therefore be speculated that, since deletion of two independent regions within both the N- or C-terminal regions of the protein did not significantly affect the expression of Rex1, these regions of Rex1 are not structurally restrained to a large degree but rather function in a partially unfolded state.The molecular functions of these distinct domains within Rex1 remain largely unclear. Data is presented in Chapter five for a role of the N-terminal region of Rex1 in targeting the protein to the nucleus through interaction with karyopherin proteins. The N- and C-terminal regions of Rex1 may be involved in other protein/protein interactions, either intramolecularly (such as in the case of RNase T) or intermolecularly, such as providing contacts within a stable protein complex or transiently interacting with other proteins during recognition of its substrate RNP complexes. Rex1 may also interact with its RNA substrates through residues outside of its catalytic domain.

Threading studies using the Phyre2 web server (Kelley et al., 2015) revealed a predicted structural similarity of high confidence (95%) between residues 428-505 of Rex1 (adjacent to the catalytic exonuclease domain and towards the C-terminus of the protein) and known crystallographic structures of cofactor-independent

phosphoglycerate mutases (PGMs) (Rigden et al., 2003; Nowicki et al., 2009; Roychowdhury et al., 2015) and phosphopentomutase (Federov et al., 2013) (see Figure 20). Phosphoglycerate mutase is a key enzyme in glycolysis that drives the isomerization of 3-phosphoglycerate into 2-phosphoglycerate. The reaction occurs by a Mn^{2+}-dependent phosphotransfer mechanism and involves the formation of a covalent phosphor-enzyme intermediate. Phosphopentomutases interconvert ribose-1-phosphate and ribose-5-phosphate as part of the pentose phosphate pathway and during purine biosynthesis, and are also phosphotransferases that function via a phospho-enzyme intermediate. It is intriguing that Rex1 has potential structural homology with enzymes that interact with phosphorylated substrates. However, the functional basis of the putative structural correlation is not clear. PGMs consist of two domains; a substrate-binding domain and a metal ion binding domain (see Figure 20). Residues 428-505 of Rex1 can be threaded with high confidence onto residues 369-441 within the defined Mn^{2+}ion binding domain of the PGM of *S. aureus*. However, some residues within PGM that are critical for coordinated ionic interactions with the Mn^{2+}ion (D397, H401) are not conserved in the Rex1 sequence, whereas others (S62, D438, H439, H456) lie outside of the mapped sequence (Roychowdhury et al., 2015). Phosphopentomutases also consist of two domains, a core domain with a protein fold similar to that of alkaline phosphatases and a cap domain (Panosian et al., 2011). The region of phosphopentomutase that the sequence of Rex1 can be mapped to has more structural integrity than that of the PGMs, constituting the upper surface of the alkaline phosphatase fold (Figure 20). Alkaline phosphatases coordinately bind two divalent metal ions that are involved in ionic interactions with the labile phosphate group. Given that residues 428-505 of Rex1 is juxtaposed to the catalytic domain, it is feasible that this region of the protein contributes to substrate binding through interaction with the RNA phosphate backbone.

Rex1 does not contain any clearly characterized RNA binding domains but does contain regions that are rich in basic residues, which can mediate interaction with

nucleic acids (Weiss and Narayana 1998; Houmani and Ruf 2009; Jones et al. 2001; Costello et al., 2011). There are two stretches of lysine-rich sequence in the N-terminal region of Rex1, between residues 42-52 and residues 19-25. These regions may also contribute to substrate binding.

Mutation of a single conserved aspartate residue within the catalytic domain prevented the protein from supporting growth in a Rex1-dependent strain and completely inhibited the final 3' end maturation of 5S rRNA. The D229A *rex1* mutation is analogous to the D238A active site mutation within Rrp6 (Phillips & Butler, 2003). This strongly suggests that the D229A mutation within Rex1 abolishes the exonucleolytic activity of this protein; this point is further addressed in the *in vitro* analyses presented in Chapter six Intriguingly, substitution of the complete catalytic domain of Rex1 for that of the functionally related exonucleases Rex2 or Rex3 failed to produce a functional chimeric protein. These experiments reveal that the catalytic domain of Rex1 is not only required for exoribonucleolytic activity but must also have one or more additional functions that impart a degree of specificity on Rex1 activity. One possibility is that the catalytic domain is involved in intramolecular interactions within Rex1 that maintain an optimal structure of the protein for RNA binding and catalysis. Alternatively, residues within the catalytic domain of Rex1 may be involved in substrate recognition or binding. Ultracentrifugation studies presented here show that the Rex1/Rex2 chimeric protein was not grossly affected in its biophysical properties. This suggests that the ability of the Rex1 catalytic domain to carry out these putative additional interactions does not require a substantially different structural organization. The following chapter describes work aimed at biophysically characterising the yeast Rex1 protein.

Chapter Four

Biophysical Analysis of the Yeast Rex1 Exoribonuclease

4.1 Introduction

Although the DEDD catalytic exonuclease domain comprises a conserved three-dimensional protein fold, the structural organization of different members of this protein family varies considerably. Some enzymes such as RNase T of *E. coli* consist of essentially only the catalytic domain, whereas in other cases, such as the yeast Rrp6 enzyme, the DEDD domain is part of a multidomain protein. Some enzymes function as monomeric proteins, whereas others are expressed as functional dimers or part of larger multimeric complexes. To date, there is no information available about the higher order structural architecture of Rex1.

RNase T and Orn (oligoribonuclease, another DEDD class enzyme from *E. coli*) are homodimeric proteins, in which the catalytic site of one subunit is positioned next to a nucleic acid binding site on the other subunit. The nucleic acid binding site is composed of three distinct peptide motifs containing clusters of lysine and arginine residues that are brought together in the three-dimensional structure and constitute a surface patch of positively charged residues (Zuo et al., 2007). The juxtaposition of the nucleic acid binding site to the catalytic active centre explains the requirement for dimerization of RNase T in order for it to carry out catalysis. The RNase T dimer interface includes a number of protuberances and cavities, with conserved hydrophobic residues L157 and W201 being buried deep within the structure of the other subunit.

The mammalian DEDD enzyme PARN (poly(A)-specific ribonuclease) is also a homodimer and, like RNase T, dimerization is required for catalytic activity because it facilitates the spatial alignment of the catalytic active site and a nucleic acid binding site. In this case, however, the substrate binding site is provided by an R3H subdomain (Grishin, 1998), which forms an additional lobe on the DEDD structural fold (Wu et al., 2005). The R3H domain lacks a significant basic patch but serves as a cap to enclose the poly(A) binding cavity at the active site of the enzyme and

contributes significantly to substrate binding and catalysis. The nuclease domain of PARN is sufficient for dimerization but it utilizes a distinct interaction surface, compared to that of RNase T and Orn (Wu et al., 2005). PARN is a multidomain protein that also contains an mRNA cap-binding domain. Interaction with the mRNA cap increases substrate binding and stimlulates the enzyme's processivity.

RNase D of *E. coli* is a monomeric protein that has, in addition to the DEDD catalytic domain, two α-helical HRDC (Helicase and RNase D C-terminal) domains that contribute to RNA binding through the presence of extended patches of basic residues on the protein's surface (Zuo et al., 2005). The three domains are arranged in a funnel-shaped ring structure that facilitates channeling of the substrate to the active site.

Rrp6 comprises a DEDD domain and an adjacent HRDC domain that are topologically equivalent to the catalytic and proximal HRDC domain of RNase D, but the mutual alignment in the two enzymes is different (Midtgaard et al., 2006). The HRDC domain is required for catalytic activity (Phillips & Butler, 2003), consistent with a role in substrate binding. Rrp6 is a component of the exosome RNase complex and it engages in two distinct modes of RNA binding, depending upon whether it mediates threading of the substrate through the central channel of the complex or actively degrades the RNA (Makino et al., 2015)(see Chapter one). The DEDD and HRDC domains are rather rigidly connected and in either case the substrate contacts residues within the HRDC domain. The active site is blocked in the substrate channeling mode by a flipped out conformation of Y361 so that it cannot interact with the phosphate group of the 3' nucleotide. Thus, the HRDC domains of RNase D and Rrp6 provide further examples of auxillary substrate binding domains for the DEDD family of exonucleases.

The DEDD domain of Pan2 is also fairly rigidly aligned to the neighbouring UCH-like (ubiquitin C-terminal hydrolase) domain. However, intermolecular interactions between the catalytic site of Pan2 and the nucleotide binding site within Pan3 are thought underlie the Pan3-dependent stimulation of Pan2 deadenylation (Schäfer et al., 2014). The Pan2/Pan3 complex is therefore an interesting example of an

RNase in which optimal substrate binding and catalysis is achieved through juxtaposition of an RNA-interacting domain and a catalytic domain from two distinct proteins.

The exonuclease Pop2 of *S. cerevisiae* lacks two of the four conserved acidic residues that are characteristic of members of the DEDD superfamily but shares the same structural fold and catalytic activity (Thore et al., 2003). Like RNase D from *E. coli*, Pop2 has a monomeric catalytic domain. However, Pop2 is a component of the multimeric Ccr4/Not complex that functions in transcription and mRNA deadenylation (Tucker et al., 2001).

There is currently no data available for the higher order structural organization of Rex1. Threading of the Rex1 sequence onto published three-dimensional structures of DEDD enzymes using the Phyre2 web server (Kelly et al., 2015) allows a comparison of potential conservation of residues that are implicated in either substrate binding or subunit dimerisation. Using Phyre2, a model of the Rex1 catalytic domain was generated by threading the Rex1 polypeptide sequence onto the three-dimensional structure of Pan2 (Figure 21). Residues 224-380 of Rex1 could be superimposed onto the structure of the DEDD domain of Pan2 with a confidence score of 100%.The secondary structure alignments between Rex1 and DEDD domain proteins generated within Phyre2 suggest that none of the basic nucleotide binding site residues found within RNase T are conserved within the predicted three-dimensional fold for Rex1 (see Figure 21). The buried residues L157 and W201 in RNase T are substituted for by residues H333 and G380 in Rex1, which are located on the surface of the modeled catalytic domain. Furthermore, the Rex1 sequence did not map onto the dimerization interface present in PARN. Thus, if Rex1 is a homodimer then it must involve a distinct dimerization interface than that seen in RNase T or PARN.

The yeast Rex1 protein has previously been purified to homogeneity from cell lysates and shown to have an apparent molecular weight of approximately 70 kDa (Frank et al., 1999). The predicted molecular weight of Rex1, based on its amino acid sequence, is 63kDa. This observation suggests that the protein is expressed as a monomeric globular protein. However, the purification procedure from Frank et al. involved exposing the proteins to buffers containing 2M sodium chloride and did not demonstrate that the purified protein had an associated ribonuclease activity. It is therefore feasible that a putative heteromeric complex involving Rex1 would be disrupted during this purification. To date, however, there are no clear candidates for potential Rex1 interacting proteins: Rex1 has not been reported to copurify with other yeast proteins in high-throughput TAP-tag purification studies, and the *REX1* gene is the only (nonessential) gene in S. cerevesiae that is required for normal 5S rRNA processing. Here I present data on the purification and biophysical characterisation of Rex1. The results of glycerol gradient sedimentation experiments and size exclusion chromatography studies show that Rex1 is expressed in yeast as part of a complex with an apparent molecular weight of approximately125kDa. Further data presented here argue against the presence of a Rex1 homodimer. Although not formally conclusive, the cumulative data strongly suggest that Rex1 is part of a heteromeric protein complex.

4.2 Results

4.2.1 *Generation of a strain expressing a TAP-tagged Rex1 fusion protein*

Strains carrying chromosomally encoded TAP-tagged alleles of the desired gene have been routinely used for the biochemical purification of yeast proteins (Puig et al., 2001). The tandem affinity purification (TAP) tag has facilitated the native purification of many proteins to apparent homogeneity (Nilsson et al, 1987) through sequential affinity chromatography procedures, coupled by a selective release from the initial resin, and consists of a calmodulin binding peptide, a recognition site for the tobacco etch virus (TEV) protease and two copies of the z domain of protein A from *S. aureus*. A strain expressing a C-terminal TAP-tagged

Rex1 fusion protein was available in the laboratory (P1022; generated by Rebecca Jones in the Mitchell lab) but details of the strain background were lacking. To generatea clearly defined strain expressing the Rex1-TAP fusion, the *rex1-TAP::URA3* allele was amplified from genomic DNA obtained from strain P1022 and the amplicon was integrated into the *REX1* locus of the standard yeast wild-type strain, BY4741.

The genomic DNA encoding the *rex1-TAP::URA3* locus was amplified using primers complementary to sequence approximately 200 nucleotides upstream and 500 nucleotides downstream of the *REX1* termination codon (primers o869 and o560, Figure 22, panel A). After transformation, candidate integrants were screened by PCR amplification of the *REX1* gene locus using primers complementary to sequences up- and downstream of the REX1 ORF (primers o559 and o560) and the products were compared to those obtained from a wild-type strain and from the original rex1-TAP strain P1022. The amplicon obtained from the P1022 strain is clearly longer than that obtained from the wild-type strain (compare lanes 2 and 3) and the electrophoretic migration of the PCR products was consistent with the predicted sizes of 2.6 kb for the *REX1* allele and 5kb for the *rex1-TAP::URA3* allele. Using genomic DNA from a candidate integrant in BY4741 as the PCR template generated an amplicon of the same size as that seen from the P1022 strain (compare lanes 2 and 4). Furthermore, Sanger sequence analysis of the gel-purified PCR product obtained from the candidate colony using a reverse primer complementary to a sequence within the TAP tag confirmed that integration had occurred at the *REX1* locus and that the sequence of the complete*REX1* coding region had not been altered.

To test for expression of the predicted fusion protein, the isolated *rex1*-TAP strain (P1810) and the isogenic wild-type strain BY4741 harbouring a suitable plasmid were grown in selective minimal medium. Whole cell extracts were prepared under alkaline denaturing conditions (see Materials and Methods) and subjected to

western analysis using the PAP antibody. The predicted molecular weight of the Rex1-TAP fusion protein, based on its amino acid sequence, is 85kDa. A polypeptide of appropriate electrophoretic mobility was detected in the lysate from the *rex1*-TAP candidate strain upon western analysisand there was no signal detected in the wild-type strain (Figure 22, panel C).

4.2.2 *Functional Analysis of the Rex1-TAP fusion protein*

Two experimental approaches were taken to address whether the Rex1-TAP fusion is a functional protein when expressed in yeast. Firstly, cellular RNA was isolated from the rex1-TAP strain and analysed for a defect in 5S rRNA maturation. In contrast to the *rex1Δ* mutant, the rex1-TAP strain did not exhibit a 5S rRNA processing defect (Figure 23, panel C). Secondly, the rex1-TAP allele was integrated into an *rrp6Δ* strain to determine whether the resultant double mutant was viable. PCR amplification of the *REX1* locus in genomic DNA from *URA3*$^{+}$ transformants revealed correct integration at the *REX1* locus (Figure 23, panel A). The correct integration of the tag into the C-terminal region of *rex1* gene was confirmed through DNA sequencing. Rex1-TAP fusion protein was then visualised by western blot analysis using the PAP antibody and the migration of the Rex1-TAP fusion protein corresponds to the expected molecular weight of ~85kDa. This shows that the *rex1* gene tagged in this work appeared correct. RNA analysis of the resultant *rex1-TAP rrp6Δ* double mutant showed no accumulation of an extended form of 5S rRNA (figure 23, panel C). Notably, spot growth assays revealed a clear growth defect for the *rex1-TAP rrp6Δ* double mutant, compared to either single mutant (Figure 23, panel B). One potential explanation for this observation is that the Rex1-TAP fusion protein is not fully functional or expressed at levels lower than the wild-type protein, but not sufficiently impaired as to impact on 5S rRNA maturation. This partial loss of function may not be sufficient to support normal growth in the absence of Rrp6. Alternatively; expression of the Rex1-TAP fusion protein may be partially dependent upon Rrp6 activity.

4.2.3 *Analysis of the relative expression level of the Rex1-TAP protein*

To compare the expression level of Rex1-TAP with that of other functionally related RNA processing factors, western analyses were performed in parallel on denatured cell extracts from the rex1-TAP strain and from isogenic strains expressing theRrp6-TAP, Csl4-TAP, Mpp6-TAP, Trf4-TAP and Mtr4-TAP fusion proteins. Csl4 is a core component of the exosome RNase complex (Allmang et al., 1999) (see Figure 2), Mpp6 is an exosome-associated nuclear protein (Milligan et al., 2008) and Trf4 and Mtr4 are components of the TRAMP complex that functions together with the exosome (Vanacova et al., 2005; Wyers et al., 2005; LaCava et al., 2005).The expression levels of these proteins have been previously reported in the literature, both through comparative western analyses of TAP-tagged strains (Ghaemmaghami et al., 2003) and in a high-throughput mass spectrometry analysis (Kulak et al., 2014).The electrophoretic mobilities of the epitope-tagged proteins (Figure 24, panel C) were consistent with their apparent molecular weights. As shown in Figure 24, the apparent expression level of Rex1-TAP (31.1%) was similar to that of Csl4-TAP (35.6%) and Mpp6-TAP (30.7%). The published expression levels are subject to a number of variables, such as stability of the protein fusion and peptide coverage of the mass spectrometry data, and vary considerably between the two experimental approaches. However, exosome core components such as Csl4 have consistently been calculated to be present at approximately 5,000 proteins per cell. It can therefore be concluded that Rex1 is also expressed at approximately 5,000 molecules per cell. As both Csl4-TAP and Mpp6-TAP have successfully been used to purify exosome complexes (Gavin et al., 2002: Milligan et al., 2008), this suggests that purification of Rex1-TAP using routine TAP purification procedures would yield sufficient material it identify the nature of any copurifying proteins. Consistent with previously published data, the expression levels of Tr4-TAP (71.7%) and Mtr4-TAP (100%) are significantly higher than that of the core exosome complex. The observed expression level of Rrp6-TAP was much higher than that of the exosome complex (Figure 24 panel C, compare lanes 2 and 3), which is in contrast to previously published findings (Ghaemmaghami et al., 2003).

This may reflect the fact that these analyses were carried out on denatured cell extracts, rather than native cell extracts.

Many constitutively expressed cellular proteins are sensitive to degradation as the culture density increases. To address the expression profile of Rex1-TAP during batch culture, cells were harvested at different points during growth and through stationary phase, and the level of Rex1-TAP was analysed by SDS-PAGE and western blotting (Figure 24, panels A and B). Rex1-TAP was stably expressed up to cell densities of $2OD_{600}$ (Figure 24, panel A) and then subsequently decreased during stationary phase (Figure 24, panel B). These data demonstrate that Rex1-TAP is stably expressed through logarithmic growth.

4.2.4 *Purification of Rex1-TAP by ion exchange chromatography*

Ion exchange chromatography provides a widely applicable purification step that is also a convenient manner in which to concentrate proteins. Lysate from a strain expressing the Rex1-TAP fusion protein was incubated with Q-sepharose and SP-sepharose beads and the lysate and non-bound fractions were assayed by SDS-PAGE and western blotting. Rex1-TAP was observed to be completely depleted from the lysate upon incubation with SP-sepharose beads using a cell lysis buffer containing 150mM NaCl (Figure 25, left panel). In contrast, there was no depletion of Rex1-TAP from the cell lysate upon incubation with Q-sepharose beads (Figure 25). It was empirically determined that increasing the salt concentration of the buffer to 450mM NaCl was sufficient to quantitatively elute the bound Rex1-TAP from the SP-sepharose beads. Based on its amino acid composition, Rex1 has a neutral isoelectric point. This suggests that the protein has a patch of positively charged residues that enable it to bind to the cation exchange resin, SP-sepharose. Many nucleic acid binding proteins bind to SP-sepharose beads through the nucleic acid binding region.

4.2.5 *Glycerol gradient analyses of Rex1 proteins*

The apparent size and heterogeneity of native Rex1 fusion proteins in yeast cell extracts were analysed by glycerol gradient centrifugation. Lysates from cells expressing either the chromosomally encoded Rex1-TAP protein or plasmid-encoded zz-Rex1 fusion protein were fractionated by utracentrifugation through glycerol gradients and the protein content of individual fractions was analysed by a combination of SDS-PAGE and either colloidal Coomassie blue staining or western blotting, using the PAP antibody complex (Figure 26). Protein standards with known sedimentation characteristics (chicken egg lysozyme, 1.9S; chicken egg ovalbumin, 3.5S; bovine serum albumin, 4.6S; yeast alcohol dehydrogenase, 7.4S; beef liver catalase, 11.3S) (Erickson, 2009) were analysed in parallel gradients or resolved through the same gradient after mixing with the SP-sepharose eluate fraction of the cell lysate. A representative example of the data from independent triplicate samples is shown in Figure 27.

Rex1-TAP sedimented as an apparently homogeneous species, with a peak in fractions 7 and 8 (Figure 26A, upper panel). The peaks of homogeneous proteins appear relatively broad upon glycerol gradient analyses (compare the distribution of Rex1 with that of the characterised protein standards such as BSA), compared to gel filtration analyses, and this is exacerbated when moderate signal strengths are obtained. The sedimentation behaviour of Rex1 was similar to that of yeast alcohol dehydrogenase (Figure 27A, lower panel), which has a sedimentation coefficient of 7.4S and a predicted molecular weight for the homotetramer of 147kDa. This would suggest that Rex1-TAP, which has a predicted molecular weight of 63kDa, is probably expressed as part of a complex rather than a monomeric protein. Comparable sedimentation profiles were obtained for the Rex1-TAP protein when whole cell lysates were analysed and after pre-fractionation of the lysate by ion exchange chromatography using SP-sepharose beads. Thus, the putative Rex1 complex is stable in moderately high salt buffers containing 450mM NaCl.

The N-terminal zz-Rex1 fusion protein consistently resolved into two peaks upon glycerol gradient centrifugation. One species was coincident with that observed for

Rex1-TAP in fractions 6 and 7, while another, slower sedimenting peak was observed in fraction 4(Figure 26). The slower sedimenting Rex1 species migrated through the gradient at a rate similar to that of BSA, the molecular weight of which (66kDa) is similar to that of the predicted molecular weight of Rex1 (63kDa). This suggests that the slower sedimenting form of Rex1 represents a monomeric species, while the faster sedimenting form represents the fraction of Rex1 that is part of a larger complex. Expression of Rex1 from the *RRP4* promoter on the plasmid led to higher expression levels than were observed for the chromosomally encoded Rex1-TAP fusion protein (Figure 9). This would be consistent with the overexpressed fraction of Rex1 being excluded from a heteromeric protein complex and being present as excess monomeric protein. From this data it can be concluded that Rex1-TAP is most likely expressed in yeast as part of a heteromeric complex.

4.2.6 *Determination of the native molecular weight of yeast Rex1*

Size exclusion chromatography is commonly used to infer the unknown molecular weight of a protein. The derived values can be fairly accurate for globular proteins but an elongated protein can elute at a volume corresponding to a molecular weight that is twice that of a globular protein of the same size. This is because a protein passes through a gel filtration column on the basis of its frictional coefficient (or Stoke's radius) rather than its molecular weight (Siegel &Monty, 1966). The Svedberg equation expresses the molecular weight of a substance in terms of its sedimentation coefficient and its frictional coefficient (Erickson, 2009). Therefore, a good estimate of the molecular weight of a protein can be obtained by determining the sedimentation coefficient by glycerol density gradient centrifugation and the frictional coefficient by size exclusion chromatography. This approach has a precision within approximately 10% and is applicable to the analysis of proteins in complex mixtures such as cell lysates, as long as a suitable antibody is available.

Glycerol gradient centrifugation analyses were performed on yeast extracts after purification by SP-sepharose ion exchange chromatography, and the yeast protein samples were mixed together with protein standards before fractionation to avoid any variation in the preparation of the gradients (Figure 27). Triplicate samples were analysed in parallel and the protein distributions were determined by a combination of colloidal Coomassie blue staining or western blotting of SDS-PAGE gels. Protein elution volumes were determined by quantifying the signal obtained for each protein and fitting the values to a gaussian distribution curve (see Table 8). By plotting the elution volume of the protein standards against their known sedimentation coefficients and mapping the elution volume of Rex1-TAP onto this standard curve, an estimate for the sedimentation coefficient of Rex1-TAP of 7.1S was obtained (the average of triplicate value).

Rex1-TAP was purified by ion exchange chromatography using SP-sepharose beads prior to analysis by gel filtration chromatography. Protein standards (alcohol dehydrogenase, ovalbumin, bovine serum albumin and catalase) that had been used for sedimentation velocity analyses were also resolved through the same Superdex 200 column, using the same buffer. As above, the elution volumes for each protein were determined by quantifying the signal in each fraction and plotting the values against a normal distribution curve and the analysis was performed on three independent samples. Rex1-TAP eluted with a peak in fraction 25 (average of trplicate samples, 26.1, 25.3, and 25.2), which partially overlapped the elution profile of yeast alcohol dehydrogenase (Figure 28). By plotting the observed elution volumes of the protein standards against their known Stoke's radii and calculating the line of best fit using Standard Curve Excel, the observed elution volume of 25.5ml for Rex1-TAP correlates with a Stoke's radius of 4.2nm.

Using the simplified Svedberg equation M=4,205(SRs) (Erickson, 2009), where M is the mass in daltons, S is the Sedimentation coefficient in Svedberg units and Rs is the Stoke's radius in nm, the native molecular mass of Rex1-TAP was determined to be 125,400 daltons.

Table 8 : The elution volume of diffent proteins of glycerole gdadient in triplicate samples

	Experiment 1		Experiment 2		Experiment 3	
	Elution volumes	S -value	Elution volumes	S -value	Elution volumes	S -value
Lysosyme	2.4	1.9	2.4	1.9	2.8	1.9
Oval Albumin	3.1	3.5	3.5	3.5	3.3	3.5
BSA	4.9	4.6	4.3	4.6	4.4	4.6
ADH	7.1	7.4	6.8	7.4	6.7	7.4
Catalase	10.5	11.3	10.1	11.3	9.3	11.3
Rex1	6.9	**7.2**	6.5	**7**	6.4	**7.2**

4.2.7 *Co-immunoprecipitation analysis of differentially tagged Rex1 proteins*

The predicted molecular weight of the Rex1-TAP fusion protein, based on its amino acid sequence, is 85kDa. In contrast, the glycerol gradient sedimentation analyses and gel filtration experiments described above suggested that the native Rex1 protein has a molecular weight of 125kDa. To rule out the possibility that Rex1 is expressed as a homodimer, pull-down experiments were performed on lysates from cells expressing two differentially tagged forms of the protein. Rex1-TAP and zz-rex1 fusion proteins were available, which enable the purification of putative Rex1 complexes on IgG sepharose beads. An additional construct was generated that allowed the expression of a Rex1-myc fusion protein.

A genomic clone of the yeast *REX1* gene (p772) was generated by PCR amplification of the locus and cloning of the gene into the centromeric vector pRS314 (Sikorski & Hieter, 1989). The clone was confirmed by restriction digestion and sequence analysis of the complete REX1 ORF (data not shown). Transformation of this *REX1* clone into the *rex1Δ, rrp47Δ* plasmid shuffle strain P596 (Costello et al., 2011) supported growth of the transformant on medium containing 5-FOA (Figure 29, panel A), demonstrating that the clone expresses a functional protein. To generate a vector expressing a rex1-13myc fusion, a cassette encoding 13 copies of the myc

tag, the terminator region of the *ADH1* gene and a downstream *kan::MX4* selectable marker (Longtine et al., 1998) was amplified by PCR and cloned into the *REX1* genomic clone by homologous recombination. A candidate clone was screened by restriction analysis and validated by sequence analysis through the region of homologous recombination (data not shown). The rex1-13myc fusion protein was shown to be functional in the plasmid shuffle assay (Figure 29, panel A). Western analysis of a cell lysate from a strain expressing the rex1-13myc fusion protein detected a single polypeptide that migrated in the SDS-PAGE gel with an electrophoretic mobility that correlates well with its predicted molecular weight of 95kDa (Figure 29, panel B). The specificity of the anti-myc antibody is demonstrated by the fact that there is no signal observed in the lysate from a wild-type yeast strain (Figure 29, panel B, compare lanes 2 and 3).

Plasmids expressing the zz-rex1 and rex1-13myc fusion proteins were transformed into a *rex1Δ* strain, cell lysate from the resulting transformant was incubated with IgG sepharose beads and retained protein was eluted by boiling in SDS-PAGE loading buffer. Aliquots of the cell lysate, bound and non-bound fractions were analysed by SDS-PAGE and western blotting (Figure 29, panel C). The zz-rex1 fusion protein was quantitatively depleted from the cell lysate upon incubation with IgG sepharose beads and efficiently eluted under denaturing conditions. In contrast, there was no clear depletion of the rex1-13myc fusion protein and there was no detectable signal in the eluate. Furthermore, a reverse pull-down experiment revealed that the rex1-13myc protein could be efficiently depleted upon incubation with beads charged with anti-13myc antibodies but no signal was observed for the zz-rex1 fusion protein (data not shown). The inability to demonstrate a physical interaction between zz-rex1 and rex1-13myc support the conclusion that Rex1 is not expressed in yeast as a homodimer. Therefore, the difference between the predicted molecular weight and apparent molecular weight of Rex1-TAP strongly suggests that the protein is associated with one or more other proteins.

4.3 Discussion

Studies on the hydrodynamic properties of Rex1 presented here have demonstrated that the native protein is expressed in yeast as part of a larger heteromeric complex. The key observations were that(i) Rex1, which has an electrophoretic mobility upon SDS-PAGE analysis that is consistent with its predicted molecular weight of 63kDa, sediments through glycerol density gradients with a higher than predicted velocity when expressed from the homologous *REX1* locus, and(ii) that higher levels of expression of Rex1 from an episomal plasmid led to the accumulation of a species with a significantly slower sedimentation velocity. These data are consistent with the faster sedimenting fraction corresponding to a heteromeric complex containing Rex1 and the slower sedimenting complex that accumulates upon Rex1 overexpression correlating to the monomeric protein. In support of the conclusion that the faster sedimenting complex is not due to a homodimeric Rex1 complex, no association was detected between two differentially tagged copies of Rex1 that were coexpressed in yeast. A combination of size exclusion chromatography and glycerol gradient sedimentation velocity analyses allowed the size of the Rex1 complex to be estimated to be 124kDa.

One possibility that cannot be excluded from the data is that the Rex1 complex reflects an association between the tagged protein and a chaperone protein that does not reflect the physical state of non-tagged Rex1 in wild-type cells. However, this is unlikely since the functional Rex1-TAPfusion protein is expressed essentially exclusively in the form of the heteromeric complex. It is also formally possible that the N-terminal zz tag and the C-terminal 13myc tag prevent Rex1 from forming a homodimer. However, the estimated molecular weight of the Rex1 complex is significantly less than the 168kDa predicted for a Rex1 homodimer. Furthermore, data presented in Chapter five provides indirect but strong evidence that the zz-Rex1 fusion protein also does not interact with another N-terminally tagged form of Rex1 (GFP-Rex1). The physical architecture of yeast Rex1 is therefore distinct from the homodimeric arrangement of the functionally homologous *E. coli* protein, RNase T. Notably; Rex1 lacks the residues that constitute the dimerization interface

of either RNase T or PARN (Figure 21). The data strongly support the conclusion that Rex1 is associated with one or more other proteins with a combined molecular weight of approximately 40kDa.

The heteromeric complexed form of Rex1 presumably reflects the functional state of the protein, since the Rex1-TAP is quantitatively expressed in this stable complex. It would therefore be predicted that mutations in other components of this complex would elicit similar defects in the 3' end maturation of 5S rRNA. Deletion of the *SNU66* gene has been reported to elicit a partial block in 5S rRNA maturation during growth at 20°C (Li et al., 2009). The 5S rRNA processing phenotype was not observed in the *snu66Δ* mutant during growth at 30°C (data not shown). The cold-sensitive 5S rRNA maturation phenotype for the *snu66Δ* mutant, which also exhibits a cold-sensitive growth phenotype (Stevens et al., 2001), suggests that Snu66 functions as a chaperone protein during 5S RNP assembly and/or processing rather than a processing factor.

Consideration of the proteins that have been shown to interact with Rex1 biochemically may potentially reveal candidates for additional components of the Rex1 heteromeric complex. A number of proteins have been identified to interact biochemically with Rex1, the majority of which are unlikely to be involved in stable interactions with Rex1 since they are protein kinases that were shown to phosphorylate Rex1 *in vitro*. Another unlikely identified candidate is Sbp1 (Mitchell et al., 2013), a cytoplasmic protein that functions in translational repression. Rex1 was identified as an interactor of the methyltransferase Hmt1in a genome-wide DHFR protein fragment complementation assay (Messier et al., 2013). Hmt1 is an abundant nuclear protein and a Rex1/Hmt1 complex would have a molecular weight of 124kDa, the estimated size of the Rex1 heteromeric complex. However, Rex1 is not known to be methylated and a potential molecular function of Hmt1 in 5S rRNA processing is not obvious. Finally, Rex1 has been shown to interact with Rpn11, a component of the 19S regulatory subunit of the proteasome (Kaake et al., 2010). The reason for a physical association between Rex1 and Rpn11 is not clear, but this may reflect targeting of Rex1 to the proteasome for degradation. Another

potential approach to identify candidate interacting proteins is to compare the expression profile of a gene. However, no other yeast gene with a significantly similar expression profile was revealed upon analysis using SPELL (serial pattern of expression levels locator) (Hibbs et al., 2007). Finally, since Rex1 appears to be primarily associated with the processing of RNA transcripts that are generated by RNA polymerase III (5S rRNA, tRNAs) it is feasible that Rex1 is associated with a regulatory component of the RNA polymerase III transcription machinery. There is a number of yeast proteins associated with RNA polymerase III that would be potential candidates (Acker et al., 2013) but there is no evidence to link any of them directly to RNA processing events.

The generation of a yeast strain expressing the Rex1-TAP fusion protein will facilitate future studies on the purification of the Rex1 heteromeric complex, identification of the interacting protein(s) and their functional analysis. These studies have established a feasible protocol for the initial stages of purification of the Rex1 protein, involving passage through Q-sepharose and retention upon SP-sepharoseion exchange chromatography media. These observations were exploited in order to purify Rex1 proteins for in vitro RNA binding and degradation assays, described in Chapter Six.

Chapter Five

Subcellular localization of wild-type and mutant Rex1 proteins

5.1 Introduction

In principle, a loss of function mutation within an enzyme may be due to defects in protein expression through misfolding and/or instability, protein localization, assembly of the protein into larger structures, substrate binding, product release or catalysis. While the *rex1* deletion mutants generated in these studies had a strong impact on protein expression levels (Figure 14) and therefore have an impact on protein folding (as would be expected for large deletions), offsetting the decreased expression level did not allow complementation of the *rex1* growth and RNA processing phenotypes. Thus, the *rex1* loss of function mutants is not limiting in terms of protein expression. In this Chapter I present the results of subcellular localization studies on the *rex1* mutants. The subsequent Chapter addresses the effects of the *rex1* mutants on substrate binding and catalysis.

The localization pathways of nuclear ribonucleases of the DEDD family have not been particularly well characterized. The nuclear exosome-associated RNase Rrp6 interacts with the importin α/β heterodimer (Srp1/Kap95 in yeast) (Peng et al., 2000). This interaction is most likely mediated through the two NLSs close to the C-terminus of Rrp6 that are required for its normal import into the cell nucleus (Phillips & Butler, 2003). The Dis3 does not clearly interact with an importin (Mitchell et al., 2003; Dziembowski et al., 2007) but the components of the core complex shows interactions with the Srp1/Kap95 heterodimer (Peng et al., 2003), suggesting the exosome is imported as a pre-assembled complex. The Rrp6-associated protein Rrp47 does not copurify with Srp1 (Feigenbutz et al., 2013), suggesting that formation of the Rrp6/Rrp47 complex occurs after import of Rrp6 into the nucleus. Interestingly, the highly conserved nuclear export factor Crm1 interacts with Rex3 and Rex4, which are both nuclear proteins (Huh et al., 2003), as well as the cytoplasmic protein Pop2 (Kirli et al., 2015).This observation may be explained by the fact that Crm1 also functions to regulate nuclear processes

through the conditional export of proteins, such as transcription factors and cell cycle factors. It is probable that Pop2, as a component of the Ccr4/Not complex, shuttles between the nucleus and the cytoplasm to fulfill roles in both transcription and mRNA turnover. Notably, Crm1 also functions to back-export cytoplasmic proteins that may have toxic effects in the nucleus (Kirli et al., 2015). Pan2 is a cytoplasmic protein (Huh et al., 2003), while Rex2 is reported to be localized to mitochondria (Hanekamp &Thorsness, 1999). There is no reported interaction between a karyopherin and the nuclear protein Rex1.

GFP fusions of the wild-type and mutant forms of Rex1 were generated and their subcellular distribution was determined by fluorescence microscopy of non-fixed cells. A small peptide sequence within the N-terminal region of Rex1 was defined that is required for nuclear import of Rex1 and sufficient to drive the nuclear localization of the GFP reporter protein. Furthermore, correct nuclear localization of Rex1 was shown to be dependent upon the yeast importin-α, Srp1.

5.2 Results

5.21 *Construction of GFP-Rex1 and GFP expression vectors*

The strategy used to generate a vector expressing the N-terminal GFP-Rex1 fusion protein was to substitute the DNA sequence encoding the zz tag in the zz-Rex1 expression vector for a sequence encoding the GFP protein. The zz tag is flanked by *Nco*I and *EcoR*I restriction sites. While there are no *EcoR*I sites within the *REX1* or GFP coding regions, there are multiple *Nco*I sites. In order to substitute the DNA tag sequences, an *EcoR*V site was first introduced directly downstream of the initiation codon of the zz tag by site-directed mutagenesis and then the GFP tag was amplified by PCR from a suitable expression vector as an *EcoR*V-*EcoR*I fragment, before substitution cloning into a zz-Rex1 expression construct based on the pRS313 vector (Sikorski & Hieter, 1989), which bears the *HIS3* marker gene. Candidate clones were initially screened by restriction digestion and then validated by sequence analysis across the complete length of the cloned GFP fragment.

The resulting GFP-Rex1 expression construct was transformed into the *rex1Δ rrp47Δ* plasmid shuffle strain P596 (Costello et al., 2011) and analysed for expression of the fusion protein and for complementation of the *rex1Δ rrp47Δ* synthetic lethality. Denatured whole cell lysates were prepared using the alkaline lysis method and analysed by SDS-PAGE and western blotting, using a GFP-specific antibody (Figure 30, panel A). The GFP-Rex1 fusion protein migrated through the SDS-PAGE gel with an electrophoretic mobility that is consistent with the predicted molecular weight, based on its amino acid sequence, of 95kDa. The detected signal was specific for the GFP fusion protein, since no signal was detected in the lysate from a strain transformed with the pRS313 control plasmid (compare lanes 2 and 3). Cells expressing the GFP-Rex1 fusion protein was are to grow on medium containing 5-FOA, whereas the transformant harbouring the pRS313 vector did not produce colonies on this medium (Figure 30, panel B). These data show that the GFP-Rex1 fusion is stably expressed in yeast and able to complement the synthetic lethality of the *rex1Δ rrp47Δ* double mutant.

To generate a plasmid that could be used in future to express N-terminal GFP fusions, the *Xba*I-*EcoR*I fragment from the GFP-Rex1 expression construct, which comprises the constitutive *RRP4* promoter and the GFP ORF with a 3' *EcoR*I site, was subcloned into the yeast shuttle plasmid pRS416. This construct is suitable for cloning genes of interest downstream of the GFP cassette but does not itself stably express GFP, since it lacks an appropriately positioned termination codon. In order to express GFP in yeast as a negative control for fluorescence localization experiments, a termination codon was introduced after the GFP encoding sequence by site-directed mutagenesis. The resultant plasmid (p824) lacks the downstream *EcoR*I site, since this was deleted to simplify screening of candidate clones. SDS-PAGE and western analysis of lysate from a strain expressing the GFP construct revealed stable expression of a protein with an electrophoretic mobility consistent with the predicted size of 28kDa (Figure 30, panel A).

5.2.2 *The GFP-Rex1 fusion is localized to the cell nucleus*

The GFP-Rex1 protein was expressed in a *rex1Δ* mutant strain (P596), together with the nuclear peripherymarker RFP-Nic96 (Huh et al., 2003; Campbell et al, 2002), and the proteins were visualized in actively dividing cells by fluorescence microscopy. Of the cells analysed that expressed GFP-Rex1, none showed a nonlocalised fluorescence and all the cells that expressed both GFP-Rex1 and RFP-Nic96 showed a clear nuclear fluorescence (Figure 31). Conversely, a nonlocalised fluorescence signal was observed in cells expressing GFP alone. The images shown are merged z stack images and so the fluorescence signal from RFP-Nic96 reflects the complete nuclear periphery, rather than providing the halo pattern seen for a single z plane image. From the data shown it can be clearly concluded that the GFP-Rex1 protein is localised to the yeast cell nucleus.

5.2.3 *The N-terminal region of Rex1 contains an NLS*

To perform fluorescence microscopy on the *rex1* mutant proteins, each deletion allele was subcloned from the constructs based on pRS415 that express zz-rex1 fusions into the GFP-Rex1 expression construct based on pRS313. Sub-cloning was carried out by restriction digestion with EcoRI and *Age*I, which excises the complete *REX1* ORF and 3' UTR. Plasmids encoding the mutant GFP-rex1 fusion proteins were then transformed into the *rex1Δ rrp47Δ* plasmid shuffle strain P596 (Costello et al., 2011) for complementation analyses, expression analyses by western blotting and for fluorescence microscopy.

Consistent with the analyses of the *zz-rex1* fusion constructs (Figure 13), spot growth analyses of the transformants on medium containing 5-FOA demonstrated that none of the GFP-*rex1* deletion mutants could complement the growth phenotype of the*rex1Δ rrp47Δ* double mutant (Figure 32, panel C). SDS-PAGE and western blot analyses of alkali-denatured cell lysates (Figure 32, panels A and B) revealed the expression of GFP fusion proteins that migrated with electrophoretic

mobilities that were consistent with their predicted molecular weights. Notably, the expression levels of all the deletion mutants are clearly lower than the full-length wild-type protein and the expression of the *GFP-rex1Δ1-82* mutant was low and below the threshold for detection by immunoblotting for some samples (Figure 32, compare panels A and B).

The subcellular localization of the mutant GFP-rex1 fusion proteins were analysed by fluorescence microscopy on cells that also expressed the nuclear periphery marker RFP-Nic96 (Figure 33). Cells expressing the full-length GFP-Rex1 fusion protein or GFP were used as controls. As shown previously, the GFP-Rex1 fusion showed a clear localization to the nuclear compartment, while GFP gave a nonlocalised pattern. The *rex1Δ528-576*, *rex1-W509X* and *rex1Δ82-202* mutants showed a clear nuclear localisation, in each case the GFP fusion protein being clearly detectable within the subcellular volume containing RFP-Nic96 (Figure 33). Of the cells analysed for each mutant, none showed detectable cytoplasmic fluorescence. These data suggest that the lack of function of these mutant alleles reflects a defect in a nuclear Rex1-dependent process. In contrast, the *rex1Δ1-202* and the *rex1Δ1-82* mutants showed a delocalized fluorescence that showed a limited overlap with the RFP-Nic96 fluorescence. The lack of function of these *rex1* mutants would therefore appear to be at least in part due to defective subcellular localization or nuclear tethering. Note that although the expression level of the *GFP-rex1Δ1-82* protein was much lower than the full-length GFP-Rex1 fusion, a signal was clearly detected by fluorescence microscopy. These data support the conclusion that the N-terminal 82 residues of Rex1 are required for its correct localization to the cell nucleus.

The *REX1* coding sequence was screened for potential NLSs using the web server-based prediction tools NLStradamus (Nguyen et al., 2009) and NLS Mapper (Kosugi et al., 2009). The NLStradamus package identified the sequence KNKKKKKAK at residues 42-50 within the *REX1* ORF as constituting a strong monopartite NLS, whereas NLS Mapper identified the longer, overlapping sequence GSKKRRLSKTSVQEDDHTNVVSEVNKNKKKK (residues 17-47) as a bipartite NLS (Figure

34). Specific deletions were generated in the GFP-Rex1 expression construct that removed either the putative monopartite or biopartite NLS and the effect of the mutations on protein function, expression and localization were assessed. To delete the putative monopartite NLS, unique *Mlu*I and *Stu*I restriction sites were introduced up- and downstream of the predicted signal sequence, respectively, by site-directed mutagenesis and the intervening sequence was removed by blunt end cloning using klenow DNA polymerase. The construct lacking the putative monopartite NLS is denoted *GFP-rex1Δ42-52*. To delete the putative bipartite NLS, an additional *Stu*I site was introduced upstream of the predicted signal sequence in the *rex1Δ42-52* mutant and the intervening was delete by digestion wit S*tu*I, followed by religation. The construct lacking the putative bipartite NLS is denoted *GFP-rex1Δ17-52*. Both constructs were verified by restriction digestion analyses and sequence analysis across the region of the mutation.

SDS-PAGE and western analysis of the candidate NLS mutants showed that the *GFP-rex1Δ42-52* mutant protein was expressed at a level similar to that of the full-length wild-type protein, whereas the expression of the *GFP-rex1Δ17-52* mutant was significantly reduced (Figure 35, panel A). Plasmid shuffle assays demonstrated that both the *rex1Δ42-52* and *rex1Δ17-52* mutants were able to substitute for loss of the wild-type *RRP47* gene in the *rex1Δ rrp47Δ* double mutant (Figure 35, panel D). These data demonstrate that both *rex1Δ42-52* and *rex1Δ17-52* alleles encode functional proteins that are able to support normal cell growth. Thus, the *rex1Δ17-52* allele was observed to be functional despite an approximately three-fold reduction in protein expression, compared to the full-length Rex1 protein. This is consistent with the conclusion that the loss of function of the *rex1* N- and C-terminal region deletion mutants (Figure 13) was not due to insufficient protein expression. Fluorescent microscopy analyses revealed that the *GFP-rex1Δ42-52* protein was localised to the cell nucleus, similar to the full-length Rex1 fusion protein (Data not shown). In contrast, the *GFP-rex1Δ17-52* protein did not accumulate in the cell nucleus but showed a more even distribution throughout the

nucleus and cytoplasm, similar to the *GFP-rex1Δ1-202* and *GFP-rex1Δ1-82* mutants (compare Figures 36 and 33).

To determine whether residues 17-52 of Rex1 are sufficient to function as an NLS, oligodeoxyribonucleotides encoding this peptide were ligated to the 3' end of the GFP ORF within the GFP expression construct and the subcellular localization of the resultant fusion protein, denoted GFP-Rex1$_{NLS}$, was determined by fluorescence microscopy. SDS-PAGE and western blot analyses revealed that the GFP-Rex1$_{NLS}$ was stably expressed in yeast (Figure 35, panel C). The GFP-Rex1$_{NLS}$ protein showed a clear nuclear localization, as demonstrated by coexpression with the RFP-Nic96 marker (Figure 36). It can be concluded from this data that residues 17-52 are necessary and sufficient for the stable accumulation of GFP-Rex1 in the cell nucleus.

5.2.4 *Overexpression of zz-Rex1 does not lead to nuclear accumulation of GFP-rex1Δ17-52*

Glycerol gradient sedimentation and gel filtration analyses revealed that the native molecular weight of Rex1-TAP is about 125 KDa which might reflect the expression of Rex1 as a homodimer or as part of a heteromeric complex. A prediction of the hypothesis that Rex1 is expressed as a homodimer is that overexpression of the wild-type form of the protein, but not of a mutant lacking the NLS, would cause the nuclear accumulation of a Rex1 mutant that lacks the NLS. To address this, a 2μ plasmid encoding zz-Rex1 was transformed into a strain expressing the *GFP-Rex1Δ17-52* fusion protein and the subcellular localization of the fluorescent protein was visualized by fluorescence microscopy. The *GFP-rex1Δ17-52* protein remained mislocalised upon overexpression of zz-Rex1 (Figure 37). This data argue strongly that Rex1 does not form a stable homodimeric complex.

5.2.5 *The rex1Δ17-52 mutant is defective in 5S rRNA processing*

Given that the *rex1Δ17-52* mutant was not localized to the cell nucleus (Figure 36) but was able to complement the *rex1Δ rrp47Δ* double mutant (Figure 35), 5S rRNA processing in the *rex1Δ17-52* single mutant and the *rex1Δ17-52 rrp47Δ* double mutant was analysed by resolving cellular RNA through denaturing acrylamide gels and performing northern blot hybridization analyses. The *rex1Δ17-52* mutant exhibited a partial defect in the 3' end maturation of 5S rRNA (figure 38 panel A, and 5 and panel B, lane 3), while the *rex1Δ42-52* mutant doesn't show this defective phenotype (figure 38 panel B lane 4). At least two distinct 5S rRNA species can be resolved in the *rex1Δ17-52* mutant that migrate closer together than the wild-type 5S rRNA and the 3' nucleotide extended form seen in the *rex1Δ* mutant (Figure 38 panel A). The *GFP-rex1Δ17-52* mutant does not accumulate in the cell nucleus but is also both excluded from the cell nucleus (Figure 36). One plausible interpretation of these results is that the mislocalization of the r*ex1Δ17-52* mutant has the consequence that its nuclear concentration is limiting for its normal RNA processing functions but sufficient for it to function partially. This would imply a very distributive mode of action of the Rex1 exonuclease, at least for 5S rRNA maturation.

Intriguingly, the partial 5S rRNA processing phenotype observed in the *rex1Δ17-52* mutant was largely suppressed in the *rex1Δ17-52 rrp47Δ* double mutant (Figure 38 panel A, compare lanes 5 and 6). This observation was reminiscent of earlier experiments that had been performed in the laboratory, where the *rrp4-1* temperature-sensitive allele of an exosome core component was shown to suppress the 5S rRNA processing defect of the *rna82-1* mutant (P. Mitchell, unpublished data). Therefore, RNA was isolated from both the *rrp4-1* single mutant and the*rrp4-1 rna82-1* double mutant during growth under nonrestrictive conditions, and the 5S rRNA profiles were compared with those of the *rex1Δ17-52* and *rex1Δ17-52 rrp47Δ* mutants. As can be seen in Figure 38, and consistent with previous studies (Allmang et al., 1999a; Allmang et al., 1999b), the *rrp4-1* single mutant has no 5S rRNA processing defect. Notably, the *rrp4-1 rna82-1* double

mutant has a clear but partial 5S rRNA processing defect that has slightly less penetrance than the *rex1Δ17-52 rrp47Δ* mutant. The *rna82-1* allele is a nonsense mutation within the codon for the W433 residue within the *REX1* ORF (van Hoof et al., 2000). It would appear from the data shown in Figure 38 that the accumulation of the aberrant, 3' extended 5.8S+30 rRNA species observed in the *rrp47Δ* mutant (Peng et al., 2003; Mitchell et al., 2003) was partially suppressed in the *rex1Δ17-52 rrp47Δ* double mutant (centre panel of Figure 38 panel A, compare lanes 4 and 6), suggesting a mutual suppression phenotype.

5.3 Discussion

Rex1 has previously been shown to be localizedto the cell nucleus in fixed cells and when expressed from the heterologous *MET25* promoter (Frank et al., 1999). Here, I extend those earlier findings by showing that a GFP-Rex1 fusion protein accumulates in the nucleus in actively dividing cells when expressed from the homologous *REX1* promoter. I have also mapped a bipartite NLS sequence between residues 17 and 52 within the Rex1 ORF that is necessary and sufficient for nuclear localisation. Since deletion of the amino terminal region of Rex1 spanning the NLS (residues 1-82) causes loss of function, it was predicted that the NLS was required for Rex1 function. However, the *rex1Δ17-52* mutant supported growth of a *rex1Δ rrp47Δ* double mutant. The phenotype observed for the *rex1Δ17-52* mutant is a nonlocalised phenotype, rather than a nuclear exclusion phenotype. One possible explanation for these observations is that the low amount of Rex1 that is present within the nucleus is sufficient to facilitate the Rex1 activity or activities that are necessary for cell growth. An alternative explanation would be that the *rex1Δ17-52* mutant may be able to carry out RNA processing functions partially within the cytoplasmic compartment. It is also possible that Rex1 contains an additional, surrogate NLS sequence, or that it can be imported into the cell nucleus inefficiently through association with one or more other proteins.

The observation that the *rex1Δ1-82* and *rex1Δ17-52* mutants have distinct phenotypes strongly supports the conclusion that the N-terminal region of Rex1 has one or more functions in addition to subcellular localization. One additional function predicted to be present within a region containing an NLS sequence would be RNA-binding activity, since NLS sequences are thought to have coevolved with RNA- and DNA-binding domains (LaCasse & Lefebvre, 1995). The N-terminal region of Rex1 shares no significant predicted structural homology with any characterised RNA-binding protein. However, BLAST searches identified homology (33% identity, 74% similarity over a 54 residue long sequence) between residues 11 to 65 of Rex1, which spans the NLS sequence, and residues 42-105 of theβ subunit of the translation initiation factor eiF2 (Sui3 in yeast) (Figure 39).Importantly, this region of eiF2β contains two of the three lysine-rich tracts that have been shown to function in mRNA binding *in vitro* and are required for the function of the protein *in vivo* (Laurino et al., 1999). The N-terminal 125 residues of eiF2β are structurally disordered (Llácer et al., 2015), suggesting it constitutes a flexible region that can make long range contacts with the mRNA.

The defined bipartite Rex1 NLS GSKKRRLSKTSVQEDDHTNVVSEVNKNKKKK has 19 amino acid linker, which is longer than the dodecapeptide linker in the bipartite NLS of nucleoplasmin but shorter than that of other characterised bipartite NLS sequences such as that of Ty1 integrase (Lange et al., 2010). Linker function is dependent upon the amino acid sequence, which most likely reflects an inherent flexibility of the peptide sequence. Bipartite (as well as monopartite) NLS sequences are recognized by importin-α. Indeed, initial results suggest that the nuclearaccumulation of GFP-Rex1 is blocked in the *srp1-31* mutant, which is defective in importin-α mediated nuclear import (Tabb et al., 2000)(data not shown).

Data presented in the previous chapter support the conclusion that Rex1 is expressed in yeast cells as a stable, heteromeric complex containing one or more additional proteins. To further scrutinize those conclusions, it was addressed whether protein localization studies could provide evidence for a Rex1 dimer. Full-length zz-Rex1 protein was overexpressed in yeast expressing the mislocalised*rex1Δ17-52* mutant. If Rex1 were expressed as a homodimeric complex, it would be anticipated that overexpression of full-length Rex1 would cause a nuclear accumulation of the *rex1Δ17-52* mutant. This effect was, however, not observed. Thus, protein localisation and pull-down approaches have both failed to provide evidence in support of a homodimeric Rex1 complex.

Mislocalisation of the *GFP-rex1Δ17-52* protein allowed partial complementation of the defect in the 3' end maturation of 5S rRNA that is observed in a *rex1Δ* mutant. There are two reasonable explanations as to how the predominantly cytoplasmic Rex1 mutant protein might facilitate the partial processing of 5S rRNA. The most obvious possibility is that the decreased nuclear concentration of the *rex1Δ17-52* mutant enables partial but incomplete processing to occur within the nucleus. Alternatively, the *GFP-rex1Δ17-52* mutant protein may exhibit activity in the cell's cytoplasm and3' end maturation of 5S rRNA might occur at a slow rate on cytoplasmic ribosomes. Both interpretations invoke a distributive mode of action of Rex1, where the enzyme readily dissociates from the 5S rRNA substrate after removal of each nucleotide. Although it cannot be formally excluded that the 3' end maturation of 5S rRNA could occur after assembly into ribosomal particles, the data presented in the following chapter is inconsistent with the ability of Rex1 to act on cytoplasmic ribosomes.

Intriguingly, the partial processing phenotype of the *rex1Δ17-52* mutant was suppressed in the absence of Rrp47, a nuclear exosome-associated protein. Similarly, a temperature-sensitive mutant allele of the core exosome component

Rrp4 suppressed the 5S rRNA processing defect of the *rna82-1* strain (an allele encoding a C-terminal deletion of Rex1). It is counterintuitive that a mutation within one nuclease would suppress the processing defect of another nuclease mutant. However, one feasible explanation for this observation is that a decreased nuclear concentration of Rex1 in the *rex1Δ17-52* mutant causes inefficient 5S rRNA processing and allows a competitive recruitment of the nuclear exosome (or the TRAMP complex) to the 5S rRNA substrate. In this scenario, the 5S rRNA would be nonproductively trapped in exosome-dependent complexes. In mutants of the exosome complex, such complexes are less readily formed and 5S rRNA would be more accessible to Rex1 when it is present at a decreased concentration. Alternatively, the accumulation of incompletely processed or degraded RNAs in exosome mutants would be expected to deplete the effective concentration of a number of important nuclear RNA binding proteins. One such protein, La (known as Lhp1 in yeast), binds to the 3' ends of RNA polymerase III transcripts and protects them against inappropriate nuclease attack (Stefano, 1984; Mathews and Francoeur, 1984; Fan*et al,* 1988; Mitchell *et al,* 1997; Teplova *et al,* 2006). It has been reported that the 3' end processing of some tRNAs is coupled to the regulated balance between the expression of La and Rex1 (Foretek et al., 2016)(see Figure 6).

Chapter Six

Analysis of RNA binding and exonuclease activity of Rex1

6.1 Introduction

Deletion analyses presented in Chapter 3 have demonstrated that the N- terminal and C-terminal regions of Rex1, in addition to the central catalytic domain, are required for its function *in vivo*. Subcellular localization studies have shown that residues 17-52 within the N-terminal region of Rex1 constitute an NLS sequence that is necessary and sufficient for Rex1 localisation to the cell nucleus. However, the function of the C-terminal region of Rex1 has yet to be established, and genetic complementation assays revealed that the N-terminal region of Rex1 has (an)other function(s) in addition to the nuclear localisation of Rex1. In this Chapter I present data addressing the contribution of the different regions of Rex1 to its ability to degrade RNA in vitro and to bind substrate RNA. Furthermore, data are presented that define the cellular RNA substrates that are recognized by Rex1 on a genome-wide scale and reveal differences in its substrate profile in the presence and absence of Rrp6.

Rex1 purified from yeast cell lysates has previously been shown to have a 3'→5' exoribonuclease activity *in vitro*, using artificial model tRNA substrates that were generated by transcription using T7 RNA polymerase (Ozanick et al., 2009). Here I report the development of a Rex1-dependent *in vitro* assay for the 3' end maturation of 5S rRNA that uses purified 5S RNP particles as substrate. Unexpectedly, all of the *rex1* deletion mutants generated in this study caused a loss in ribonuclease activity *in vitro*. *In vitro* poly(U)-binding assays suggest that this may reflect a compromised ability to bind the RNA substrate.

Cross-linking and analysis of cDNAs (CRAC) is a versatile approach to map the sites on cellular RNAs that are bound by RNA binding proteins (Granneman et al., 2009).

The approach is applicable to analyses of actively growing cells and provides nucleotide resolution of the protein/RNA interaction sites. Cross-links are induced by irradiation with UV light and so reflect juxtapositions of amino acid and nucleotide residues within 1 to 2 angstrom. CRAC was developed from similar "individual nucleotide resolution cross-linking and immunoprecipitation" (iCLIP) techniques (reviewed by Huppertz et al., 2014) and exploits the ability to purify yeast proteins highly selectively using tandem affinity purification tags involving at least one purification step under highly denaturing conditions, and the development of high throughput sequencing technologies that permit the generation of millions of sequence reads from short cDNA libraries. Variations on the CRAC technique have been developed that allow the analysis of tertiary inter- and intramolecular RNA interactions (Kudla et al., 2011), the resolution of RNA interactions with distinct domains within a single RNA-binding protein (Schneider et al., 2012), and the resolution of RNA interactions involving an RNA-binding protein that is present in more than one functionally distinct complex (Thoms et al., 2015). Although originally developed for use in yeast, the expression of suitable fusion proteins has also allowed CRAC to be applied to the analysis of RNA-binding proteins in bacteria (Winther et al., 2016; Waters et al., 2017) and mammalian cells (Libri et al., 2012; Helwak et al., 2013).

Here I present the results of a genome-wide CRAC analysis of the RNAs that interact with Rex1 in yeast. The data reveal that the predominant Rex1 substrate is tRNA, although the protein does interact with a broad range of cellular RNAs including mRNA transcripts, snoRNAs and rRNA. There is a pronounced bias in the tRNA reads, indicating a level of selective binding to specific tRNAs. One hypothesis was that the RNA interaction profile for Rex1 would be altered in the absence of Rrp6, and that substrates showing a significantly increased association with Rex1 in an *rrp6Δ* mutant would reflect those substrates that are dependent upon either Rex1 or Rrp6 for their processing or degradation. These data may therefore shed

some light on the basis of the synthetic lethal interaction between *rex1Δ* and *rrp6Δ* alleles.

6.2 Results

6.2.1 *Establishing an in vitro assay for Rex1 exonuclease activity*

Previous studies have demonstrated a Rex1-associated RNase activity using an artificial in vitro-transcribed tRNA substrates (Ozniack et al., 2009). To establish a more appropriate *in vitro* assay for Rex1 exonuclease activity, it was considered preferable that an RNA substrate was used that accumulated in the *rex1Δ* mutant. 5S rRNA was chosen as a potential substrate for an in vitro assay for two reasons. Firstly, 5S rRNA is a highly abundant cellular RNA and therefore could be expected to be readily isolated in suitable quantities. Secondly, 5S rRNA is expressed in clearly distinct forms in wild-type cells and *rex1Δ* mutants that are readily resolved by gel electrophoresis. Thus, a conversion of substrate to product could be assayed by gel electrophoresis.

zz-Rex1 fusion proteins were purified from yeast cell lysates using protocols that had been previously established for the biophysical analysis of Rex1, as outlined in Chapter 4. In brief, cell lysates were prepared in a low salt buffer and incubated first with a Q-sepharose anion exchange resin(that does not bind Rex1) and then the non-bound fraction was incubated with an SP-sepharosecation exchange resin (that captures Rex1 from the lysate). The bound material was then eluted from the SP sepharose beads in a buffer containing 300mM NaCl and the Rex1 protein was captured by affinity chromatography on IgG sepharose beads. The proteins were incubated with substrate while attached to the beads. Fortunately, full-length wild-type Rex1 and all the *rex1* deletion mutants showed the same binding characteristics with respect to the ion exchange resins, and so could be purified using the same protocol. To maximise Rex1 protein yield for the assays, the wild-type and mutant zz fusion proteins were expressed from high copy number 2μ vectors.

5S rRNA substrate was initially gel-purified from total cellular RNA from the *rex1Δ* mutant after electrophoresis through urea-containing acrylamide gels, recovered by extraction in the presence of phenol and ethanol precipitation, and refolded by renaturation in digestion buffer. Despite relevant precautions against ribonuclease contamination, gel purification of 5S rRNA proved problematic and the RNA was consistently recovered in a partially degraded state. As an alternative and more stable source of 5S rRNA substrate, 60S ribosomal subunits were isolated from the *rex1Δ* strain by sucrose density gradient centrifugation. Inspection of a recent cryoelectron microscopy reconstruction of the yeast 60S subunit at 3.9 angstrom resolution (PDB file 5GAK) reveals that the 3' end of 5S rRNA, which is located in the "central protuberance" of the large subunit, is on the surface of the complex and projected towards the solvent (Schmidt et al., 2016). No alteration in electrophoretic mobility of the 5S rRNA could be detected when on-bead assays were performed using purified wild-type Rex1 protein and 60S subunits from the *rex1Δ* strain as the substrate (data not shown). It is possible that the 3' end of the 5S rRNA may not be sufficiently accessible within the context of the 60S subunit to allow processing by Rex1, or that substrate recognition involves contacts at other sites within 5S rRNA or associated proteins that are shielded upon assembly of the 60S subunit. To circumvent such potential limitations in substrate accessibility, 5S rRNP particles were dissociated from the larger ribosomal complexes by sucrose gradient centrifugation in buffers containing EDTA (Comb & Sakaer, 1967 (Blobel, 1971; Steitz et al., 1988). After fractionating the sucrose gradient, the RNA content of each fraction was assayed by acrylamide gel electrophoresis. Fractions containing 5S rRNA but clear of 5.8S rRNA (as a marker for ribosomal subunits) (see Figure 40) were pooled and made up to 10mM $MgCl_2$.

Upon incubation of the purified 5S RNP substrate with the wild-type zz-Rex1 fusion protein, the 5S rRNA was processed within 10 minutes to a product with the same electrophoretic mobility as 5S rRNA from a wild-type strain (Figure 41, panel A). Further incubation of the mixture for up to 30 minutes did not alter the

electrophoretic mobility of the RNA, demonstrating that the 3' extended 5S rRNA substrate underwent limited and accurate trimming in the presence of Rex1. The lack of 5S rRNA species of intermediate length suggests that the processing reaction involves a processive enzymatic activity, consistent with previous analyses of Rex1 (Ozanick et al., 2009). The 3' end maturation of the 5S rRNA substrate was shown to be dependent upon Rex1, since assays performed in parallel on the D229A mutant protein did not cause an apparent shortening of the RNA. Western analyses of the purified proteins revealed that the amount of mutant D229A protein used in the assay was at least as much as the amount of wild-type Rex1 (Figure 41, panel B). Control reactions wherein the 5S RNP substrate was incubated with a mock purification of Rex1 from cells harbouring the vector alone did show a slow and limited shortening of the substrate over the period of the assay, and this effect was also visible upon incubation with the catalytic inactive mutant at the longer time-points. These observations show that there is an additional activity present in the purified protein samples that causes a limited shortening of the substrate but which requires prolonged incubation and does not act on 5S rRNA of wild-type length. These data demonstrate a Rex1-dependent nuclease activity that is able to recapitulate the accurate processing of a 3' extended 5S rRNA precursor to mature 5S rRNA and confirm that the D229A mutant blocks this nuclease activity.

In vitro assays performed on purified *W509X*, *Δ428-476*, *Δ1-82* and *Δ82-202rex1* mutant proteins using the 5S rRNP substrate revealed that all the *rex1* deletion mutants were defective in catalytic activity and failed to generate a detectable level of normal length 5S rRNA, even after 30 minutes incubation (Figure 42, panel A). In contrast, the wild-type Rex1 protein showed a robust 5S RNA processing activity as before (Figure 41) and completely processed the substrate within 10 minutes. Western analyses of the proteins assayed revealed that the amount of mutant and wild-type proteins assayed were comparable (Figure 42, panels B and C). These data demonstrate that the DEDD catalytic domain of Rex1 is insufficient

for catalysis in vitro, and suggest that each deletion impacts on the ability of the Rex1 protein to interact with its RNP substrate.

6.2.2 *The N- and C-terminal regions of Rex1 are required for RNA binding*

An in vitro RNA-binding assay was established to address how the loss of function *rex1* mutants is affected in their ability to interact with RNP substrates. A poly(U) binding assay was used, since Rex1 acts predominantly on RNA polymerase III transcripts, which typically have 3' terminal oligo(U) tracts. Poly(U) RNA was chemically linked through its 3' hydroxyl group to adipic acid dehydrazide agarose beads and, after incubation with partially purified zz-Rex1 proteins, retained protein was specifically eluted by incubation with RNase A (Michlewski & Cáceres, 2010) and the amount of Rex1 protein in the bound and non-bound fraction was assayed by SDS-PAGE and western blotting. Binding of the catalytic inactive D229A mutant was initially assayed, since this mutant would not be able to degrade RNA to which it bound and thereby prevent its own retention, and non-charged beads lacking RNA were used as a control for nonspecific binding. Binding reactions were also carried out in buffer containing EDTA to block catalysis. As can be seen in Figure 43, the *rex1* D229A mutant was detected in the bound fraction upon incubation with beads linked to RNA but no protein was observed in the bound fraction upon incubation with the control beads lacking poly(U) (panel A, compare lanes 1 and 2). Incubation with full-length wild-type Rex1 revealed stable binding with poly(U)-agarose beads (Figure 43 panel A, lanes 3 and 4). These data suggest thatRex1 is able to bind RNA without positioning the 3' end of the RNA in the catalytic centre, since the RNA is immobilised on the solid support through its 3' hydroxyl group, and are consistent with an additional RNA binding site within the protein or an associated factor.

Assays on the *rex1Δ1-202*, *rex1Δ426-478* and *rex1W509X* mutants failed to show clear binding to poly(U) RNA in three independent experiments. Some of the W509X mutant protein is retained on the poly(U)-agarose beads in the example shown in Figure 43 (panel B, lanes 3 and 4) but there is also a low level of retention of the D229A mutant in the control reaction using beads lacking poly(U) RNA

(Figure 43 panel B, lane 2). These data suggest that the N- and C-terminal regions of Rex1 are both required for stable interaction with RNA.

6.2.3 *Generation of strains expressing the Rex1-HTP fusion protein*

In order to perform CRAC analyses on Rex1, a derivative of the BY4741 wild-type strain was generated that expresses a C-terminal Rex1 fusion protein containing a His(6) tag, a TEV protease cleavage site and two copies of the z domain of protein A from *S. aureus* (the "HTP" tag).

Genomic DNA from an *lcp5-HTP* strain available in the laboratory (Turner and Mitchell, unpublished data) was used to amplify the DNA sequence encompassing the HTP tag and the downstream *URA3* selectable marker, and the resulting amplicon was transformed into the BY4741 wild-type strain and an isogenic *rrp6Δ* strain. Integrants were screened by PCR amplification of the *REX1* locus (Figure 44, panel A). As seen in Figure 44, amplification of the *REX1* locus from the wild-strain gave rise to a product with the predicted size of 2.6kb while amplification of the *REX1* locus from either the *rex1-HTP* or*rex1-HTP rrp6Δ* transformants gave rise to a single product that was approximately 2kb longer. Sanger sequence analysis of the gel-purified PCR product using a primer that is complementary to a sequence within the HTP confirmed that integration had occurred at the *REX1* locus and that the sequence of the REX1 coding region had not been altered. PCR amplification of the *RRP6* locus from genomic DNA of a wild-type strain, the *rex1-HTP rrp6Δ* candidate and an *rrp6Δ* control strain confirmed that the presence of the *rrp6Δ* allele in the *rex1-HTP rrp6Δ* candidate strain (Figure 44, panel B, lanes 4-6).

SDS-PAGE and western blotting analysis of denatured cell extracts using the PAP antibody revealed the expression of Rex1-HTP fusion proteins in the *rex1-HTP* and *rex1-HTP rrp6Δ* strains with an apparent molecular weight of approximately 80kDa (Figure 44, panel C). This is in close agreement with the predicted molecular weight of the fusion protein of 83kDa. There was no significant difference in the expression level of the rex1-HTP fusion protein in the presence or absence of Rrp6 (Figure 44 panel C, compare lanes 2 and 3), suggesting that Rex1 expression is not

regulated by Rrp6. The expression level of the rex1-HTP fusion was approximately 20% higher than the expression of the rex1-TAP fusion protein (Figure 44, panel D).

6.2.4 *Functional analysis of the rex1-HTP fusion protein*

Since *rex1Δ rrp6Δ* double mutants are nonviable (van Hoof et al., 2000), the successful isolation of a *rex1-HTP rrp6Δ* double mutant strain demonstrates that the *rex1-HTP* fusion protein is functional. Spot growth analyses revealed that the *rex1-HTP rrp6Δ* double mutant grew more slowly than the wild-type strain. The *rex1-HTP rrp6Δ* double mutant also grew more slowly than the *rrp6Δ* or the *rex1-HTP* single mutant strain (Figure 45, panel B). These data demonstrate that the r*ex1-HTP* fusion protein is able to support growth in the absence of Rrp6 but is compromised to some degree in its ability to carry out a growth rate-limiting process. Denaturing acrylamide gel electrophoresis of total cellular RNA from the *rex1-HTP* single mutant and the *rex1-HTP rrp6Δ* mutant revealed that neither strain exhibited the defect in the 3' end maturation of 5S rRNA that is characteristic of *rex1 Δ* mutants (Figure 45, panel A).These data are consistent with the *rex1-HTP* fusion protein being a functional form of the protein.

6.2.5 *CRAC analyses of the rex1-HTP fusion protein*

CRAC analyses of the *rex1-HTP* single mutant, the *rex1-HTP rrp6Δ* double mutant and wild-type control strain were performed by the Tollervey lab. The catalytically active*rex1-HTP* fusion protein cross-linked to RNA in dividing cells and sequence analyses of the cDNAs identified 129,753 reads in the *RRP6* strain and 115,381 reads from the analysis of the *rrp6Δ* mutant. In contrast, 17,584 reads were obtained from the control strain. A similar ratio of mapped reads between HTP-tagged proteins and non-tagged strains has been previously observed (Granneman et al., 2009). All of the cDNA reads obtained could be mapped to the reference yeast genome (*S. cerevisiae* genome, ensemblerelease 74). The distribution of reads between different classes of transcripts that were obtained for the *rex1-HTP*, *rex1-HTP rrp6Δ* and wild-type strains are shown in Figure 46.

The majority of reads recovered from the *rex1-HTP* strain mapped to tRNAs (62,412 reads; 48% of the total number of reads), but there were also significant numbers of cDNA reads from rRNA (53,274 reads; 41% total reads), mRNA (21,902 reads; 17% total reads) and snoRNA (5904 reads; 5% total reads). A similar but distinct profile was observed in the absence of Rrp6; although the majority of hits were still seen for tRNA (50237 reads; 44% total reads), rRNA (43642 reads; 38% total reads) and mRNA (16777; 15% total reads),a significantly larger percentage of reads were observed for snoRNAs, intergenic transcripts and 5.8S rRNA. These RNAs are characterized substrates of Rrp6 (Briggs et al. 1998; Allmang et al., 1999; Wyers et al., 2005). These observations suggest that Rex1 is recruited tosubstrates that are normally processed or degraded by Rrp6in the *rrp6Δ* mutant.

The enrichment of tRNA reads in the Rex1 CRAC data is consistent with the known role of Rex1 in the 3' end processing of tRNAs (Copela et al, 2008; Foretek et al, 2016). Rex1 has been shown to act on $tRNA^{Arg}_{UCU}$ species that is processed from a dicistronic transcript (Piper& Straby, 1989) and 3' trimming of $tRNA^{Tyr}_{GUA}$ and $tRNA^{Lys}_{UUU}$(Copela et al., 2008). To address whether the number of cDNA reads for a particular tRNA transcript reflects a specificity of binding or rather simply its relative cellular abundance, the number of reads obtained for Rex1 for each tRNA were plotted against the number of reads obtained in the CRAC dataset for the Rpo31 core subunit of RNA polymerase III (Turowski et al., 2016) (Figure 47). It can be seen that there is not a direct correlation between the number of tRNA sequence reads for Rex1 and Rpo31, indicating that some tRNA species are over-represented in the Rex1-HTP dataset and others are under-represented. The tRNAs that were most frequently crosslinked withRex1 were $tRNA^{Lys}_{UUU}$and $tRNA^{Ile}_{UAU}$species, while there was also a high representation of $tRNA^{Trp}$, $tRNA^{Ile}$ and certain $tRNA^{Arg}$species. Notably, $tRNA^{Lys}_{UUU}$, $tRNA^{Ile}_{UAU}$ and $tRNA^{Trp}_{UGG}$species contain introns. However, not all intron-containing tRNAs are preferentially crosslinked to Rex1. For example, $tRNA^{Ser}_{GCU}$and $tRNA^{Pro}_{UGG}$intron-containing transcripts are not enriched in the Rex1 cDNA reads.

6.3 Discussion

Here I have described the development of an *in vitro* assay for the 3' end maturation of 5S rRNA. RNA processing in the *in vitro* assay was accurate at the nucleotide level 3' and shown to be dependent upon Rex1, since no processing was observed upon incubation of the substrate with the *rex1* D229A active site mutant. Incubation of the 3' extended 5S RNP particle with Rex1 caused the conversion of substrate to mature 5S rRNA without the detection of RNAs of intermediate length, which is indicative (but not formal proof) of a processive rather than distributive mechanism. The inability of Rex1 to trim 5S rRNA further may be related to the secondary structure of this RNA, which has a double-stranded terminal stem, and/or the association of 5S rRNA-binding proteins such as Rpl5.

Unusually, when compared to other nuclease assays published in the literature (e.g. Mitchell et al., 1997; Burkard & Butler, 2000; Ozanick etal., 2009), this RNA processing reaction utilizes an RNP particle substrate rather than an in vitro transcribed RNA. The detected Rex1 activity was substrate-dependent, the enzyme acting on the 5S RNP particle substrate but not on 60S ribosomal subunits containing a 3' extended 5S rRNA. The fact that differences in substrates have a significant impact on enzyme activity emphasizes the importance of performing such assays on a biologically relevant substrate. Distinct structural contexts of a substrate RNA can impact on the three-dimensional structure of the RNA, affect the accessibility of the substrate for the enzyme, and change the provision of additional structural features such as domains within RNA-associated proteins that contribute to substrate recognition and/or a stable enzyme/substrate interaction. The 3' end of the 5S rRNA is accessible to the solvent in the 60S ribosomal subunit (Schmidt et al., 2016), suggesting that Rex1 makes additional contacts with its substrate that are not possible after assembly of the 5S RNP particle into the 60S subunit. The 5S RNP particle is an appropriate substrate with which to assay Rex1 activity, since 3' end processing of 5S rRNA occurs before assembly of the complex into the 60S subunit (Steitz et al., 1988).

In vitro assays performed on the *rex1* mutants revealed that the catalytic domain is not sufficient for RNA processing. Furthermore, deletion of four distinct regions outside of the catalytic domain of Rex1 (residues 1-82, 82-202, 428-476 and 509-553) inhibited both Rex1-dependent RNA degradation and RNA binding. Inspection of the polypeptide sequence of Rex1 reveals that there are stretches of basic residues within each of the regions deleted in this study (K_{42}NKKKKKAK$_{50}$, K_{166}MEKINKLKELQKKKK$_{181}$; K_{462}KPRK$_{466}$ and K_{522}KERLDKRRER$_{532}$: the position of the first and last residue are given in subscript) that could potentially contribute to interactions between Rex1 and its RNA substrate. It is tempting to speculate that these stretches of amino acids might be juxtaposed in the three-dimensional structure of Rex1 and comprise a compound RNA interaction surface. Given that the poly(U) substrate used in the binding assays was coupled to the beads through its 3' hydroxyl group, retention of Rex1 on the poly(U)-coupled beads strongly implies that Rex1 contains an RNA binding site in addition to the catalytic centre. The loss of RNA binding upon deletion of any one of four regions within the protein would suggest that they contribute to RNA binding in a highly synergistic manner. Alternatively, the relatively large deletions made in this study could simply block the correct folding of Rex1 and therefore inhibit RNA binding. Given the indications that Rex1 is assembled into a larger heteromeric complex, is also feasible that one or more deletion may block the ability of Rex1 to remain stably bound to an associated protein that is required for its activity. More specific mutations within each of these stretches of basic amino acids would be required to address their potential role in RNA binding.

The Rex1-HTP fusion protein was cross-linked to cellular RNAs upon irradiation of growing cells with UV light. These interactions reflect direct contacts between the Rex1 protein and RNA within the cell. Most interactions were observed with tRNA, although there were a significant number of interactions with other classes of RNA. Approximately 10% of the CRAC cDNA reads in the *rex1-HTP* strain were mapped to 5S rRNA. The RNA interaction profile of Rex1 is clearly distinct from that of other cellular RNA binding proteins reported in the literature (e.g. Granneman et al.,

2009) and consistent with the *in vivo* RNA processing defects observed in *rex1* mutants. This is strongly indicative that the CRAC dataset for Rex1 represents specific interactions, rather than reflecting a nonspecific affinity of the protein for cellular RNA.

Some tRNAs were cross-linked to Rex1 at a much higher frequency than others and the distribution of cDNA reads obtained for Rex1 did not reflect the relative abundance of tRNAs within the cellular pool, as judged by comparison with the CRAC data for the catalytic subunit of RNA polymeraseIII. A high yield of cross-links were obtained for specific tRNAs that are aminoacylated with particular amino acids, notably $tRNA^{Lys}$, $tRNA^{Ile}$, $tRNA^{Trp}$ and $tRNA^{Arg}$. These four aminoacyl-tRNAs comprised the 38 most frequently cross-linked tRNAs of the 292 different tRNA transcripts, and 33% of the total number of tRNA reads. There is a strong correlation between high binding to Rex1 and tRNA molecules that contain introns. Thus, the intron-containing $tRNA^{Lys}_{UUU}$ species was crosslinked to Rex1 with an approximately five times higher yield than itsnon-spliced isoacceptor $tRNA^{Lys}_{CUU}$ species. Similarly, crosslinking to the intron-containing $tRNA^{Ile}_{UAU}$ species was higher than the non-spliced $tRNA^{Ile}_{AAU}$ and $tRNA^{Ile}_{GAU}$ species. There are 6 $tRNA^{Trp}_{CCA}$ transcripts, all of which contain an intron. The most abundant cellular tRNA molecule, the intron-containing $tRNA^{Ser}_{GCU}$ transcript, was cross-linked to Rex1 with only moderate frequency but was crosslinked more frequently than other $tRNA^{Ser}$ species. It is interesting to note that some previously identified Rex1 tRNA substrates such as $tRNA^{Tyr}_{GUA}$ (Copela et al, 2008) were identified at low frequency in the CRAC dataset. A large number of cDNA reads may reflect a high throughput of a specific enzyme substrate or an increased residence time for a particular substrate due to the formation of a stalled complex. Hence, it is feasible that the apparent bias towards intron-containing tRNAs may result from a kinetic delay in their processing. More detailed future analyses of the CRAC data will reveal the precise points of contact within the specific RNAs and resolve whether the tRNAs bound to Rex1 are spliced or unspliced. Furthermore, more detailed analyses of the RNA processing defects of *rex1* mutants are required to validate whether the

identified interacting RNAs are substates of the enzyme. It is not clear at present whether the identified interactions reflect Rex1-mediated productive tRNA processing events or whether the intron-containing tRNAs are being targeted to a Rex1-dependent tRNA surveillance pathway.

In the absence of Rrp6, an increased proportion of the Rex1 cross-links were observed for known Rrp6 substrates such as snoRNA, 5.8S rRNA and intergenic transcripts. The number of reads from both snoRNAs and intergenic transcripts approximately doubled in the *rex1-HTP rrp6Δ* strain, compared to the *rex1-HTP* strain. This is indicative of a degree of redundancy for Rex1 and Rrp6 activities in the processing or turnover of these RNAs and is consistent with the previously published finding that a conditional*rex1Δ rrp6* mutant exhibits a block in the 3' end processing of snoRNAs (Garland et al., 2013). The CRAC data presented here offer a possible explanation for the basis of the synthetic lethality of the *rex1Δ rrp6Δ* double mutant, suggesting that the double mutant may be defective in a combination of snoRNA production and the turnover of noncoding RNA arising from intergenic regions of the genome. Further analyses of conditional *rex1 rrp6* mutants would be required to test this interpretation.

Bibliography

Aasland R, Gibson TJ, Stewart AF., 1995. The PHD finger: implications for chromatin-mediated transcriptional regulation. Trends in biochemical sciences 20: 56-59.

Adam SA, Gerace L, 1991. Cytosolic proteins that specifically bind nuclear location signals are receptors for nuclear import. *Cell*, 66:837-847.

Albuqueque CP, Smolka MB, Payne SH, Bafna V, Eng J, and Zhou H., 2008. A multidimentional chromatography technology for in-depth phsphoproteome analysis. Molecular and cell Proteomics: MCP7:1389-1396

Aldrich TL, Di Segni G, McConaughy BL, Keen NJ, Whelen S, Hall BD., 1993. Structure of the yeast TAP1 protein: dependence of transcription activation on the DNA context of the target gene. *Mol Cell Biol* 13: 3434-3444

Allen, T. D., Cronshaw, J. M., Bagley, S., Kiseleva, E., and Goldberg, M. W., 2000. The nuclear pore complex: mediator of translocation between nucleus and cytoplasm . *J. Cell Sci.* 113, 1651–1659

Allmang C, Kufel J, Chanfreau G, Mitchell P, Petfalski E, Tollervey D., 1999a. Functions of the exosome in rRNA, snoRNA and snRNA synthesis. *EMBO J* 18: 5399-5410

Allmang C, Petfalski E, Podtelejnikov A, Mann M, Tollervey D, Mitchell P., 1999b. The yeast exosome and human PM-Scl are related complexes of 3' → 5' exonucleases. *Genes Dev* 13 2148-2158

Allmang, C., Mitchell, P., Petfalski, E., Tollervey, D., 2000. Degradation of ribosomal RNA precursors by the exosome. Nucleic Acids Res 28, 1684–1691.

Aloy P, Ciccarelli FD, Leutwein C, Gavin AC, Superti-Furga G, Bork P, Bottcher B, Russell RB., 2002. A complex prediction: three-dimensional model of the yeast exosome. *EMBO Rep* 3: 628-635

Anderson, J.S., Parker, R.P., 1998. The 3' to 5' degradation of yeast mRNAs is a generalmechanism for mRNA turnover that requires the SKI2 DEVH box protein and 3' to 5' exonucleases of the exosome complex. EMBO J. 17, 1497- 1506.

Andrade JM, Cairrao F & Arraiano CM., 2006. RNase R affects gene expression in stationary phase: regulation of ompA. Mol Microbiol 60: 219–228.

Andrade JM, Hajnsdorf E, R´egnier P &Arraiano CM., 2009a. The poly(A)-dependent degradation pathway of rpsO mRNA is primarily mediated by RNase R. RNA 15: 316–326.

Arraiano, C.M., Andrade, J.M., Domingues, S., Guinote, I.B., Malecki, M., Matos, R.G., *et al*. (2010). The critical role of RNA processing and degradation in the control of gene expression. *FEMS Microbiol Rev* 34: 883–923.

Aso T., Haque D. , Barstead R.J., Conaway R.C., Conaway J.W., 1996. The inducible elongin A elongation activation domain: structure, function and interaction with the elongin BC complex, EMBO J. 15 :5557–5566.

Apollon P. and Hans J. GROSS. , 1996. Pre-tRNA 3'-processing in Saccharomyces cerevisiae Purification and characterization of exo- and endoribonucleases. Eur. J. Biochem. 242, 747-759.

Araki, Y., S. Takahashi, T. Kobayashi, H. Kajiho, S. Hoshino, and T. Katada., 2001. Ski7p G protein interacts with the exosome and the Ski complex for 3'-to-5' mRNA decay in yeast. EMBO J. 20:4684–4693.the Degradation of Noncoding RNA Transcripts. Mol. Cell. Biol. 28(17):5446.

Auweter SD, Oberstrass FC, Allain FH., 2006. Sequence-specific binding of single-stranded RNA: is there a code for recognition? *Nucleic acids research* 34: 4943-4959.

Awano N, Inouye M & Phadtare S., 2008. RNase activity of polynucleotide phosphorylase is critical at low temperature in Escherichia coli and is complemented by RNase II. J Bacteriol 190: 5924–5933.

Awano N, Rajagopal V, Arbing M, Patel S, Hunt J, Inouye M & Phadtare S., 2010. Escherichia coli RNase R has dual activities, helicase and RNase. J Bacteriol 192: 1344–1352.

Backe PH, Messias AC, Ravelli RB, Sattler M, Cusack S., 2005. X-ray crystallographic and NMR studies of the third KH domain of hnRNP K in complex with single-stranded nucleic acids. *Structure* 13: 1055-1067.

Bailey, S.L., Harvey, S., Perrino, F.W. and Hollis, T., 2012. Defects in DNA degradation revealed in crystal structures of TREX1 exonuclease mutations linked to autoimmune disease. *DNA Repair(Amst)*, 11, 65-73.

Bailey, S.L., Witte, T., Vyse, T.J. *et al.,* 2007.Mutations in the gene encoding the 3'-5' DNAexonuclease TREX1 are associated with systemic lupus erythematosus. *Nat Genet*, 39, 1065-1067.

Banner. W. M., 1978. Protein migration and accumulation in nuclei. In The Cell Nucleus, 4, H. Busch, ed. (New York: Academic Press), pp. 97-148.

Bao J, Wu Q, Song R, Jie Z, Zheng H, Xu C, Yan W., 2011. RANBP17 is localized to the XY body of spermatocytes and interacts with SPEM1 on the manchette of elongating spermatids. Mol Cell Endocrinol 333:134–142.

Barber, G.N., 2011. Cytoplasmic DNA innate immune pathways. *Immunol Rev*, 243, 99-108.

Barnes M.H., Spacciapoli,P., Li,D.H. and Brown,N.C. , 1995. The 3'–5' exonuclease site of DNA polymerase III from gram-positive bacteria: definition of a novel motif structure. Gene, 165, 45–60.

Bally, M., Hughes, J., and Cesareni, G. 1988. SnR30: a new, essential small nuclear RNA from Saccharomyces cerevisiae. Nucleic Acids Research 16: 5291-5303.

Bernstein J., Toth E. A., (2012) Yeast nuclear RNA processing. *World J Biol Chem* 2012 January 26; 3(1):7 -26

Blobel, G. (1971) Proc. Natl. Acad. Sci. USA 68, 1881-1885.

Becker, J., Melchior, F., Gerke, V., Bischoff, F. R., Ponstingl, H., and Wittinghofer,A, 1995 RNA1 Encodes a GTPase-activating Protein Specific for Gsp1p, the Ran/TC4 Homologue of *Saccharomyces cerevisiae* .*J. Biol. Chem.* 270, 11860–11865

Beese LS, Steitz TA., 1991. Structural basis for the 3'-5' exonuclease activity of Escherichia coli DNA polymerase I: a two metal ion mechanism. *EMBO J* 10: 25-33

Beese, L. S., V. Derbyshire and T. A. Steitz, 1993. Structure of DNA polymerase I Klenow fragment bound to duplex DNA. Science 260: 352–355

Benitez1, Shunbin Ning2, Arun Malhotra1, Murray P. Deutscher1, and Yanbin Zhang., 2015. Human DNA exonuclease TREX1 is also an exoribonuclease that acts on single-stranded RNA. JBC.10: 1-10.

Beran, R. K., and R. W. Simons., 2001. Cold-temperature induction of *Escherichia coli* polynucleotide phosphorylase occurs by reversal of its autoregulation. Mol. Microbiol. 39:112–125.

Bermu´ dez-Cruz RM, Fernandez-Ram´ırez F, Kameyama-Kawabe L & Monta˜nez C (2005) Conserved domains in polynucleotide phosphorylase among eubacteria. Biochimie 87: 737–745.

Bernad, A., Blanco, L., L, zaro, J., Mart, n, G., & Salas, M., 1989. A conserved 3' to 5' exonuclease active site in prokaryotic and eukaryotic DNA polymerases. *Cell*, *59*(1), 219–228.

Bischoff, F. R., and Ponstingl, H, 1991 . Catalysis of guanine nucleotide exchange on Ran by the mitotic regulator RCC1 .*Nature* 354, 80–82

Blondel, M., Alepuz, P. M., Huang, L. S., Shaham, S., Ammerer, G., andPeter, M., 1999 . Nuclear export of Far1p in response to pheromones requires the export receptor Msn5p/Ste21p .*Genes Dev.* 13, 2284–2300

Boeck, R., S. Tarun Jr., M. Rieger, J. A. Deardorff, S. Muller-Auer et al., 1996. The yeast Pan2 protein is required for poly(A)- binding protein-stimulated poly(A)-nuclease activity. J. Biol. Chem. 271: 432–438.

Bonneau F, Basquin J, Ebert J, Lorentzen E, Conti E., 2009. The yeast exosome functions as a macromolecular cage to channel RNA substrates for degradation. *Cell* 139: 547-559

Braithwaite,D. and Ito,J., 1993. Compilation, alignment, and phylogenetic relationships of DNA polymerases . *Nucleic Acids Res.*, 21, 787–802.

Brautigam C.A., Sun,S., Piccirilli,J.A. and Steitz,T.A., 1999. Structures of normal single-stranded DNA and deoxyribo-3'-*S*-phosphorothiolates bound to the 3'–5' exonucleolytic active site of DNA polymerase I from *Escherichia coli*. Biochemistry, 38, 696–704.

Briani F, Del Favero M, Capizzuto R et al., 2007. Genetic analysis of polynucleotide phosphorylase structure and functions. Biochimie 89: 145–157.

Briggs, M.W., Burkard, K.T., Butler, J.S., 1998. Rrp6p, the Yeast Homologue of the Human PMScl 100-kDa Autoantigen, Is Essential for Efficient 5.8S rRNA 3' End Formation. J Biol Chem 273:13255–13263.

Brown, C.E., Tarun, S.Z., Boeck, R. & Sachs, A.B., 1996. PAN3 encodes a subunit of the Pab1p-dependent poly(A) nuclease in *Saccharomyces cerevisiae*. *Mol. Cell. Biol.* 16, 5744–5753.

Bruce Alberts, Alexander Johnson, Julian Lewis, MartinRaff, Keith Roberts, and Peter Walter., 2008. All cells Transcribe Portions of Their Hereditary Information into the Same Intermediary Form (RNA). In: Molecular Biology of the Cell. Fifth Ed.Garland Science, Taylor and Francis Group, LLC,USA. pp: 4,336.

Burd CG, Dreyfuss G.,1994. Conserved structures and diversity of functions of RNA-binding proteins. *Science* 265: 615-621.

Burkard KT, Butler JS., 2000. A nuclear 3'-5' exonuclease involved in mRNA degradation interacts with Poly(A) polymerase and the hnRNA protein Npl3p. *Mol Cell Biol* 20: 604-616

Butler JS, Mitchell P, 2011. Rrp6, rrp47 and cofactors of the nuclear exosome. Med Biol. 702:91-104.

Butler JS., 2002. The yin and yang of the exosome. *Trends Cell Biol* 12: 90-96

Büttner K, Wenig K, Hopfner KP., 2005. Structural framework for the mechanism of archaeal exosomes in RNA processing. *Mol Cell* 20: 461-471

Cairra˜o F, Cruz A, Mori H & Arraiano CM., 2003. Cold shock induction of RNase R and its role in the maturation of the quality control mediator SsrA/tmRNA. Mol Microbiol 50: 1349–1360.

Callahan KP, Butler JS., 2008. Evidence for core exosome independent function of the nuclear exoribonuclease Rrp6p. *NucleicAcids Res* 36: 6645-6655

Callahan KP, Butler JS., 2010. TRAMP complex enhances RNA degradation by the nuclear exosome component Rrp6. *J BiolChem* 285: 3540-3547

Canavan R, Bond U., 2007. Deletion of the nuclear exosome component RRP6 leads to continued accumulation of the histone mRNA HTB1 in S-phase of the cell cycle in Saccharomyces cerevisiae. *Nucleic Acids Res* 35: 6268-6279

Canadien, V., Richards, D., Beattie, B., Wu, L.F., Altschuler, S.J., Roweis, S., Frey, B.J., Emili, A., Greenblatt, J.F., Hughes, T.R. 2003. A panoramic view of yeast noncoding RNA processing. *Cell* 113: 919-933.

Cannistraro VJ & Kennell D., 1999. The reaction mechanism of ribonuclease II and its interaction with nucleic acid secondary structures. Biochim Biophys Acta 1433: 170–187.

Campbell, R. E. Tour O, Palmer AE, Steinbach PA, Baird GS, Zacharias DA, aand Tsien RY, 2002. A monomeric red fluorescent protein. Proc. Natl Acad. Sci. USA 99, 7877–7882.

Carneiro T, Carvalho C, Braga J, Rino J, Milligan L, Tollervey D, Carmo-Fonseca M., 2007. Depletion of the yeast nuclear exosome subunit Rrp6 results in accumulation of polyadenylated RNAs in a discrete domain within the nucleolus. *Mol Cell Biol* 27: 4157-4165

Chakshusmathi, G., Kim, S.D., Rubinson, D.A., and Wolin, S.L., 2003.A La protein requirement for efficient pre-tRNA folding. EMBO J.22: 6562–6572.

Chang KY, Ramos A., 2005. The double-stranded RNA-binding motif, a versatile macromolecular docking platform. *The FEBS journal* 272: 2109-2117.

Chen, C.-Y.A. & Shyu, A.-B., 2011. Mechanisms of deadenylation-dependent decay. Wiley Interdiscip. Rev. *RNA* 2, 167–183.

Cheng ZF & Deutscher MP., 2002. Purification and characterization of the Escherichia coli exoribonuclease RNase R. Comparison with RNase II. J Biol Chem 277: 21624–21629.

Cheng ZF & Deutscher MP., 2003. Quality control of ribosomal RNA mediated by polynucleotide phosphorylase and RNase R. P Natl Acad Sci USA 100: 6388–6393.

Cheng ZF & Deutscher MP., 2005. An important role for RNase R in mRNA decay. Mol Cell 17: 313–318.

Chernyakov I, Whipple JM, Kotelawala L, Grayhack EJ, Phizicky EM., 2008. Degradation of several hypomodified mature tRNA species in Saccharomyces cerevisiae is mediated by Met22 and the 5'-3' exonucleases Rat1 and Xrn1. *Genes Dev* 22: 1369-1380

Choi JM, Park EY, Kim JH, Chang SK & Cho Y., 2004. Probing the functional importance of the hexameric ring structure of RNase PH. J Biol Chem 279: 755–764.

Chlebowski, A., Lubas, M., Jensen, T.H., Dziembowski, A., 2013. RNA decay machines: The

exosome. Biochim Biophys Acta 1829, 552–560.Christie, M., Boland, A., Huntzinger, E., Weichenrieder, O. & Izaurralde, E., 2013. Structure of the PAN3 pseudokinase reveals the basis for interactions with the PAN2 deadenylase and the GW182 proteins. *Mol. Cell* 51, 360–373.

Christopher J. Yoo and Sandra L. Wolin., 1997. The Yeast La Protein Is Required for the 39 Endonucleolytic Cleavage That Matures tRNA Precursors . Cell, Vol. 89, 393–402.

Connelly S, Manley JL., 1988. A functional mRNA polyadenylation signal is required for transcription termination by RNA polymerase II. *Genes Dev* 2: 440-452

Conti, E., and Kuriyan, J, 2000. Crystallographic analysis of the specific yet versatile recognition of distinct nuclear localization signals by karyopherin α .*Structure* 8, 329–338

Cook A, Bono F, Jinek M, Conti E., 2007. Structural biology of nucleocytoplasmic transport. Annu Rev Biochem;76:647–671.

Copela,L.A., Fernandez,C.F., Sherrer,R.L. and Wolin,S.L., 2008. Competition between the Rex1 exonuclease and the La protein affects both Trf4p-mediated RNA quality control and pre-tRNA maturation. RNA, 14, 1214–1227.

Corbett, A. H., Koepp, D. M., Lee, M. S., Schlenstedt, G., Hopper, A. K.,and Silver, P. A, 1995 . Rna1p, a Ran/TC4 GTPase activating protein, is required for nuclear import. . *J. Cell Biol.* 130, 1017–1026

Cordin O, Banroques J, Tanner NK, Linder P., 2006. The DEAD-box protein family of RNA helicases. Gene. 15;367:17-37.

Costello, J.L., Stead, J., Feigenbutz, M., Jones, R.M., Mitchell, P., 2011. The C-terminal region of the exosome-associated protein Rrp47 is specifically required for box C/D small nucleolarRNA 3'-maturation. J Biol Chem 286, 4535–4543.

Crow, Y.J., Hayward, B.E., Parmar, R., Robins, P., Leitch, A., Ali, M., Black, D.N., van Bokhoven, H., Brunner, H.G., Hamel, B.C. *et al.,* 2006. Mutations in the gene encoding the 3'-5' DNA exonuclease TREX1 cause Aicardi-Goutieres syndrome at the AGS1 locus. *Nat Genet*, 38:917-920.

Cudny H & Deutscher MP., 1980. Apparent involvement of ribonuclease D in the 30 processing of tRNA precursors. P Natl Acad Sci USA 77: 837–841.

Cudny H, Zaniewski R & Deutscher MP, 1981. Escherichia coli RNase D. Catalytic properties and substrate specificity. J Biol Chem 256: 5633–5637.

Das B, Butler JS, Sherman F., 2003 Degradation of normal mRNA in the nucleus of Saccharomyces cerevisiae. *Mol Cell Biol* 23: 5502-5515

de Keizer PL, Burgering BM, Dansen TB., 2011 Forkhead box o as a sensor, mediator, and regulator of redox signaling. Antioxid Redox Signal;14:1093–1106.

Derbyshire, V., P. S. Freemont, M. R. Sanderson, L. Beese, J. M. Friedman et al., 1988 Genetic and crystallographic studies of 3',5'-exonucleolytic site of DNA polymerase I. Science 240:199–201

Deutscher MP & Marlor CW., 1985. Purification and characterization of Escherichia coli RNase T. J Biol Chem 260: 7067–7071.

Deutscher MP & Reuven NB., 1991. Enzymatic basis for hydrolytic versus phosphorolytic mRNA degradation in Escherichia coli and Bacillus subtilis. P Natl Acad Sci USA 88: 3277–3280.

Deutscher MP, Marlor CW & Zaniewski R., 1985. RNase T is responsible for the end-turnover of tRNA in Escherichia coli. P Natl Acad Sci USA 82: 6427–6430.

Deutscher MP, Marshall GT & Cudny H., 1988. RNase PH: an Escherichia coli phosphate-dependent nuclease distinct from polynucleotide phosphorylase. P Natl Acad Sci USA 85: 4710–4714.

DeVit, M.J. and Johnston, M. 1999. The nuclear exportin Msn5 is required for nuclear export of the Mig1 glucose repressor of Saccharomyces cerevisiae. Curr. Biol. 9: 1231–1241.

de la Cruz J, Kressler D, Tollervey D, Linder P, 1998. Dob1p (Mtr4p) is a putative ATP-dependent RNA helicase required for the 3’ end formation of 5.8S rRNA in Saccharomyces cerevisiae. *EMBO J* ; 17: 1128-1140

Dingwall, C., and Laskey, R. A, 1991. Nuclear targeting sequences — a consensus? .*Trends Biochem. Sci* 16, 478–481

Donald G. Comb And Nilima Sarkar, 1967. The Binding of 5s Ribosomal Ribonucleic Acidto Ribosomal Subunits. J. iMo2. Biol. 25:317-330

Donovan WP & Kushner SR., 1986. Polynucleotide phosphorylase and ribonuclease II are required for cell viability and mRNA turnover in Escherichia coli K-12. P Natl Acad Sci USA 83: 120–124.

Dong, B., and Silverman, R.H. (1999). Alternative function of a protein kinase homology domain in 20, 50-oligoadenylate dependent RNase L. Nucleic Acids Res. 27, 439–445.

Dopie J, Skarp KP, Rajakyla EK, Tanhuanpaa K, Vartiainen MK., 2012. Active maintenance of nuclear actin by importin 9 supports transcription. Proc Natl Acad Sci U S A 109:544–552.

Dreyfuss G, Kim VN, Kataoka N., 2002. Messenger-RNA-binding proteins and the messages they carry. *Nature reviews Molecular cell biology* 3: 195-205.

Dziembowski A, Lorentzen E, Conti E, Séraphin B., 2007. A single subunit, Dis3, is essentially responsible for yeast exosome core activity. *Nat Struct Mol Biol* 14: 15-22

Egecioglu, D. E., A. K. Henras, and G. F. Chanfreau, (2006). *Contributions of Trf4p- and Trf5p-dependent polyadenylation to the processing and degradative functions of the yeast nuclear exosome*. RNA 12:26–32.

El Hage A, Koper M, Kufel J, Tollervey D., 2008. Efficient termination of transcription by RNA polymerase I requires the 5' exonuclease Rat1 in yeast. *Genes Dev* 22: 1069-1081

Evans D, Marquez SM, Pace NR. 2006. RNase P: Interface of the RNA and protein worlds. Trends Biochem Sci 31: 333–341

Etxebeste O, Markina-Inarrairaegui A, Garzia A, Herrero-Garcia E, Ugalde U, Espeso EA., 2009. KapI, a non-essential member of the Pse1p/Imp5 karyopherin family, controls colonial and asexual development in Aspergillus nidulans. Microbiology 155:3934–3945.

Fahrenkrog, B., and Aebi, U., 2002. The Vertebrate Nuclear Pore Complex: From Structure to Function. *Results Probl. Cell Differ.* 35, 25–48

Fahrenkrog, B., and Aebi, U., 2003. The nuclear pore complex: nucleocytoplasmic transport and beyond. *Nat. Rev. Mol. Cell. Biol.* 4, 757–766

Fang F, Phillips S, Butler JS (2005). Rat1p and Rai1p function with the nuclear exosome in the processing and degradation of rRNA precursors. *RNA*; 11: 1571-1578

Feigenbutz, M., Jones, R., Besong, T.M.D., Harding, S.E., Mitchell, P., 2013b. Assembly of the yeast exoribonuclease Rrp6 with its associated cofactor Rrp47

occurs in the nucleus and is critical for the controlled expression of Rrp47. J Biol Chem 288, 15959–15970.

Fenghua Yuan1, Tanmay Dutta1, Ling Wang2, Lei Song1, Liya Gu3, Liangyue Qian1, Anaid,Benitez1, Shunbin Ning2, Arun Malhotra1, Murray P. Deutscher1, and Yanbin Zhang., 2015. Human DNA exonuclease TREX1 is also an exoribonuclease that acts on single-stranded RNA. JBC.10: 1-10.

Fedorov, AA, Fedorove, E.V, Bonanno, J., Burley, S.K, Almo, S.C., 2013. Crystal structure of phosphorylated phosphopentomutase from streptococcus mutants. New YorkSGX Research Centre for Structural Genomics, New York Structural Genomic research Consortium. PDB file 4N7T

Floyd-Smith, G., Slattery, E., and Lengyel, P. (1981). Interferon action: RNA cleavage pattern of a (20-50)oligoadenylate-dependent endonuclease. Science 212, 1030–1032.

Fontes, M. R., Teh, T., and Kobe, B, 2000 . Structural basis of recognition of monopartite and bipartite nuclear localization sequences by mammalian importin-α .*J. Mol. Biol.* 297, 1183–1194

Foretek, D., Wu, J., Hopper, A. K., & Boguta, M. , 2016. Control of Saccharomyces cerevisiae pre-tRNA processing by environmental conditions. *RNA (New York, N.Y.)*, 339–349.

Frank,P., Braunshofer-Reiter,C., Karwan,A., Grimm,R. and Wintersberger,U., 1999. Purification of Saccharomyces cerevisiae RNase H (70) and identification of the corresponding gene. FEBS Lett., 450, 251–256.

Fraza˜o C, McVey CE, Amblar M, Barbas A, Vonrhein C, Arraiano CM & Carrondo MA., 2006. Unravelling the dynamics of RNA degradation by ribonuclease II and its RNA-bound complex. Nature 443: 110–114.

Freemont,P., Friedman,J., Beese,L., Sanderson,M. and Steitz,T., 1988. Cocrystal structure of an editing complex of Klenow fragment with DNA. *Proc. Natl. Acad. Sci*. *USA*, 85, 8924–8928.

Fried H, Kutay U., 2003. Nucleocytoplasmic transport: taking an inventory. Cell Mol Life Sci;60:1659–1688.

Fye, J.M., Orebaugh, C.D., Coffin, S.R., Hollis, T. and Perrino, F.W. (2011) Dominant mutationof the TREX1 exonuclease gene in lupus and Aicardi-Goutieres syndrome. *J Biol Chem*, 286,32373-32382.

Gamsjaeger R, Liew CK, Loughlin FE, Crossley M, Mackay JP., 2007. Sticky fingers: zinc-fingers as protein-recognition motifs. *Trends in biochemical sciences* 32: 63-70.

Garc´ıa-Mena J, Das A, S´anchez-Trujillo A, Portier C & Montanez C., 1999. A novel mutation in the KH domain of polynucleotide phosphorylase affects autoregulation and mRNA decay in Escherichia coli. Mol Microbiol 33: 235–248.

Garland, W., Feigenbutz, M., Turner, M., Mitchell, P., 2013. Rrp47 functions in RNA surveillance and stable RNA processing when divorced from the exoribonuclease and exosome-binding domains of Rrp6. RNA 19, 1659–1668.

Gilchrist, D., and Rexach, M, 2003. Molecular Basis for the Rapid Dissociation of Nuclear Localization Signals from Karyopherin α in the Nucleoplasm .*J. Biol. Chem.* 278, 51937–51949

Gilchrist, D., Mykytka, B., and Rexach, M. (2002) . Accelerating the Rate of Disassembly of Karyopherin·Cargo Complexes .*J. Biol. Chem.* 277:18161–18172

Go¨rlich, D., Kostka, S., Kraft, R., Dingwall, C., Laskey, R. A., Hartmann, E.,and Prehn, S. ,1995. Two different subunits of importin cooperate to recognize nuclear localization signals and bind them to the nuclear envelope .*Curr. Biol.* 5, 383–392

Golomb L, Bublik DR, Wilder S, Nevo R, Kiss V, Grabusic K, Volarevic S, Oren M., 2012. Importin 7 and exportin 1 link c-Myc and p53 to regulation of ribosomal biogenesis. Mol Cell 45:222–232.

Gongora, C., David, G., Pintard, L., Tissot, C., Hua, T.D., Dejean, A. and Mechti, N.,1997. Molecular cloning of a new interferon-induced PML nuclear body-associated protein J. Biol. Chem. 272, 19457-19463.

Gorlich, D., Prehn, S., Laskey, R. A., and Hartmann, E., 1994 . Isolation of a protein that is essential for the first step of nuclear protein import . *Cell* 79, 767–778

Graves JD and krebs EG., 1999. Protein phosphorylation and signal transduction. Pharmacol Ther. 82:111-21.

Greimann JC, Lima CD., 2008. Reconstitution of RNA exosomes from human and Saccharomyces cerevisiae cloning, expression, purification, and activity assays. *Methods Enzymol* 448: 185-210

Grishin NV., 2001. KH domain: one motif, two folds. *Nucleic acids research* 29: 638-643.

Grishin, N.V., 1998. The R3H motif: a domain that binds single-stranded nucleic acids. Trends Biochem. Sci. , 23, 329 –330.

Grossman D & van Hoof A., 2006. RNase II structure completes group portrait of 30 exoribonucleases. Nat Struct Mol Biol 13: 760–761.

Hall TM., 2005. Multiple modes of RNA recognition by zinc finger proteins. *Current opinion in structural biology* 15: 367-373.

Hamamoto T, Gunji S, Tsuji H, Beppu T., 1983. Leptomycins A and B, new antifungal antibiotics. I. Taxonomy of the producing strain and their fermentation, purification and characterization. J Antibiot (Tokyo) 36:639–645.

Hanekamp,T. and Thorsness,P.E.., 1999. YNT20, a bypass suppressor of yme1 yme2, encodes a putative 3_-5_ exonuclease localized in mitochondria of *Saccharomyces cerevisiae. Curr. Genet.*, 34, 438–448.

Harlow LS, Kadziola A, Jensen KF & Larsen S., 2004. Crystal structure of the phosphorolytic exoribonuclease RNase PH from Bacillus subtilis and implications for its quaternary structure and tRNA binding. Protein Sci 13: 668–677.

Harold P. E., 2009. Size and Shape of Protein Molecules at the Nanometer LevelDetermined by Sedimentation, Gel Filtration, and Electron Microscopy. Biological Procedures Online, 11,:32-50

Hasan, M., Koch, J., Rakheja, D., Pattnaik, A.K., Brugarolas, J., Dozmorov, I., Levine, B.,Wakeland, E.K., Lee-Kirsch, M.A. and Yan, N. (2013) Trex1 regulates lysosomal biogenesis andinterferon-independent activation of antiviral genes. *Nat Immunol*, 14, 61-71.

Hartmann RK, Gössringer M, Späth B, Fischer S, Marchfelder A. 2009. The making of tRNAs and more—RNase P and tRNase Z. Prog Mol Biol Transl Sci 85: 319–368

Henras AK, Soudet J, Gérus M, Lebaron S, Caizergues- Ferrer M, Mougin A, Henry Y (2008). The post-transcriptional steps of eukaryotic ribosome biogenesis. *Cell Mol Life Sci*; 65: 2334-2359

Helwak A, Kudla G, Dudnakova T, Tollervey D. 2013. Mapping the human miRNA interactome by CLASH reveals frequent noncanonical binding. Cell 153:654–665

Hibbs MA, Hess DC, Myers CL, Huttenhower C, Li K, Troyanskaya OG., 2007. Exploring the functional landscape of gene expression: directed search of large microarray compendia, Bioinformatics, vol. 23 (pg. 2692-2699)

Hodel, A. E., Harreman, M. T., Pulliam, K. F., Harben, M. E., Holmes, J. S., Hodel, M. R., Berland, K. M., and Corbett, A. H, 2006. Nuclear Localization Signal Receptor Affinity Correlates with *in Vivo* Localization in *Saccharomyces cerevisiae .J. Biol. Chem.* 281, 23545–23556

Hodel, M. R., Corbett, A. H., and Hodel, A. E. (2001) . Dissection of a Nuclear Localization Signal .*J. Biol. Chem.* 276,1317–1325

Hollis, T., Gahr, M., Perrino, F.W. *et al.* , 2007. A mutation in TREX1 that impairs susceptibility

Hood, J. K., and Silver, P. A, 1998. Cse1p Is Required for Export of Srp1p/Importin-α from the Nucleus in*Saccharomyces cerevisiae .J. Biol. Chem.* 273, 35142–35146

Hoss, M., Robins, P., Naven, T.J., Pappin, D.J., Sgouros, J. and Lindahl, T., 1999. A human DNA editing enzyme homologous to the Escherichia coli DnaQ/MutD protein. *The EMBO journal*, 18: 3868-3875.

Houmani, J.L., and Ruf, I.K. 2009. Clusters of basic amino acids contribute to RNA bind-ing and nucleolar localization of ribosomal protein L22. PloS One 4: e5306.

Hopper, A.K. (2006). Cellular dynamics of small RNAs. Crit. Rev. Biochem. Mol. Biol. 41: 3–19.

Houseley J, Tollervey D., 2006. Yeast Trf5p is a nuclear poly(A) polymerase. *EMBO Rep* 7: 205-211

Huang S. and Deutscher,M.P., 1992. Sequence and transcriptional analysis of the *Escherichia coli rnt*gene encoding RNase T. J. Biol. Chem., 267, 25609–25613.

Huang, Y., Bayfield, M.A., Intine, R.V., and Maraia, R.J., 2006. Separate RNA-binding surfaces on the multifunctional La protein mediate distinguishable activities in tRNA maturation. Nat. Struct.Mol. Biol. 13: 611–618.

Huang, H. et al., 2014. Dimeric structure of pseudokinase RNase L bound to 2-5A reveals a basis for interferon-induced antiviral activity. Mol. Cell 53, 221–234.

Hughes, J.M., and Ares, M. 1991. Depletion of U3 small nucleolar RNA inhibits cleavage in the 5' external transcribed spacer of yeast pre-ribosomal RNA and impairs formation of 18S ribosomal RNA. EMBO J 10: 4231-4239.

Huh, W.K., Falvo, J.V., Gerke, L.C., Carroll, A.S., Howson, R.W., Weissman, J.S. and O'Shea, E.K. (2003) Global analysis of protein localization in budding yeast. Nature, 425, 686-691.

Houseley, J., Tollervey, D., 2009. The many pathways of RNA degradation. Cell 136, 763–776.

Huppertz I., Attig J., D'Ambrogio A., Easton L.E., Sibley C.R., Sugimoto Y., Tajnik M., König J., Ule J. (2104). iCLIP: protein-RNA interactions at nucleotide resolution Methods, 65, pp. 274–287

Ibrahim H, Wilusz J, Wilusz CJ. RNA recognition by 3'-to-5' exonucleases: the substrate perspective. *Biochim Biophys Acta* 2008; 1779: 256-265

Ingmar B Schäfer, Michaela Rode, Fabien Bonneau, Steffen Schüssler & Elena Conti., 2014. The structure of the Pan2–Pan3 core complex reveals cross-talk between deadenylase and pseudokinase. nature structural & molecular biology. 21:591-598.

Ishii R, Nureki O & Yokoyama S., 2003. Crystal structure of the tRNA processing enzyme RNase PH from Aquifex aeolicus. J Biol Chem 278: 32397–32404.

Itaya, M., McKelvin, D., Chatterijie, S.K. and Crouch, R.J., 1991. Selective cloning of genes encoding RNase H from Salmonella typhimurium, Saccharomyces cerevisiae and Escherichia coli rnh mutant. Mol. Gen. Genet. 227,438-445.

Ito T, Tashiro K, Muta S, Ozawa R, Chiba T, Nishizawa M, Yamamoto K, Kuhara S, Sakaki Y., 2000. Toward a protein-protein interaction map of the budding yeast: A comprehensive system to examine two-hybrid interactions in all possible combinations between the yeast proteins. *Proc Natl Acad Sci USA* 97: 1143-1147

Ito,J. and Braithwaite,D., 1991. Compilation and alignment of DNA polymerase sequences. . *Nucleic Acids Res.*, 19, 4045–4057.

Jason Ptacek , Geeta Devgan , Gregory Michaud , Heng Zhu, Xiaowei Zhu, Joseph Fasolo, Hong Guo, Ghil Jona, Ashton Breitkreutz, Richelle Sopko, Rhonda R. McCartney, Martin C. Schmidt, Najma Rachidi, Soo-Jung Lee, Angie S. Mah, Lihao Meng, Michael J. R. Stark, David F. Stern, Claudio De Virgilio, Mike Tyers, Brenda Andrews , Mark Gerstein, Barry Schweitzer, Paul F. Predki& Michael Snyder., 2005. Global analysis of protein phosphorylation in yeast. Nature 438, 679-684.

Jans, D.A.; Briggs, L.J.; Gustin, S.E.; Jans, P.; Ford, S.; Young, I.G. The cytokine interleukin-5 (IL-5) effects cotransport of its receptor subunits to the nucleus in vitro. FEBS lett., 1997, 410, 368- 372.

Jackowiak, P., Nowacka, M., Strozycki, P.M., Figlerowicz, M., 2011. RNA degradome--its
biogenesis and functions. Nucleic Acids Res 39, 7361–7370.

Jensen KF, Andersen JT & Poulsen P., 1992. Overexpression and rapid purification of the orfE/rph gene product, RNase PH of Escherichia coli. J Biol Chem 267: 17147–17152.

Jimeno-González S, Haaning LL, Malagon F, Jensen TH., 2010. The yeast 5’-3’ exonuclease Rat1p functions during transcription elongation by RNA polymerase II. *Mol Cell* 37: 580-587

Joanna K. and David T., 2003. 3'-processing of yeast tRNATrp precedes 5'-processing. RNA 2003 9: 202-208.

Johnson, M.S., McClur, M.A. Feng, D.F. Grey, J and Doolittle, R.F.,1986. Computer analysis of retroviral poi genes: Assignment of enzymatic functions to specific sequences and homologies with nonviral enzymes Proc. Natl. Acad.. Sci. USA 83, 7648-7652.

Jonathan A. Stead, Joe L. Costello, Michaela J. Livingstone and Phil Mitchell, 2007. The PMC2NT domain of the catalytic exosome subunit Rrp6p provides the interface for binding with its cofactor Rrp47p, a nucleic acid-binding protein. Nucleic Acids Research. Vol. 35, No. 16, 5556–5567.

Jones, T.A., Uhlén, M., 1987. A synthetic IgG-binding domain based on staphylococcal

Jones, S., Daley, D.T., Luscombe, N.M., Berman, H.M., and Thornton, J.M. 2001. Protein-RNA interactions: a structural analysis. Nucleic Acids Research 29: 943-954.

Joyce, C. and Steitz,T., 1994. FUNCTION AND STRUCTURE RELATIONSHIPS IN DNA POL YMERASES . *Annu. Rev. Biochem.*, 63, 777–822.

Joël Acker, Christine Conesa, Olivier Lefebvre (2013). Yeast RNA polymerase III transcription factors and effectors. Biochimica et Biophysica Acta (BBA), Volume 1829, Pages 283-295

Granneman, S., Kudla, G., Petfalski, E., and Tollervey, D., 2009. Identification of protein binding sites on U3 snoRNA and pre-rRNA by UV cross-linking and high-throughput analysis of cDNAs. Proc. Nat. Acad. Sci. 106, 9613–9618.

Garrett K.P., Aso T., Bradsher J.N., Foundling S.I., Lane W.S. , Conaway R.C., Conaway J.W., 1995. Positive regulation of general transcription factor SIII by a tailed ubiquitin homolog, Proc. Natl. Acad. Sci. USA 92 7172–7176.

Kadaba,S., Wang,X. and Anderson,J.T., 2006. Nuclear RNAsurveillance in Saccharomyces cerevisiae: Trf4p-dependent polyadenylation of nascent hypomethylated tRNA and an aberrant form of 5S rRNA. RNA, 12, 508–521.

Kaffman, A., Rank, N. M., O'Neill, E. M., Huang, L. S., and O'Shea, E. K., 1998 . The receptor Msn5 exports the phosphorylated transcription factor Pho4 out of the nucleus .*Nature* 396, 482–486

Kahvejian A, Svitkin YV, Sukarieh R, M'Boutchou MN, Sonenberg N., 2005. Mammalian poly(A)-binding protein is a eukaryotic translation initiation factor, which acts via multiple mechanisms. *Genes & development* 19: 104-113.

Kalab, P., Weis, K., and Heald, R, 2002.Visualization of a Ran-GTP Gradient in Interphase and Mitotic *Xenopus* Egg Extracts.*Science* 295, 2452–2456

Kalderon, D., Richardson, W. D., Markham, A. F., and Smith, A. E, 1984 . Sequence requirements for nuclear location of simian virus 40 large-T antigen .*Nature* 311, 33–38

Kavanagh, D., Spitzer, D., Kothari, P.H., Shaikh, A., Liszewski, M.K., Richards, A. and Atkinson, J.P., 2008. New roles for the major human 3'-5' exonuclease TREX1 in human disease. *Cell Cycle*, 7, 1718-1725.

Kaake R. M., Milenkovic T., Przulj N., Kaiser P., Huang L. (2010). Characterization of cell cycle specific protein interaction networks of the yeast 26s proteasome complex by the Qtax strategy. J. Proteome Res. 9, 2016–2029

Kadaba, S., A. Krueger, T. Trice, A. M. Krecic, A. G. Hinnebusch et al., 2004 Nuclear surveillance and degradation of hypomodified initiator tRNAMet in S. cerevisiae. Genes Dev. 18: 1227– 1240

Kadaba, S., X. Wang, and J. T. Anderson, 2006 Nuclear RNA surveillance in Saccharomyces cerevisiae: Trf4p-dependent polyadenylation of nascent hypomethylated tRNA and an aberrant form of 5S rRNA. RNA 12: 508–521

Kirli K, Karaca S, Dehne HJ, Samwer M, Pan KT, Lenz C, Urlaub H, Gorlich D. (2015). A deep 784 proteomics perspective on CRM1-mediated nuclear export and nucleocytoplasmic partitioning. 785 Elife 4. doi:10.7554/eLife.11466.

Koonin E.V., Deutscher M.P., 1993. RNase T shares conserved sequence motifs with DNA proofreading exonucleases, Nucleic Acids Res. 21:2521–2522.

Kelly KO & Deutscher MP (1992) Characterization of Escherichia coli RNase PH. J Biol Chem 267: 17153–17158.

Kelly KO, Reuven NB, Li Z & Deutscher MP., 1992. RNase PH is essential for tRNA processing and viability in RNase-deficient Escherichia coli cells. J Biol Chem 267: 16015–16018.

Kelley, L. A., Mezulis, S., Yates, C. M., Wass, M. N. & Sternberg, M. J. E. (2015). The Phyre2 web portal for protein modeling, prediction and analysis. Nat. Protocols 10, 845–858

Kim M, Krogan NJ, Vasiljeva L, Rando OJ, Nedea E, Greenblatt JF, Buratowski S., 2004. The yeast Rat1 exonuclease promotes transcription termination by RNA polymerase II. *Nature* 432: 517-522

Klebe, C., Prinz, H., Wittinghofer, A., and Goody, R. S, 1995 . The kinetic mechanism of Ran-nucleotide exchange catalyzed by RCC1 .*Biochemistry*34, 12543–12552

Kobe, B, 1999. Autoinhibition by an internal nuclear localization signal revealed by the crystal structure of mammalian importin*Nat. Struct. Biol.* 6, 301–304

Koch P, Bohlmann I, Schafer M, Hansen-Hagge TE, Kiyoi H, Wilda M, Hameister H, Bartram CR, Janssen JW., 2000. Identification of a novel putative Ran-binding protein and its close homologue. Biochem Biophys Res Commun 278:241–249.

Kogoma, T., 1997. Stable DNA Replication: Interplay between DNA Replication, Homologous Recombination, and Transcription Microbiology . Mol. Biol. Rev. 61: 212-238.

Koonin E.V., 1997. A conserved ancient domain joins the growing superfamily of 3’–5’ exonucleases.Curr. Biol., 7:604–606.

Körner CG, Wormington M, Muckenthaler M, Schneider S, Dehlin E, Wahle E., 1998. The deadenylating nuclease (DAN) is involved in poly(A) tail removal during the meiotic maturation of Xenopus oocytes. EMBO J. 18:5427-37.

Kosugi S., Hasebe M., Tomita M., and Yanagawa H., 2009. Systematic identification of yeast cell cycle-dependent nucleocytoplasmic shuttling proteins by prediction of composite motifs. Proc. Natl. Acad. Sci. USA 106, 10171-10176.

Kudla, G., Granneman, S., Hahn, D., Beggs, J., and Tollervey, D. (2011). Crosslinking, ligation, and sequencing of hybrids reveals RNA-RNA interactions in yeast. Proc. Natl. Acad. Sci. USA 108, 10010–10015

Kuai L, Das B, Sherman F., 2005. A nuclear degradation pathway controls the abundance of normal mRNAs in Saccharomyces cerevisiae. *Proc Natl Acad Sci USA* 102: 13962-13967

Kutay, U., Bischoff, F. R., Kostka, S., Kraft, R., and Go¨rlich, D,1997. Export of Importin α from the Nucleus Is Mediated by a Specific Nuclear Transport Factor . *Cell*90, 1061–1071

Lam YW, Yuan Y, Isaac J, Babu CV, Meller J, Ho SM., 2010. Comprehensive identification and modified-site mapping of S-nitrosylated targets in prostate epithelial cells. PLoS One 5:9075.

Laura Milligan, Laurence Decourty, Cosmin Saveanu, Juri Rappsilber, Hugo Ceulemans, Alain Jacquier and David Tollervey., 2008. A Yeast Exosome Cofactor, Mpp6, Functions in RNA Surveillance and in the Degradation of Noncoding RNA Transcripts Molecular and Cellular Biologyp5446-5457.

LaCava, J., Houseley, J., Saveanu, C., Petfalski, E., Thompson, E., Jacquier, A., Tollervey, D.,2005. RNA degradation by the exosome is promoted by a nuclear polyadenylation complex.Cell 121, 713–724.

Lange A., McLane L.M., Mills R.E., Devine S.E., Corbett A.H. 2010. Expanding the definition of the classical bipartite nuclear localization signal Traffic, 11, pp. 311-323

Laurino J. P., Thompson G. M., Pacheco E., Castilho B. A. (1999). The β subunit of eukaryotic translation initiation factor 2 binds mRNA through the lysine repeats and a region comprising the C2-C2 motif. Mol. Cell. Biol. 19:173–181

LaCasse E.C., Lefebvre Y.A. 1995. Nuclear localization signals overlap DNA- or RNA-binding domains in nucleic acid-binding proteins. Nucleic Acids Res. 23:1647–1656.

Leslie, D.M.; Zhang, W.; Timney, B.L.; Chait, B.T.; Rout, M.P.; Wozniak, R.W.; Aitchison, J.D. Characterization of karyopherin cargoes reveals unique mechanisms of kap121-p mediated nuclear import. *Mol. Cell. Biol.,* 2004, *24,* 8487-8503.

Lebreton A, Tomecki R, Dziembowski A, Séraphin B., 2008. Endonucleolytic RNA cleavage by a eukaryotic exosome. Nature. 7224:993-6.

Lee, S. J., Matsuura, Y., Liu, S. M., and Stewart, M, 2005. Structural basis for nuclear import complex dissociation by RanGTP .*Nature* 435,693–696

Lee-Kirsch, M.A., Gong, M., Chowdhury, D., Senenko, L., Engel, K., Lee, Y.A., de Silva, U.,Letian K., Feng F. J. Scott , and Fred S., 2004. Polyadenylation of rRNA in Saccharomyces cerevisiae. Proc Natl Acad Sci U S A. 23:8581-6.

Lemay, V., Hossain, A., Osheim, Y.N., Beyer, A.L., and Dragon, F. 2011. Identification of novel proteins associated with yeast snR30 small nucleolar RNA. Nucleic Ac-ids Research.

Lee, J.Y., Rohlman, C.E., Molony, L.A., and Engelke, D.R. (1991). Characterization of RPR1, an essential gene encoding the RNA component of Saccharomyces cerevisiae RNase P. Mol. Cell. Biol. 11: 721– 730.

Lewis HA, Chen H, Edo C, Buckanovich RJ, Yang YY, Musunuru K, Zhong R, Darnell RB, Burley SK., 1999. Crystal structures of Nova-1 and Nova-2 K-homology RNA-binding domains. *Structure* 7: 191-203.

Li, H.D., Zagorski, J., and Fournier, M J. 1990. Depletion of U14 small nuclear RNA (snR128) disrupts production of 18S rRNA in Saccharomyces cerevisiae. Mo-lecular and Cellular Biology 10: 1145-1152.

Li Z & Deutscher MP., 1995. The tRNA processing enzyme RNase T is essential for maturation of 5S RNA. P Natl Acad Sci USA 92: 6883–6886.

Li Z, Pandit S & Deutscher MP., 1998. 30 Exoribonucleolytic trimming is a common feature of the maturation of small, stable RNAs in Escherichia coli. P Natl Acad Sci USA 95: 2856–2861.

Li Z, Pandit S & Deutscher MP., 1999a. Maturation of 23S ribosomal RNA requires the exoribonuclease RNase T. RNA 5: 139–146.

Li Z, Zhan L & Deutscher MP., 1996. Escherichia coli RNase T functions in vivo as a dimer dependent on cysteine 168. J Biol Chem 271: 1133–1137.

Li Z, Deutscher MP. Cell., 1996. Maturation pathways for E. coli tRNA precursors: a random multienzyme process in vivo.3:503-12.

Libri V, Helwak A, Miesen P, Santhakumar D, Borger JG, Kudla G, Grey F, Tollervey D , Buck AH. (2012). Murine cytomegalovirus encodes a miR-27 inhibitor disguised as a target. Proc. Natl Acad. Sci. USA 109, 279–284.

Lin PH & Lin-Chao S., 2005. RhlB helicase rather than enolase is the beta-subunit of the Escherichia coli polynucleotide phosphorylase (PNPase)-exoribonucleolytic complex. P Natl Acad Sci USA 102: 16590–16595.

Liou GG, Chang HY, Lin CS & Lin-Chao S., 2002. DEAD box RhlB RNA helicase physically associates with exoribonuclease PNPase to degrade double-stranded RNA independent of the degradosome-assembling region of RNase E. J Biol Chem 277: 41157–41162.

Liszewski, M.K., Barilla-Labarca, M.L., Terwindt, G.M., Kasai, Y. *et al.,*2007. C-terminal

truncations in human 3'-5' DNA exonuclease TREX1 cause autosomal dominant retinal

vasculopathy with cerebral leukodystrophy. *Nature genetics*, 39, 1068-1070.

Logan J, Falck-Pedersen E, Darnell JE, Shenk T., 1987. A poly(A) addition site and a downstream termination region are required for efficient cessation of transcription by RNA polymerase II in the mouse beta maj-globin gene. *Proc Natl AcadSci USA* 84: 8306-8310

Lodish HF, Berk A, Kaiser C, Krieger M, Scott MP, Bretscher A, Ploegh H, Matsudaira PT, 2007. "Chapter 8: Post-transcriptional Gene Control". *Molecular Cell .Biology*. San Francisco: WH Freeman. ISBN 0-7167-7601-4.

Lla´ cer, J.L., Hussain, T., Marler, L., Aitken, C.E., Thakur, A., Lorsch, J.R., Hinnebusch, A.G., and Ramakrishnan, V. (2015). Conformational Differences between Open and Closed States of the Eukaryotic Translation Initiation Complex. Mol. Cell 59, 399–412

Lorentzen E, Basquin J, Conti E., 2008. Structural organization of the RNA-degrading exosome. *Curr Opin Struct Biol* 18: 709-713

Lorentzen E, Basquin J, Tomecki R, Dziembowski A, Conti E., 2008. Structure of the active subunit of the yeast exosome core, Rrp44: diverse modes of substrate recruitment in the RNase II nuclease family. *Mol Cell* 29: 717-728

Lorentzen E, Conti E. The exosome and the proteasome: nano-compartments for degradation. *Cell* 2006; 125: 651-654 68 Lorentzen E, Conti E., 2005. Structural basis of 3' end RNA recognition and exoribonucleolytic cleavage by an exosome RNase PH core. *Mol Cell* 20: 473-481

Lorentzen E, Dziembowski A, Lindner D, Seraphin B, Conti E., 2007. RNA channelling by the archaeal exosome. *EMBO Rep* 8: 470-476

Lorentzen E, Walter P, Fribourg S, Evguenieva-Hackenberg E, Klug G, Conti E., 2005. The archaeal exosome core is a hexameric ring structure with three catalytic subunits. *Nat Struct MolBiol* 12: 575-581

Lorsch JR., 2002. RNA chaperones exist and DEAD box proteins get a life. Cell 109:797‑800.

Loughlin FE, Mansfield RE, Vaz PM, McGrath AP, Setiyaputra S, Gamsjaeger R, Chen ES, Morris BJ, Guss JM, Mackay JP., 2009. The zinc fingers of the SR-like protein ZRANB2 are single-stranded RNA-binding domains that recognize 5' splice site-like sequences. *Proceedings of the National Academy of Sciences of the United States of America* 106: 5581-5586.

Loveland KL, Hogarth C, Szczepny A, Prabhu SM, Jans DA., 2006. Expression of nuclear transport importins beta 1 and beta 3 is regulated during rodent spermatogenesis. Biol Reprod 74:67–74.

Lu Z, Xu S, Joazeiro C, Cobb MH, Hunter T., 2002. The PHD domain of MEKK1 acts as an E3 ubiquitin ligase and mediates ubiquitination and degradation of ERK1/2. *Molecular cell* 9: 945-956.

Luo W, Johnson AW, Bentley DL., 2006. The role of Rat1 in coupling mRNA 3'-end processing to transcription termination: implications for a unified allosteric-torpedo model. *GenesDev* 20: 954-965

Lupas, A., Van Dyke, M. & Stock, J., 1991. prediction coiled coil from protein sequences . Science 252: 1162–1164.

Luttinger A, Hahn J & Dubnau D., 1996. Polynucleotide phosphorylase is necessary for competence development in Bacillus subtilis. Mol Microbiol 19: 343–356.

Luz JS, Tavares JR, Gonzales FA, Santos MC, Oliveira CC., 2007. Analysis of the Saccharomyces cerevisiae exosome architecture and of the RNA binding activity of Rrp40p. *Biochimie* 89: 686-691

Lykke-Andersen S, Brodersen DE, Jensen TH., 2009. Origins and activities of the eukaryotic exosome. *J Cell Sci* 122: 1487-1494

Mahanty, S. K., Wang, Y., Farley, F. W., and Elion, E. A. (1999) *Cell* 98,501–512

Maillet, L. & Collart, M.A., 2002. Interaction between Not1p, a component of the Ccr4-not complex, a global regulator of transcription, and Dhh1p, a putative RNA helicase. *J. Biol. Chem.* 277, 2835–2842.

Major AT, Whiley PA, Loveland KL., 2011. Expression of nucleocytoplasmic transport machinery: clues to regulation of spermatogenic development. Biochim Biophys Acta 1813;:1668–1688.

Makhnevych T, Lusk CP, Anderson AM, Aitchison JD, Wozniak RW., 2003. Cell cycle regulated transport controlled by alterations in the nuclear pore complex. Cell 115:813–823.

Mangus, D.A. *et al.*, 2004.Positive and negative regulation of poly(A) nuclease. *Mol. Cell. Biol.* 24, 5521–5533.

Marelli M, Aitchison JD, Wozniak RW., 1998. Specific binding of the karyopherin Kap121p to a subunit of the nuclear pore complex containing Nup53p, Nup59p, and Nup170p. J Cell Biol 143:1813–1830.

Mathy, N., A. C. Jarrige, M. Robert-Le Meur, and C. Portier., 2001. Increased expression of *Escherichia coli* polynucleotide phosphorylase at low temperatures is linked to a decrease in the efficiency of autocontrol. J. Bacteriol. 183:3848–3854.

Matsuura, Y., and Stewart, M, 2004. Structural basis for the assembly of a nuclear export complex .*Nature* 432, 872–877

Matsuura, Y., and Stewart, M, 2005. Nup50/Npap60 function in nuclear protein import complex disassembly and importin recycling .*EMBO J.* 24, 3681–3689

Matsuura, Y., Lange, A., Harreman, M. T., Corbett, A. H., and Stewart, M, 2003. Structural basis for Nup2p function in cargo release and karyopherin recycling in nuclear import .*EMBO J.* 22, 5358–5369

Matthews JM, Sunde M., 2002. Zinc fingers--folds for many occasions. *IUBMB life* 54: 351-355.

Matthias Mann, Shao-En Ong, Mads Grønborg, Hanno Steen, Ole N. Jensen and Akhilesh Pandey ., 2002. Analysis of protein phosphorylation using mass spectrometry: deciphering the phosphoproteome. Trends in Biotechnology,20: 261-268.

Matus-Ortega ME, Regonesi ME, Pina-Escobedo A, Tortora P, Deho` G & Garc´ıa-Mena J., 2007. The KH and S1 domains of Escherichia coli polynucleotide phosphorylase are necessary for autoregulation and growth at low temperature. Biochim Biophys Acta 1769: 194–203.

Mazur, D.J. and Perrino, F.W., 2001. Structure and expression of the TREX1 and TREX2 3' --> 5'exonuclease genes. *J Biol Chem*, 276, 14718-14727.

Mazur,S.J. and Record,M.T.Jr, 1989. Association kinetics of site-specific protein–DNA interactions: Roles of nonspecific DNA sites and of the molecular location of the specific site. Biopolymers, 28, 929–953.

Mazza C, Segref A, Mattaj IW, Cusack S., 2002. Large-scale induced fit recognition of an m(7)GpppG cap analogue by the human nuclear cap-binding complex. *The EMBO journal* 21: 5548-5557.

Meyer S., Temme C., and Wahle E., 2004. Messenger RNA turnover in eukaryotes: pathways and enzymes. Crit. Rev. Biochem. Mol. Biol. 39: 197-216.

Mian IS ., 1997 Comparative sequence analysis of ribonucleases HII, III, II PH and D. Nucleic Acids Res 25: 3187–3195.

Midtgaard SF, Assenholt J, Jonstrup AT, Van LB, Jensen TH, Brodersen DE., 2006. Structure of the nuclear exosome component Rrp6p reveals an interplay between the active site and the HRDC domain. *Proc Natl Acad Sci USA* 103:11898-11903

Miller J, McLachlan AD, Klug A., 1985. Repetitive zinc-binding domains in the protein transcription factor IIIA from Xenopus oocytes. *The EMBO journal* 4: 1609-1614.

Min Hu, Pingwei Li, Muyang Li, Wenyu Li, Tingting Yao, Jia-Wei Wu, Wei Gu, Robert E. Cohen, and Yigong Shi., 2002.Crystal structure of a UBP-family deubiquitinating enzyme in isolation and in complex with ubiquitin aldehyde. *Cell* 111, 1041–1054.

Mishiro S, Hoshi Y, Takeda K, Yoshikawa A, Gotanda T, Takahashi K, Akahane Y, Yoshizawa H, Okamoto H, Tsuda F, et al., 1990. Non-A, non-B hepatitis specific antibodies directed at host-derived epitope: implication for an autoimmune process. Lancet.8728:1400–1403

Mitchell P, E. Petfalski, A.Shevchenko, M. Mann, and D. Tollervey., 1997. The Exosome: A Conserved Eukaryotic RNA Processing Complex Containing Multiple 3'-5' Exoribonucleases . Cell 91:457-466.

Mitchell P, Petfalski E, Houalla R, Podtelejnikov A, Mann M, Tollervey D., 2003. Rrp47p is an exosome-associated protein required for the 3’ processing of stable RNAs. *Mol Cell Biol* 23: 6982-6992

Mitchell, S.F., Jain, S., She, M. & Parker, R. (2013). Global analysis of yeast mRNPs. Nat. Struct. Mol. Biol. 20, 127–133.

Messier V., Zenklusen D., Michnick S.W. (2013). A nutrient-responsive pathway that determines M phase timing through control of B-cyclin mRNA stability Cell, 153, pp. 1080-1093

Moras, D., & Argos, P., 1990. An attempt to unify the structure of polymerases. *Protein Engineering, Design and Selection*, *3*(6), 461–467.

Morozov V, Mushegian AR, Koonin EV, Bork P., 1997. A putative nucleic acid-binding domain in Bloom’s and Werner’s syndrome helicases. *Trends Biochem Sci* 22: 417-418

Moser M.J., Holley,W.R., Chatterjee,A. and Mian,I.S., 1997. The proofreading domain of *Escherichia coli* DNA polymerase I and other DNA and/or RNA exonuclease domains. Nucleic Acids Res., 25, 5110–5118.

Moser MJ, Holley WR, Chatterjee A, Mian IS., 1997. The proofreading domain of Escherichia coli DNA polymerase I and other DNA and/or RNA exonuclease domains. *Nucleic AcidsRes* 25: 5110-5118

Morrissey, J.P., and Tollervey, D. 1997. U14 small nucleolar RNA makes multiple con-tacts with the pre-ribosomal RNA. Chromosoma 105: 515-522.

Morrissey, J.P., and Tollervey, D. 1993. Yeast snR30 is a small nucleolar RNA required for 18S rRNA synthesis. Molecular and Cellular Biology 13: 2469-2477.

Murthi A, Shaheen HH, Huang HY, Preston MA, Lai TP, Phizicky EM, Hopper AK (2010). Regulation of tRNA bidirectional nuclear-cytoplasmic trafficking in S. cerevisiae. Mol Biol Cell 21, 639–649.

Nariai M, Tanaka T, Okada T, Shirai C, Horigome C, and Mizuta K., 2005. Synergistic defect in 60S ribosomal subunit assembly caused by a mutation of Rrs1p, a ribosomal protein L11-binding protein, and 3'-extension of 5S rRNA in Saccharomyces cerevisiae. Nucleic Acids Research 14:4553-4562.

Neuhoff V, Stamm R and Eibl H. Clear background and highly sensitive protein staining with Coomassie Blue dyes in polyacrylamide gels: A systematic analysis. Electrophoresis. 1985, 6, 427-448. 225

Nowicki, M.W., Kuaprasert, B., McNae, I.W., Morgan, H.P., Harding, M.M., Michels, P.A.M., Fothergill-Gilmore, L.A. & Walkinshaw, M.D. 2009. Crystal structures of Leishmania mexicana phosphoglycerate mutase suggest a one-metal mechanism and a new enzyme subclass. J. Mol. Biol. 394: 535-543

Nguyen Ba AN, Pogoutse A, Provart N, Moses AM., 2009. NLStradamus: a simple Hidden Markov Model for nuclear localization signal prediction. *BMC Bioinformatics.* Jun 29;10(1):202.

Nguyen L.H., Erzbergr,J.P., Root,J. and Wilson,D.M.,III., 2000. The human homolog of *Escherichia coli*orn degrades small single-stranded RNA and DNA oligomers. J. Biol. Chem., 275, 25900–25906.

Nilsson, B., Moks, T., Jansson, B., Abrahmsén, L., Elmblad, A., Holmgren, E., Henrichson, C.,Jones, T.A., Uhlén, M., 1987. A synthetic IgG-binding domain based on staphylococcal

Nolwenn Le Meur and Robert Gentleman., 2008. Modeling synthetic lethality. Genome Biology 9:R135.

Nurmohamed S, Vaidialingam B, Callaghan AJ & Luisi BF., 2009. Crystal structure of Escherichia coli polynucleotide phosphorylase core bound to RNase E, RNA and manganese: implications for catalytic mechanism and RNA degradosome assembly. J Mol Biol 389: 17–33.

Oddone A, Lorentzen E, Basquin J, Gasch A, Rybin V, Conti E, Sattler M., 2007. Structural and biochemical characterization of the yeast exosome component Rrp40. *EMBO Rep* 8: 63-69

Oeffinger M, Zenklusen D, Ferguson A, Wei KE, El Hage A, Tollervey D, Chait BT, Singer RH, Rout MP., 2009. Rrp17p is a eukaryotic exonuclease required for 5' end processing of Pre- 60S ribosomal RNA. *Mol Cell* 36: 768-781

Ollis,D., Brick,P., Hamlin,R., Xuong,N. and Steitz,T., 1985. Structure of large fragment of *Escherichia coli* DNA polymerase I complexed with dTMP . *Nature*, 313,762–766.

Ooi SL, Samarsky DA, Fournier MJ, Boeke JD., 1998. Intronic snoRNA biosynthesis in Saccharomyces cerevisiae depends on the lariat-debranching enzyme: intron length effects and activity of a precursor snoRNA. *RNA* 4: 1096-1110

Ost KA & Deutscher MP., 1991. Escherichia coli orfE (upstream of pyrE) encodes RNase PH. J Bacteriol 173: 5589–5591.

Oubridge C, Ito N, Evans PR, Teo CH, Nagai K., 1994. Crystal structure at 1.92 A resolution of the RNA-binding domain of the U1A spliceosomal protein complexed with an RNA hairpin. *Nature* 372: 432-438.

Orebaugh, C.D., Fye, J.M., Harvey, S., Hollis, T. and Perrino, F.W. (2011) The TREX1

exonuclease R114H mutation in Aicardi-Goutieres syndrome and lupus reveals dimeric structurerequirements for DNA degradation activity. *J Biol Chem*, 286, 40246-40254.

Oussenko IA, Abe T, Ujiie H, Muto A & Bechhofer DH., 2005. Participation of 30-to-50 exoribonucleases in the turnover of Bacillus subtilis mRNA. J Bacteriol 187: 2758–2767.

Paine, P. L., Moore, L. C., and Horowitz, S. B., 1975 . Nuclear envelope permeability..*Nature* 254, 109–114

Peng SC, Lai YT, Huang HY, Huang HD, Huang YS., 2010. A novel role of CPEB3 in regulating EGFR gene transcription via association with Stat5b in neurons. Nucleic Acids Res 38:7446–7457.

Peng, W.T., Robinson, M.D., Mnaimneh, S., Krogan, N.J., Cagney, G., Morris, Q., Davierwala,A.P., Grigull, J., Yang, X., Zhang, W., Mitsakakis, N., Ryan, O.W., Datta, N., Jojic, V., Pal, C.,Canadien, V., Richards, D., Beattie, B., Wu, L.F., Altschuler, S.J., Roweis, S., Frey, B.J.,Emili, A., Greenblatt, J.F., Hughes, T.R., 2003. A panoramic view of yeast noncoding RNAprocessing. Cell 113, 919–933.

Pentecost,B.T., 1998. Expression and estrogen regulation of the HEM45mRNA in human tumor lines and in the rat uterus. *J. Steroid Biochem.Mol. Biol.*, 64, 25–33.

Perez-Terzic C, Faustino RS, Boorsma BJ, Arrell DK, Niederlander NJ, Behfar A, Terzic A. , 2007. Stem cells transform into a cardiac phenotype with remodeling of the nuclear transport machinery. Nat Clin Pract Cardiovasc Med 4(Suppl. 1):S68–S76.

Peter W. PIPER, Nita PATEL, and Alan LOCKHEART., 1984. Processing of the 3' sequence extensions upon the 5S rRNA of a mutant yeast in *Xenopus laevis* germinal vesicle extract. 141: 115–118.

Mitchell P and David tollervey., 2000. Musing on the Structural Organization of the Exosome Complex. Natural Structure Biology. Volume 7 number 10.

Phillips S., Butler JS, 2003. Contribution of domain structure to the RNA 3' end processing and degradation functions of the nuclear exosome subunit Rrp6p. RNA. 9:1098-107.

Piazza F, Zappone M, Sana M, Briani F & Deho` G ., 1996. Polynucleotide phosphorylase of Escherichia coli is required for the establishment of bacteriophage P4 immunity. J Bacteriol 178: 5513–5521.

Piper, P.W., Bellatin, J.A. and Lockheart,A., 1983. Altered maturation of sequences at the 30 terminus of 5S gene transcripts in a Saccharomyces cerevisiae mutant that lacks a RNA processing endonuclease. EMBO J., 2, 353–359.

Piper,P.W. and Straby,K.B., 1989. Processing of transcripts of a dimeric tRNA gene in yeast uses the nuclease responsible for maturation of the 30 termini upon 5 S and 37 S precursor rRNAs. FEBS Lett., 250, 311–316.

Planta RJ, Mager WH., 1998. The list of cytoplasmic ribosomal proteins of Saccharomyces cerevisiae. Yeast 14: 471–477.

Portier C & Regnier P., 1984. Expression of the rpsO and pnp genes: structural analysis of a DNA fragment carrying their control regions. Nucleic Acids Res 12: 6091–6102.

Pradeepa MM, Manjunatha S, Sathish V, Agrawal S, Rao MR., 2008. Involvement of importin-4 in the transport of transition protein 2 into the spermatid nucleus. Mol Cell Biol 28:4331–4341.

Price SR, Evans PR, Nagai K., 1998. Crystal structure of the spliceosomal U2B"-U2A' protein complex bound to a fragment of U2 small nuclear RNA. *Nature* 394: 645-650.

Pruijn GJ., 2005. Doughnuts dealing with RNA. Nat Struct Mol Biol 12: 562–564.

Purusharth RI, Madhuri B & Ray MK., 2007. Exoribonuclease R in Pseudomonas syringae is essential for growth at low temperature and plays a novel role in the 30 end processing of 16 and 5 S ribosomal RNA. J Biol Chem 282: 16267–16277.

Parker R., and Song H., 2004. The enzymes and control of eukaryotic mRNA turnover. Nat. Struct. Mol. Biol.11:121-127

Parker, R., 2012. RNA degradation in Saccharomyces cerevisae. Genetics 191, 671–702.
Ptsahne,M., 1986. Gene regulation by proteins acting nearby and at a distance. Nature, 322, 697–701.

Park, M. Y., Wu, G., Gonzalez-Sulser, A., Vaucheret, H. & Poethig, R. S., 2005. Proc. Natl. Acad. Sci. USA 102, 3691–3696.

Panosian T. D., Nannemann D. P., Watkins G. R., Phelan V. V., McDonald W. H., Wadzinski B. E., Bachmann B. O., Iverson T. M. (2011). Bacillus cereus Phosphopentomutase Is an Alkaline Phosphatase Family Member That Exhibits an Altered Entry Point into the Catalytic Cycle. J. Biol. Chem. 286, 8043–8054

Putker M, Madl T, Vos HR, de Ruiter H, Visscher M, van den Berg MC, Kaplan M, Korswagen HC, Boelens R, Vermeulen M, Burgering BM, Dansen TB., 2013. Redox-dependent control of FOXO/DAF-16 by transportin-1. Mol Cell 49:730–742.

Qiu, J., Qian,Y., Frank,P., Wintersberger,U. and Shen,B., 1999. *Saccharomyces cerevisiae* RNase H functions in RNA primerremoval during lagging-strand DNA synthesis, most efficiently incooperation with Rad27 nuclease. *Mol. Cell. Biol.*, 19, 8361–8371.

Quimby, B. B., and Dasso, M. (2003) *Curr. Opin.* The small GTPase Ran: interpreting the signs .*Cell Biol.* 15, 338–344

Radu, A., Blobel, G., and Moore, M. S., 1995. Identification of a protein complex that is required for nuclear protein import and mediates docking of import substrate to distinct nucleoporins. . *Proc. Natl. Acad. Sci. U. S. A.* 92, 1769–1773

Rafal Tomecki, Karolina Drazkowska, and Andrezi Dziembowski., 2010. Mechanism of RNA Degradation by the Eukaryotic Exosome. Chemobiochem 11: 938-942.

Rajkowitsch L, Chen D, Stampfl S, Semrad K, Waldsich C, Mayer O, Jantsch MF, Konrat R, Bläsi U, Schroeder R., 2007. RNA chaperones, RNA annealers and RNA helicases.RNA Biol. 3:118-30.

Reuven,N. and Deutscher,M., 1993. Multiple exoribonucleases are required for the 3' processing of Escherichia coli tRNA precursors in vivo . *FASEB J.*, 7, 143–148.

Richards, A., van den Maagdenberg, A.M., Jen, J.C., Kavanagh, D., Bertram, P., Spitzer, D.,Liszewski, M.K., Barilla-Labarca, M.L., Terwindt, G.M., Kasai, Y. *et al.* (2007) C-terminaltruncations in human 3'-5' DNA exonuclease TREX1 cause autosomal dominant retinalvasculopathy with cerebral leukodystrophy. *Nature genetics*, 39, 1068-1070.

Riddick, G., and Macara, I. G, 2005 . A systems analysis of importin-α–β mediated nuclear protein import .*J. Cell Biol.* 168, 1027–1038

Rigden DJ, Lamani E, Mello LV, Littlejohn JE &Jedrzejas MJ (2003) Insights into the catalyticmechanism of cofactor-independent phosphoglyceratemutase from X-ray crystallography, simulated dynamicsand molecular modeling. J Mol Biol 328, 909–920.

Roychowdhury, A., Kundu, A., Rose, M., Gujar, A., Mukherjee, S. & Das, A.K. 2015. Complete catalytic cycle of cofactorindependent phosphoglycerate mutase involves a springloaded mechanism. FEBS J. 282: 1097-1110

Robbins, J., Dilworth, S. M., Laskey, R. A., and Dingwall, C, 1991. Two interdependent basic domains in nucleoplasmin nuclear targeting sequence: Identification of a class of bipartite nuclear targeting sequence .*Cell* 64,615–623

Robert S. Sikorski and Philip Hieter., 1989. A System of Shuttle Vectors and Yeast Host Strains Designed for Efficient Manipulation of DNA in Saccharomyces ceratisiae . Genetics 122: 19-27.

Roppelt V, Klug G, Evguenieva-Hackenberg E., 2010. The evolutionarily conserved subunits Rrp4 and Csl4 confer different substrate specificities to the archaeal exosome. *FEBS Lett* 584: 2931-2936

Ross N. Nazar., 2004. Ribosomal RNA Processing and Ribosome Biogenesis in Eukaryotes. IUBMB Life, 56(8): 457–465.

Ruzzi M, Marconi A, Saliola M, Fabiani L, Montebove F, Frontali L., 1997. The sequence of a 8 kb segment on the right arm of yeast chromosome VII identifies four new open reading frames and the genes for yTAFII145. Yeast. 4:365-8.

Sachs, A.B. & Deardorff, J.A., 1992.Translation initiation requires the PAB-dependent poly(A) ribonuclease in yeast. *Cell* 70, 961–973.

Sachs, A.B. Bond, M.W. and Kornberg, R.D., 1986. A single gene from yeast for both nuclear and cytoplasmic polyadenylate-binding proteins: domain structure and expression. Cell 45, 827-835.

Sambrook J, Russell DW, 2006 . Preparation of plasmid DNA by alkaline lysis with SDS: minipreparation.Cold Spring Harb. Protoc.

Sarah G. Ozanick1, Xuying Wang1, Michael Costanzo2, Renee L. Brost2,Charles Boone2 and James T. Anderson1., 2009. Rex1p deficiency leads to accumulation of precursor initiator tRNAMet and polyadenylation of substrate RNAs in Saccharomyces cerevisiae. Nucleic Acids Research, 37: 298–308

Siegel L. M., Monte K. J., 1966. Determinationof molecular weights and frictionalratios of proteins in impure systems by useof gel filtration and density gradient centrifugation. Biochim Biophys Acta 112:346– 362

Schneider C, Anderson JT, Tollervey D., 2007. The exosome subunit Rrp44 plays a direct role in RNA substrate recognition. *Mol Cell* 27: 324-331

Schneider, C., Kudla, G., Wlotzka, W., Tuck, A., and Tollervey, D., 2012. Transcriptome-wide analysis of exosome targets. Mol. Cell 48, 422-433.

Schneider C, Leung E, Brown J, Tollervey D., 2009. The N-terminal PIN domain of the exosome subunit Rrp44 harbors endonuclease activity and tethers Rrp44 to the yeast core exosome. *Nucleic Acids Res* 37: 1127-1140

Schürer H, Schiffer S, Marchfelder A, Mörl M., 2001. This is the end: processing, editing and repair at the tRNA 3'-terminus. Biol Chem. 8:1147-56.

Schultz, J., Milpet z,F., Bork, P. and Ponting, C.P. (1998). SMART, a simple modular architecture research tool: identification of signaling domains. Proc. Natl Acad. Sci. USA , 95 , 5857 –5864.

Schafer, T., D. Strauss, E. Petfalski, D. Tollervey, and E. Hurt, 2003 The path from nucleolar 90S to cytoplasmic 40S pre ribosomes. EMBO J. 22: 1370–1380.

Steinmetz, E.J., Conrad, N.K., Brow, D.A., Corden, J.L., 2001. RNA-binding protein Nrd1 directs poly(A)-independent 3’-end formation of RNA polymerase II transcripts. Nature 413, 327–331.

Shaheen HH, Hopper AK (2005). Retrograde movement of tRNAs from the cytoplasm to the nucleus in S. cerevisiae. Proc Natl Acad Sci USA 102, 11290–11295.

Stephen F. Altschul, Thomas L. Madden, Alejandro A. Schäffer, Jinghui Zhang, Zheng Zhang, Webb Miller, and David J. Lipman (1997), "Gapped BLAST and PSI-BLAST: a new generation of protein database search programs", Nucleic Acids Res. 25:3389-3402.

Shaheen HH, Horetsky RL, Kimball SR, Murthi A, Jefferson LS, Hopper AK (2007). Retrograde nuclear accumulation of cytoplasmic tRNA in rat hepatoma cells in response to amino acid deprivation. Proc Natl Acad Sci USA 104, 8845–8850

Stevens S.W. , Barta I. , Ge H.Y., Moore R.E., Young M.K., Lee T.D., Abelson J. (2001). Biochemical and genetic analyses of the U5, U6, and U4/U6 x U5 small nuclear ribonucleoproteins from Saccharomyces cerevisiae RNA, 7, pp. 1543–1553

Sekimoto T, Miyamoto Y, Arai S, Yoneda Y., 2011. Importin alpha protein acts as a negative regulator for Snail protein nuclear import. J Biol Chem 286:15126–15131.

Shi Z, Yang WZ, Lin-Chao S, Chak KF & Yuan HS., 2008. Crystal structure of Escherichia coli PNPase: central channel residues are involved in processive RNA degradation. RNA 14: 2361–2371.

Siddiqui, N. *et al.,* 2007. Poly(A) nuclease interacts with the C-terminal domain of polyadenylate-binding protein domain from poly(A)-binding protein. *J. Biol. Chem.* 282, 25067–25075.

Sievers, F., Wilm, A., Dineen, D., Gibson, T.J., Karplus, K., Li, W., Lopez, R., McWilliam, H.,

Skowronek, E. W. a, Grzechnik, P., Marchfelder, A., & Kufel, J., 2013. Rex1 , and Rrp6, 115 130.

Shiota, C.; Coffey, J.; Grimsby, J.; Grippo, J.F.; Magnuson, M.A. Nuclear import of hepatic glucokinase depends upon glucokinase regulatory protein, whereas export is due to a nuclear export signal sequence in glucokinase. J. Biol. Chem., 1999, 274, 37125-37130.
Steitz J.A., Berg C., Hendrick J.P., La Branche-Chabot H., Metspalu A., Rinke J., Yario T.(1988) A 5S rRNA/L5 complex is a precursor to ribosome assembly in mammalian cells. J. Cell. Biol. 106:545–556.

Smith, A. E., Slepchenko, B. M., Schaff, J. C., Loew, L. M., and Macara, I. G, 2002 .Systems Analysis of Ran Transport .*Science* 295, 488–491

Soren L. A. et al , 2011. The eukaryotic RNA exosome. RNA Biology 8:1,61-66.

Sowadski, J. M., Handschumacher, M. D., Murthy, H. M. K., Foster, B. A., and Wyckoff, H. W., 1985 . Refined structure of alkaline phosphatase from Escherichia coli at 2.8 Å resolution . J. Mol. Biol. 186, 417–433

Spickler C & Mackie GA., 2000. Action of RNase II and polynucleotide phosphorylase against RNAs containing stemloops of defined structure. J Bacteriol 182: 2422–2427.

Stade, K., Ford, C. S., Guthrie, C., and Weis, K., 1997 . Exportin 1 (Crm1p) Is an Essential Nuclear Export Factor.*Cell* 90, 1041–1050.

Staub E, Fiziev P, Rosenthal A, Hinzmann B.,2004. Insights into the evolution of the nucleolus by an analysis of its protein domain repertoire. *Bioessays* 26: 567-581

Stead JA, Costello JL, Livingstone MJ, Mitchell P., 2007. The PMC2NT domain of the catalytic exosome subunit Rrp6p provides the interface for binding with its cofactor Rrp47p, a nucleic acid-binding protein. *Nucleic Acids Res* 35:5556-5567

Stefl R, Skrisovska L, Allain FH., 2005. RNA sequence- and shape-dependent recognition by proteins in the ribonucleoprotein particle. *EMBO reports* 6: 33-38.

Steitz T.A. and Steitz,J.A., 1993. A general two metal-ion mechanism for catalytic RNA. Proc. Natl Acad. Sci. USA, 90, 6498–6502.

Stevens A, Maupin MK., 1987. A 5'----3' exoribonuclease of Saccharomyces cerevisiae: size and novel substrate specificity. *Arch Biochem Biophys* 252: 339-347

Stevens SW, Abelson J, 1999. Purification of the yeast U4/U6.U5 small nuclear ribonucleoprotein particle and identification of its proteins. Proc Natl Acad Sci U S A 96: 7226–7231.

Stewart, M., Baker, R. P., Bayliss, R., Clayton, L., Grant, R. P., Littlewood, T., and Matsuura, Y., 2001. Molecular mechanism of translocation through nuclear pore complexes during nuclear protein import. *FEBS Lett.* 498, 145–149

Stoffler, D., Fahrenkrog, B., and Aebi, U., 1999. The nuclear pore complex: from molecular architecture to functional dynamics. *Curr. Opin. Cell Biol.* 11,391–401

Späth B, Canino G, Marchfelder A. 2007. tRNase Z: The end is not in sight. Cell Mol Life Sci 64: 2404–2412

Su, J.Y. and Maller, J.L. (1995). Cloning and expression of a *Xenopus* gene that prevents mitotic catastrophe in fission yeast. Mol. Gen. Genet. 246, 387-396.

Suntharalingam, M., and Wente, S. R., 2003 . Peering through the Pore: Nuclear Pore Complex Structure, Assembly, and Function .*Dev. Cell* 4, 775–789

Symmons MF, Jones GH & Luisi BF., 2000. A duplicated fold is the structural basis for polynucleotide phosphorylase catalytic activity, processivity, and regulation. Structure 8: 1215–1226.

Tabb MM, Tongaonkar P, Vu L, Nomura M. (2000). Evidence for separable functions of Srp1p, the yeast homolog of importin alpha (Karyopherin alpha): role for Srp1p and Sts1p in protein degradation. Mol Cell Biol. 2000, 20: 6062-6073. 10.1128/MCB.20.16.6062-6073.

Taro Shuin,b and Teijiro Aso., 2003. Identification of EloA-BP1, a novel Elongin A binding protein with an exonuclease homology domain. Biochemical and Biophysical Research

Takano A, Endo T, Yoshihisa T (2005). tRNA actively shuttles between the nucleus and cytosol in yeast. Science 309, 140–142.

Tettelin H et al, 1997. The nucleotide sequence of Saccharomyces cerevisiae chromosome VII. Nature. 29;387(6632 Suppl):81-4.

Thomson, E., Tollervey, D., 2010. The final step in 5.8S rRNA processing is cytoplasmic into granzyme A-mediated cell death underlies familial chilblain lupus. *J Mol Med (Berl)*, 85, 531-

Thoms, M., Thomson, E., Baßler, J., Gna¨ dig, M., Griesel, S., and Hurt, E. (2015). The exosome is recruited to RNA substrates through specific adaptor proteins. Cell 162, 1029–1038.

Tran, E. J., and Wente, S. R., 2006. Dynamic Nuclear Pore Complexes: Life on the Edge. *Cell* 125, 1041–1053

Tucker, M., Staples, R.R., Valencia-Sanchez, M.A., Muhlrad, D. & Parker, R., 2002. Ccr4p is the catalytic subunit of a Ccr4p/Pop2p/Notp mRNA deadenylase complex in *Saccharomyces cerevisiae*. *EMBO J.* 21, 1427–1436.

Turowski TW, Lesniewska E, Delan-Forino C, Sayou C, Boguta M, Tollervey D. Global analysis of transcriptionally engaged yeast RNA polymerase III reveals extended tRNA transcripts. Genome research. 2016;26(7):933–44. doi: 10.1101/gr.205492.116

Van der Giessen K, Gallouzi IE., 2007. Involvement of transportin 2-mediated HuR import in muscle cell differentiation. Mol Biol Cell;18:2619–2629.

Van Hoof A, Lennertz P, Parker R., 2000a. Yeast exosome mutants accumulate 3'-extended polyadenylated forms of U4 small nuclear RNA and small nucleolar RNAs. *Mol Cell Biol* 20: 441-452

Van Hoof, A., R. R. Staples, R. E. Baker, and R. Parker., 2000c. Function of the Ski4p (Csl4p) and Ski7p proteins in 3'-to-5' degradation of mRNA. Mol. Cell. Biol. 20:8230–8243.

Van Hoof,A., Lennertz,P. and Parker,R., 2000b. Three conserved members of the RNase D family have unique and overlapping functions in the processing of 5S, 5.8S, U4, U5, RNase MRP and RNase P RNAs in yeast. EMBO J., 19, 1357–1365.

Van Horn, D.J., Yoo, C.J., Xue, D., Shi, H., and Wolin, S.L., 1997. TheLa protein in Schizosaccharomyces pombe: a conserved yet dispensablephosphoprotein that functions in tRNA maturation. RNA 3: 1434–1443.

Vanácová, S., Wolf, J., Martin, G., Blank, D., Dettwiler, S., Friedlein, A., Langen, H., Keith, G.,
Keller, W., 2005. A new yeast poly(A) polymerase complex involved in RNA quality control.
PLoS Biol 3, e189.

Vanacova, S., J. Wolf, G. Martin, D. Blank, S. Dettwiler et al., 2005 A new yeast poly(A) polymerase complex involved in RNA quality control. PLoS Biol. 3: e189

Vasiljeva L and Buratowski S., 2006. Nrd1 interacts with the nuclear exosome for 3' processing of RNA polymerase II transcripts. Mol Cell.2:239-48.

Venema,J. and Tollervey,D. (1999) Ribosome synthesis in Saccharomyces cerevisiae. Annu. Rev. Genet., 33, 261±311.

Vincent HA & Deutscher MP., 2006. Substrate recognition and catalysis by the exoribonuclease RNase R. J Biol Chem 281: 29769–29775.

Viswanathan M, Dower KW & Lovett ST., 1998. Identification of a potent DNase activity associated with RNase Tof Escherichia coli. J Biol Chem 273: 35126–35131.

von Hippel,P.H. and Berg,O.G. (1989) Facilitated target location in biological systems. J. Biol. Chem., 264, 675–678.

Vogtle FN, Wortelkamp S, Zahedi RP, Becker D, Leidhold C, Gevaert K, Kellermann J, Voos W, Sickmann A, Pfanner N, Meisinger C,2009. Global analysis of the mitochondrial N-proteome identifies a processing peptidase critical for protein stability. Cell 139(2):428-39.

Wahle, E. & Winkler, G.S., 2013. RNA decay machines: deadenylation by the Ccr4-Not and Pan2-Pan3 complexes. *Biochim. Biophys. Acta* 1829, 561–570.

Wang HW, Wang J, Ding F, Callahan K, Bratkowski MA, Butler JS, Nogales E, Ke A., 2007. Architecture of the yeast Rrp44 exosome complex suggests routes of RNA recruitment for 3’ end processing. *Proc Natl Acad Sci USA* 2 104: 16844–16849.

Wang P, Liu GH, Wu K, Qu J, Huang B, Zhang X, Zhou X, Gerace L, Chen C., 2009. Repression of classical nuclear export by S-nitrosylation of CRM1. J Cell Sci 122:3772–3779.

Wang R, Shen J, Huang P, Zhu X., 2013. CCCTC-binding factor controls its own nuclear transport via regulating the expression of importin 13.Mol Cells 35:388–395.

Wang, W., and D. H. Bechhofer., 1996. Properties of a *Bacillus subtilis* polynucleotide phosphorylase deletion strain. J. Bacteriol. 178:2375–2382.

Wang, J., Yu,P., Lin,T., Konigsberg,W. and Steitz,T., 1996. Wang,J., Yu,P., Lin,T., Konigsberg,W. and Steitz,T. (1996) *Biochemistry*, 35, 8110–8119 .*Biochemistry*, 35, 8110–8119.

Waters SA, McAteer SP, Kudla G, Pang I, Deshpande NP, Amos TG, et al. (2017) Small RNA interactome of pathogenic E. coli revealed through crosslinking of RNase E. EMBO J.;36(3):374–87.

Weiss, M.A., and Narayana, N. 1998. RNA recognition by arginine-rich peptide motifs. Biopolymers 48: 167-180.

Wen-Tao Peng, Mark D. Robinson, Sanie Mnaimneh, Nevan J. Krogan, Gerard Cagney, Quaid Morris, Armaity P. Davierwala, Jo¨ rg Grigull, Introduction Xueqi Yang, Wen Zhang, Nicholas Mitsakakis, Owen W. Ryan, Chris Pal, Veronica Canadien, Dawn Richards, Bryan Beattie, Lani F. Wu, Steven J. Altschuler, Sam Roweis, Brendan J. Frey, Andrew Emili, Jack F. Greenblatt, and Timothy R. Hughes, 2003. A Panoramic View of Yeast Noncoding RNA Processing. Cell. Vol. 113, 919–933.

Wintersberg, U., 1990. Ribonucleases H of retroviral and cellular origin. Pharmacol. Ther. 48, 259-280.

Whitney ML, Hurto RL, Shaheen HH, Hopper AK (2007). Rapid and reversible nuclear accumulation of cytoplasmic tRNA in response to nutrient availability. Mol Biol Cell 18, 2678–2686.

Winther K. , Tree J.J., Tollervey D., Gerdes K. VapCs., 2016. Mycobacterium tuberculosis cleave RNAs essential for translation. Nucleic Acids Res.; 44:9860–9871.

Wolin, S.L. and Cedervall, T., 2002. The La protein. Annu. Rev. Biochem. 71: 375–402.

Wolin,S.L. and Matera,A.G., 1999. The trials and travels of tRNA. Genes Dev., 13, 1–10.

Wolf, J., Valkov, E., Allen, M.D., Meineke, B., Gordiyenko, Y., McLaughlin, S.H., Olsen, T.M., Robinson, C.V., Bycroft, M., Stewart, M. et al. (2014) Structural basis for Pan3 binding to Pan2 and its function in mRNA recruitment and deadenylation. EMBO J 33, 1514–1526

Wu M, Reuter M, Lilie H., Liu Y., Wahle E. (2005). Song Structural insight into poly(A) binding and catalytic mechanism of human PARN EMBO J., 24, pp. 4082-4093

Wyers, F., Rougemaille, M., Badis, G., Rousselle, J.-C., Dufour, M.-E., Boulay, J., Régnault, B.,
Devaux, F., Namane, A., Séraphin, B., Libri, D., Jacquier, A., 2005. Cryptic pol II transcripts
are degraded by a nuclear quality control pathway involving a new poly(A) polymerase. Cell
121, 725–737.

Xia, Y.-P.; Yeh, C.-T.; Ou, J.-H.; Lai, M.M.C. Characterization of nuclear targeting signal of hepatitis delta antigen: nuclear transport as a protein complex. J. Virol., 1992, 66, 914-921.

Xue Y, Bai X, Lee I, Kallstrom G, Ho J, Brown J, Stevens A, Johnson AW., 2000. Saccharomyces cerevisiae RAI1 (YGL246c) is homologous to human DOM3Z and encodes a protein that binds the nuclear exoribonuclease Rat1p. *Mol Cell Biol* 20: 4006-4015

Yamaguchi YL, Tanaka SS, Yasuda K, Matsui Y, Tam PP., 2006. Stage-specific Importin13 activity influences meiosis of germ cells in the mouse. Dev Biol 297:350–360.

Yamada-Okabe, Toshiko; Mio, Toshiyuki; Matsui, Mitsuaki; Arisawa, Mikio; Yamada-Okabe, Hisafumi (November 1999). The Candida albicans gene for mRNA 5'-cap methyltransferase: identification of additional residues essential for catalysis. . *Microbiology*. 145 (11): 3023–3033. ISSN 1350-0872. PMID 10589710. doi:10.1099/00221287-145-11-3023. Retrieved January 7, 2011.

Yan, N., Regalado-Magdos, A.D., Stiggelbout, B., Lee-Kirsch, M.A. and Lieberman, J., 2010. The cytosolic exonuclease TREX1 inhibits the innate immune response to human immunodeficiency virus type 1. *Nat Immunol*, 11, 1005-1013.

Yoo, C.J. and Wolin, S.L., 1997. The yeast La protein is required forthe 39 endonucleolytic cleavage that matures tRNA precursors. Cell 89: 393–402.

Yoshihisa, T, Yunoki-Esaki, K., Ohshima, C., Tanaka, N. & Endo, T. (2003) Mol. Biol. Cell 14, 3266–3279.

Yoshida, K., and Blobel, G., 2001. The Karyopherin Kap142p/Msn5p Mediates Nuclear Import and Nuclear Export of Different Cargo Proteins. *J. Cell Biol.* 152, 729–740

You P, Peng Z, Wang Y, Tao T., 2013 Expression and subcellular distribution of imp13 are regulated in brain development. In Vitro Cell Dev Biol Anim 49:346–353.

Yoo, C J. and Wolin, S L., 1994. La proteins from Drosophila melanogaster and Saccharomyces cerevisiae: a yeast homolog of the La autoantigen is dispensable for growth. Mol. Cell. Biol. 8:5412.

Yuhong Zuo and Murray P. Deutscher., 2001. Exoribonuclease superfamilies: structuralanalysisandphylogeneticdistribution. *NucleicAcidsResearch, .29: 1017–1026*

Zangrossi S, Briani F, Ghisotti D, Regonesi ME, Tortora P & Deho` G., 2000. Transcriptional and post-transcriptional control of polynucleotide phosphorylase during cold acclimation in Escherichia coli. Mol Microbiol 36: 1470–1480.

Zhang JR & Deutscher MP., 1988b. Transfer RNA is a substrate for RNase D in vivo. J Biol Chem 263: 17909–17912.

Zhihua Li1, Insuk Lee1,2, Emily Moradi1, Nai-Jung Hung3, Arlen W. Johnson3, Edward M. Marcotte1., 2009. Rational Extension of the Ribosome Biogenesis Pathway Using Network-Guided Genetics. PLoS Biology. 7 :10: 1-17.

Zhou, Z., and M. P. Deutscher., 1997. An essential function for the phosphate-dependent exoribonucleases RNase PH and polynucleotide phosphorylase.

Zilha˜o R, Caillet J, Regnier P & Arraiano CM., 1995a. Precise physical mapping of the Escherichia coli rnb gene, encoding ribonuclease II. Mol Gen Genet 248: 242–246.

Zilha˜o R, Cairra˜o F, R´egnier P & Arraiano CM., 1996a. PNPase modulates RNase II expression in Escherichia coli: implications for mRNA decay and cell metabolism. Mol Microbiol 20: 1033–1042.

Zilha˜o R, Camelo L & Arraiano CM., 1993. DNA sequencing and expression of the gene rnb encoding Escherichia coli ribonuclease II. Mol Microbiol 8: 43–51.

Zilha˜o R, Plumbridge J, Hajnsdorf E, Regnier P & Arraiano CM., 1996b. Escherichia coli RNase II: characterization of the promoters involved in the transcription of rnb. Microbiology 142: 367–375.

Zilha˜o R, R´egnier P & Arraiano CM., 1995b. The role of endonucleases in the expression of ribonuclease II in Escherichia coli. FEMS Microbiol Lett 130: 237–244.

Zuo Y & Deutscher MP., 2001. Exoribonuclease superfamilies:structural analysis and phylogenetic distribution. Nucleic Acids Res 29: 1017–1026. *Design and Selection*, *3*(6), 461–467. http://doi.org/10.1093/protein/3.6.461

Zuo Y, Wang Y & Malhotra A, 2005. Crystal structure of Escherichia coli RNase D, an exoribonuclease involved in structured RNA processing. Structure 13: 973–984.

Zuo, Y. and Deutscher, M.P., 2002. Mechanism of action of RNase T. I. Identification of residues required for catalysis, substrate binding, and dimerization. *J Biol Chem*, 277, 50155-50159.

Zuo, Y., & Deutscher, M. P., 2001. Exoribonuclease superfamilies: structural analysis and phylogenetic distribution. *Nucleic Acids Research*, *29*(5), 1017–1026.

Zuo,Y., Zheng,H., Wang,Y., Chruszcz,M., Cymborowski,M.,Skarina,T., Savchenko,A. and Minor,W., 2007. Crystal structureof RNase T, an exoribonuclease involved in tRNA maturation and end turnover. Structure, 15, 417–428.

Zhou, A., Hassel, B.A., and Silverman, R.H. (1993). Expression cloning of 2-5Adependent RNAase: a uniquely regulated mediator of interferon action. Cell 72, 753–765.

Zhou, A., Paranjape, J., Brown, T.L., Nie, H., Naik, S., Dong, B., Chang, A., Trapp, B., Fairchild, R., Colmenares, C., and Silverman, R.H. (1997). Interferon action and apoptosis are defective in mice devoid of 20,50-oligoadenylate-dependent RNase L. EMBO J. 16, 6355–6363.

Figures

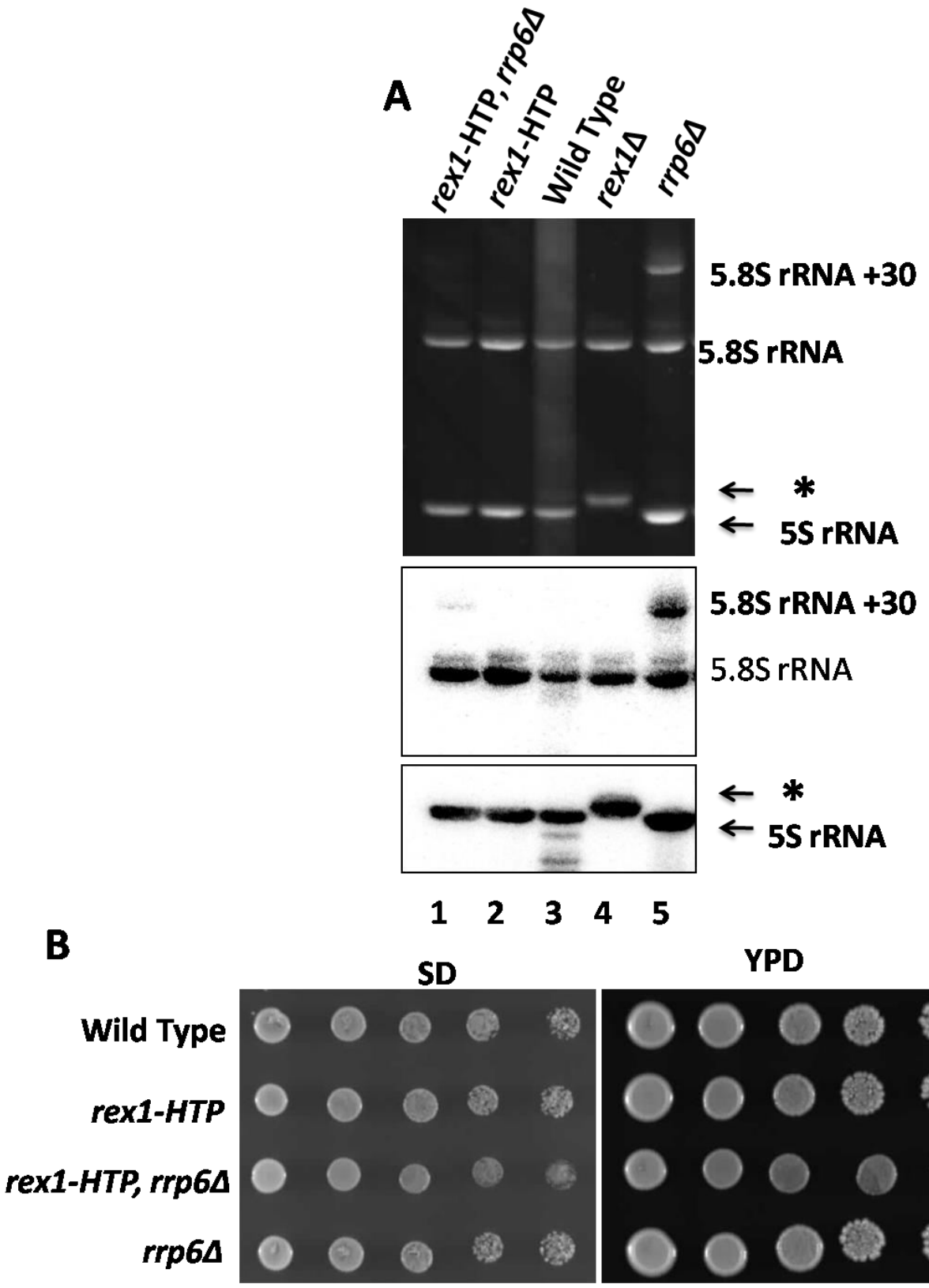

Figure 45 The *rex1*-HTP fusion protein processes 5S rRNA in both wild type and *rrp6Δ* strains.

(A) Analysis of 5S and 5.8S rRNA species in the *rex1-HTP* and *rex1-HTP rrp6Δ* strains. Total cellular RNA was resolved through denaturing polyacrylamide gels, transferred to membranes and hybridised with probes specific to the 5.8S and 5S rRNAs. Upper panel, image of the ethidium stained polyacrylamide gel. Centre panel, northern blot hybridised with a 5.8S rRNA probe. Lower panel, northern blot hybridised with a 5S rRNA probe. The relevant strain genotypes are indicated at the top. The asterisk indicates the 3' extended form of 5S rRNA seen in rex1 loss of function mutants. The "5.8S+30" band is characteristic of rrp6Δ mutants. **(B)** Spot growth analysis of a wild-type strain and isogenic *rex1-HTP* and *rrp6Δ* single mutants and the *rex1-HTP rrp6Δ* double mutant. Strains were pregrown in YPD medium and then serial dilutions were applied to minimal and rich medium plates. The plates were photographed after incubation at 30°C for three days.

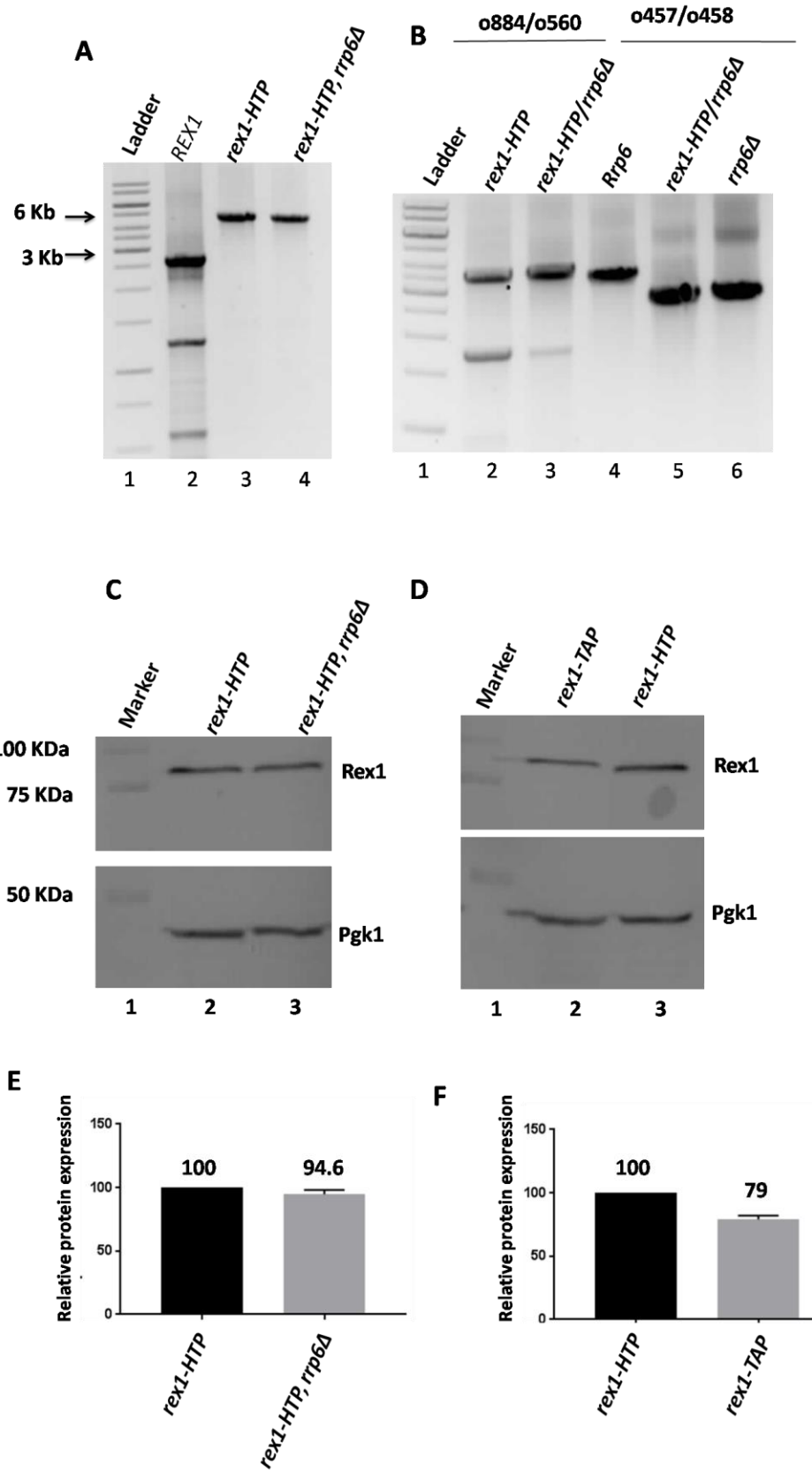

Figure 44 Generation of a *rex1-HTP* strain.

The HTP epitope tag was amplified from yeast genomic DNA with primers showing homology to the *REX1* locus and the PCR product was transformed into a wild-type strain and an isogenic *rrp6Δ* strain. Transformants were recovered by growth on selective medium and validated by PCR amplification of the *REX1* and *RRP6* genes and by western blot analyses of cell lysates **(A)** Validation of *rex1-HTP* and *rex1-HTP rrp6Δ* integrants by PCR. PCR was performed on yeast genomic DNA using the *REX1*-outlying primers o559 and o560, and the products were resolved by agarose gel electrophoresis. Lane1, DNA markers; lane 2, genomic DNA from a wild type *REX1* strain; lane 3, genomic DNA from a *rex1-HTP* isolate; lane 4, genomic DNA from a *rex1-HTP* isolate in an *rrp6Δ* strain background. **(B)** Further validation of the *rex1-HTP* strains by PCR. The lanes labelled o880/o560 are reactions using the forward primer o880, which anneals to a site within the *REX1* ORF, and the o560 reverse primer. The lanes labelled o457/o458 are reactions using primers outlying the *RRP6* gene. The relevant genotype of the strains are indicated above the panel. **(C)** Western analysis of the Rex1-HTP protein. Lysates from *rex1-HTP* and *rex1-HTP rrp6Δ* candidates were resolved by SDS-PAGE and analysed by western blotting. Detected Rex1 and Pgk1 proteins are indicated. **(D)** Comparative analysis of the expression of *rex1-HTP* and *rex1-TAP* proteins. **(E)** Quantification of the relative expression level of rex1-HTP in a RRP6 and rrp6Δ strain. **(F)** Quantification of the relative expression level of rex1-HTP and rex1-TAP proteins. The error bars indicate the standard deviation of the mean of three replicates in each case.

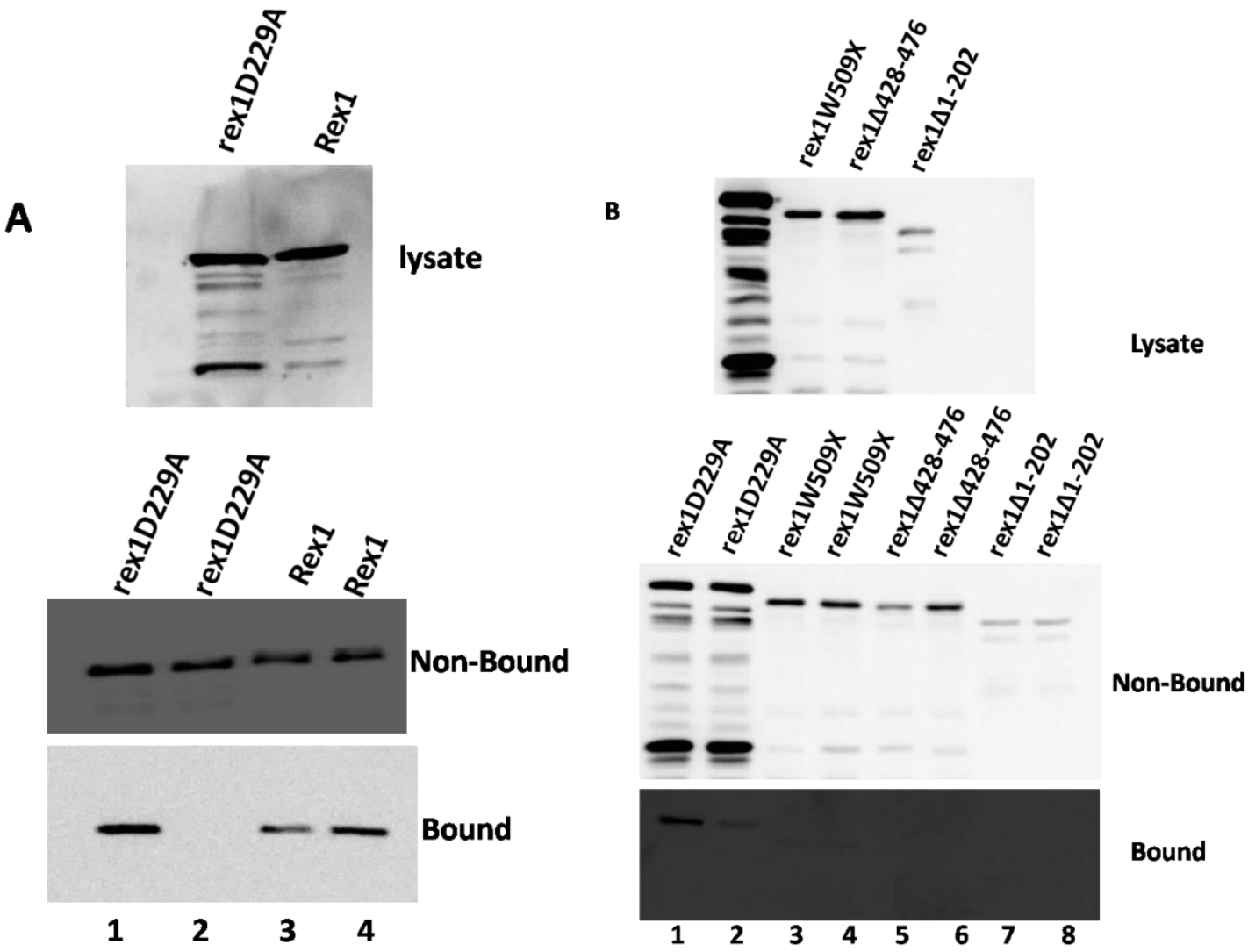

Figure 43 The N- and C-terminal regions of Rex1 are required for RNA binding in vitro.

RNA binding assays were performed on Rex1 proteins after purification by ion exchange chromatography using poly(U)-agarose beads. Retained protein was specifically eluted by treatment with RNase. Rex1 protein in the lysate, the non-bound fraction and the bound (specifically eluted) fractions was detected by SDS-PAGE and western blotting, using the PAP antibody complex. **(A)** RNA binding assay of full-length Rex1 and the catalytically inactive D229A mutant. Lane 1, incubation of the D229A mutant with poly(U)-agarose beads; lane 2, incubation of the D229A mutant with control beads lacking poly(U). Lanes 3 and 4, duplicate samples of full-length zz-Rex1 incubated with poly(U) beads. **(B)** RNA binding assay of the rex1 deletion mutants. Upper panel, western blot analysis of the cell lysates. Lower panels, western blot analyses of non-bound and bound fractions of duplicate reactions for each mutant.

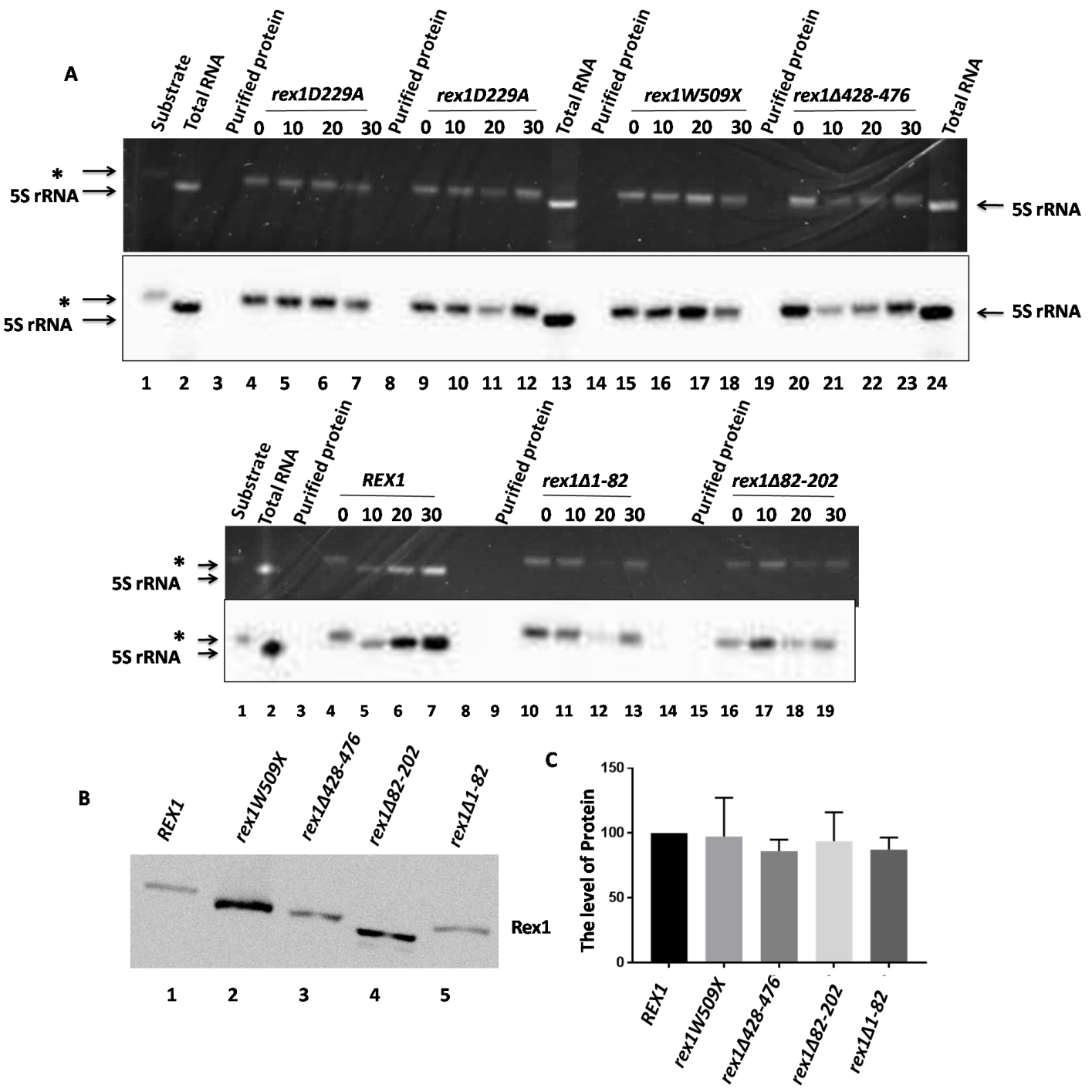

Figure 42 Yeast *rex1* mutants are unable to process 5S rRNA *in vitro*.

(A) *In vitro* 5S rRNA processing assay. Rex1 proteins tethered to IgG sepharose beads were incubated with purified 5S rRNP complexes from a r*ex1Δ* strain. Aliquots of the reaction mixtures were removed at various time points (in minutes) and the RNA was resolved by PAGE through a denaturing gel. RNA was detected by ethidium staining of the gels and by northern blot hybridisation after transferring the RNA to a nylon membrane, using a probe specific to the 5S rRNA. Lane 1, 5S RNP substrate from a *rex1Δ* strain; lane 2, total celluar RNA from a wild-type strain; lane 3, control sample without added RNA substrate; lanes 4-7, time-course of incubations with purified wild-type and mutant Rex1 proteins, including the catalytically inactive D229A *rex1* mutant. **(B)** Western analysis of Rex1 proteins after recovery from the beads. Lane 1, wild-type Rex1, lane2, *rex1W509X mutant*; lane 3*, rex1Δ428-476*; lane 4, *rex1Δ82-202*; lane 5, the *rex1Δ1-82* mutant. **(C)** The level of protein measured by ECL is indicated in the histogram, the error bar indicating the standard deviation of the mean of three independent assays.

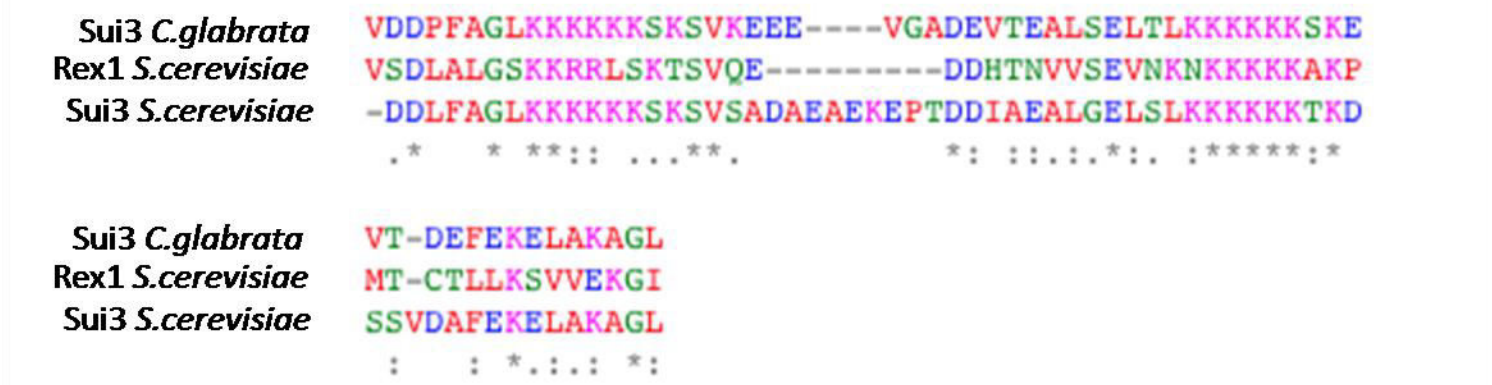

Figure 39 Sequence alignment of Rex1 and Sui3 sequences.

A BLAST search using the N-terminal 82 residues of Rex1 from *S. cerevisiae* identified homology with a the N-terminal region of eiF2β from Candida glabrata. The homologous sequence in the S. cerevisiae eiF2β protein (Sui3) was identified through a further BLAST search. The three sequences were then aligned using T-Coffee. The sequences shown are residues 10-69 of Sui3 from *C. glabrata*, residues 11-65 of Rex1 from *S. cerevisiae* and residues 42-105 of Sui3 from *S. cerevisiae*. Conserved residues are indicated by asterisks. Similar and highly similar residues are indicated by one or two dots, respectively.

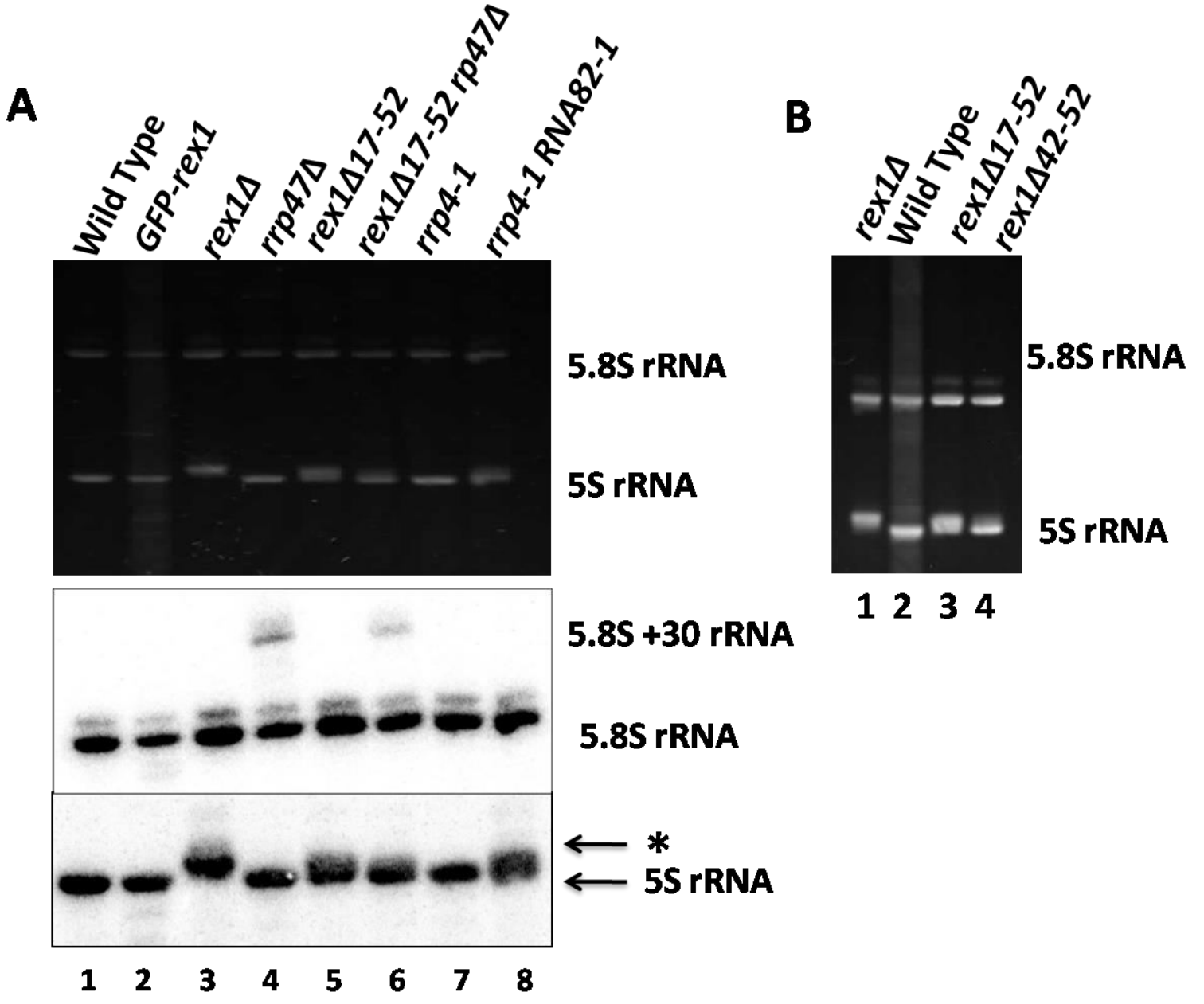

Figure 38 **The *rex1Δ17-52* mutant shows a 5S rRNA processing is defect.**

Total cellular RNA was extracted from yeast, resolved through an 8% denaturing polyacrylamide gel and visualised by staining with ethidium bromide. The RNA was then transferred to a nylon membrane and the northern blot was hybridised with probes complementary to the 5S and 5.8S rRNAs. Relevant strain genotypes are indicated at the top of the figure. The asterisk indicates 3' extended forms of 5S rRNA

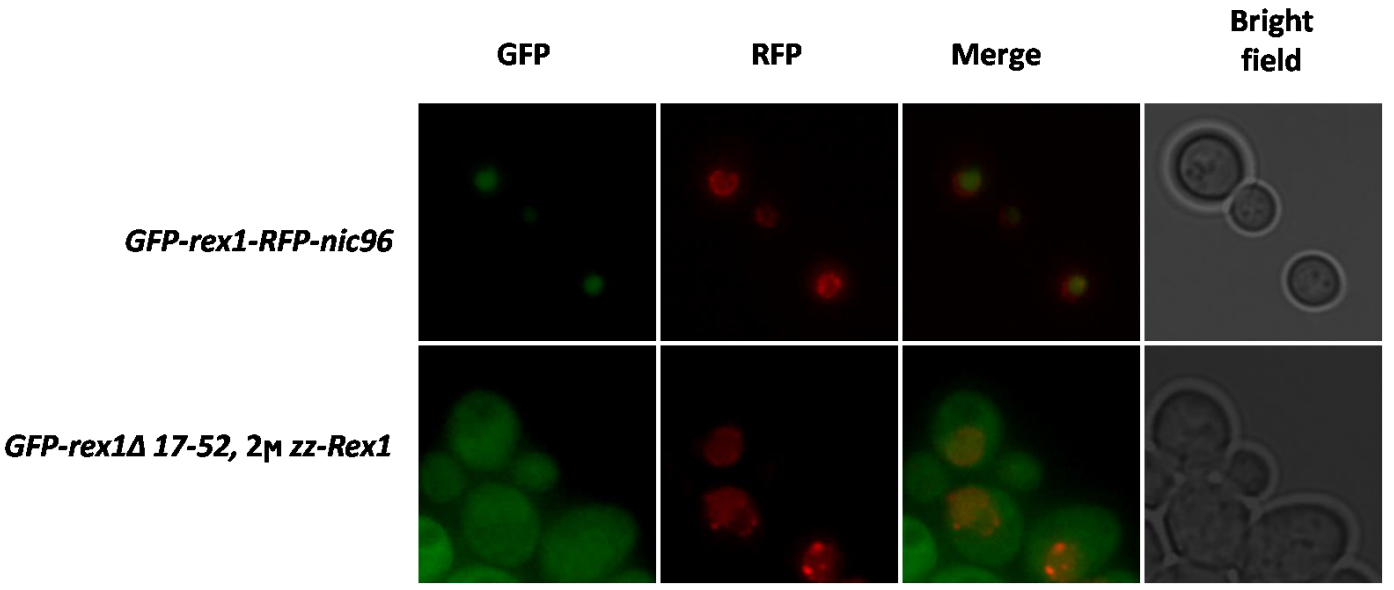

Figure 37 Expression of *zz-rex1* from a 2μ vector does not lead to nuclear accumulation of *GFP-rex1Δ17-52*.

Fluorescence microscopy analyses were performed on living cells expressing both the GFP-rex1Δ17-52 fusion protein and the nonfluorescent zz-Rex1 protein from a high copy number 2μ plasmid. Cells expressing the GFP-Rex1 protein were analysed in parallel. Both strains also expressed the mRFP-Nic96 protein. Representative images of cells that were obtained using the GFP channel, the RFP channel, merged channels and the bright field objective are shown.

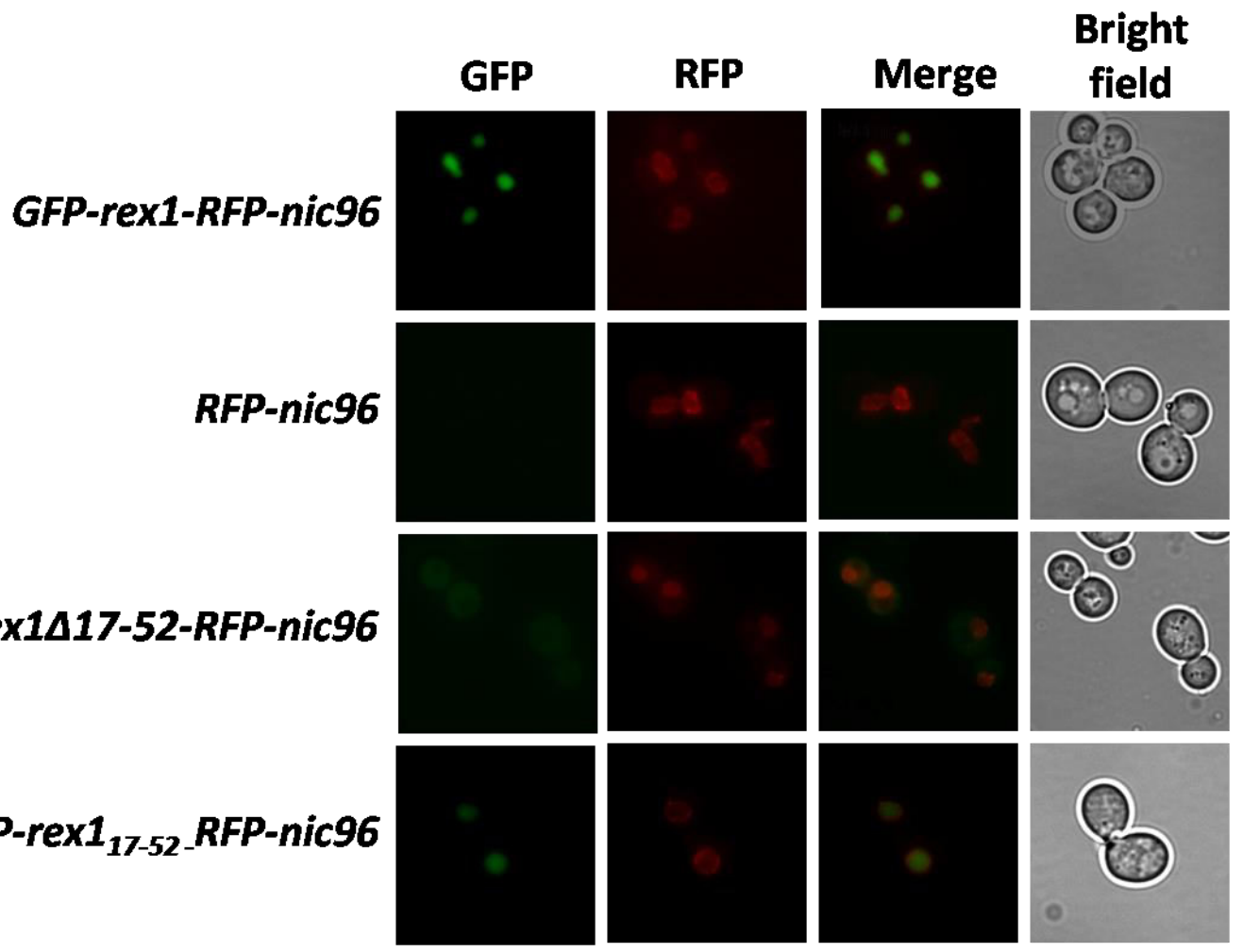
GFP
RFP
Merge
Bright field
GFP-rex1-RFP-nic96
RFP-nic96
GFP-rex1Δ17-52-RFP-nic96
GFP-rex1$_{17-52}$-RFP-nic96

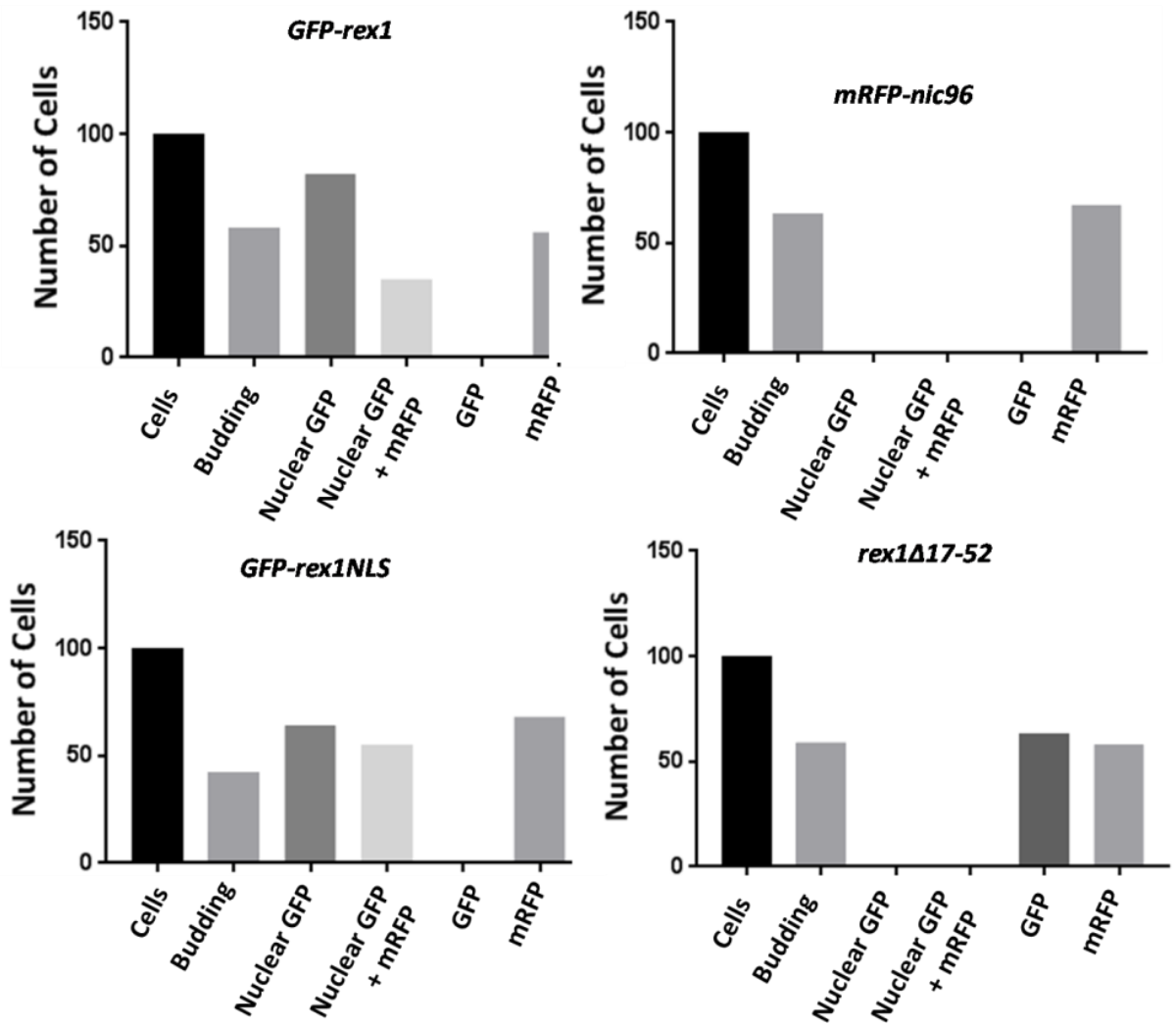

Figure 36 Residues of 17-52 of Rex1 constitute a nuclear localization signal sequence.

Cells expressing GFP fusions and the mRNP-Nic96 protein were analysed by fluorescence microscopy. 100 randomly selected cells were phenotypically scored for budding, the nuclear or cytoplasmic distribution of the GFP fusion and for coexpression of both fluorescent proteins. Data are presented as histograms. GFP channel, RFP channel, merged channel and bright field images of representative cells are shown.

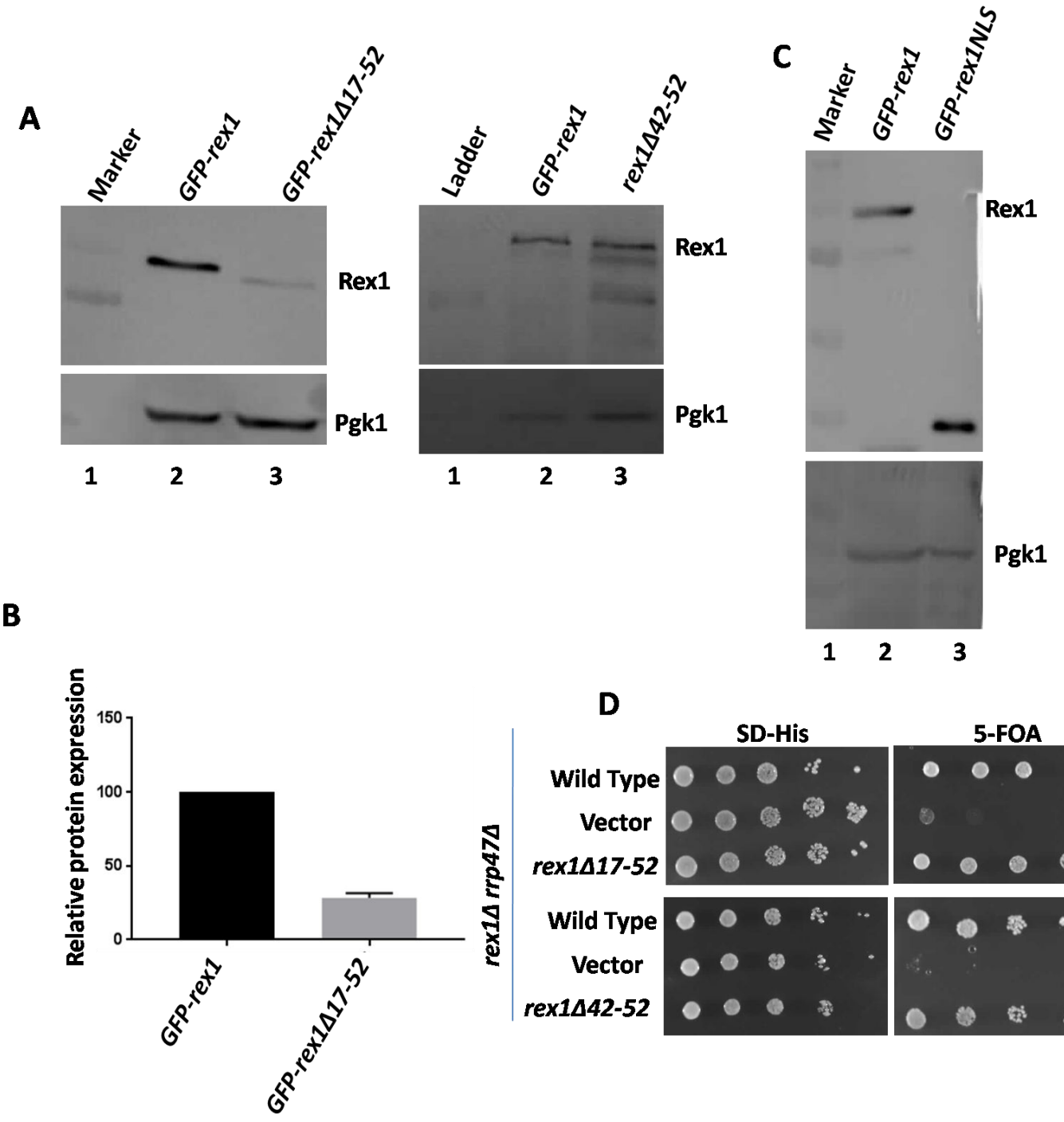

Figure 35 Deletion of residues 17-52 of Rex1 causes reduced expression but does not block activity.

(A) Western analysis of the GFP-rex1Δ17-52 and GFP-rex1Δ42-52 fusion. Extracts from cells expressing full-length GFP-rex1 , the GFP-rex1Δ17-52 or GFP-rex1Δ42-52 deletion mutant were resolved by SDS-PAGE and analysed by western blotting, using an anti-GFP antibody. Pgk1 was also anlaysed as a loading control. (**B**) Quantitation of the expression level of the GFP-rex1Δ17-52 mutant, relative to that of the full-length GFP-rex1 protein. The error bar indicates the standard deviation of the mean of three biological replicates. (**C**) Western analysis of the expression of GFP fused to residues 17-52 of Rex1. The expression level of the GFP-rex1NLS was compared to that of the full-length GFP-rex1 protein. (D) Complementation assay of the *rex1Δ rrp47Δ* double mutant with the GFP-rex1Δ17-52 allele. The plasmid shuffle strain was transformed with plasmids encoding the full-length GFP-rex1 protein, the GFP-rex1Δ17-52 mutant, or the cloning vector, and the transformants were assayed for growth on selective minimal medium and on medium containing 5-FOA. The plates were photographed after incubation at 30°C for 3 days.

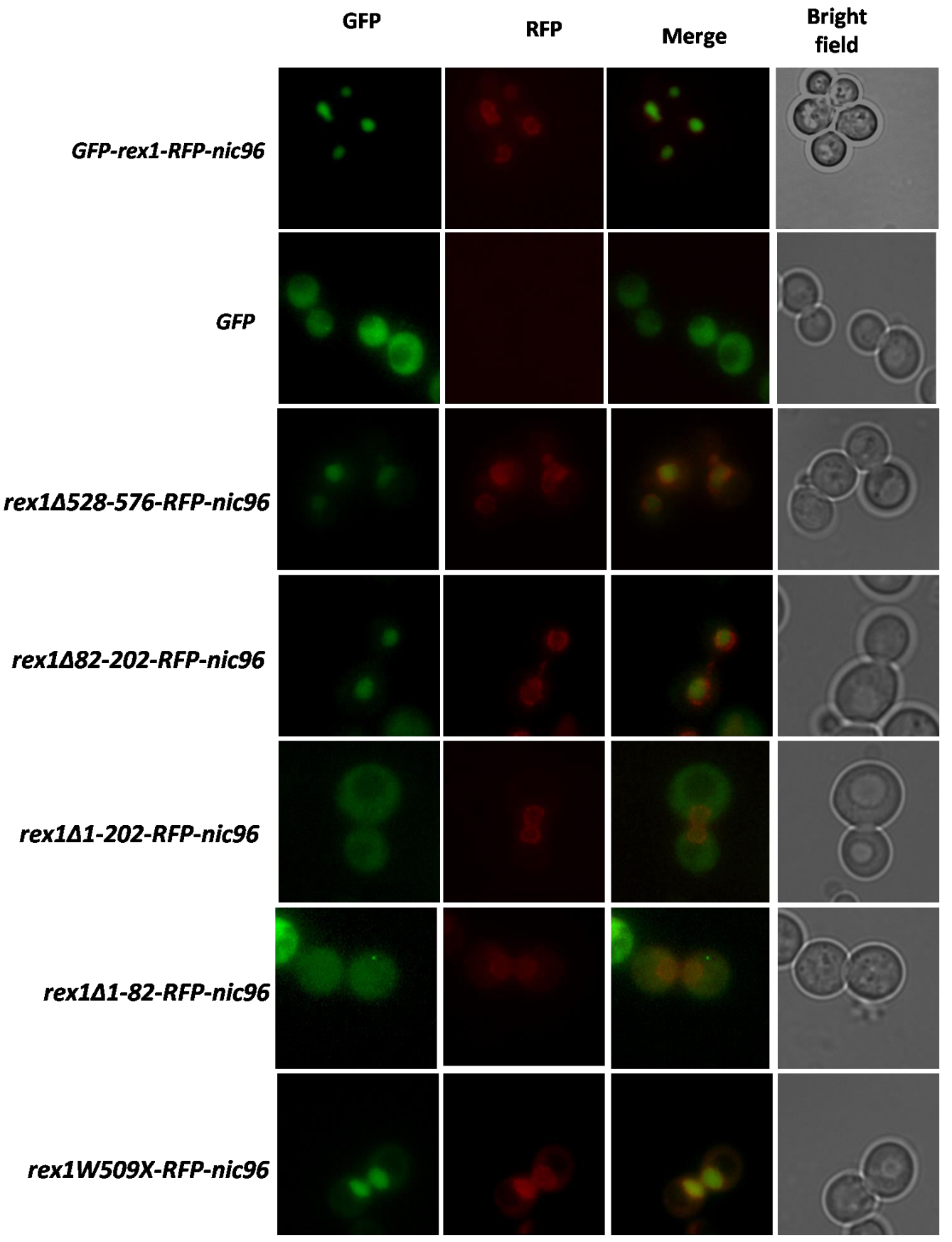
GFP
RFP
Merge
Bright field
GFP-rex1-RFP-nic96
GFP
rex1Δ528-576-RFP-nic96
rex1Δ82-202-RFP-nic96
rex1Δ1-202-RFP-nic96
rex1Δ1-82-RFP-nic96
rex1W509X-RFP-nic96

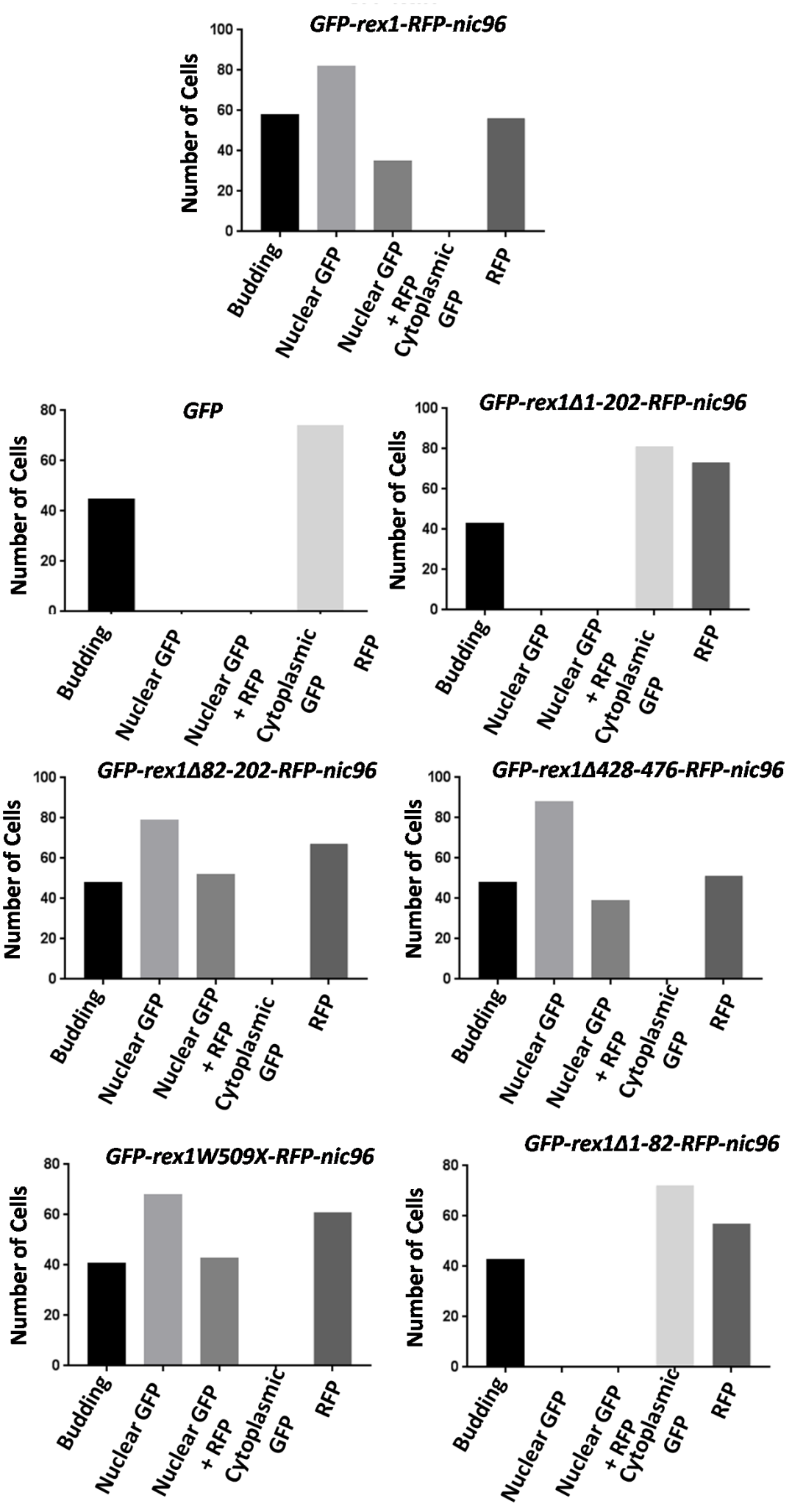

Figure 33 The N-terminal region of Rex1 is important for nuclear localization.
The subcellular localisation of the GFP-rex1 fusion proteins was analysed by fluorescence microscopy on living cells. The GFP fusions were expressed in a *rex1Δ* mutant, together with the nuclear periphery marker mRFP-Nic96. 100 randomly selected individual cells from each transformant were visually scored for the presence of a bud, a nuclear GFP signal, both a nuclear GFP signal and an RFP signal, a cytoplasmic GFP signal, and an RFP signal. The number of cells in each category are shown for each mutant. GFP channel, RFP channel, merged channel and bright field images are shown of representative cells for each mutant.

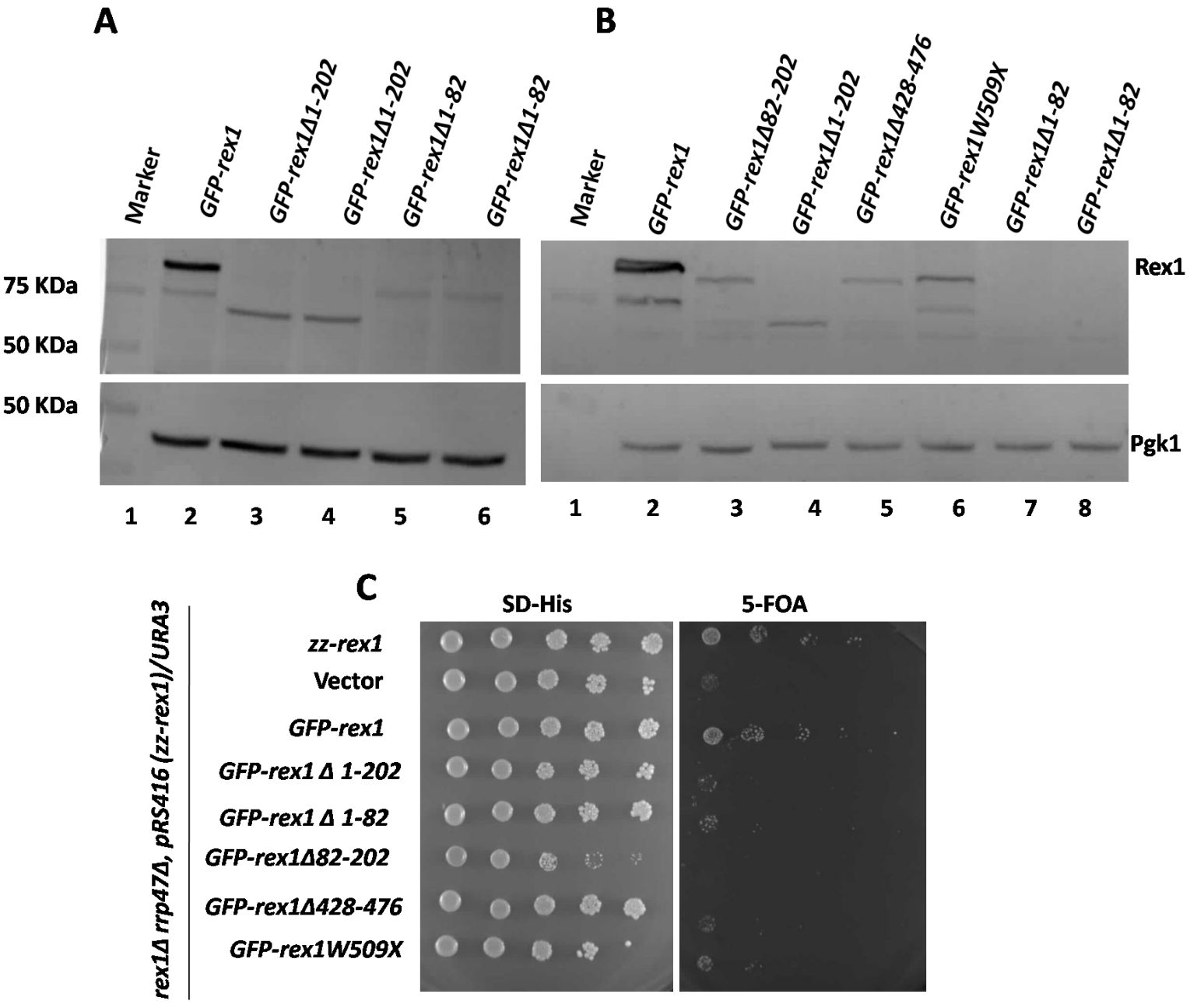

Figure 32 Functional and western analysis of different mutants of *GFP-rex1*.

(A and B) Western analysis of the *GFP-rex1* mutants. Cell extracts were resolved by SDS-PAGE and analysed by western blotting, using an anti-GFP antibody and an anti-Pgk1 antibody (lower panel). **(C)** Complementation assay of the *GFP-rex1* mutant alleles, using the *rex1Δ rrp47Δ* plasmid shuffle strain. Transformants expressing the full-length zz-rex1 allele, the GFP fusion alleles or harbouring the cloning vector were assayed for growth on selective minimal medium and on medium containing 5-FOA using a spot growth assay. Plates were photographed after incubation at 30°C for 3 days.

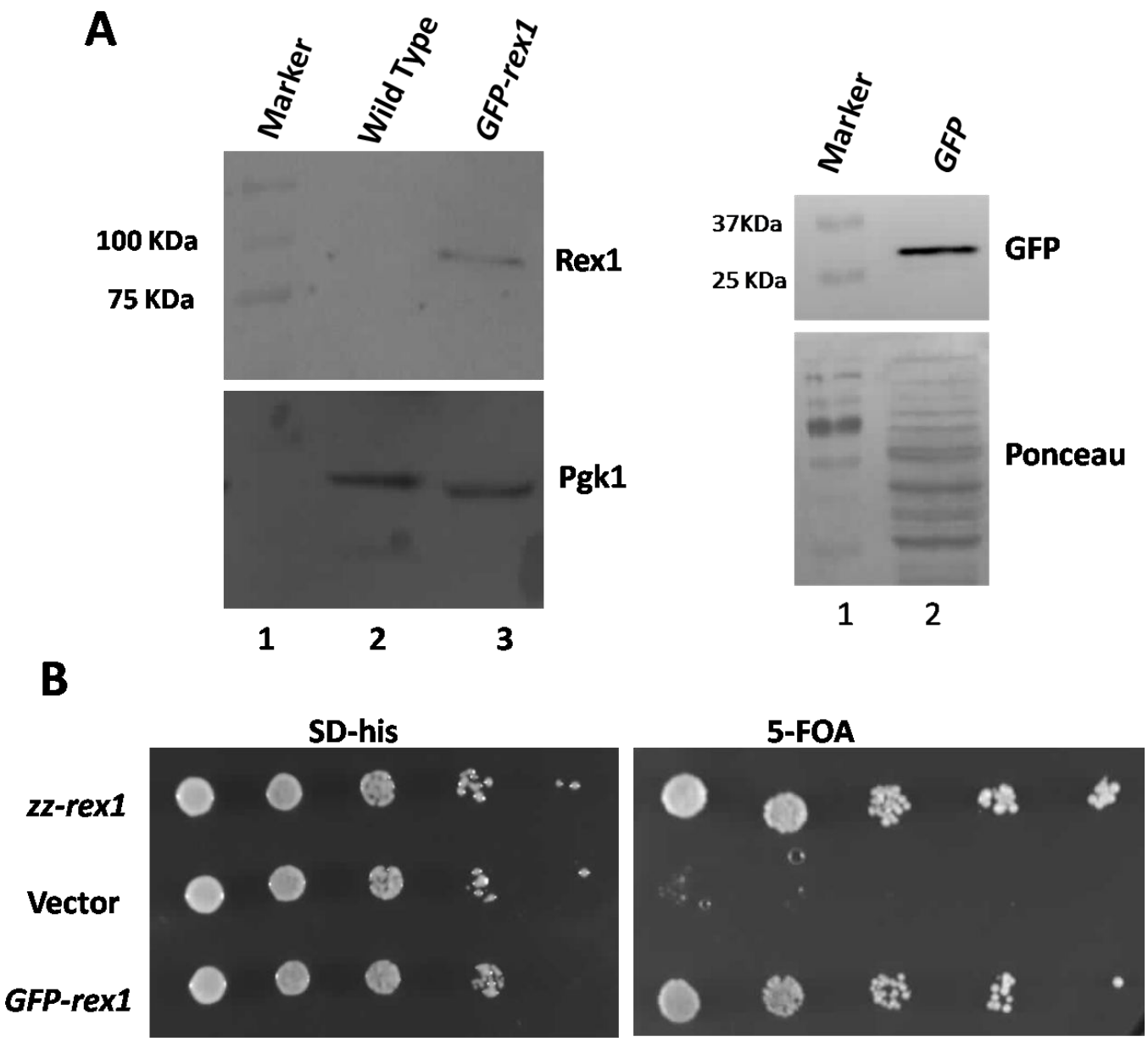

Figure 30 Western and functional analysis of the GFP-Rex1 protein.

(A) Western analysis of GFP-Rex1. Cell lysate from a strain expressing the GFP (the right panel) and GFP-Rex1 fusion protein (the left panel, lane 3) or harbouring the vector control (lane 2) were resolved by SDS-PAGE and analysed by western blotting, using an anti-GFP antibody (upper panel) and an anti-Pgk1 antibody (lower panel). **(B)** Spot growth analysis of the *rex1Δ rrp47Δ* plasmid shuffle strain P596 after transformation with a plasmid encoding either the zz-Rex1 or GFP-Rex1 fusion protein, or the vector control. The left hand panel shows growth on medium lacking histidine. The right hand panel shows growth on medium containing 5-FOA.

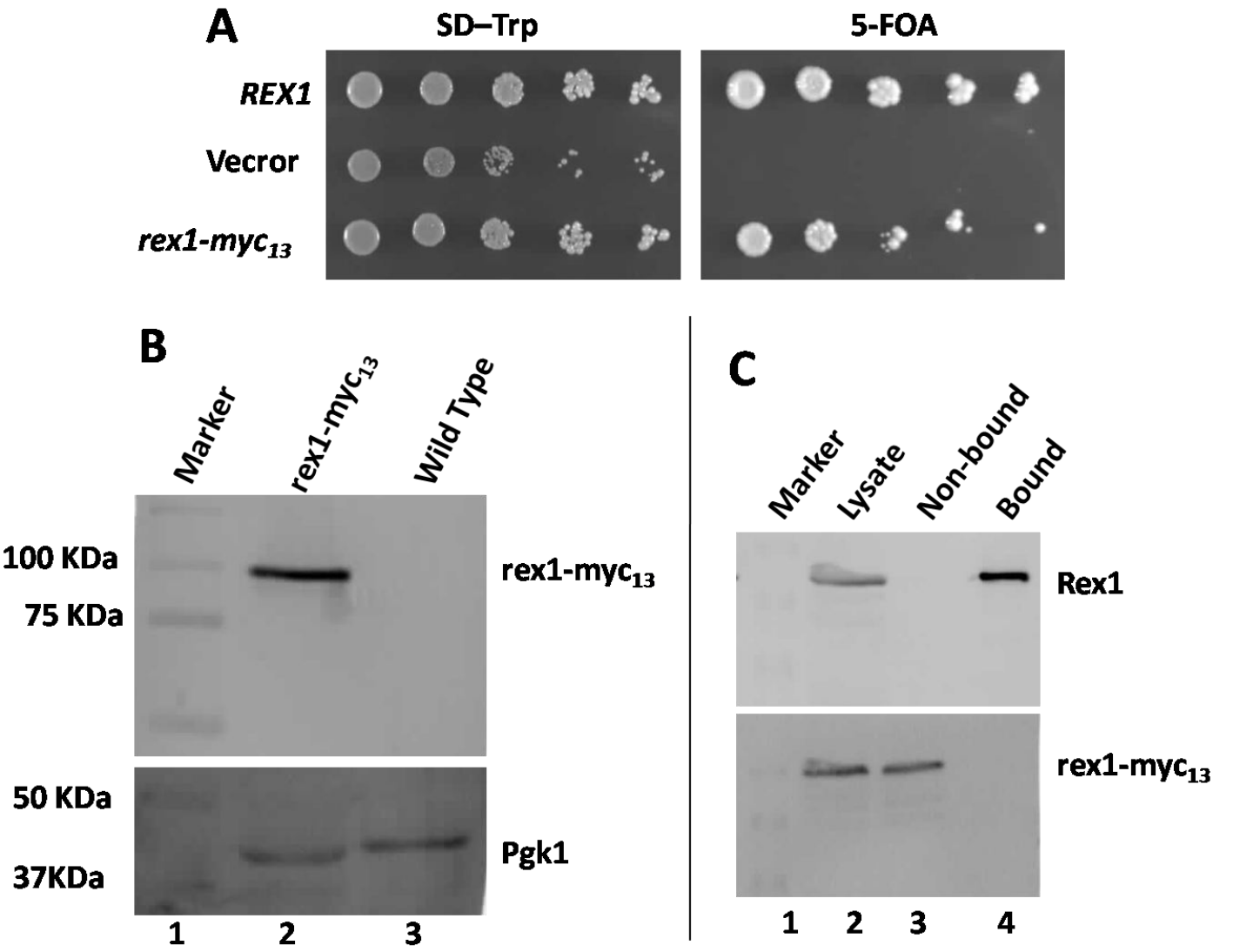

Figure 29 **Rex1 is not expressed in yeast as a homodimer.**

(A) Plasmid shuffle assay to test for complementation of the *rex1Δ rrp47Δ* strain with the *rex1-myc13* allele. The plasmid shuffle strain was transformed with plasmids containing the wild-type REX1 gene, the rex1-myc13 allele or lacking an insert. Transformants were grown up in selective minimal medium and their growth was compared on minimal medium and on medium containing 5-FOA, using a spot growth assay. (**B**) Western blot assay of rex1-myc13 expression. Cell extracts were resolved by SDS-PAGE and analysed by western blotting using an atnibody specific to the myc tag. The blot was also probed for Pgk1. (**C**) Pull-down analysis of two forms of functional Rex1 coexpressed in the same cell. Pull-downs were performed on extracts from a strain expressing zz-Rex1 and Rex1-myc13 using IgG sepharose beads. Whole lysate, supernatant and eluate fractions were resolved by SDS-PAGE and analysed by western blotting, using antibodies specific to the two epitope tags.

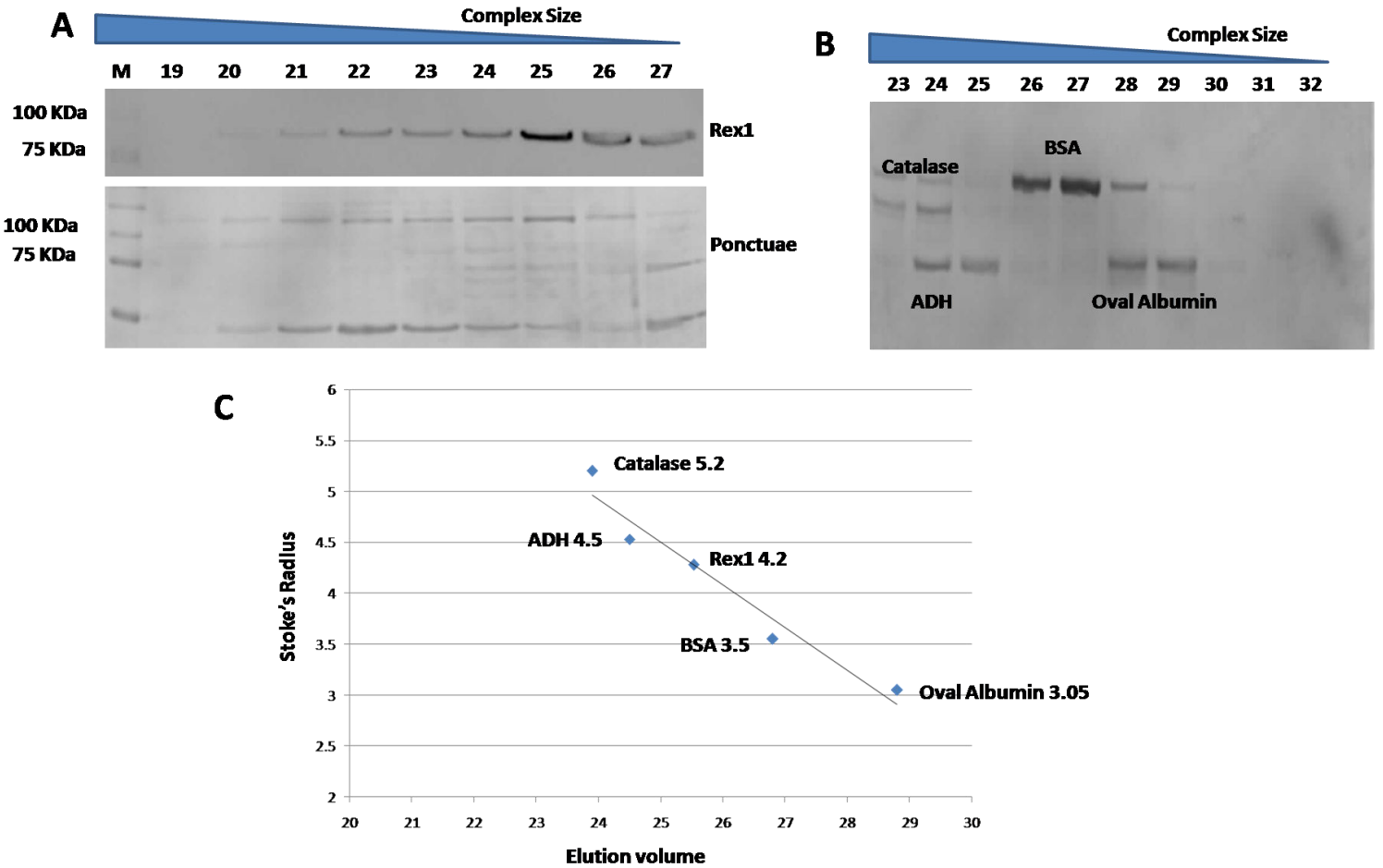

Figure 28 Size exclusion chromatographic analysis of Rex1-TAP.

Rex1-TAP was partially purified from cell lysates by ion exchange chromatography and the mixture was resolved by size exclusion chromatography using a Superdex 200 column. The elution volume of Rex1-TAP was determined by SDS-PAGE and western blot analyses of the column fractions. A mixture of marker proteins of known Stoke's radius were resolved through the same column and their elution volumes were determined by SDS-PAGE analysis of the column fractions. (**A**) Western blot analysis of Rex1-TAP elution. The upper panel shows the western signal, the lower panel is an image of the Ponceau red-stained western blot. (**B**) SDS-PAGE analysis of the protein markers. Bands corresponding to ovalbumin, BSA, ADH and catalase are labelled. (**C**) Plot and line of best fit of the average elution volume of the protein standards obtained from three independent runs against their known Stoke's radii. The average elution volume for Rex1-TAP from three biological replicates is indicated.

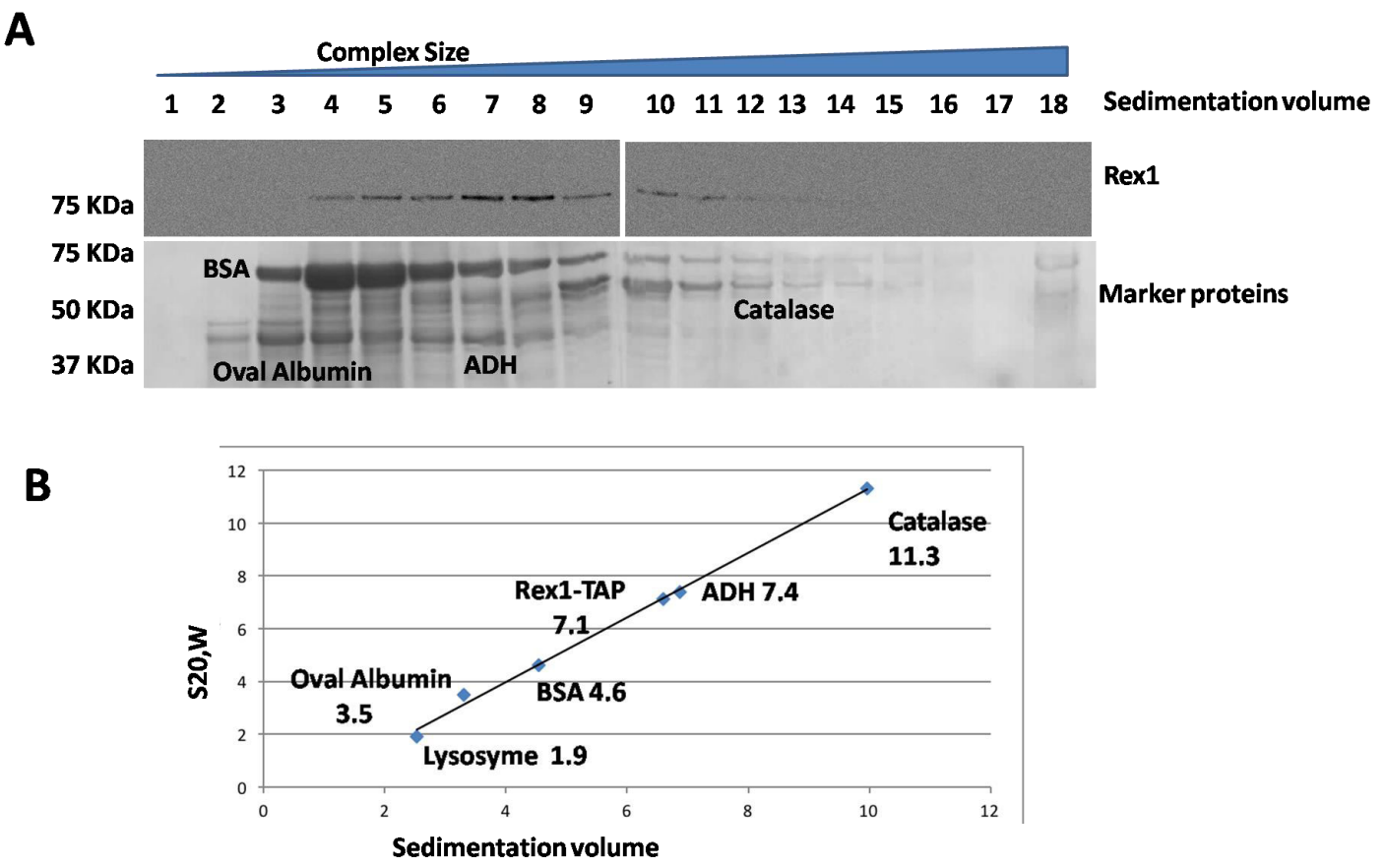

Figure 27 **Glycerol gradient sedimentation analysis of the Rex1-TAP protein**

(A) Rex1-TAP was partially purified from cell lysates by ion exchange chromatography, combined with a mixture of protein standards (lysozyme, ovalbumin, BSA, ADH and catalase) and the mixtures were resolved by velocity sedimentation ultracentrifugation through glycerol gradients. The sedimentation profile analysis of Rex1-TAP was determined by SDS-PAGE and western analysis of the gradient fractions. The sedimentation profiles of the marker proteins were determined by SDS-PAGE separation of proteins within the gradient fractions followed by colloidal coomassie staining. Fractions 1-18 are numbered from th etop to the bottom of the gradient. **(B)** Plot of the sedimentation volume of each protein against its sedimentation coefficient. Data is shown for the average value of three independent experiments.

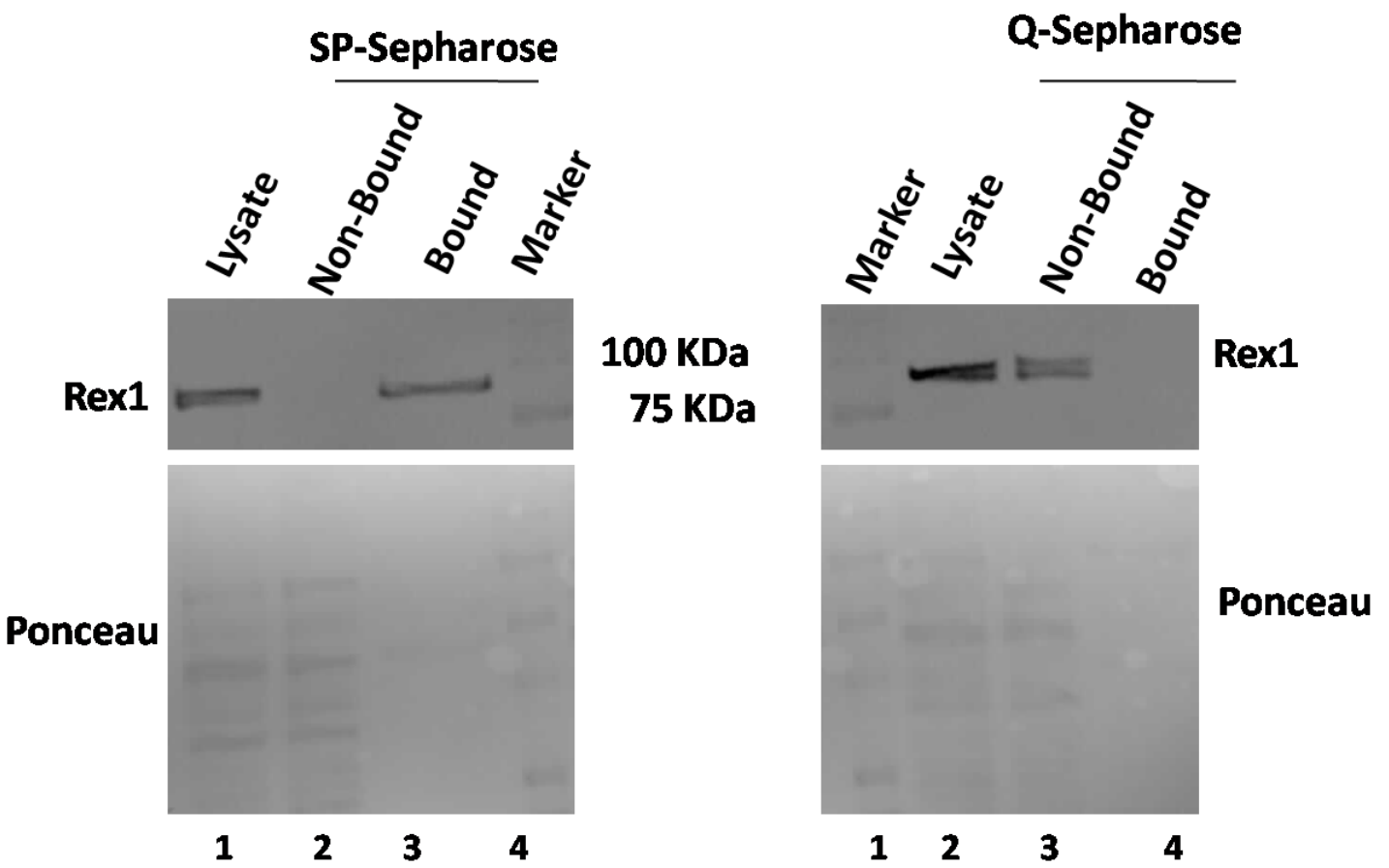

Figure 25 Rex1-TAP binds to SP-Sepharose beads very efficiently.

Cell lysates were fractionated by ion exchange chromatography using SP-Sepharose (left panel) and Q-Sepharose beads (right panel). Whole lysate, bound and non-bound fractions were resolved by SDS-PAGE and analysed by western blotting, using the PAP antibody. Ponceau-stained blots are shown to visualise the protein content of each fraction.

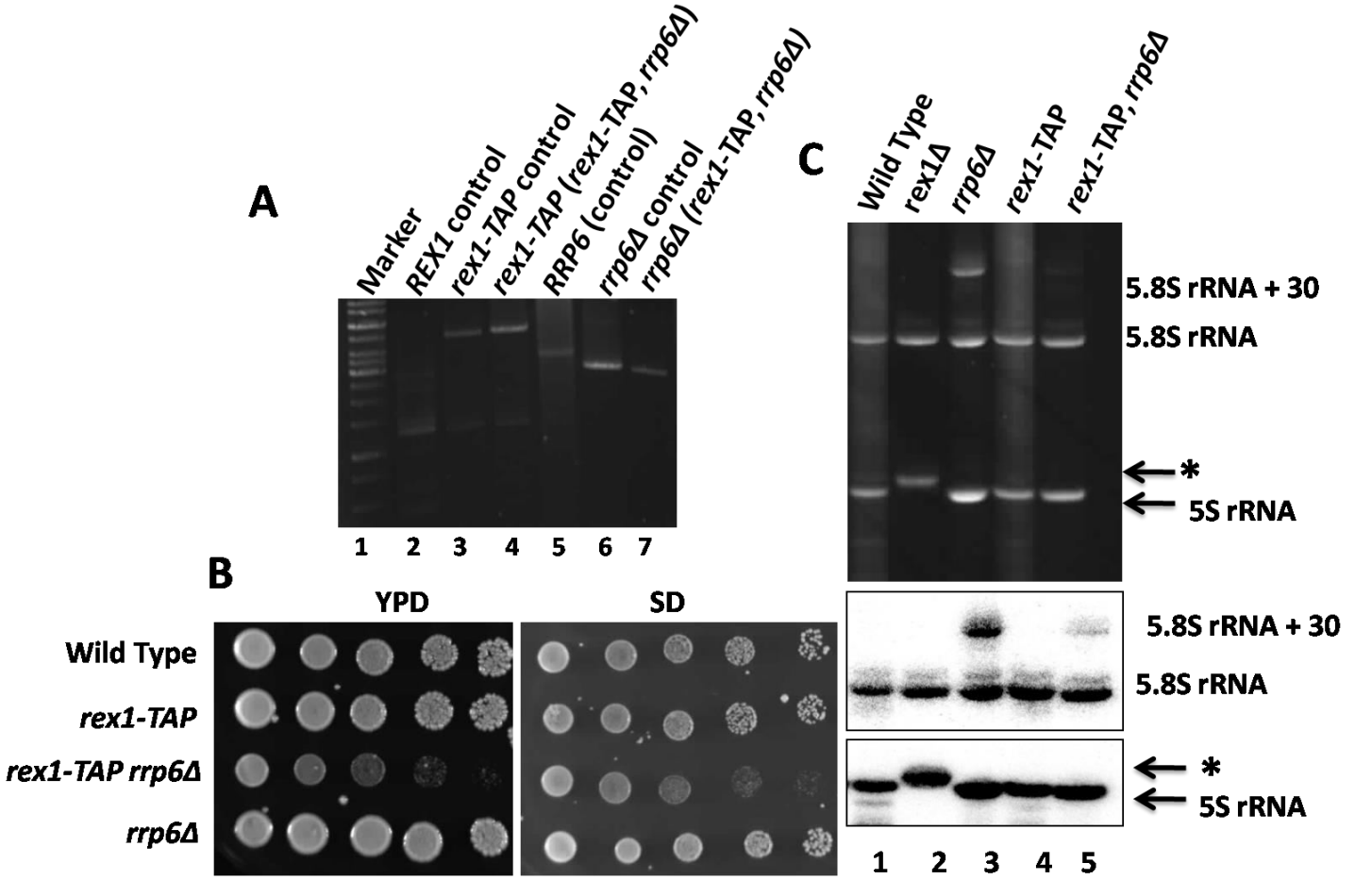

Figure 23 The *rex1-TAP* allele encodes a functional protein.

(A) Validation of the *rex1-TAP allele* in an *rpp6Δ* strain. Yeast genomic DNA samples were analysed by PCR using *REX1* and *RRP6* primers and the products resolved by agarose gel electrophoresis. Lane 1, DNA molecular weight markers; lanes 2 and 5, wild-type strain; lane 3, *rex1-TAP* strain; lanes 4 and 7, *rex1-TAP rrp6Δ* candidate; lane 6, *rrp6Δ* strain. Amplicons in lanes 2-4 and 5-7 were generated with *REX1* and *RRP6* specific primers, respectively. **(B)** Spot growth analysis comparing the growth of a wild-type strain against isogenic *rex1-TAP*, *rrp6Δ* and *rex1-TAP rrp6Δ* mutants. Assays were performed on YPD and minimal media. Plates were photographed after incubation at 30°C for 3 days. **(C)** Comparison of small rRNAs in the *rex1-TAP rrp6Δ* strain with those seen in a wild-type strain, the *rex1Δ* mutant and an *rrp6Δ* mutant. RNA was visualised by staining with ethidium bromide (upper panel) and by Northern blot hybridisation using probes specific to 5.8S (centre panel) and 5S (lower panel) rRNAs. The extended 5S rRNA indicated with an asterisk is characteristic of the *rex1Δ* mutant.

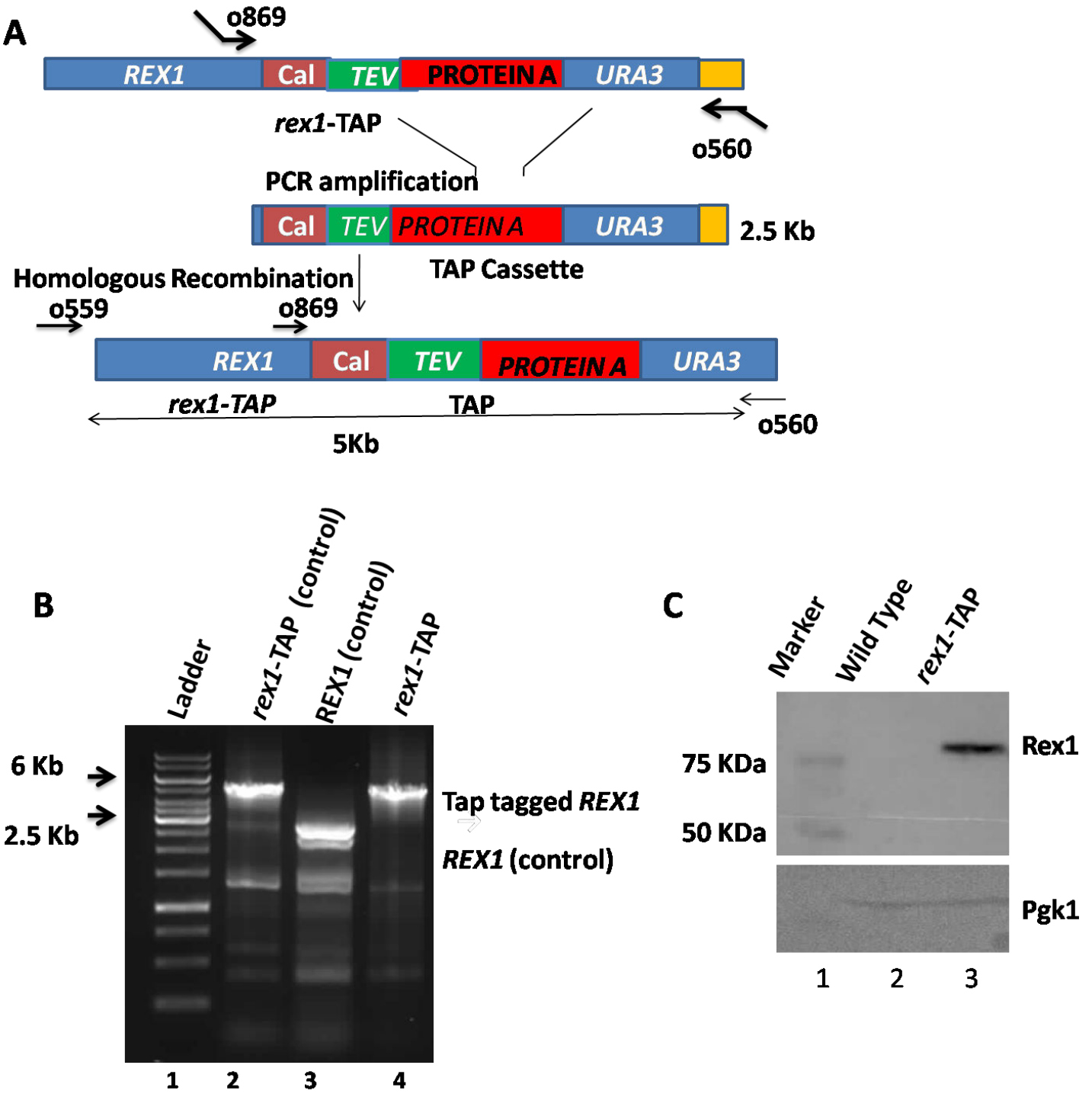

Figure 22 **Generation of a *rex1*-TAP strain.**

Schematic depicting the strategy for PCR amplification of the *rex1*-TAP allele of the P1022 strain and integration into the *REX1* locus of the BY4741 strain. Distinct functional elements of the amplicon (calmodulin binding domain, TEV protease cleavage site and zz domain of protein A, together with a downstream *URA3* marker gene) are indicated. **(B)** The *REX1* locus was amplified from genomic DNA isolated from the initial rex1-TAP strain, a wild-type strain and the new *rex1*-TAP isolate and the products were resolved by agarose gel electrophoresis. Lane 1, DNA ladder; lane2, DNA from the original *rex1*-TAP strain, P1022; lane 3, DNA from the wild-type strain BY4741; lane 4, DNA from the *rex1*-TAP candidate in BY4741. **(C)** Western analysis of *rex1*-TAP expression. Whole cell extracts from the wild-type strain and the *rex1*-TAP isolate were resolved by SDS-PAGE and analysed by western blotting, using the PAP antibody (upper panel) and an antibody specific to Pgk1 protein (lower panel).

A

```
Rex1        HIFALDCEMC L---SEQG-- ----LVLTRI SLVNFDN--- -----EVIYE ELVKP----D VPIVDYLTRY SG---ITEEK
RNase T     YPVVIDVETA G---FNAK-- ---TDALLEI AAITLKMDEQ GWLMPDTTLH FHVEPFV--G ANLQPEALAF NG---IDPND
Pan2        TLVAIDAEFV S(7)IDHQG( 7)KRTALARI SIIRGEEGE- --LYGVPFVD DYVVN----T NHIEDYLTRY SG---ILPGD
Rex2        PLVWIDCEMT G---LDHVN- ----DRIIEI CCIITDGHL( 7)GQGDSHYE SVIHYGPEVM NKMNEWCIEH HGNSGLTAKV

Rex1        LTVG--AKKT LR--EVQKDL LKIISRS--- --DILIGHSL QNDLKVMKLK HP-------- ----LVVDT- ----AIIYHH
RNase T     PDRG--AVSE YE--ALHEIF KVVRKGIKA( 6)IMVAHN-A NFDHSFMMAA AERASLKRNP FHPFATFDT- ----AALAGL
Pan2        LDPEKSTKRL VRRNVVYRKV WLLMQLG--- --CVFVGHGL NNDFKHININ VPRNQ----- -----IRDT- ---AIYFLQG
Rex2        LAS----EKT LA--QVEDEL LEYIQRYIP( 5)-VLAGNSV HMDRLFMVRE FPK------- -----VIDH- ----LFYRIV

Rex1        KAG------- DPFKPSFKYF SETFLNKSIQ NG----EHDS VEDARACLEL TKLKILNGLA
RNase T     ALG------- --RQTVFSKA CQTAGMDFDS TQ----AHSA LYDTERTAVL FCEIVNRWKR
Pan2        KR-------- ---YLSFRYF AYVLLGMNIQ EG----NHDS IEDAHTALIL YKKYLHLKEK
Rex2        DVS------- -----SIMEV ARRHNPALQA RNP(4)AHTA YSDIKESIAQ LQWYMDNYLK
```

B

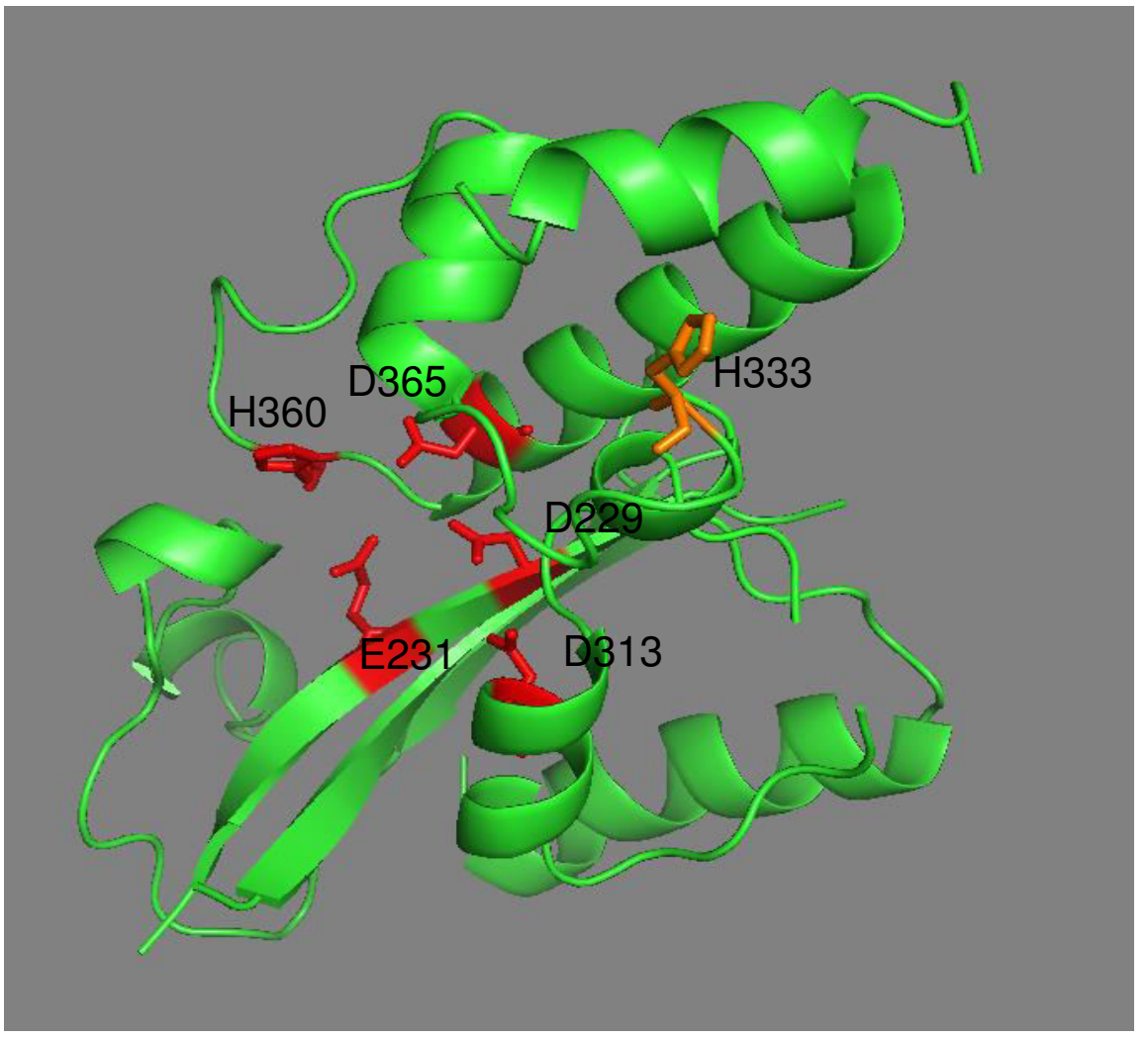

Figure 21

(A) Family alignment of selected members of the EXOIII (DEDD) domain (SMART accession number SM00479). The alignment was generated using SMART (Simple Modular Architecture Research Tool) (Schultz et al., 1998). The conserved acidic residues and the histidine residue characteristic of the DEDDh domain are boxed. Basic residues in the RNase T sequence that comprise the nucleotide binding sequence (Zuo et al., 2007) are underlined. **(B)** Model of the DEDD domain of Rex1. The Rex1 sequence was threaded to the Pan2 structure using Phyre2 and represented using MacPyMOL. The residues that constitute the catalytic site (D229, E231, D313, H360, D365) are highlighted, as is H333, the residue equivalent to L157 of RNase T.

A

```
Rex1                    FGIGINTENLFTKLHRFEVKTVLLNDMIIKNHTEDDSKGQLIRCVEDDETWTHIHENLNK
PGM S. mutans_          YALSPFAPTVLNKLADAGVSTYAVGKINDI-FNGSGITNDMGHNKSNSHGVDTLIKTMGL
PGM B. stear_                                                  SAYEVTDALLKEIEA
PGM L. mexicana_                                               QSAAITEAAIEALKS
AP-like fold            TEPSPFAPTVLNKLADAGVSTYAVGKINDIFNGSGI-TNDMGHNKSNSHGVDTLIKTMGL
PGM S. aureus _         ---------------------------------------------SAYEVKDALLEELNK
                                 HHHH      BBBBB  HHHH                HHHHHHHHHHHHHH

Rex1                   D---VKLIVGRIKNLERSRNYNKKPRKETPSFDASMVLHDIGQHLTQLYENA-TPGTMILI
PGM S. mutans _        SAFTKGFSFTNLVDFDALYGHRRNA------HGYRDCLHEFDERLPEIIAAM-KVDDLLLI
PGM B. stear _         DK--YDAIILNY-------ANPDMVGHSGKLEPTIKAVEAVDECLGKVVDAILAKGGIAII
PGM L. mexicana _      GM—YNVVRINFPNGDMVGHTGDL--------KATITGVEAVDESLAKLKDAVDSVNGVYIV
AP-like fold           SAFTKGFSFTNLVDFDALYGHRRNA------HGYRDCLHEFDERLPEIIAAM-KVDDLLLI
PGM S. aureus _        GD--LDLIILNF------ ANPDMVGHSGMLEPTIKAIEAVDECLGEVVDKILDMDGYAII
                             BBBBBB           BBB     HHHHHHHHHHHHHHHHHHHHH      BBBB

Rex1                   MSGTGDT
PGM S. mutans _        TADHGN
PGM B. stear _         TADHGN
PGM L. mexicana _      TADHGN
AP-like fold           TADHGND
PGM S. aureus _        TADHGN
                       B
```

B

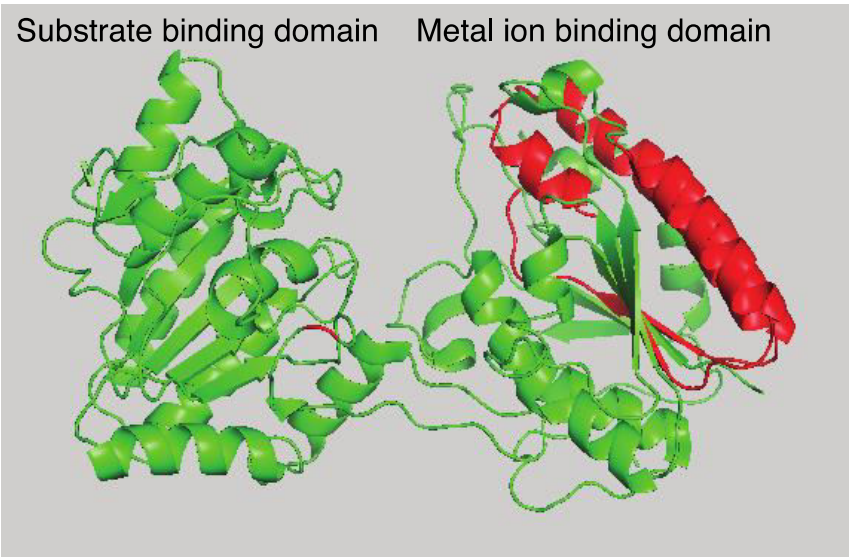

C

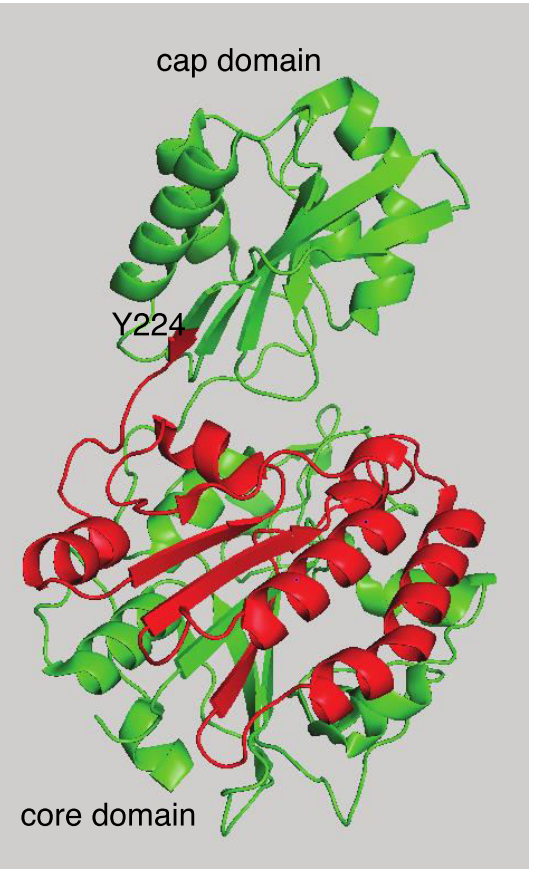

Figure 20 A threading-based model of the three-dimensional fold of residues 428-505 of Rex1.

(**A**) Sequence alignment of Rex1 with phosphoglycerate mutases from *Streptococcus mutans*, *Bacillus stearothermophilus*, *Leishmania mexicana* and *Staphylococcus aureus*, together with an alkaline phosphatase-like fold from phosphopentomutase from *S. mutans*. (**B**) Structure of phosphoglycerate mutase from *S. aureus* (PDB file 4my4), with the region of structural homology to Rex1 residues 428-505 shown in red. The distinct substrate binding and metal ion binding domains are indicated. (**C**) Structure of phosphopentomutase from *S. mutans* (PDB file 3M7V). The “cap” and “core” domains are labelled. The sequence that can be matched to Rex1 residues 428-505 is highlighted in red. Residue Y224 denotes the N-terminal end of the highlighted sequence.

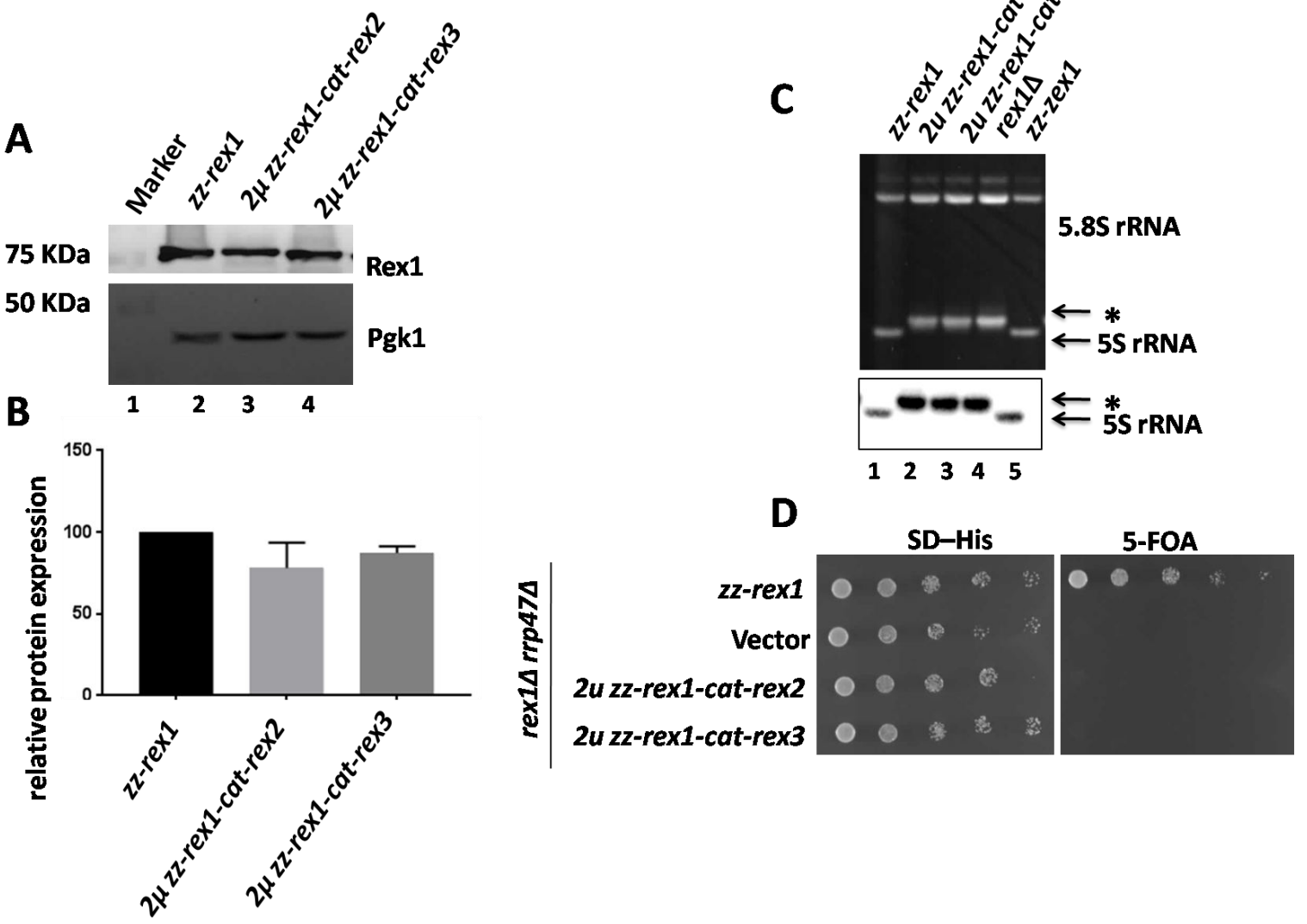

Figure 18 Loss of function of the rex1 catalytic domain substitution mutations is not due to limited protein expression levels.

(A) Western blotting analysis of the *rex1* catalytic domain substitution mutants expressed from a 2µ vector. The upper panel shows expression of the Rex1 proteins. The lower panel shows the Pgk1 loading control. (**B) T**he expression levels of the rex1 mutant proteins are shown, relative to the zz-rex1 wild-type protein. The error bar indicates the standard deviation of the mean from three independent biological replicates. (**C)** Analysis of 5S rRNA expression in the rex1 mutants. RNA isolated from cells expressing wild-type zz-rex1, the rex1 catalytic domain substitution mutants from a high copy number plasmid, or lacking Rex1 protein was resolved through denaturing polyacrylamide gels, transferred to nylon membranes and hybridised with a probe complementary to the 5S rRNA. Upper panel, ethidium-stained acrylamide gel. Lower panel, northern blot probed for 5S rRNA. The asterisk indicates a 3' extended form of 5S rRNA. **(D)** Plasmid shuffle assay to test for function of the catalytic domain substitution mutants upon expression from a high copy number plasmid. Transfromants were pre-grown in selective medium and serial dilutions were spotted onto selective medium and onto medium containing 5-FOA. Plates were photographed after incubation for 3 days at 30 °C.

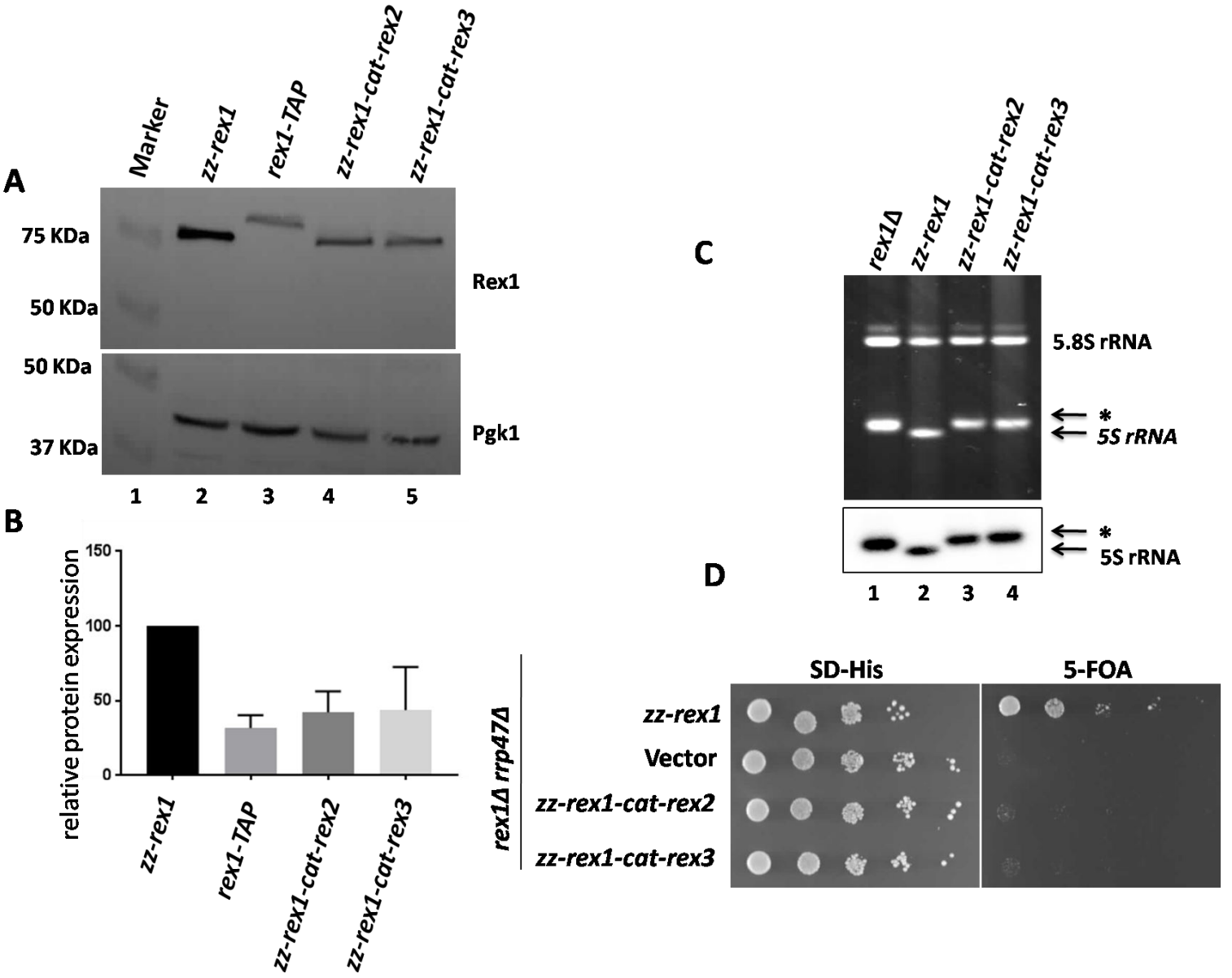

Figure 17 The catalytic domain of Rex1 cannot be substituted by the same domain from Rex2 or Rex3.

(A) Western blotting analysis of the catalytic domain substitution mutants. Total cell lysate from strains expressing wild-type or mutant *rex1* proteins was fractionated through a 10% SDS-PAGE gel and the Rex1 protein was detected by western blot analysis, using the PAP antibody complex (upper panel). The loading control Pgk1 was detected using anti-Pgk1 antibodies (lower panel). Lane 1, molecular weight marker; lane 2, full length zz-Rex1 protein; lane 3, chromosomally encoded Rex1-TAP from an isogenic strain; lane 4, the zz-rex1-cat-rex2 mutant protein; lane 5, the zz-rex1-cat-rex3 mutant protein **(B)** Histogram showing the relative expression level of the rex1 proteins. Levels were standardised to the amount of Pgk1 and are expressed relative to the plasmid-encoded, wild-type zz-rex1 protein. Error bars indicate the standard deviation of the mean from three biological replicates. **(C)** 5S rRNA analyses of the rex1 mutants. Total cellular RNA isolated from a *rex1Δ* strain, a strain expressing the wild-type zz-rex1 protein and from strains expressing the catalytic domain substitution mutants was resolved through a urea/polyacrylamide gel and transferred to a Hybond N+ membrane for northern hybridisation using a probe specific to the 5S rRNA. Upper panel, ethidium-stained polyacrylamide gel. Lower panel, northern blot of the same gel after hybridisation with the 5S rRNA probe. The asterisk indicates the extended form of 5S rRNA characteristic of loss of function *rex1* mutants. **(D)** Plasmid shuffle assay of the catalytic domain substitution mutants. The *rex1Δ rrp47Δ* plasmid shuffle strain was transformed with plasmids encoding the wild-type zz-rex1 fusion protein, the domain swap constructs or the plasmid vector alone, grown in selective medium lacking histidine and then ten-fold serial dilution of mutants were spotted onto permissive medium and medium containing 5-FOA. Images were taken after incubation for 3 days at 30 °C.

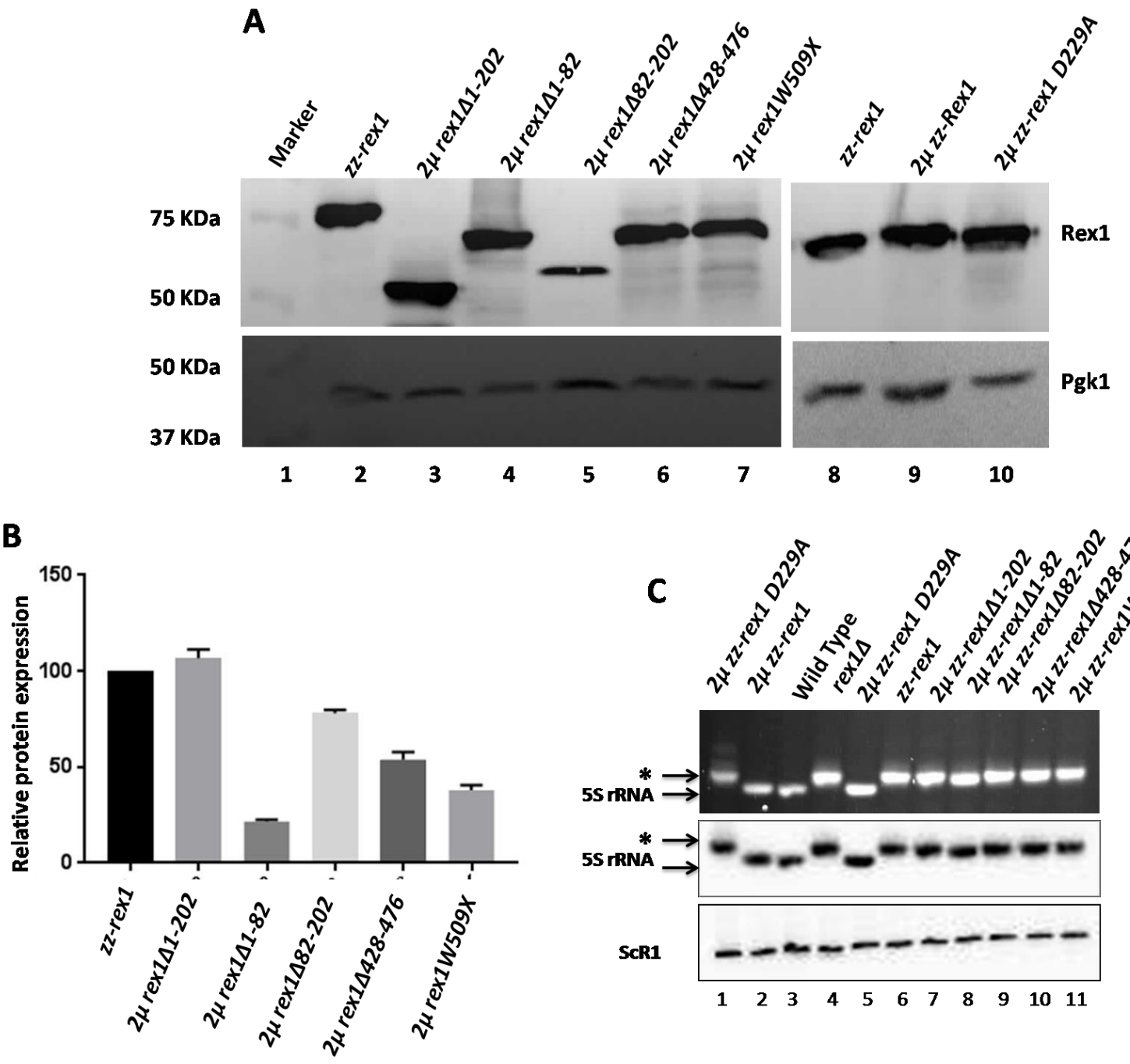

Figure 16 The loss of function phenotypes of the *rex1* alleles are not due to limited protein expression.

(A) Western analysis of *rex1* mutants expressed from 2µ high copy number plasmids. Cell extracts from strains expressing the wild-type or mutant *zz-rex1* fusion proteins were resolved by SDS-PAGE and analysed by western blotting using the PAP antibody complex. Pgk1 levels were determined as a loading control. Lane 1, molecular weight markers; lanes 2 and 8, *zz-rex1* expressed from a CEN plasmid; lanes 3-7 and 10, *rex1* mutants expressed from a high copy number 2µ plasmid. Lane 9, *zz-rex1* expressed from a high copy number 2µ plasmid. **(B)** Histogram of the relative expression levels of the *rex1* mutants. Error bars indicate the standard deviation of the mean of three independent biological replicate assays. **(C)** Northern analysis of 5S rRNA expression in the *rex1* mutants. The top panel shows an ethidium bromide-stained urea/polyacrylamide gel containing total cellular RNA from strains expressing wild-type Rex1, a *rex1Δ* mutant and the *rex1* mutants expressed from a high copy number 2µ plasmid. The lower panels are northern blots of the acrylamide gel that have been hybridised with probes complementary to sequences within 5S rRNA and within the ScR1 RNA, which serves as a loading control. The asterisk indicates the 3' extended 5S rRNA species that is a characteristic of strains lacking Rex1 or expressing a non-functional Rex1 protein.

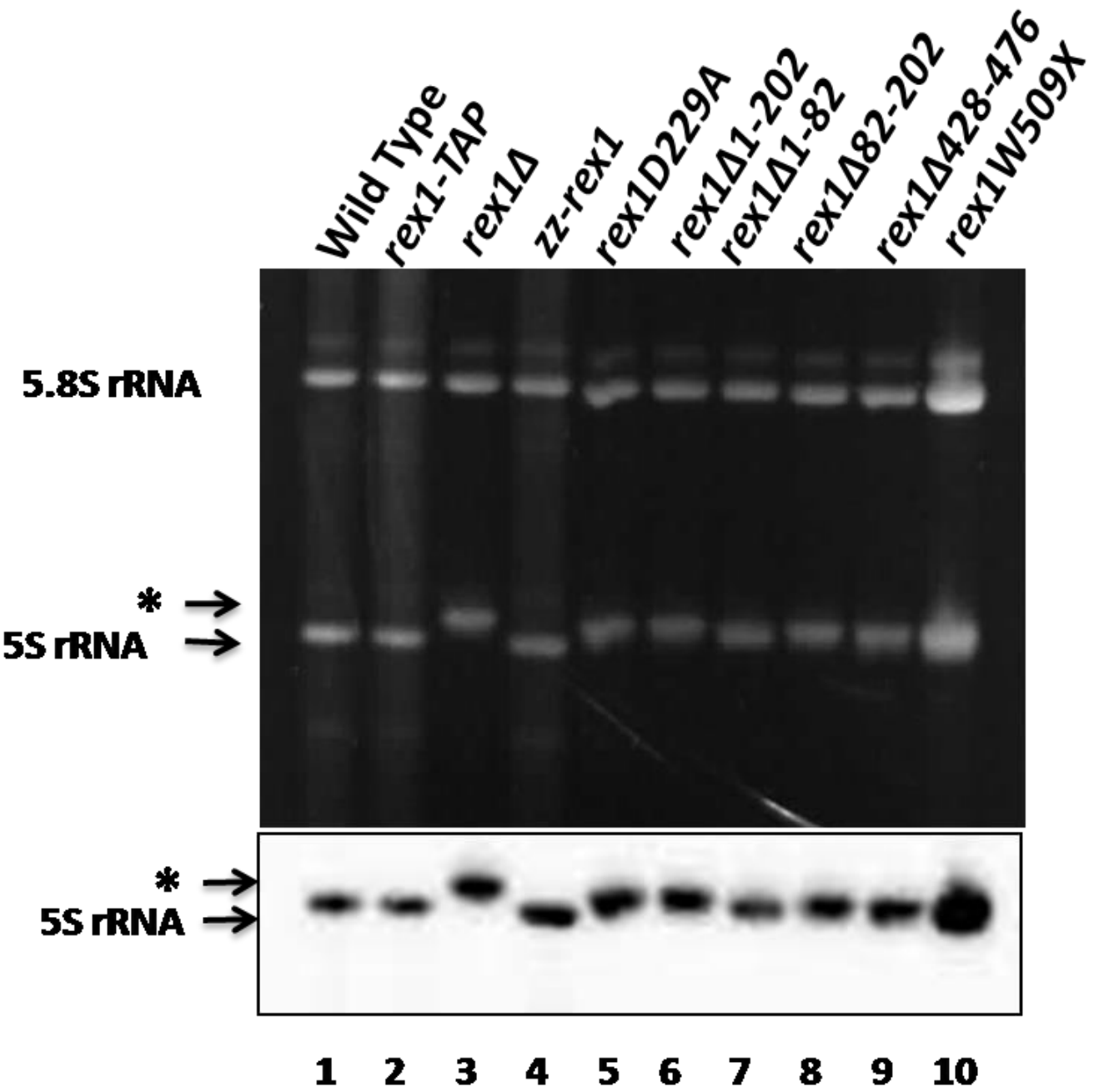

Figure 15 Northern blot analysis of cellular RNA from the *rex1* mutants.

Total cellular RNA was fractionated through a 6% denaturing polyacrylamide gel and visualized using ethidium bromide (upper panel). The RNA was transferred to a Hybond N+ membrane and the blot was hybridised with a probe complementary to the 5S rRNA (lower panel). The asterik indicates the extended 5S rRNA species that is characteristic of strains lacking Rex1 protein.

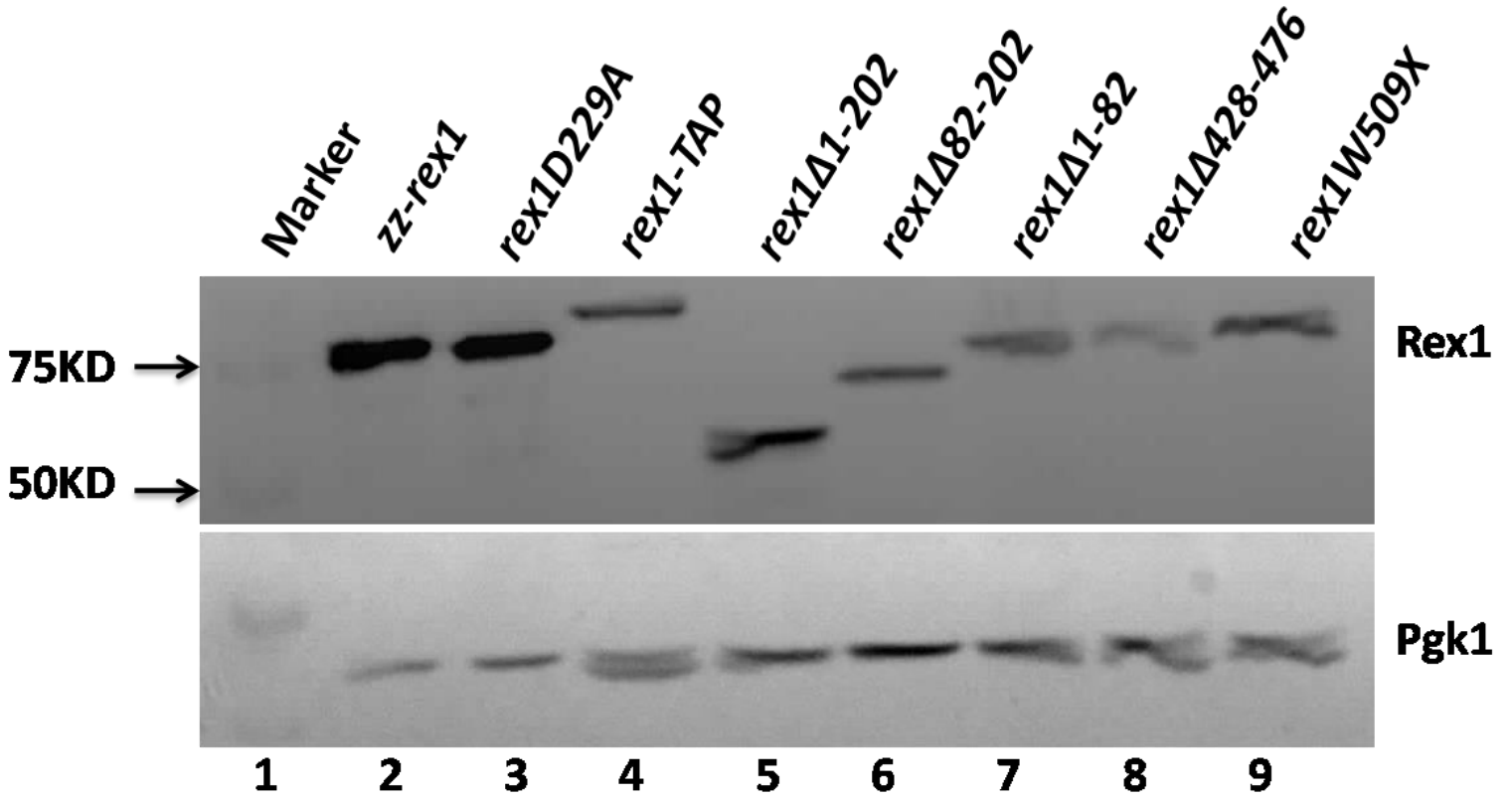

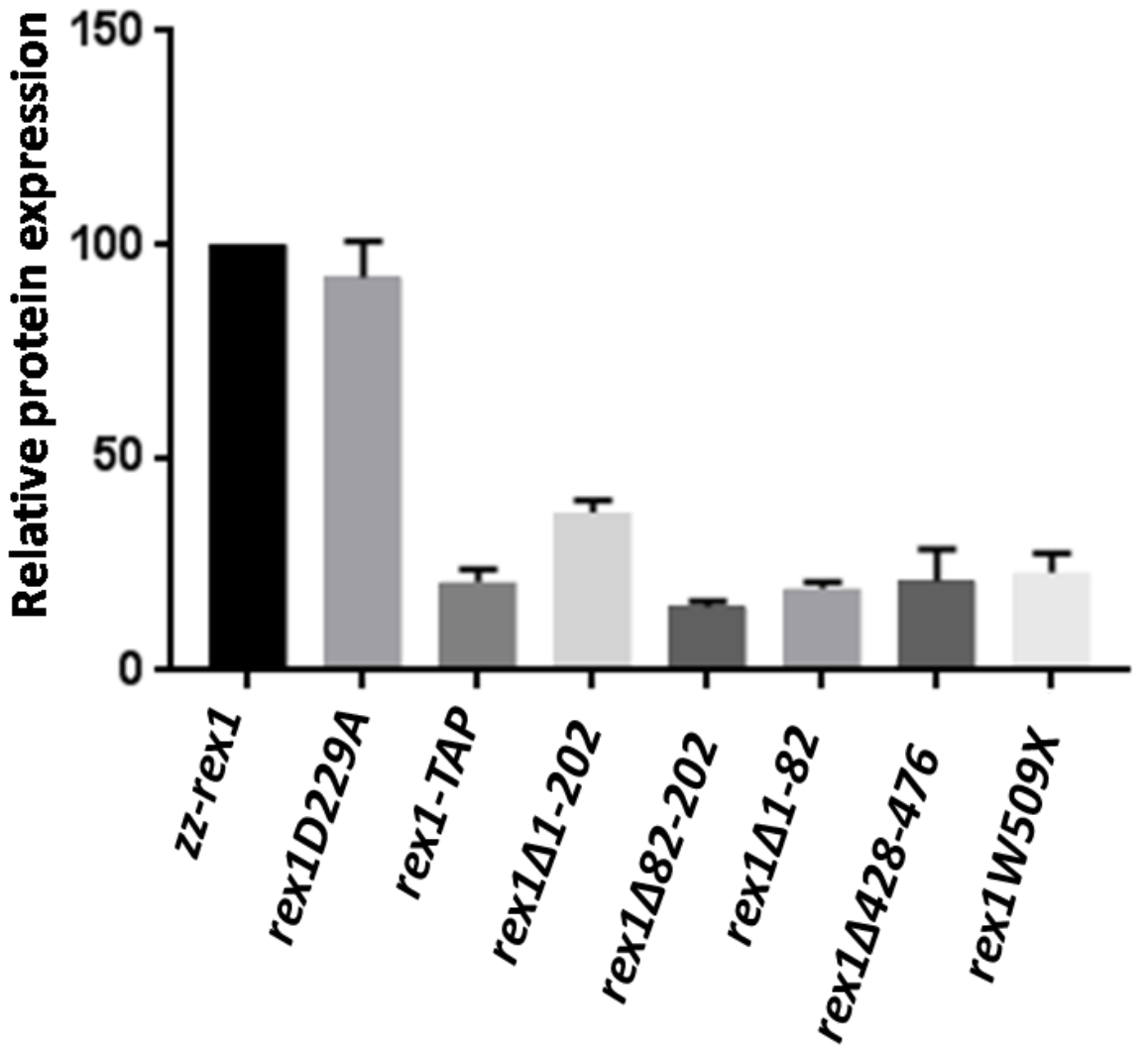

Figure 14 Western blot analysis of *rex1* mutants.

Lysates from cells expressing zz-Rex1 and Rex1-TAP fusion proteins were resolved by SDS-PAGE and analysed by western blotting, using the peroxidase/anitperoxidase (PAP) conjugate, which binds to the epitope tag, and a Pgk1-specific antibody. Lane 1, molecular weight markers; lane 2, full-length wild-type zz-Rex1; lane 3, the D229A *rex1* active site point mutant; lane 4, chromosomally encoded Rex1-TAP fusion protein; lanes 5-9, *zz-rex1* deletion mutants. The upper panel shows a western blot to visualise the Rex1 proteins. The lower panel shows the detection of Pgk1 on the same blot. The histogram shows the level of protein expression for each mutant, relative to the full-length, wild-type zz-rex1 protein. Expression levels were normalized to the Pgk1 signal and show the average of three biological replicates. Error bars indicate the standard deviation of the mean.

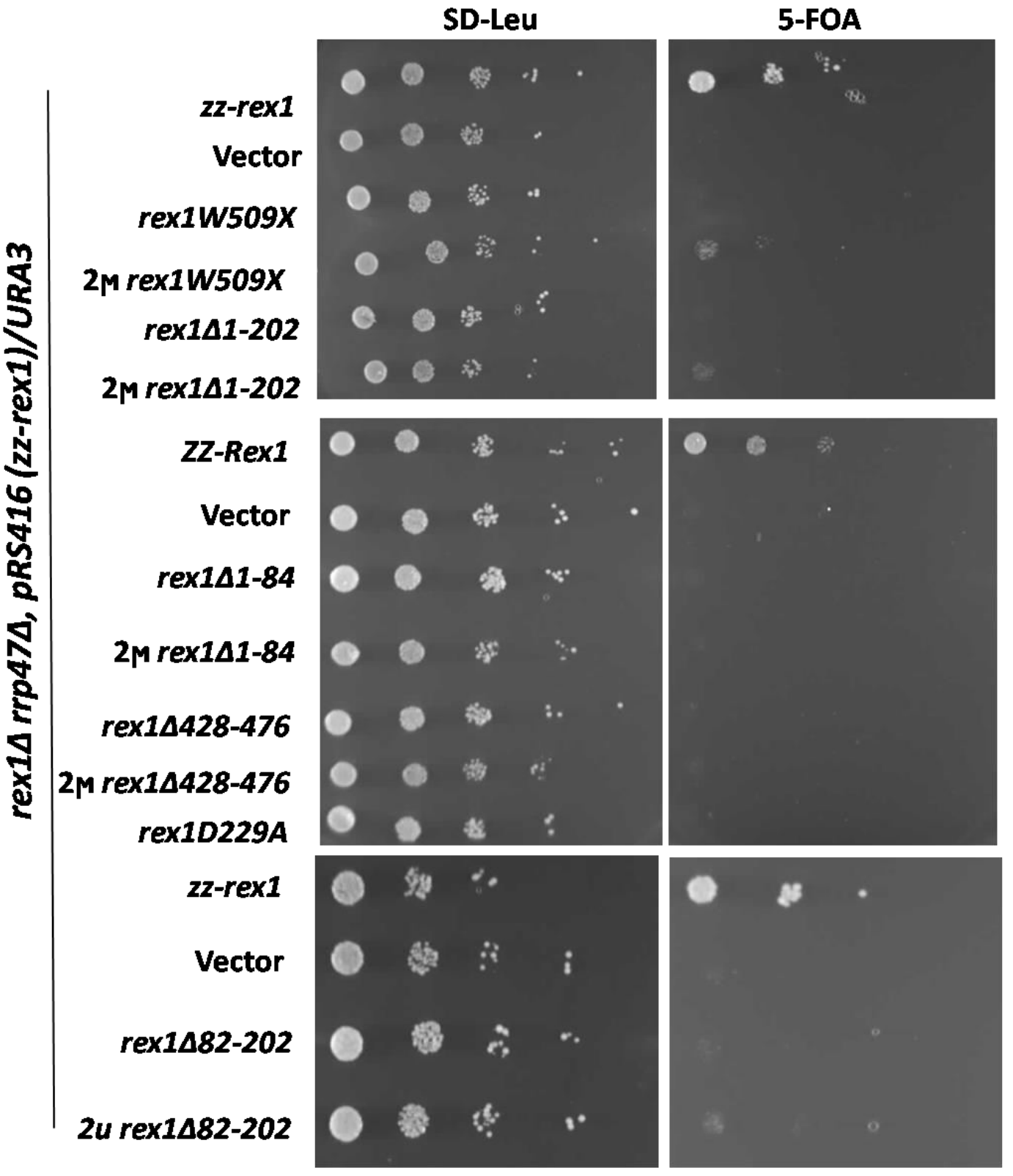

Figure 13 **Complementation analysis of *rex1* mutants.**

Centromeric and high copy number plasmids encoding the rex1 alleles were transformed into a rex1Δ rrp47Δ plasmid shuffle strain. Transformants were grown up in selective minimal medium (SD-Leu) and ten-fold serial dilutions of the cultures were spotted onto selective minimal medium and onto medium containing 5-FOA, as indicated. Plates were photographed after incubation for 3-4 days at 30°C.

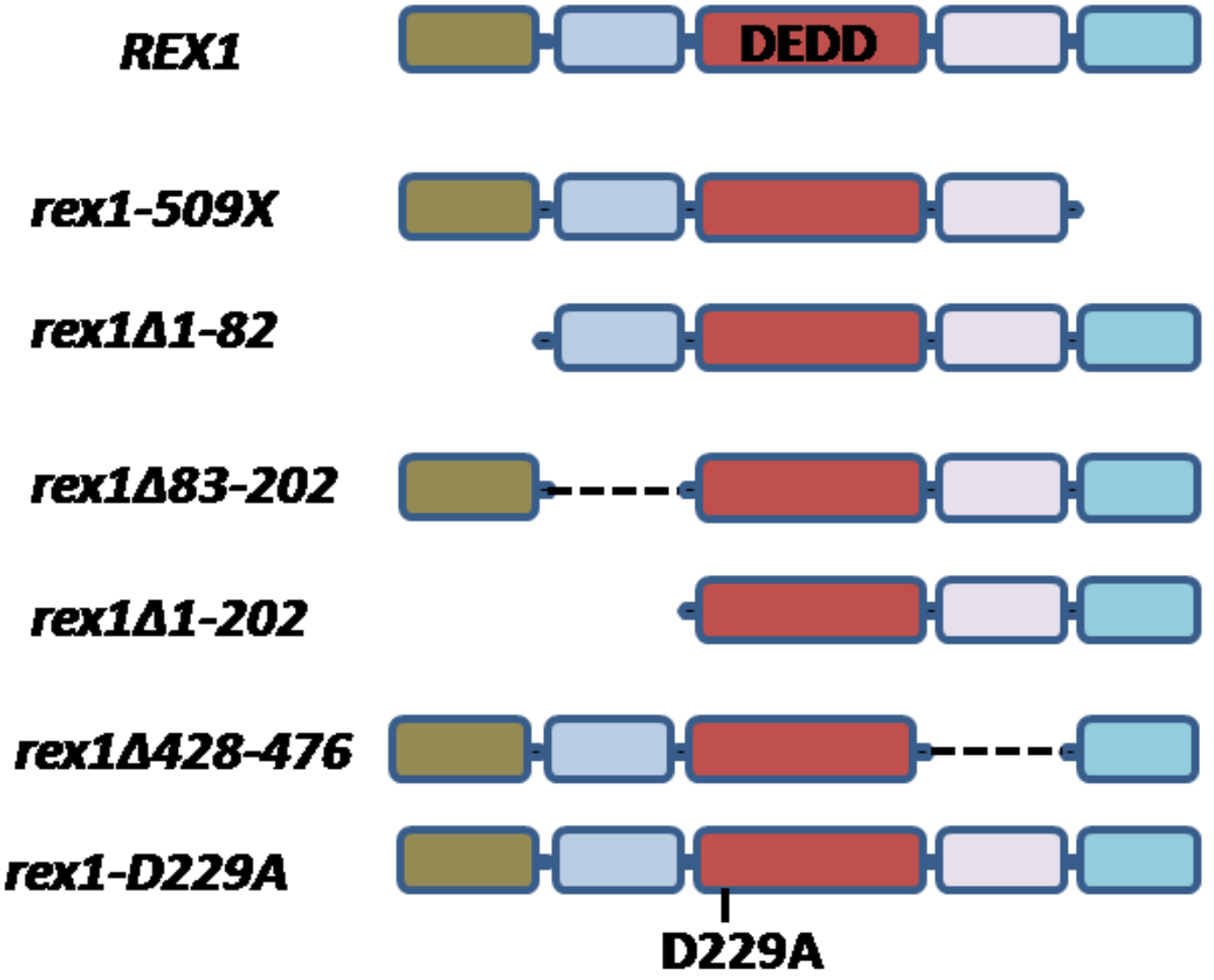

Figure 12. Generation of *rex1* mutants.

The *REX1* gene was cloned by PCR into a plasmid that drives the expression of N-terminal zz-tagged fusion proteins from the *RRP4* promoter. N- or C-terminal truncations and internal deletions were produced by site-directed mutagenesis and restriction cloning. A D229A point mutant was generated, which alters a conserved aspartate residue that is required for the exonuclease activity of related DEDD domain proteins such as Rrp6.

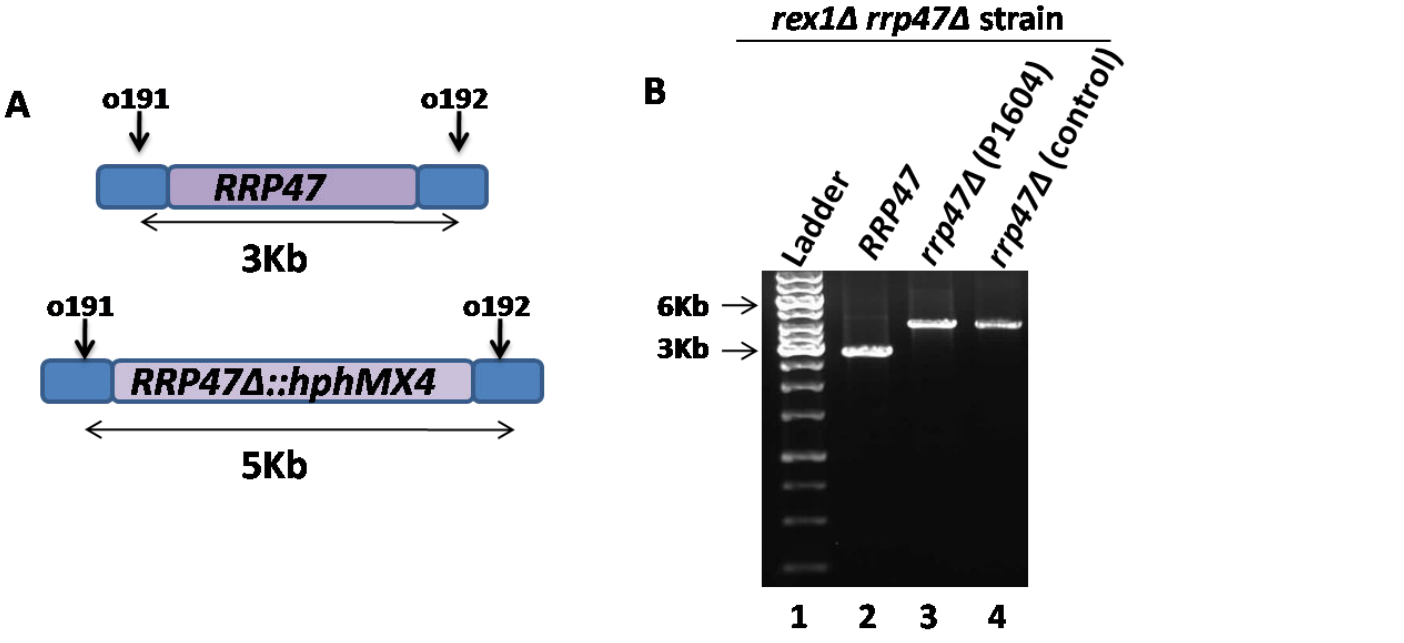

Figure 11 **Generation and validation of a *rex1Δ rrp47Δ* shuffle strain.**

(A) Schematic illustration of the products obtained upon amplification of the *RRP47* and *rrp47::hphMX4* loci with primers o191 and o192. Sites of complementarity to the primers and sizes of the PCR products are indicated. **(B)** Agarose gel electrophoresis of the PCR reaction mixtures. Lane 1, DNA ladder; lanes 2-4, reactions with *RRP47*-specific primers. Lane 2, genomic DNA from wild-type, *RRP47* strain. Lane 3, genomic DNA from a candidate rex1Δ::kanMX4 rrp47Δ:hphMX4 strain; lane 4, DNA from a control rrp47::hphMX4 strain. **(C)** Spot growth assays of the candidate *rex1Δ::kanMX4 rrp47::hphMX4* double mutant on medium containing 5-FOA and on medium lacking leucine. The strain was transformed with a plasmid expressing the zz-rex1 fusion protein (lower row) or the cloning vector (centre row) and compared with the growth of a *rex1Δ* single mutant (upper row).

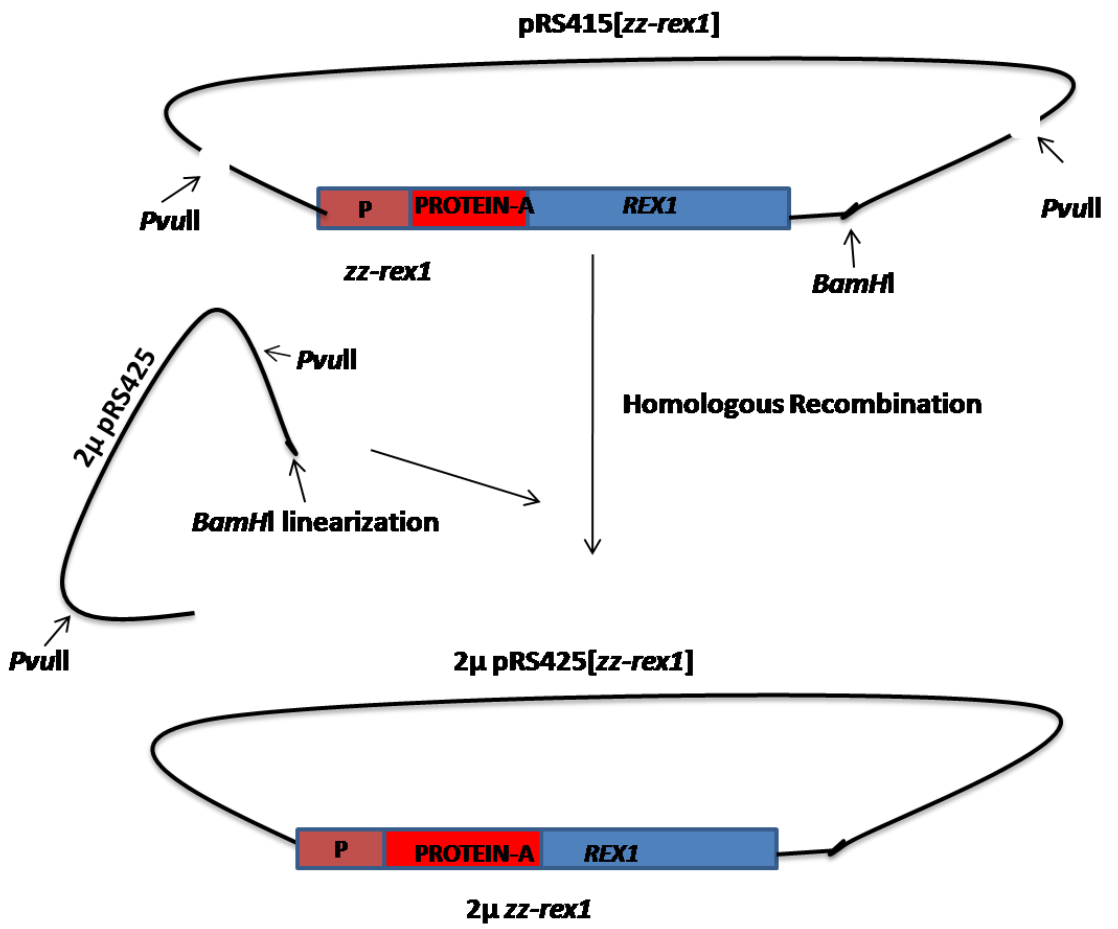

Figure 10 Generation of *REX* 1 construct on a high copy number plasmid to overexpress *Rex1* proteins.

Schematic illustration of subcloning of zz-*Rex1* from a single copy centromeric plasmid *pRS415* into a high copy number plasmid by homologous recombination. The restriction site of *Pvu*II is indicated by arrow. *zz-rex1* gene flanked by 200 bases of either up and down stream as indicated is prepared for homlogous recombination.

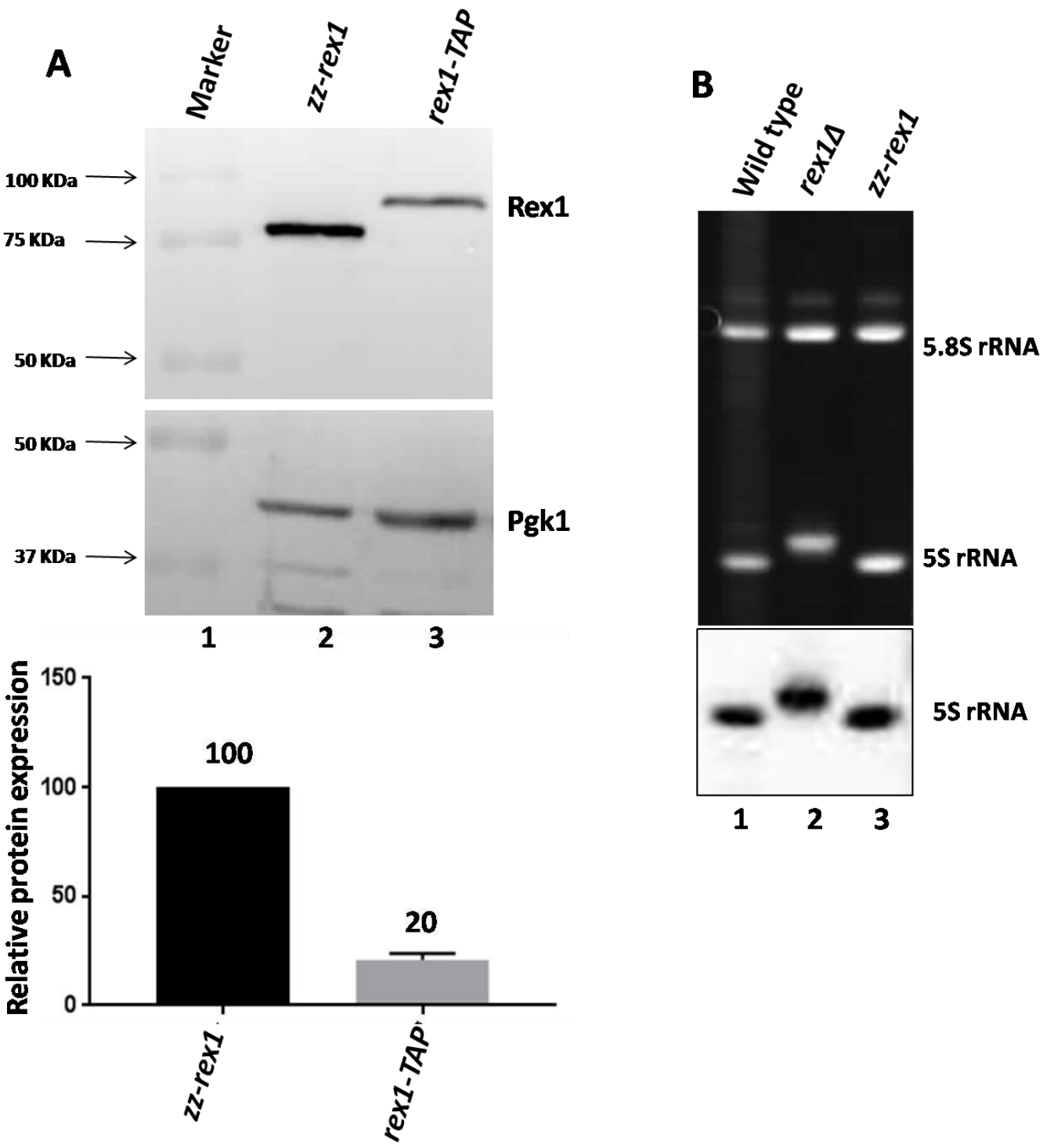

Figure 9 Western blot analysis of *zz-Rex1* protein expression.

(A) Cell lysates were resolved by SDS-PAGE and analysed by western blotting. The zz-Rex1 and Rex1-TAP fusion proteins were visualised using the PAP antibody (the upper image upper panel) and the Pgk1 loading control was detected using anti-pgk1 antibody (the lower panel). Lane 1, molecular weight markers; lane 2, extract from cells expressing zz-Rex1; lane 3, extract from cells expressing the chromosomally encoded Rex1-TAP protein. The histogram show the relative level of protein expression after normalisation to the expression level of Pgk1. Assays were performed on three biological replicates. The error bar indicates the standard deviation of the mean. **(B)** zz-Rex1 protein processes 5S rRNA**.** Total cellular RNA was extracted from yeast, resolved through an 8% denaturing polyacrylamide gel and visualised by staining with ethidium bromide. The RNA was then transferred to a nylon membrane and the northern blot was hybridised with probes complementary to the 5S. Relevant strain genotypes are indicated at the top of the figure.

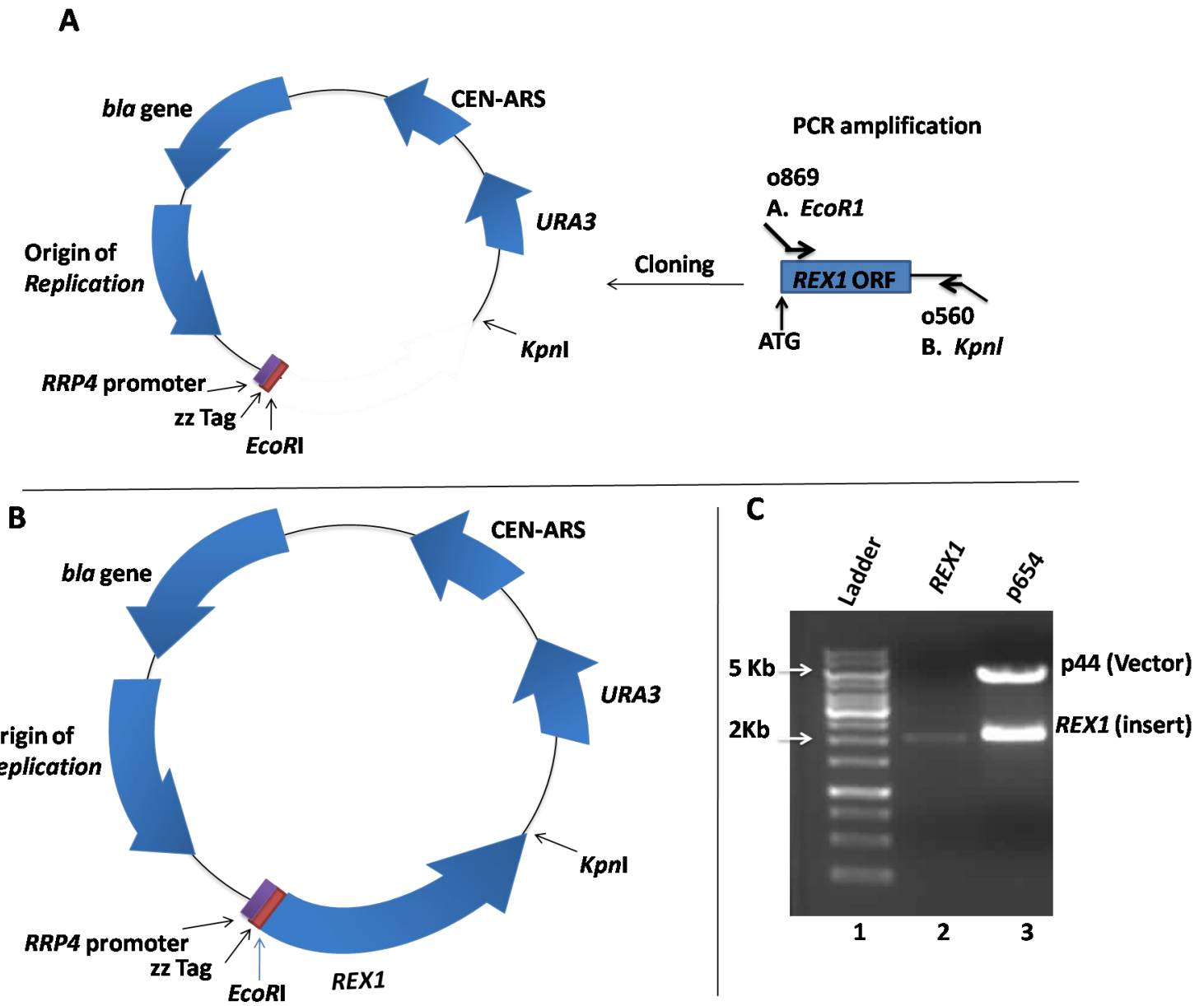

Figure 8 **Generation of a yeast plasmid construct expressing zz tagged Rex1.**

(**A**) Schematic illustration of the PCR-mediated amplification of the *REX1* allele and cloning into the p44 expression vector. The primer numbers and introduced restriction site locations are indicated. **(B)** Plasmid map of the pRS416[zz-rex1] construct bearing the *URA3* marker. The construct expresses the *REX1* ORF as a zz-Rex1 protein fusion from the constitutive *RRP4* promoter. (**C**) Screening of candidate clones by restriction digestion with EcoRI and KpnI. Lane 1, DNA ladder, 2. PCR product obtained by amplification of the *REX1* gene with primers o869 and o560. Lane 3, EcoRI/KpnI digestion of a candidate clone.

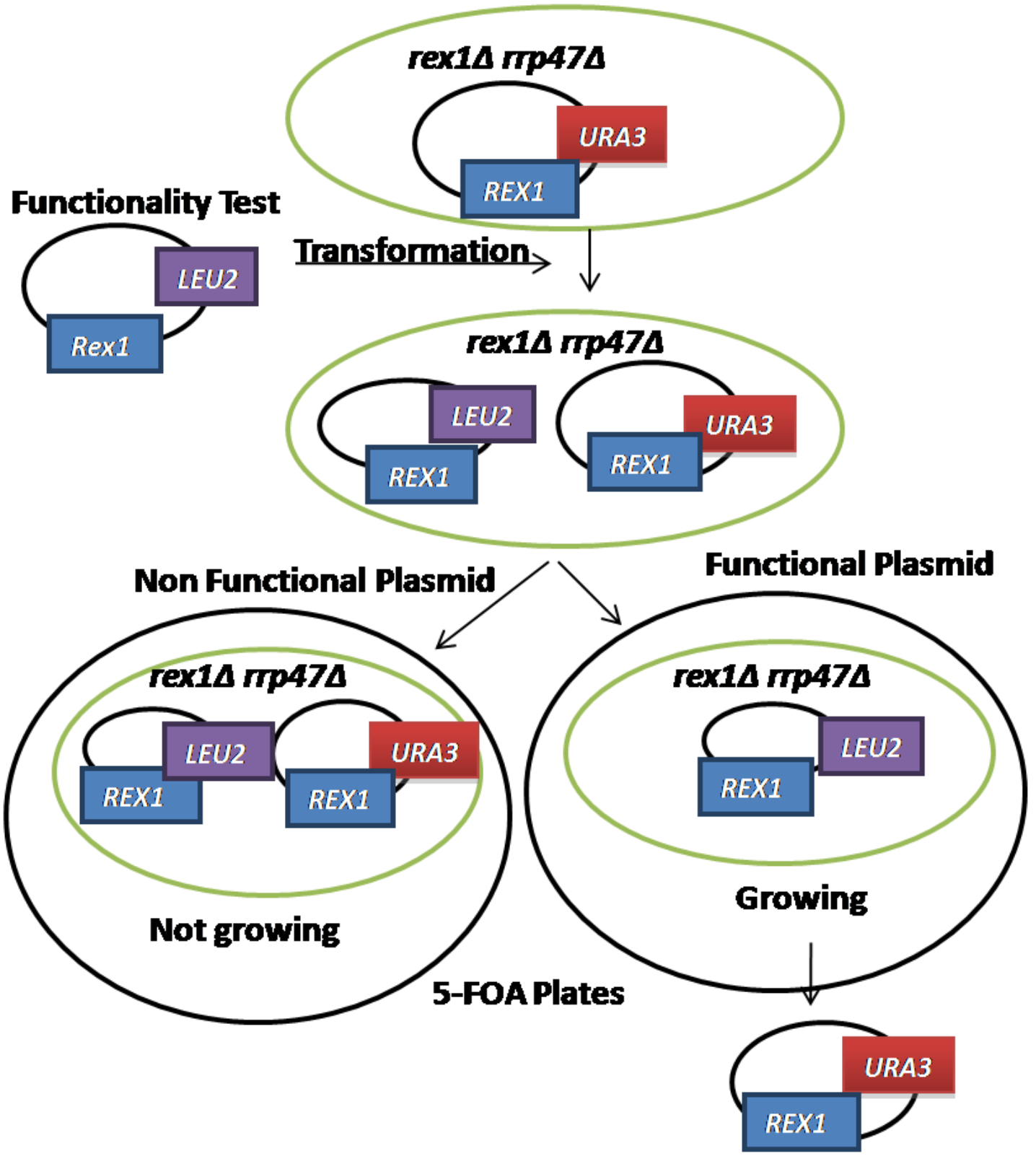

Figure 7 Schematic of a *rex1Δ rrp47Δ* shuffle assay.

A *rex1Δ rrp47Δ* strain is synthetic lethal (Peng *et al*., 2003) but cell growth of the double mutant can be supported by a plasmid with a wild type allele of *REX1* . This plasmid also harbours the counterselectable *URA3* marker. A second plasmid is then introduced that harbours a distinct selectable marker gene, e.g. the LEU2 marker, together with the test *rex1* allele. If the *rex1* allele is functional then the first plasmid can be lost and the transformant is viable on medium containing 5-FOA (right hand side of the panel). In contrast, if the *rex1* allele is not functional then growth is dependent upon the initial plasmid and the strain cannot grow on medium containing 5-FOA (left hand side of the panel).

.

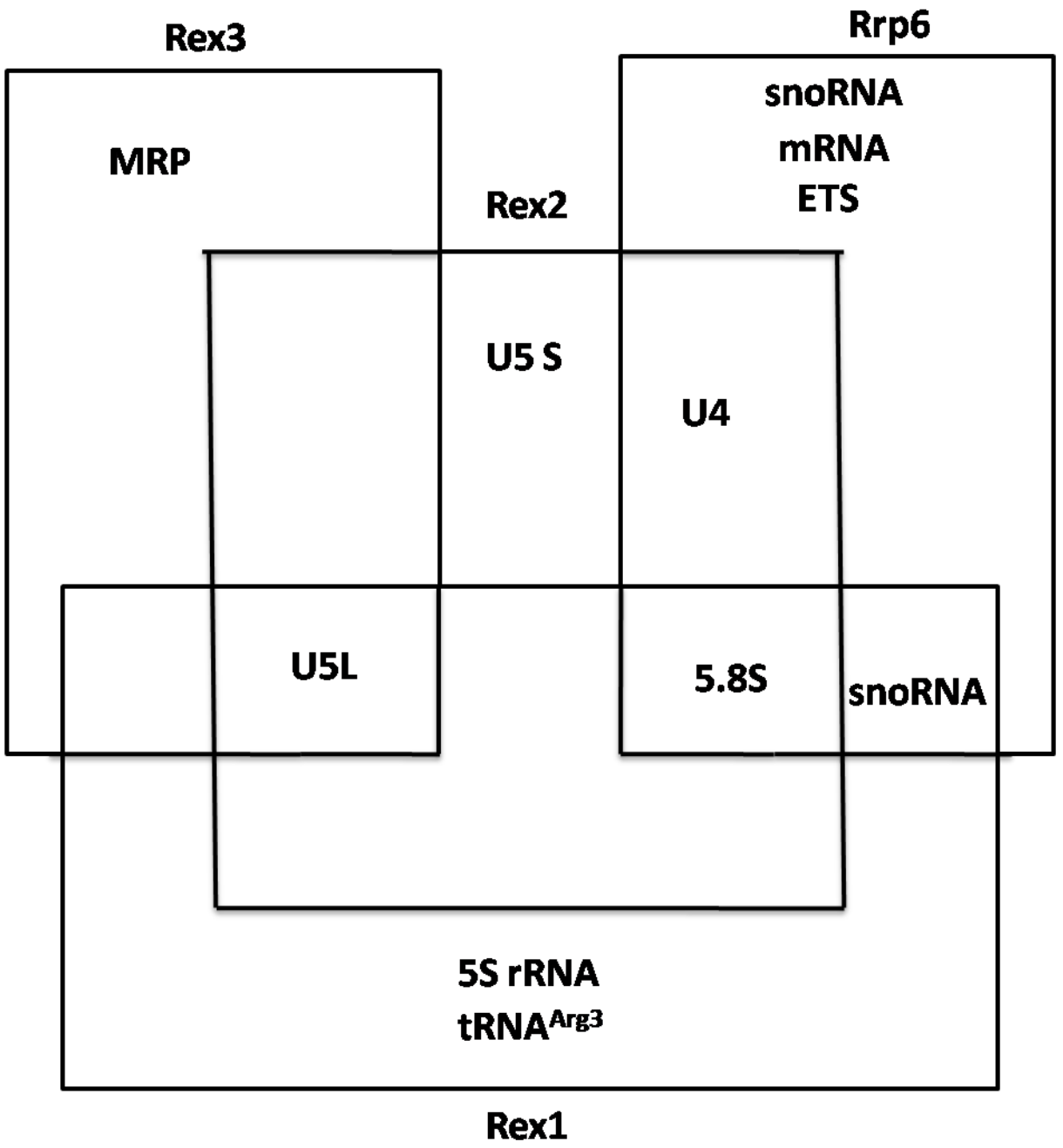

Figure 5 Functional overlap of Rex1, Rex3 and Rrp6 RNases.

A Venn diagram showing the functional overlap and specificities of the Rex1, Rex3 and Rrp6 RNases. RNA substrates of a specific protein are indicated inside the box of the same protein. RNA substrates that depend on the redundant functions of different proteins (van Hoof et al*,* 2000; Garland et al*,* 2013) are indicated in the overlap of different boxes.

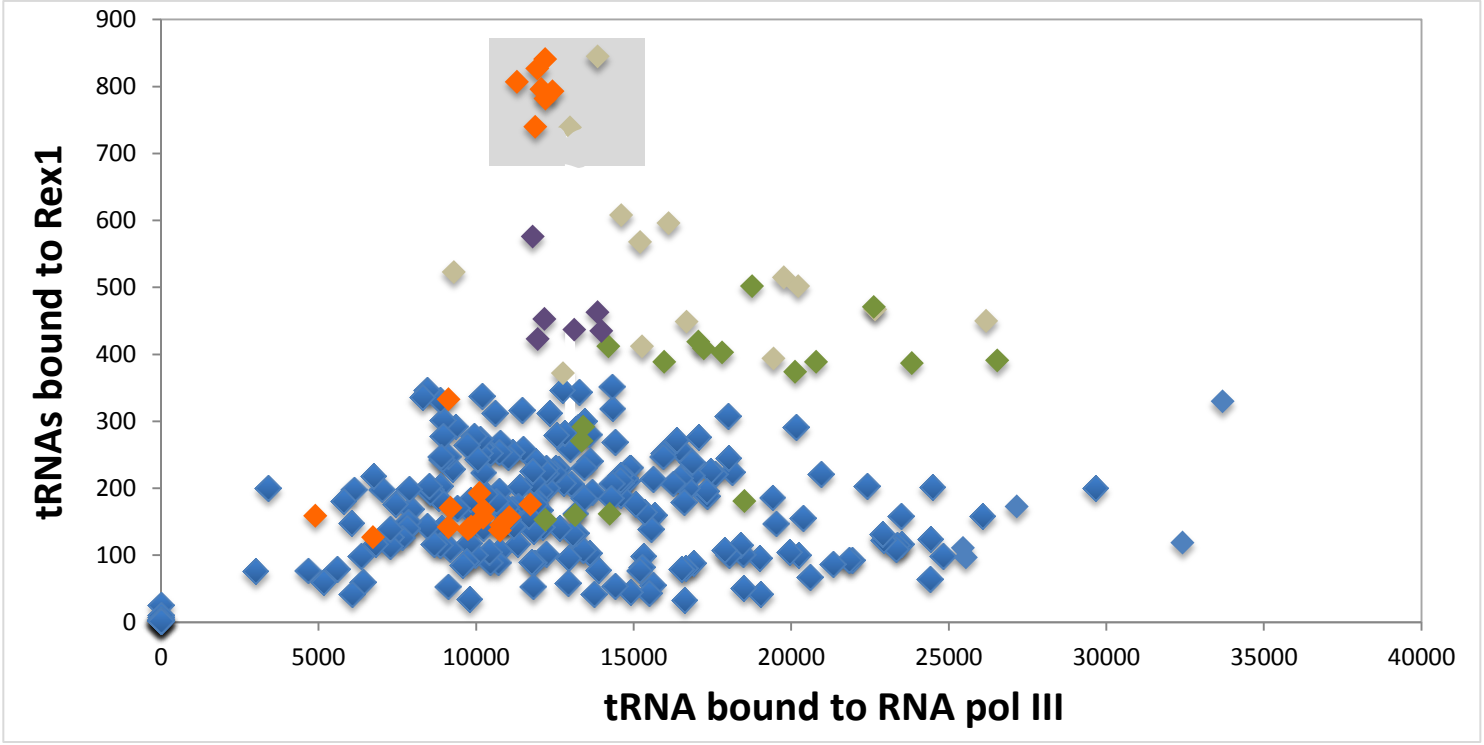

Figure 47 Scatter plot of comparing the number of tRNA cDNA reads obtained for Rex1 and RNA pol III.

The number of CRAC reads obtained for Rex1 for each tRNA transcript in yeast is plotted against the number of reads obtained with the Rpo31 subunit of RNA Polymerase III. Data points obtained for $tRNA^{Lys}$ (orange), $tRNA^{Trp}$ (purple), $tRNA^{Ile}$ (silver) and $tRNA^{Arg}$ (green) species are highlighted. Data points from $tRNA^{Lys}_{UUU}$ and $tRNA^{Ile}_{UAU}$ transcripts that contain introns are boxed.

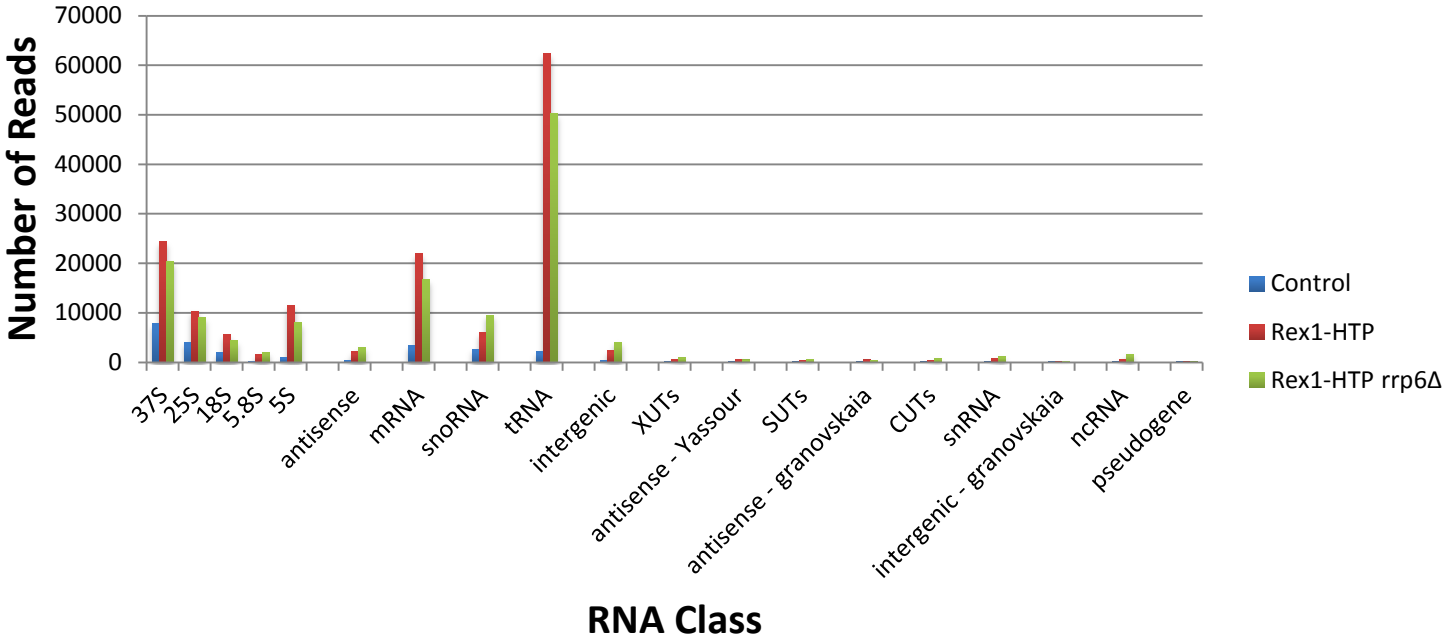

Figure 46 Overview of the Rex1-HTP CRAC data in the presence and absence of Rrp6.

The total number of hits in the Rex1-HTP CRAC dataset are given for different classes of RNA.

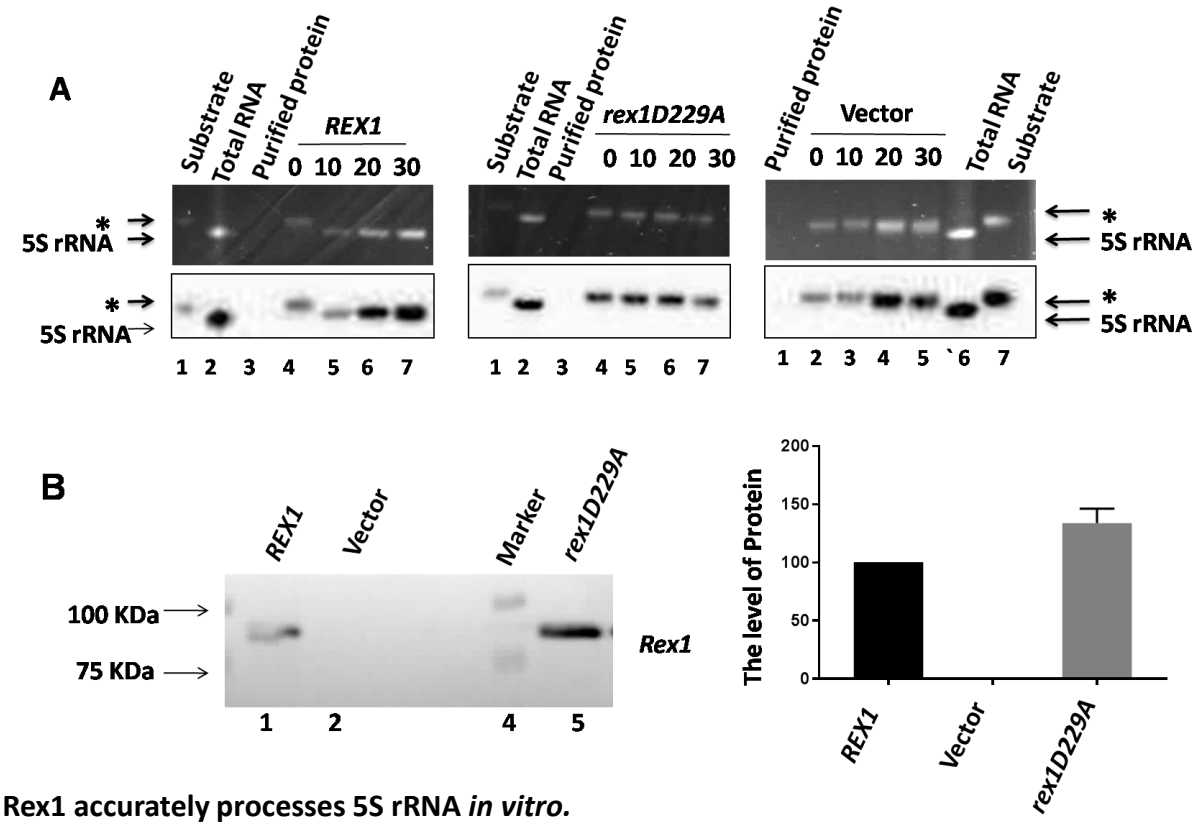

Figure 41 **Rex1 accurately processes 5S rRNA *in vitro.***

(A) *In vitro* on-bead exonuclease activity of yeast Rex1. Reaction mixtures were resolved on a 6 % RNA polyacrylamide gel and visualised by ethidium bromide staining (upper panels) and by northern blot hybridisation using a 5S rRNA specific probe (lower panels). Lane 1, 5S RNP substrate from a *rex1Δ* strain; lane 2, total RNA from a wild-type strain; lane 3, control sample without added RNA substrate; lanes 4-7, time-course (in minutes) of incubations with purified wild-type Rex1, the catalytically inactive D229A *rex1* mutant and a vector control. **(B)** Western analysis of the epitope-tagged protein recovered from the beads after the assay. Lane 1, wild-type Rex1; lane 2, vector control; lane 4, molecular weight marker; lane 5, the *rex1* D229A mutant. The level of protein measured by ECL is indicated in the histogram, the error bar indicating the mean and standard deviation.

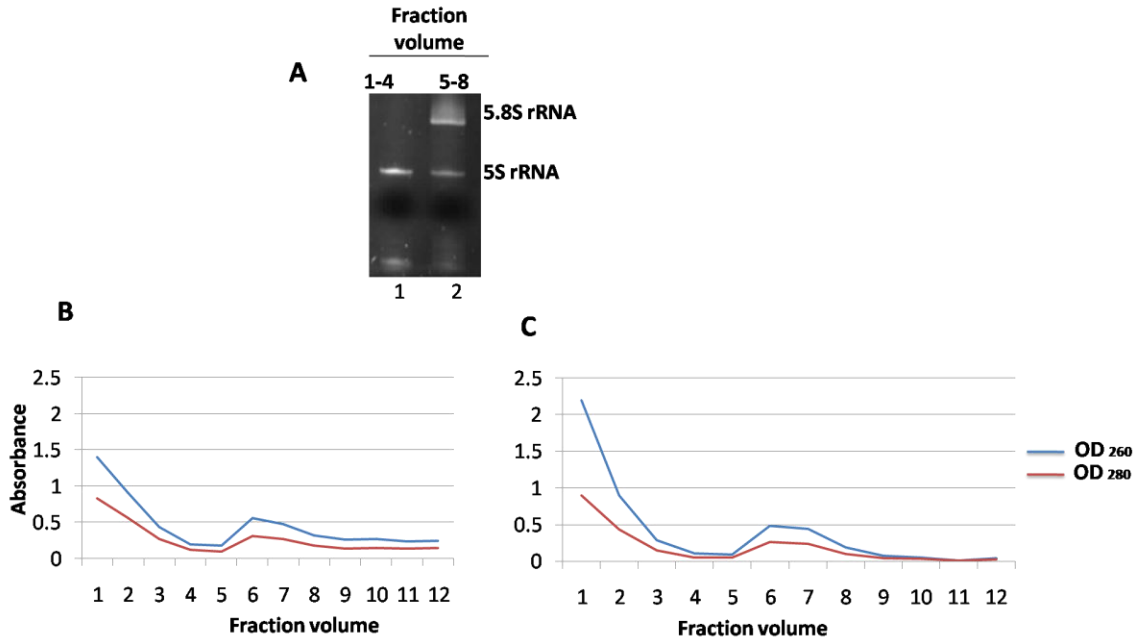

Figure 40 Analysis of purified rRNP complexes

rRNP complexes were purified from cytoplasmic extracts of a *rex1Δ* strain by sucrose gradient ultracentrifugation. **(B)** Purification of the large and small ribosomal subunits by centrifugation through gradients in a low salt buffer. The OD of each gradient fraction, numbered 1-12 from top to the bottom of the gradient, is plotted. Ribosomal subunits were detected in fractions 6 and 7. (**C)** Glycerol gradient analyses of EDTA-washed ribosomes. The OD of each gradient fraction is plotted. Ribosomal subunits were detected in aliquots 6 and 7. (**A)** Acrylamide gel electrophoresis of RNA from the gradient shown in panel (C). Lane 1, pooled gradient fractions 1-4; lane 2, pooled gradient fractions 5-8. Major RNA species are indicated to the right.

A

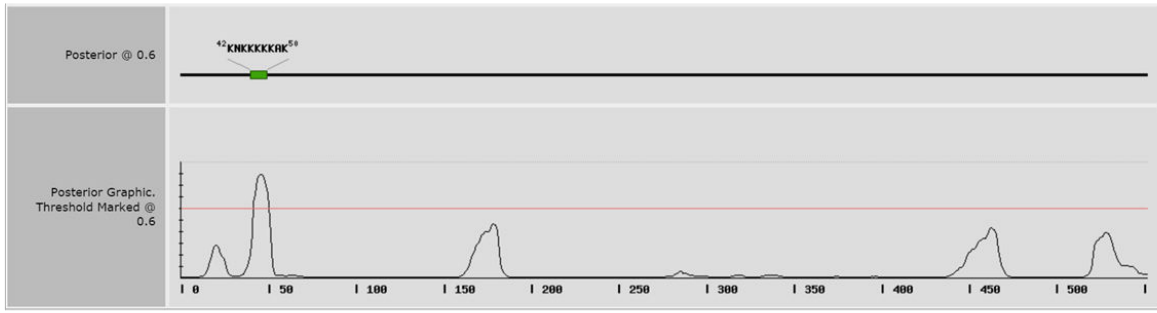

B

Predicted bipartite NLS		
Pos.	Sequence	Score
17	GSKKRRLSKTSVQEDDHTNVVSEVNKNKKKK	8.2
21	RRLSKTSVQEDDHTNVVSEVNKNKKKKKAKP	5.1

Figure 34 NLS prediction software define a putative NLS in the N-terminal region of Rex1.

(A) Prediction of an NLS within Rex1 using the online prediction database, NLStradamus (Nguyen *et al,* 2009). **B)** According to a second online prediction tool (NLS_Mapper) (Kosugi *et al*., 2009), a bipartite Rex1-NLS is located at N-terminal residues 17-52. The residues underlined in red are present in both putative NLS sequences.

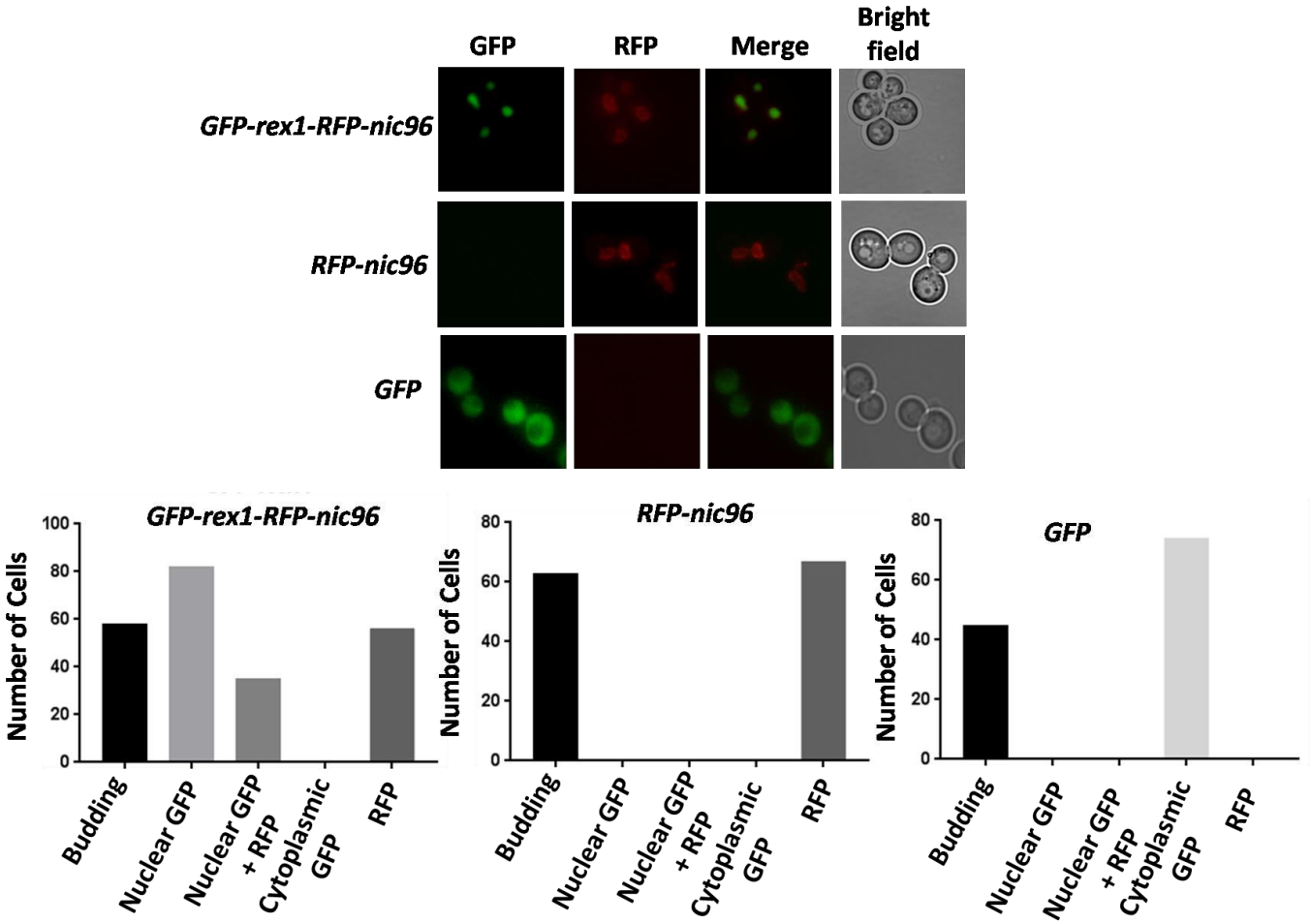

Figure 31 GFP-Rex1 is localized to the cell nucleus.

Actively dividing cells expressing GFP, RFP-Nic96 or both GFP-Rex1 and RFP-Nic96 were imaged by fluorescence microscopy. GFP channel, RFP channel, merged and bright field Images are shown for selected representative cells. The data from 100 randomly selected cells are presented for each strain as histograms.

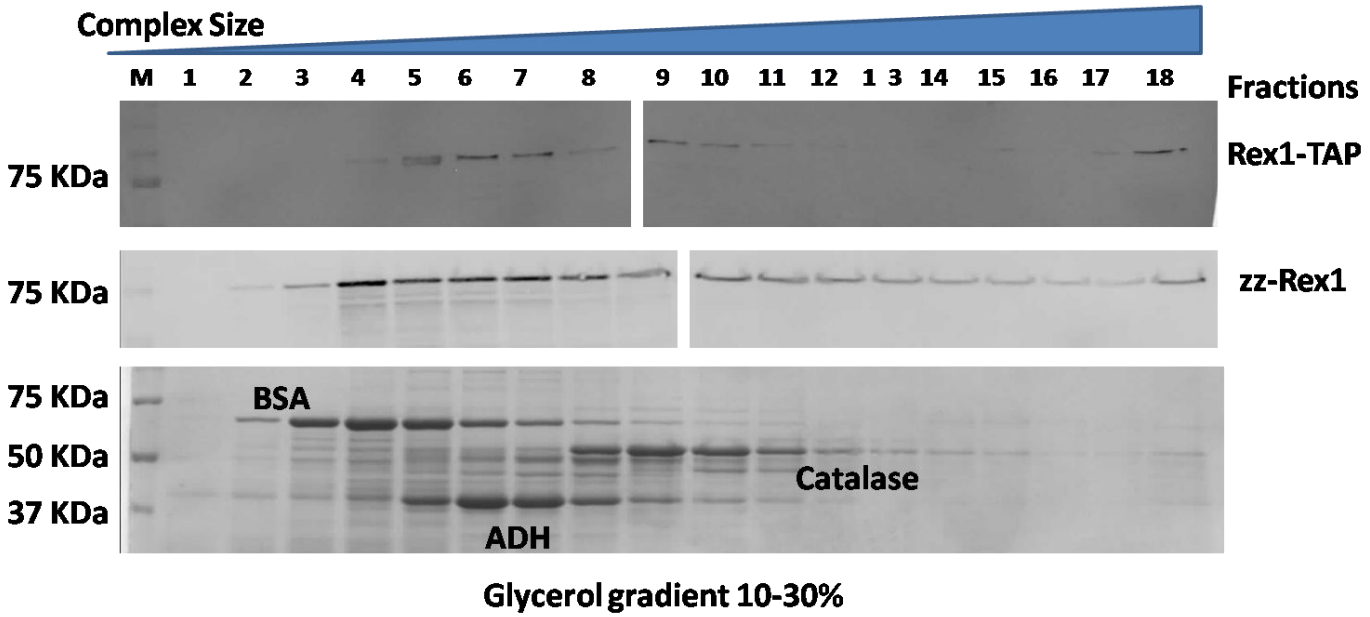

Figure 26 Rex1 is expressed as part of a larger protein complex.

Cell lysates were fractionated through glycerol gradients and analysed by SDS-PAGE and western blotting. The sedimentation velocity of Rex1-TAP and zz-Rex1 proteins were analysed using the PAP antibody, while the sedimentation velocity of standard proteins (BSA, catalase and ADH) were analysed by coomassie staining (lower panel). Fractions are numbered 1-18 from the top to the bottom of the gradient.

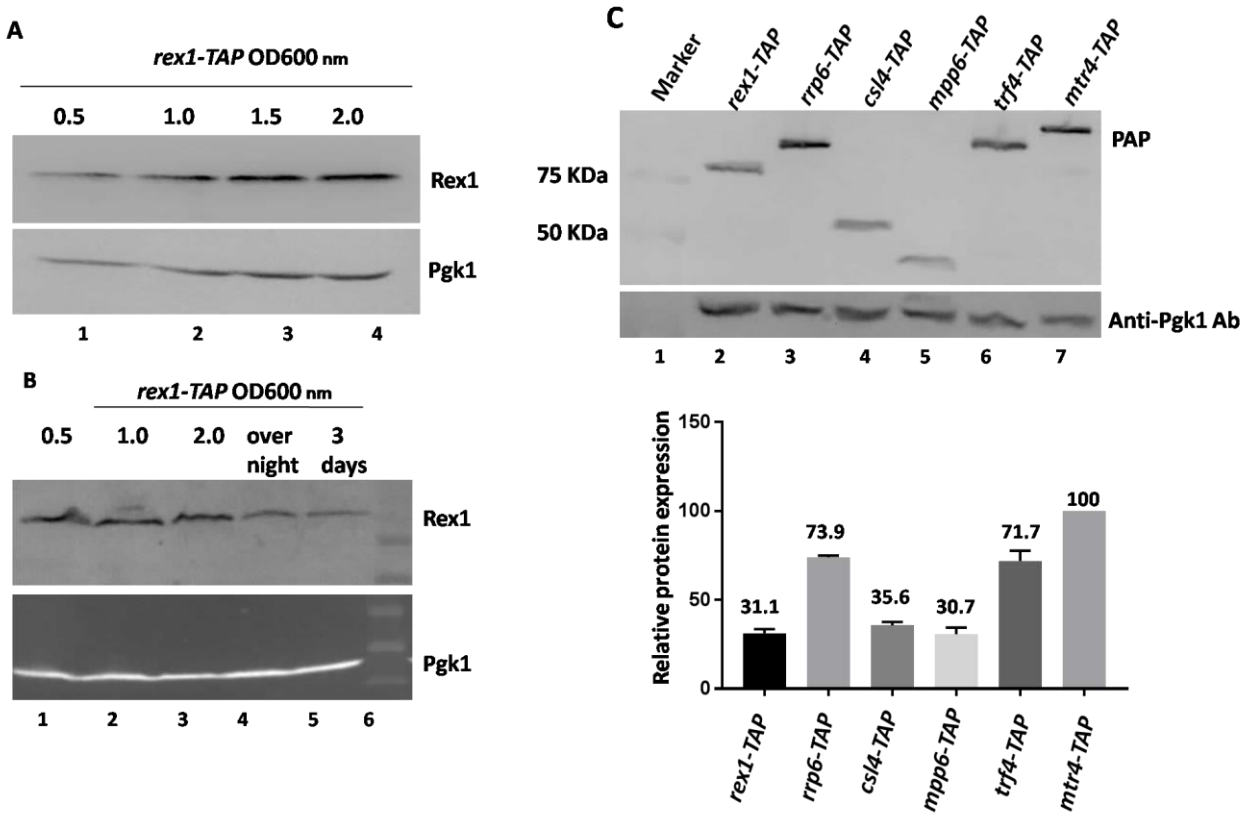

Figure 24 Rex1-TAP is stably expressed in stationary phase

(A,B) Western analyses of rex1-TAP expression during logarithmic growth and upon incubation in stationary phase. Cells were harvested at the OD shown, cell extracts were resolved by SDS-PAGE and Rex1-TAP and Pgk1 levels were analyzed by Western blotting. **(C)** The expression level of Rex1 was compared to the expression level of Rrp6, Csl4, Mpp6, Trf4 and Mtr4. Expression levels were standardized to the level of Pgk1. The upper panel shows a representative Western blot. The lower panel shows the quantification of the western signals from three independent biological replicates. Error bars indicate the standard deviation of the mean values.

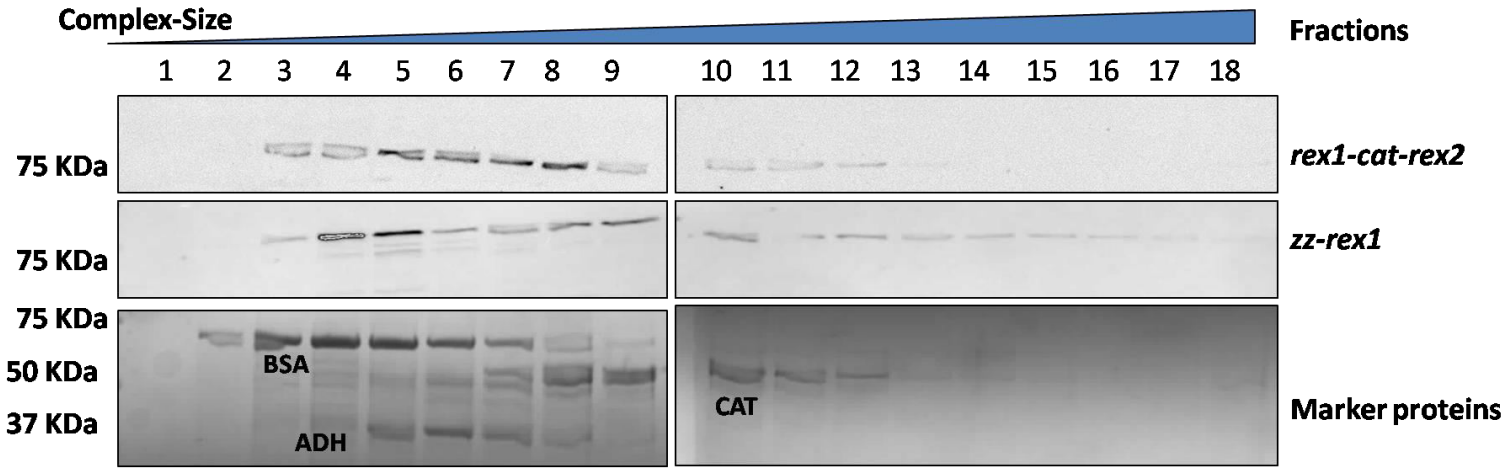

Figure 19 The sedimentation velocity of the *zz-rex1-cat-rex2* mutant is similar to ADH

Cell lysate from a strain expressing the epitope-tagged *rex1-cat-rex2* mutant was resolved through 10-30% glycerol gradients. After fractionation, aliquots were resolved by SDS-PAGE and analysed by Western blotting. Lanes 1-18, aliquots of fractions taken from the top to the bottom of the gradient. The *rex1-cat-rex2* mutant was detected by Western analysis (upper panels). Protein standards were detected by staining with colloidal Coomassie Blue (lower panels). Images of the western blots were captured at the same time to generate identical exposures. The molecular weight markers are indicated to the left.

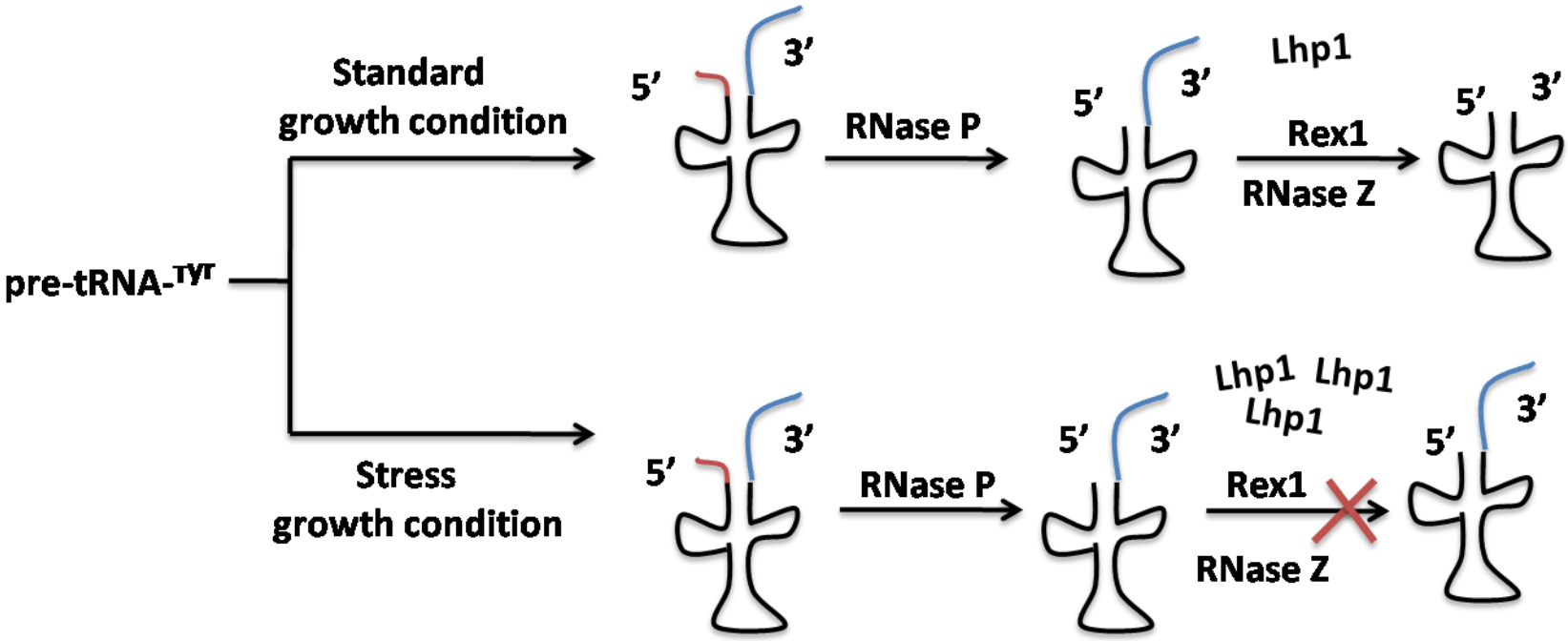

Figure 6 **Schematic presentation of pre-tRNA^{Tyr} processing under normal growth and during stress.**

Processing of pre-tRNA^{Tyr} involves initial endonucleolytic cleavage by RNase P to generate the mature 5' end, followed by 3' end processing involving both endo- and exoribonucleases. Under standard growth conditions, 3' end processing involves Rex1 and RNase Z. Under stress conditions (the lower route), 3’ processing is inhibited (indicated by the red cross) due to increased expression of Lhp1 and saturation of its substrate binding sites at 3’ end of the tRNA (Foretek *et al,* 2016).

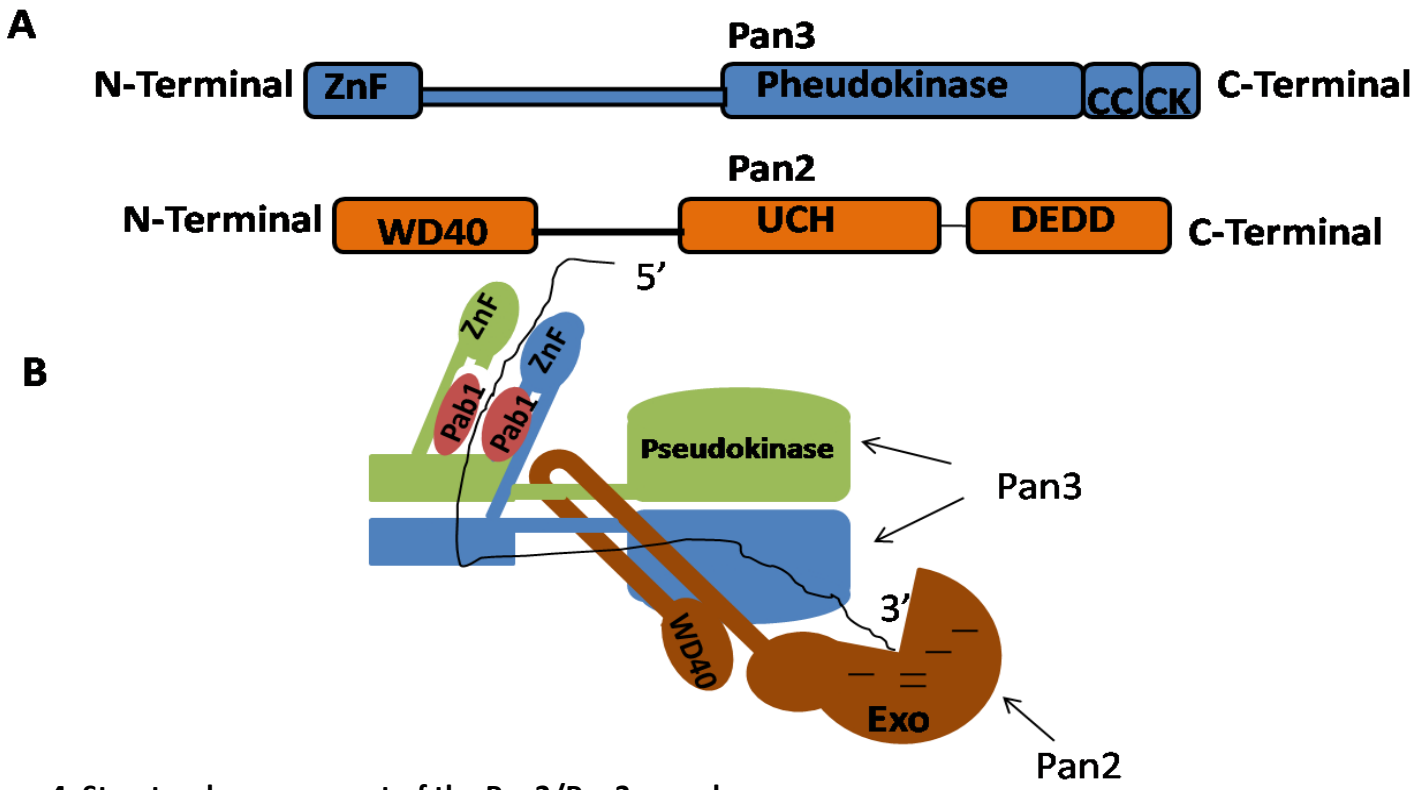

Figure 4. Structural arrangement of the Pan2/Pan3 complex.

(**A**) Domain structure of Pan2 and Pan3 proteins. ZnF, Zinc finger; UCH, ubiquitin C-terminal hydrolase, CK, C-terminal knob domain; CC, coiled coil. (**B**) Structural arrangement of the Pan2/Pan3 heterotrimeric complex. Pan3 is a homodimer with the two subunits being aligned in a "head to head, tail to tail" manner. The Pan2/Pan3 complex binds to the poly(A) RNA via the Znf and psuedokinase domain at its C-terminal and threads RNA into the catalytic domain of Pan2. The image was taken and adapted from Wolf et al, 2014 and Schäfer et al., 2014).

A

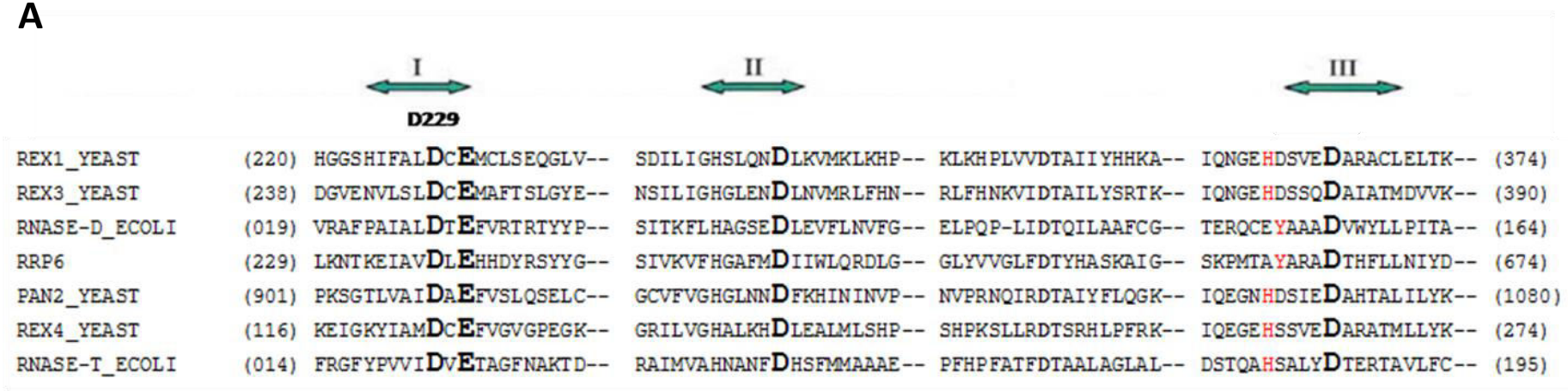

B

Figure 3 Sequence alignment of the catalytic domain of yeast DEDD family members.

(A) Sequence alignment of the catalytic domain of yeast DEDD family members. Clustal-Omega (Sievers et al, 2011) was used to align yeast proteins Rrp6, Pan2, Rex1, Rex4 and Rex3 sequences and some editing has been done from BLAST search. Acidic residues shown in bold are highly conserved and required for catalysis. DEDD domains are subdivided onto DEDDy and DEDDh groups, based on the presence of either conserved amino acid Y or H (highlighted in red in motif III). D229 (indicated in motif I) was mutated to generate the *rex1* inactivate mutant. The figure is Modified from Yuhong and Murray, 2001. **(B)** Domain organisation of the Rex1 protein. ExPASy coils (Lupas *et al,* 1991) was used to predict different coiled-coil regions of Rex1 that are indicated in different colour boxes.

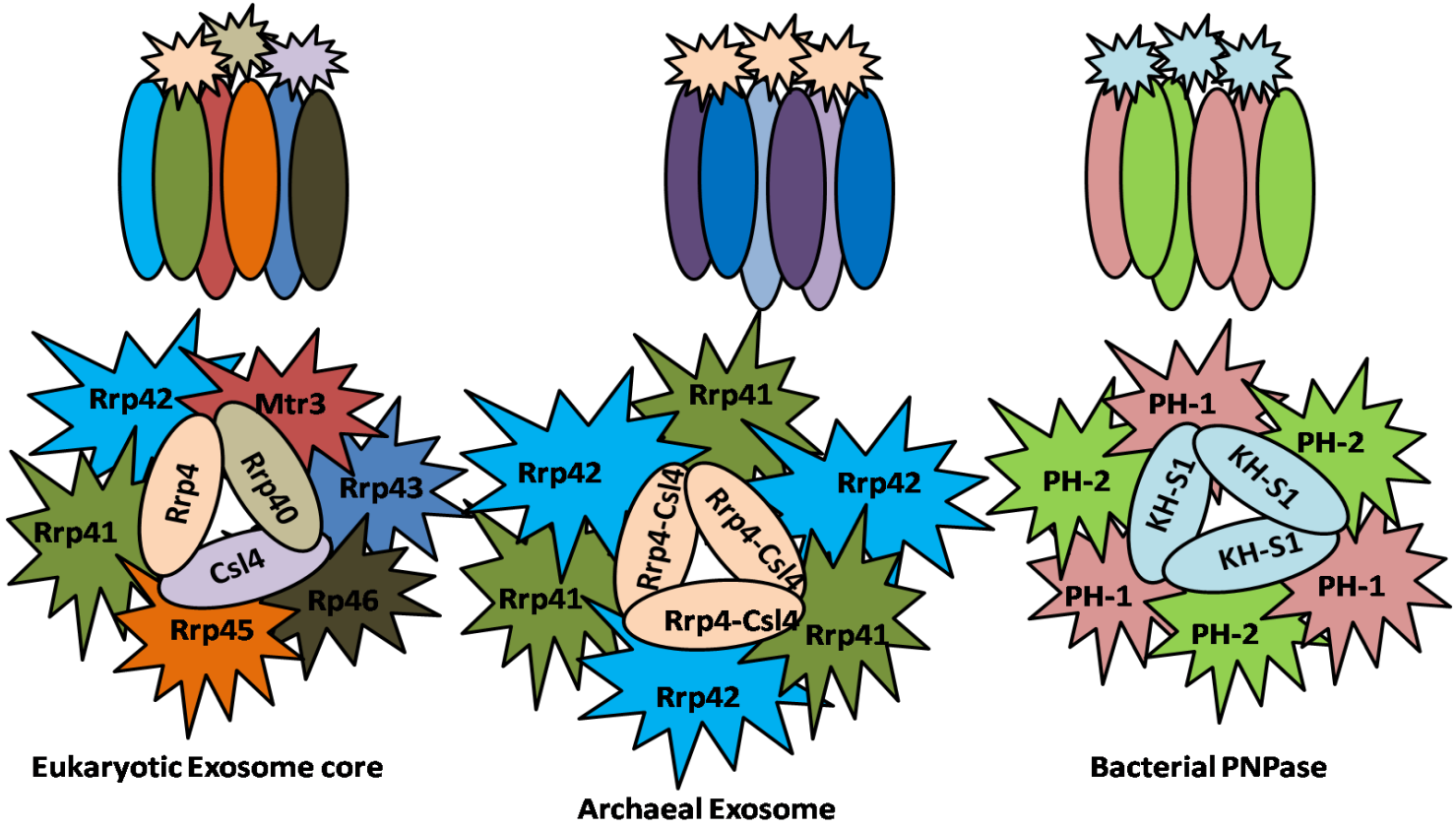

Figure 2. The structure of the Exosome is conserved and related to PNPase.

The cartoon images show the composition of the exosome core in top view (lower panel) and side view (upper panel) in eukaryotic and archaeal systems, and compare them to prokaryotic PNPase.

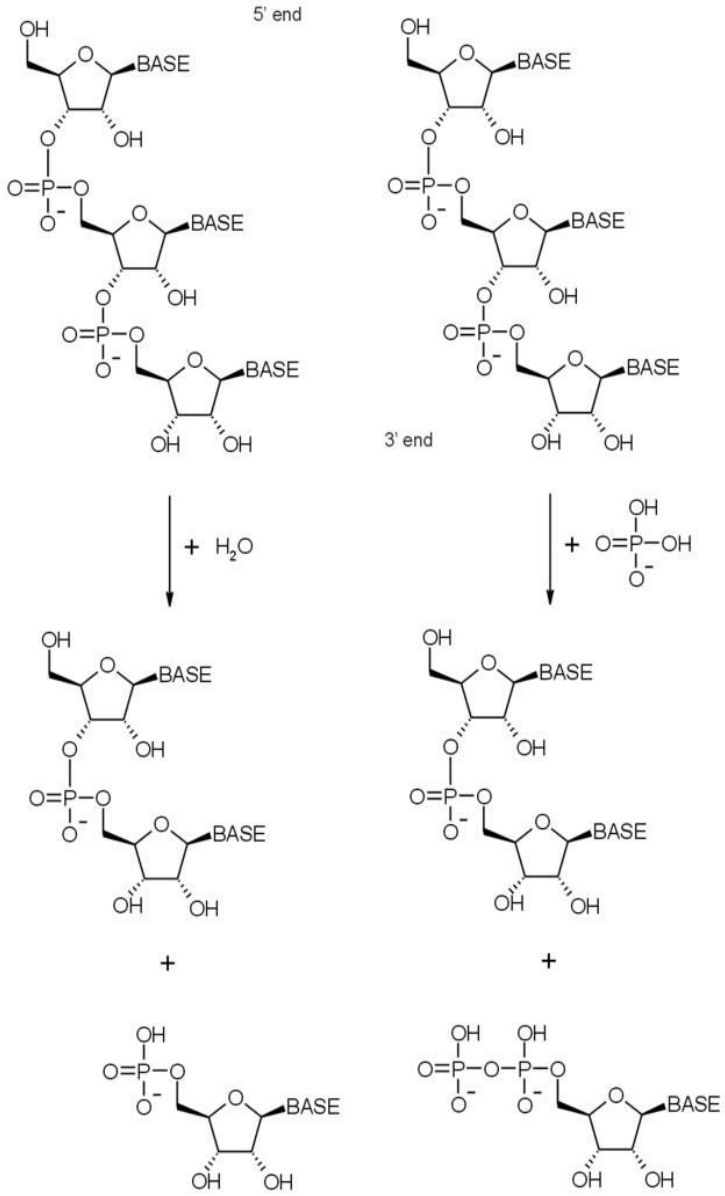

Figure 1. Hydrolytic and Phosphorolytic mechanisms of RNA Degradation.

Phosphorolytic exoribonucleases use an inorganic phosphate ion to attack the 5’ phosphodiester linkage of the terminal nucleotide, leaving a 3’ hydroxyl group and releasing a nucleoside 5’ diphosphate (right hand side panel). Hydrolytic exoribonucleases use a water molecule to attack the phosphodiester bond and release nucleoside 5’ monophosphates (left hand side panel).